SEISMIC SEQUENCE STRATIGRPAPHY AND RESERVOIR CHARACTER OF DEEPWATER SETTING IN M11 BLOCK, MARTABAN BASIN, MYANMAR

By

PONGSIT CHONGRUEANGLAP

B.S. Geology, Chulalongkorn University, 2012

A thesis submitted to the
Faculty of the Graduate School of the
University of Colorado in partial fulfillment
of the requirement for the degree of
Master of Science
Department of Geological Sciences
2019

This thesis entitled:
Seismic Sequence Stratigraphy and Reservoir Character of Deepwater setting in M11 block, Martaban Basin, Myanmar
written by Pongsit Chongrueanglap
has been approved for the Department of Geological Sciences

____

(Dr. Paul Weimer)

____

(Dr. Charles Stern)

____

(Dr. Tomas Villamil)

Date______________

The final copy of this thesis has been examined by the signatories, and we find that both the content and the form meet acceptable presentation standards of scholarly work in the above mentioned discipline.

Chongrueanglap, Pongsit (M.S., Geology)

Seismic Sequence Stratigraphy and Reservoir Character of Deepwater setting in M11 block, Martaban Basin, Myanmar

Thesis directed by Professor Paul Weimer.

ABSTRACT

The Martaban basin, located offshore Myanmar. The sequence stratigraphic framework of upper Miocene to Pliocene was defined using a 2,261 sq.km. 3D-PSTM seismic survey, in addition to a nearby well data. The depositional environments and the reservoir potential are analyzed. The study area was segmented into three parts, based on different tectonic settings in the focus stratigraphic section.

Eight megasequences were clearly defined from early Miocene (?) to Top Pliocene. Each megasequence consists of base-of-slope turbidite system, comprising channel-fill, levee, and overbanks. System is primarily mud, with sands restricted to specific environments. Sedimentary supply primarily from N and NNE, part of Ayeyarwardy delta.

The overall sea level changes present major in relative sea level rise, which is part of lower Bathyal from biostratigraphic report. For system tracts interpretation, all of megasequences are primarily thick LSTs with thin condensed sections, equivalent to PGC, TST and HST.

The erosional nature of sequence boundaries varies from the older (Megasequences 1-4) to the younger (Megasequences 5-8). Substantial erosion of the lower slope is presented approximately 300 meters in maximum at Miocene and lower Pliocene megasequences, likely enhanced by tectonism causing to the sudden increase in volume of the sediment gravity flows. These might be 2nd order of sequence boundaries. In Pliocene, less erosion feature recorded at the lower boundaries. Possibly 3rd order of sequence boundaries is interpreted in Pliocene, with less tectonic enhancement.

The channel-fill reservoirs are thicker in the shallow megasequences in both Miocene and Pliocene. During Pliocene, two zones are recognized as lower (Megasequences 4–6) and upper Pliocene (Megasequences 7-8). Levees and overbank thickness are varies based on the width and the channel geometry, which cut through the area. In addition, carbonate reservoir in late Miocene is considering part of the reservoir as well. Typical of the stacking reservoir from the prediction of channel-filled is about 120 meters, from each 30 meters individual channel in average.

For other elements in petroleum system analysis, significant unknown of petroleum systems elements are listed as source rock presence and kerogen types with timing of the HC generation and charging.

CONTENTS

LIST OF TABLES

TABLE

LIST OF FIGURES

FIGURE

INTRODUCTION

The Martaban basin, located offshore Myanmar, is one of the biggest sedimentary basins near the Ayeyarwardy Delta (Figures 1, 2). Nine geological sedimentary basins are present in this offshore area: Rakhine, Andaman, Preparis, Central Andaman, Martaban, Tanintharyi, North Mali, South Mali and Mergui basins (Figure 1).

The Martaban basin has had a complex tectonic evolution since late Oligocene. The basin initially formed as a back-arc basin associated with the oblique subduction of the Indian plate. After subduction was initiated, a trans-tensional pull-apart basin developed associated with regional strike-slip faults during middle Miocene. Later, during the Pleistocene, movement of microplates created local contraction and inversion, creating possible drillable structural traps in this area.

The Martaban basin is an active exploration area with many possible lease blocks (Figure 2). Myanmar Oil and Gas Enterprise (MOGE) defined three petroleum regions covering this area: Rakhine, Moattama and Tanintharyi (Figure 3).

The Neogene stratigraphy of the area developed primarily in two phases (Figure 4): (1) a wedge of late Oligocene to early Miocene localized carbonated buildups, overlaid and lateral to (2) thick siliciclastic sediments derived from the Ayeyarwardy Delta to the north. The petroleum potential of these siliciclastic deposits is of great interest to oil and gas exploration companies.

Thus, this thesis focuses on the seismic sequence stratigraphy of upper Miocene to Pliocene sediments in the M11 block and their petroleum potential (Figure 3). The M11 block is 5,373 km^2 in area, is approximately 300 km away from Yangon, and is close to the main gas production in the Yadana, Yetagun and Zawtika fields (Figure 3). First, the sequence stratigraphic framework is defined based on the important surfaces defined using a 2,261 sq.km.

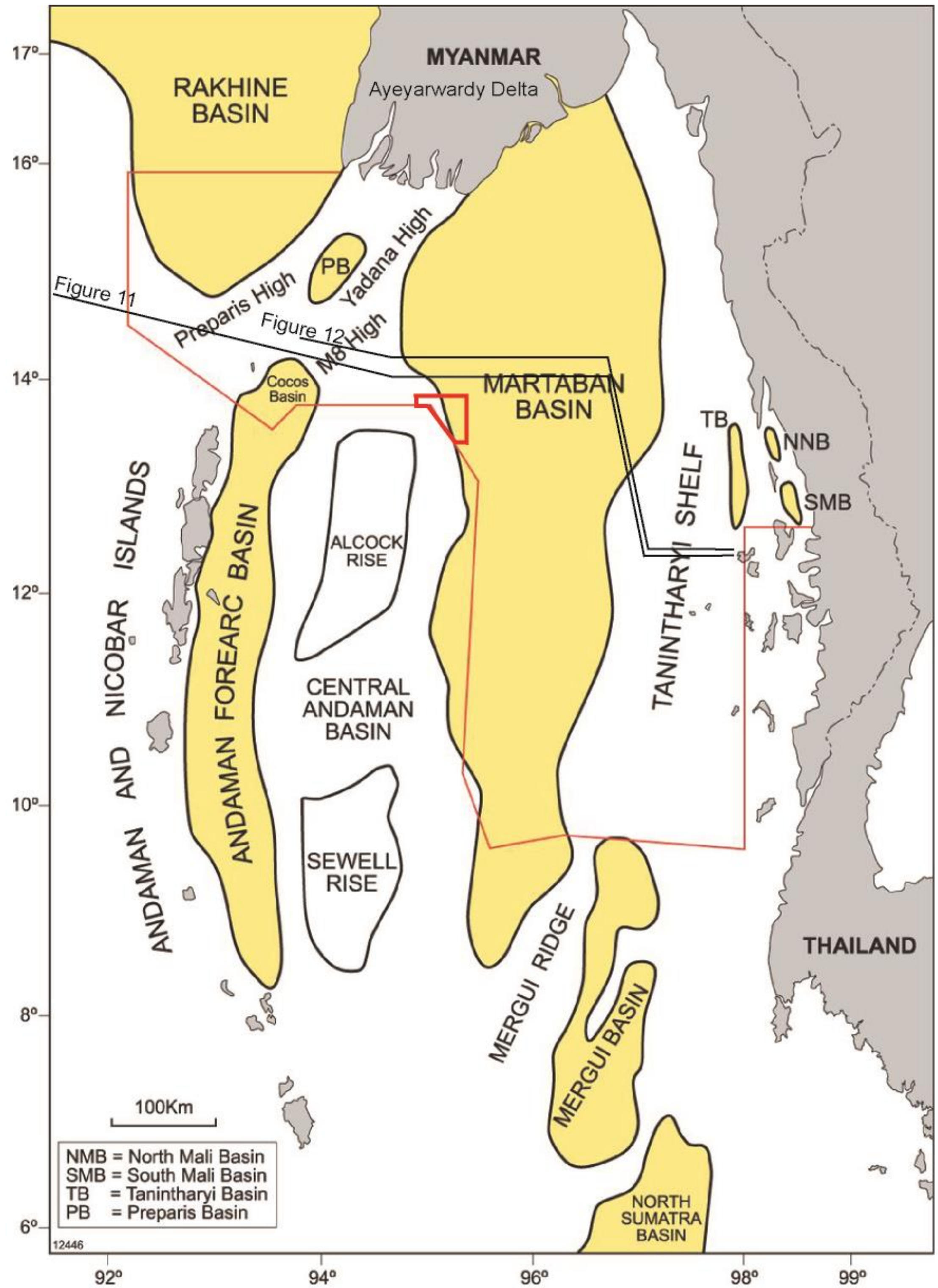

Figure 1: Location map of Martaban and surrounding basins, offshore Myanmar. Red line is the exploration and production boundary of the Martaban basin. M11 block, study area, is shown by red outlines. Location of figure 11, 12 are shown (modified from Racey and Ridd, 2015).

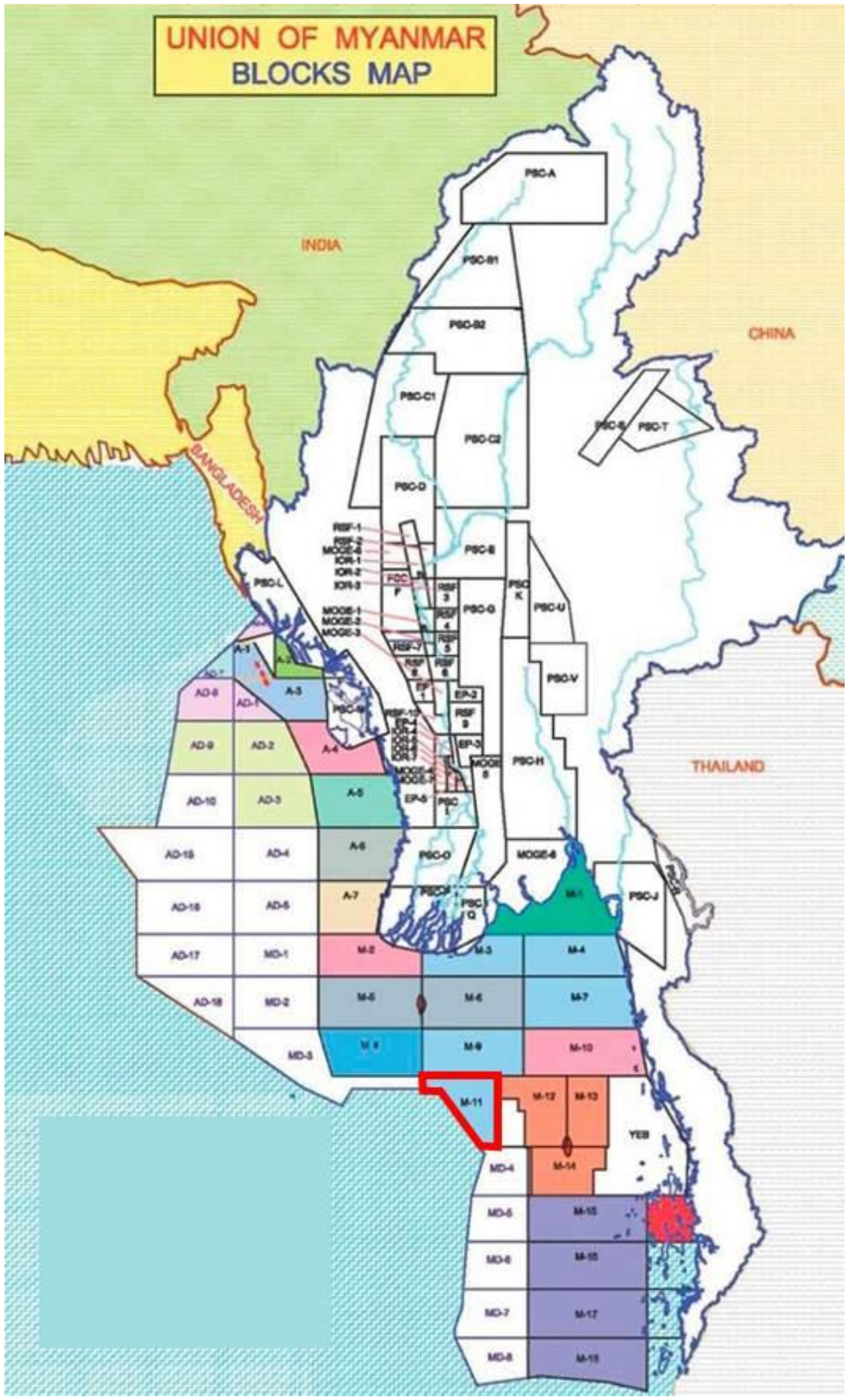

Figure 2: Map showing Exploration blocks of onshore and offshore Myanmar. The study area M11 block is outlined in thick-red line block (modified from Thiha, 2014).

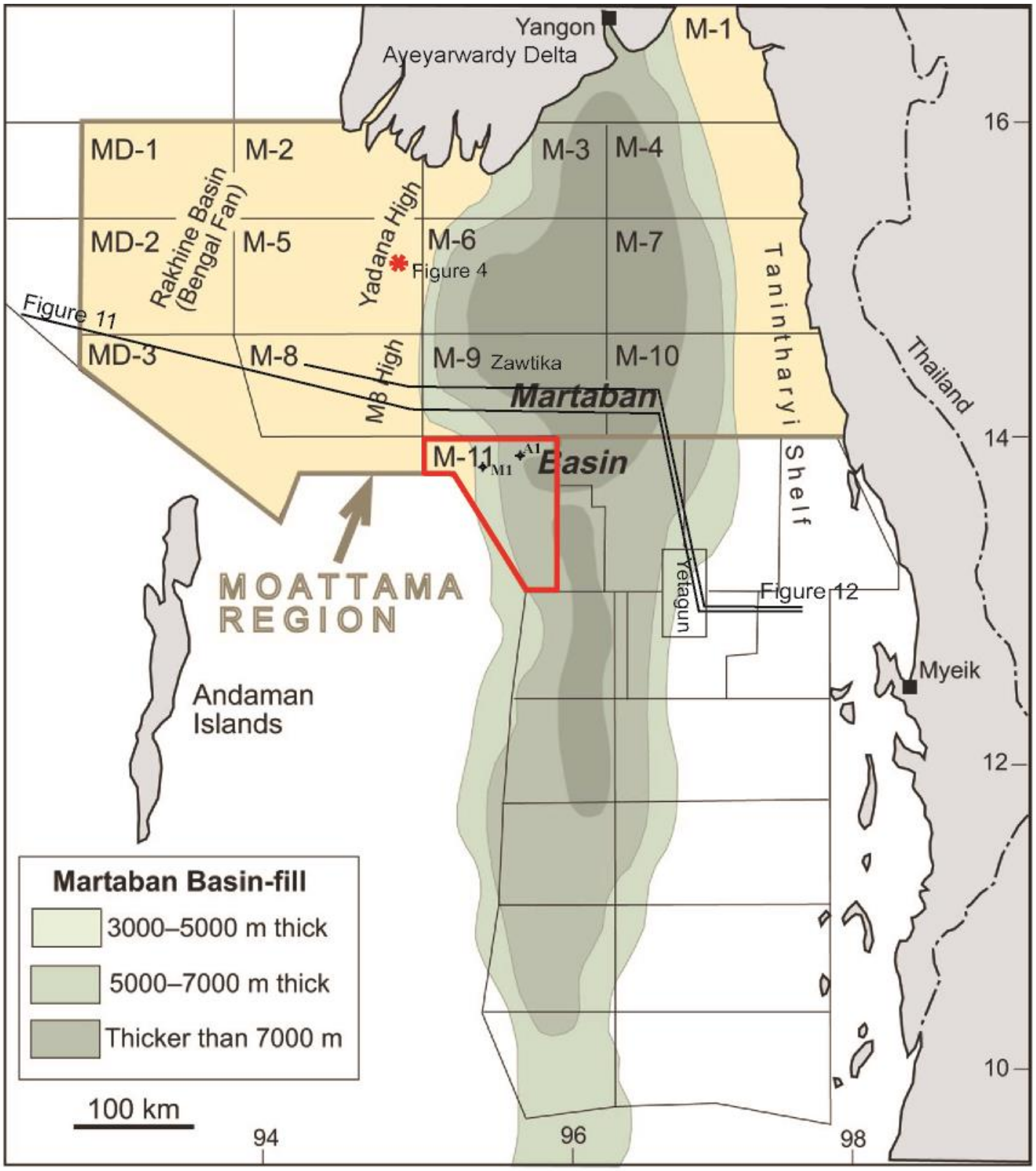

Figure 3: Map showing the thickness of late Oligocene to present sediments of the Martaban basin, offshore Myanmar. Location of the study area (red outline) is on the central west flank of depocenter. Yadana, Yetagun and Zawtika production areas are shown. Mottama Region is highlighted (brown outline with yellow fill). Location of Figures 11 and 12 are shown (modified from Racey and Ridd, 2015).

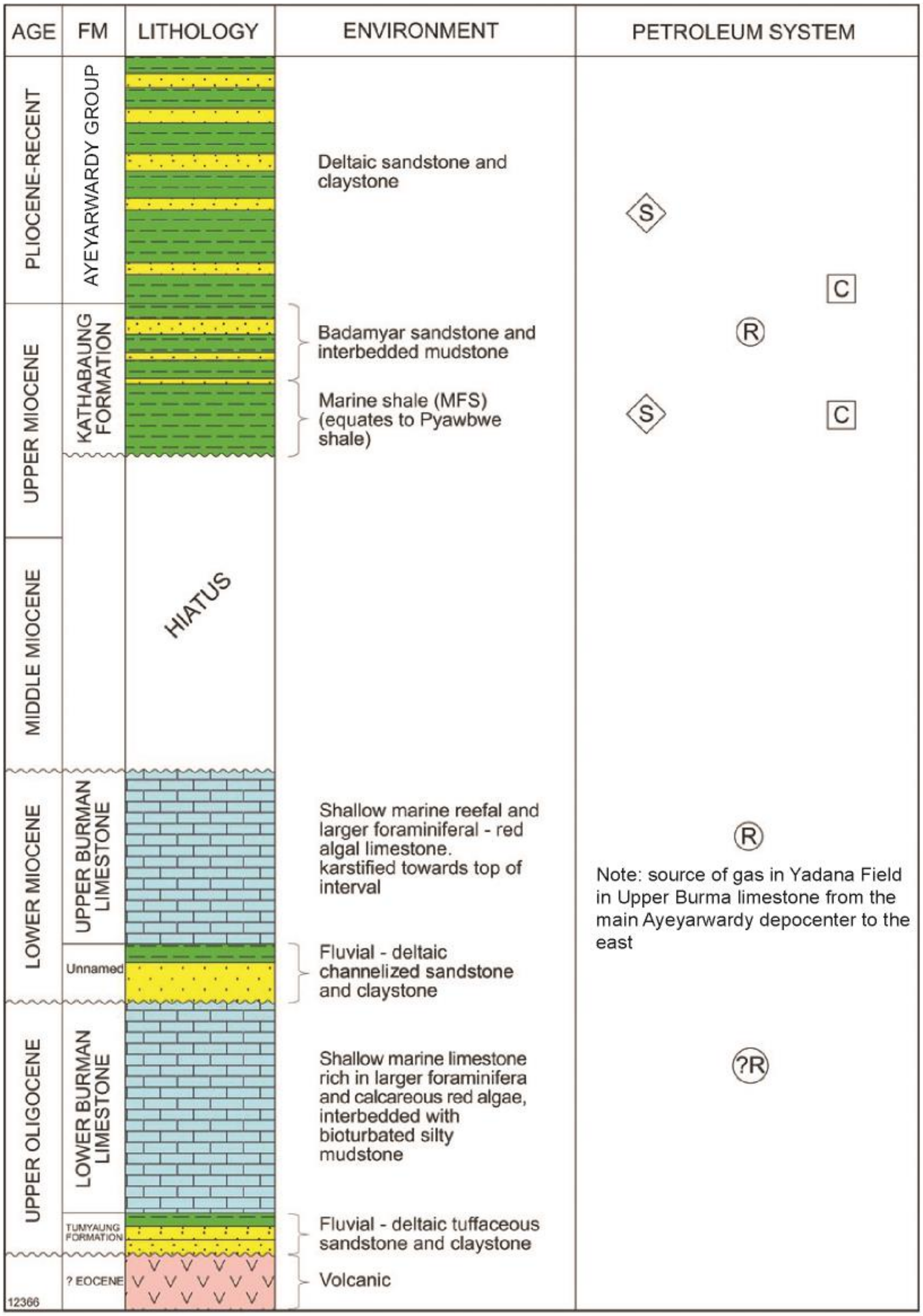

Figure 4: Stratigraphic column, environments of deposition, and petroleum systems elements of the Yadana Field, Martaban basin. See Figure 3 for location of the Yadana High field. S = source rocks, R = reservoirs, and C = seal rocks (modified from Racey and Ridd, 2015).

3D-PSTM seismic survey acquired in 2016 (Figure 5). Second, the depositional environments are interpreted based primarily on seismic facies and their attributes and geometries. Finally, the play potential for the study area is evaluated for future exploration of this area. Specifically, the reservoir potential of the Neogene siliciclastic sediments are analyzed, as well as other elements.

Exploration History

Myanmar Oil Company (MOC) began offshore exploration in 1972 using 2D seismic data. The first 18 exploration wells were drilled based only on 2D seismic data. 5 wells had significant gas shows (Racey and Ridd, 2015). Later, the acquisition of 3D seismic data made significant changes in the Moattama region. The new 3D survey allowed better observation of nature therefore decreased exploration risk. In early 21st century, PTT Exploration and Production LCC (PTTEP) entered Myanmar, and they drilled 27 wells more between 2005 and 2013 based on new 3D seismic technology. The Zawtika producing area is one of the most recent discoveries from this exploration campaign (Figure 3).

Today, all 11 shallow-water blocks (M1-M11) have exploration wells drilled in them, whereas the deepwater MD1 to MD3 blocks to the west have yet to be drilled (Figure 3) (Racey and Ridd, 2015). The M1 well is the deepest water depth drilled in to date is 1,003 m in the study area (Figure 3). The other wells, except the well in M8 block, were drilled in between 8 and 200 m water depth. The M8 well is in 500m.

Two exploration wells have been drilled in M11 block area: A1 well (1976) and M1 well (2013) (Figures 4, 5). Although the wells did not result in significant discoveries, the results were key to guiding the next phase of exploration. These two wells focused on the Miocene carbonate play, similar to the Yadana producing field (Figures 1, 3). Today, the area remains underexplored with only 2 wells in 5,300 sq.km.

The objectives of the A1 well were to explore the high structure as carbonate play exploration based on 2D seismic interpretation. Unexpected overpressured sediments were penetrated, resulting in the well being abandoned shallower than the original target. The upper Pliocene section was penetrated, and it consists primarily of shale with low N/G sands and thin siltstones. The poor reservoir quality of clastic reservoirs has been of concern since then.

The M1 well is the most recent exploration well drilled in this area, using the same play concept as A1 well, i.e. to test the carbonate play, based on the interpretation of the 2012 3D-PSTM seismic survey (Figure 6). This zone was dry. A secondary exploration zone of interest was in the lower Pleistocene, which is the same age as the producing reservoir in the Zawtika field to the north (M8 lease block) (Figure 3). However, the gas accumulation was too small to develop economically. Thermogenic gas was found in Pliestocene reservoir, based on C1 – C3 analysis.

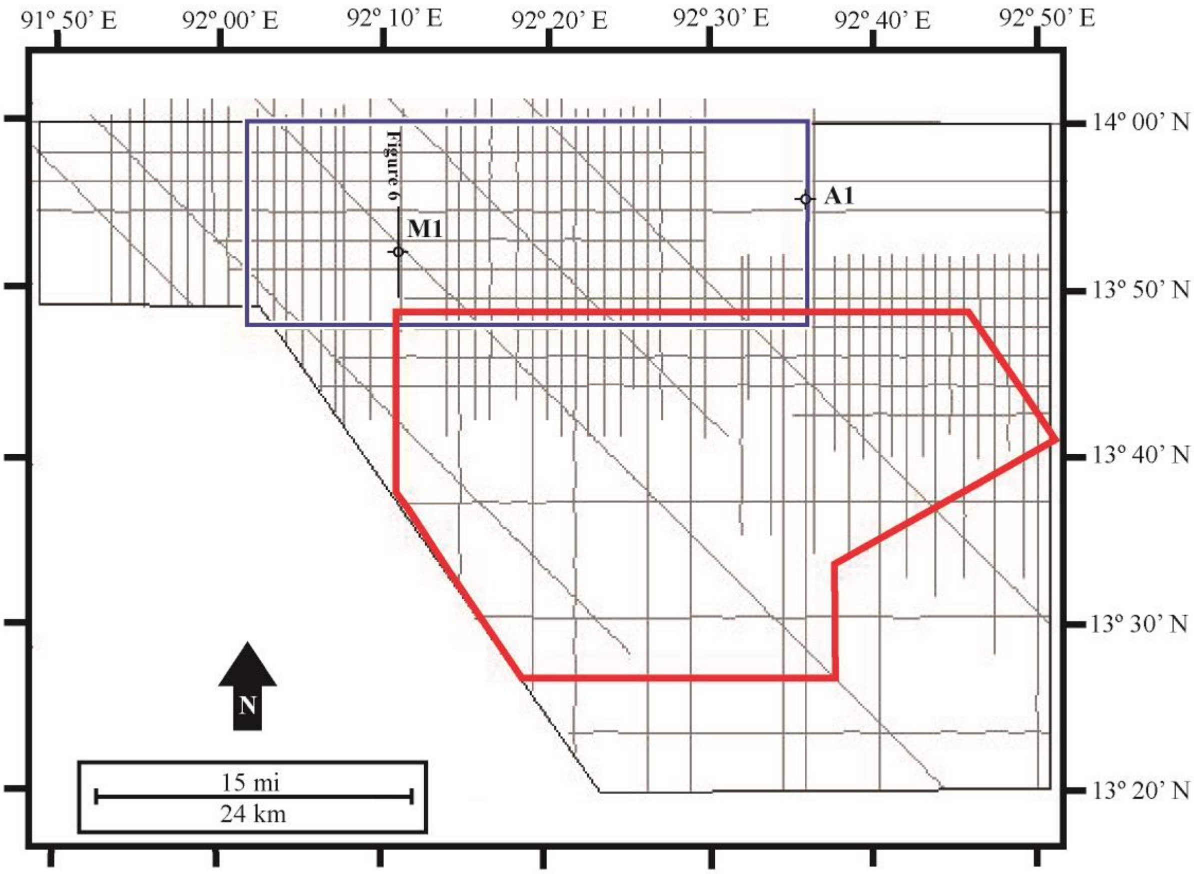

Figure 5: Basemap of M11 area included in black irregular box. The 2012 3D-PSTM seismic survey is outlined by purple boundary, and the 2016 3D-PSTM seismic survey is outlined by red boundary. 2D seismic profiles are shown by black lines. M1 and A1 exploration wells and location of figure 6 are shown.

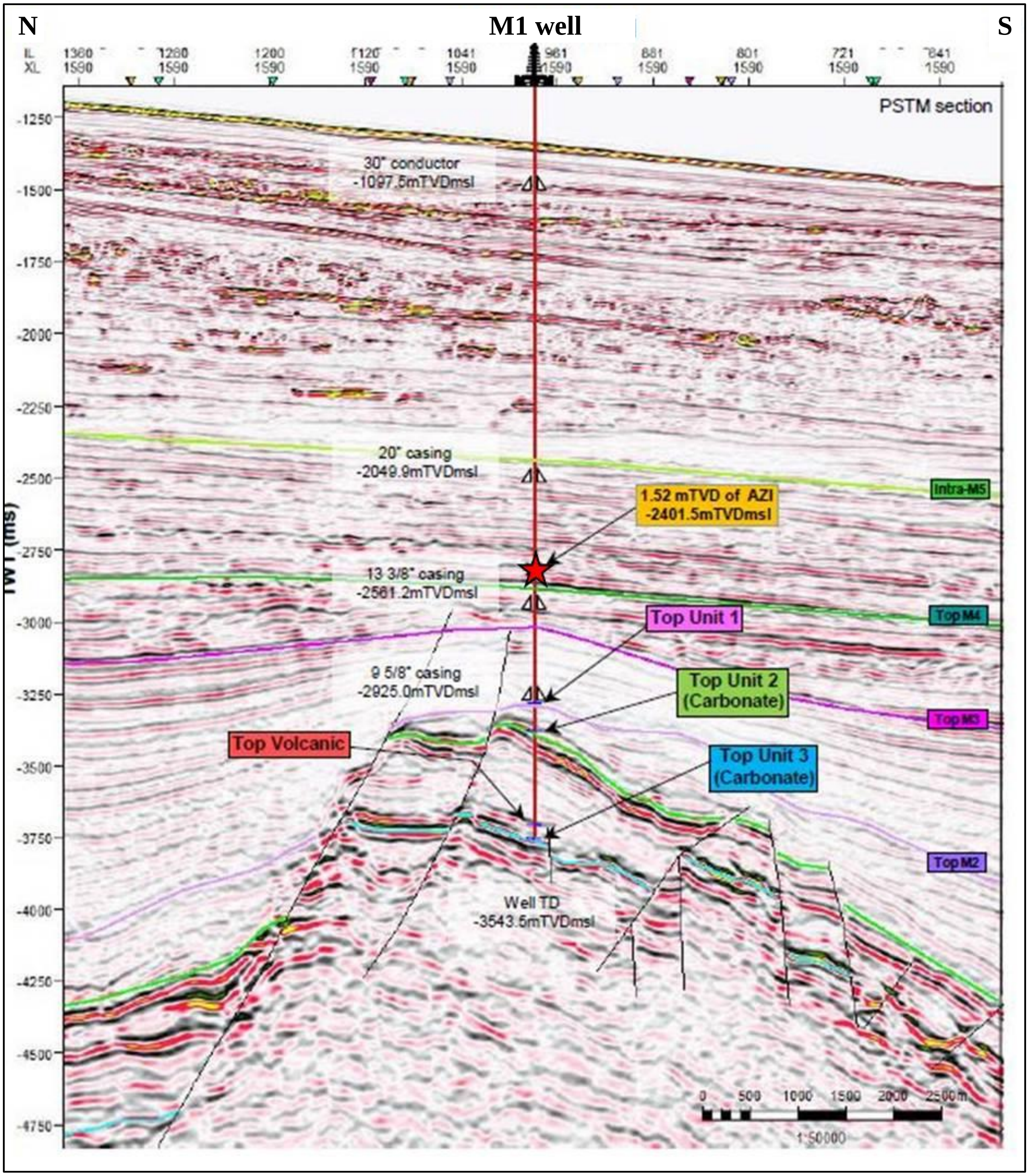

Figure 6: Seismic section along M1 well, part of the 2012 3D-PSTM seismic cube. AZI = Additional Zone of Interest. Red star shows zone of gas shows in Pleistocene. See the location in Figure 5 (PTTEP internal report, 2014).

DATA SET

The seismic reflection data set interpreted in this study consists of 2D seismic information, and 2 cubes of 3D seismic data (Figure 5). All available seismic and well information are provided by PTT Exploration and Production LCC (PTTEP). For the 2D seismic data, there are 41 east-west and 25 north-south profiles, which total 400 km-length. These data are primarily in the northern part of M11 block. The data quality is generally poor, especially in the deeper section; however, the main structures within the basin can be defined.

Both 3D seismic data cubes in this study were analyzed. They consist of pre-stack time migration with peak zero-phase appearance, representing positive reflection coefficients (RC). The 2012 3D-PSTM seismic covers 1,230 km^2, and 8 seconds TWTT of moderate to high quality. The recent M1 exploration well, is located in this seismic cube, so the well results can be integrated into the seismic data.

The primary seismic reflection data cube interpreted in this study is 2016 3D-PSTM. The cube covers 2,261 km^2, and 8.1 second TWTT (approximately 4800 m) with moderate to high reflection quality. The data were processed by CGG Services (Singapore) in 2016. The survey data is 12.5 x 12.5 m bin size and 81 fold coverage. The inline direction is 145-325 degrees perpendicular with crossline direction. Additional acquisition and processing parameters are listed in Table 1.

Exploration well data are available only for M1 well, consisting of wireline logs, mudlog data and biostratigraphic report (Figures 5, 7). The wireline data include gamma-ray, resistivity, sonic, porosity, and density logs. A checkshot velocity survey was also available. A biostratigraphic report for the M1 well summarizes the ages of each key surface marker (Figure 7). The biostratigrahic analyses include palynology, foraminifera (both planktonic, benthonic),

Survey Definition	
Survey Orientation	NW-SE
Line Orientation	145 / 325
Number of primes lines	146
Water depths	200 to 2000 m
Source	
Number of sources	2
Volume	3480 cubic inches
Nominal source depth	6 m
Shot point interval	25 m flip-flop
Source	Air gun arrays 50 m apart
Streamers	
Number of stremers	12
Streamer active length	8100 m
Streamer seperation	100 m
Number of groups per streamer	648
Group Interval	12.5 m
Streamer depth	18 - 30 m Salnt
Recording System	
Sample rate	2 ms
Recording length (ms)	8200 ms
Low cut filter	2 Hz@6dB/Octave - 200 Hz@370dB/Octave
Fold coverage of data	81
Recording time delay	-200 ms
Offset	
Near channel inline offset	176 m
Far channel inline offset	8250 m
Processing Parameter	
Processing Length	8000 ms
Processing sample rate	2 ms
Final Bin Size	12.5 x 12.5 m
Datum Plane	Mean Sea Level (MSL)
Low frequency filtering	2.5 Hz
Phase Conversion	Zero Phase with Normal SEG polarity
Offset	250 - 8250 m
Demultiple 1	3D SRME
Demultiple 2	High resolution Radon demultiple
PSTM (Pre-Stack)	Using Tomographic velocity function
Demultiple 3	High resolution Radon demultiple
Stacking	Denoise and Trim statics
Acquisition Footprint removal	Crossline direction smoothing of 600 m

Table 1: Summary of the acquisition and processing parameters of 2016 3D-PSTM seismic data. (adapted from CGG final processing report, 2016)

(A)

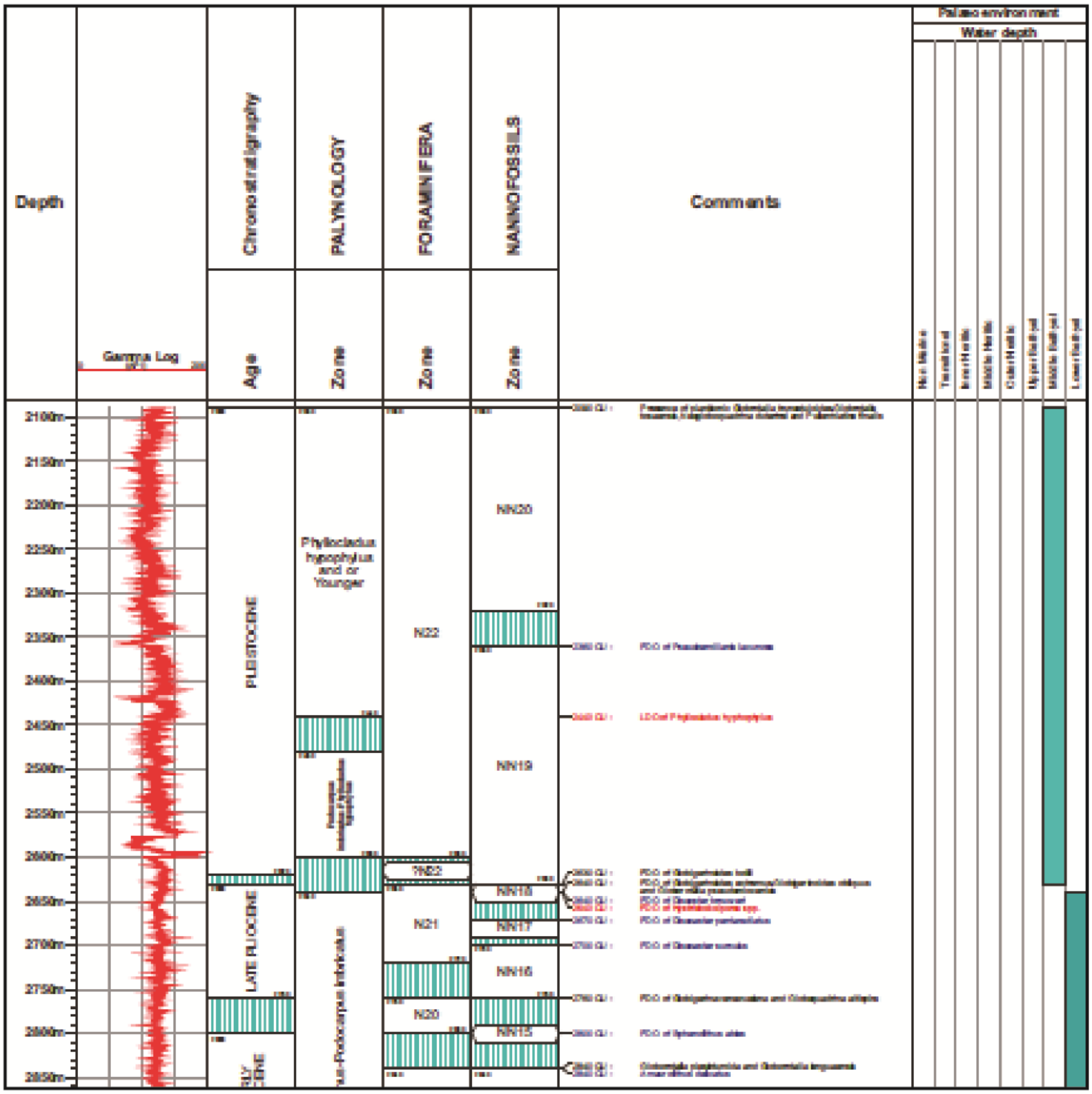

Figure 7: Biostratigraphic summary of M1 well in the study area. **(A)** and **(B)** The chronology is a composite of foraminifers, calcareous nanofossils and palynology show with a gamma-ray curve. The paleoenvironment of water depth interpretation in each zone is included as shown in numbers. The relative sea level change is interpreted. **(C)** and **(D)** The relative distribution of forams of each biozone are shown. (Modified from PTTEP internal report, 2013)

(B)

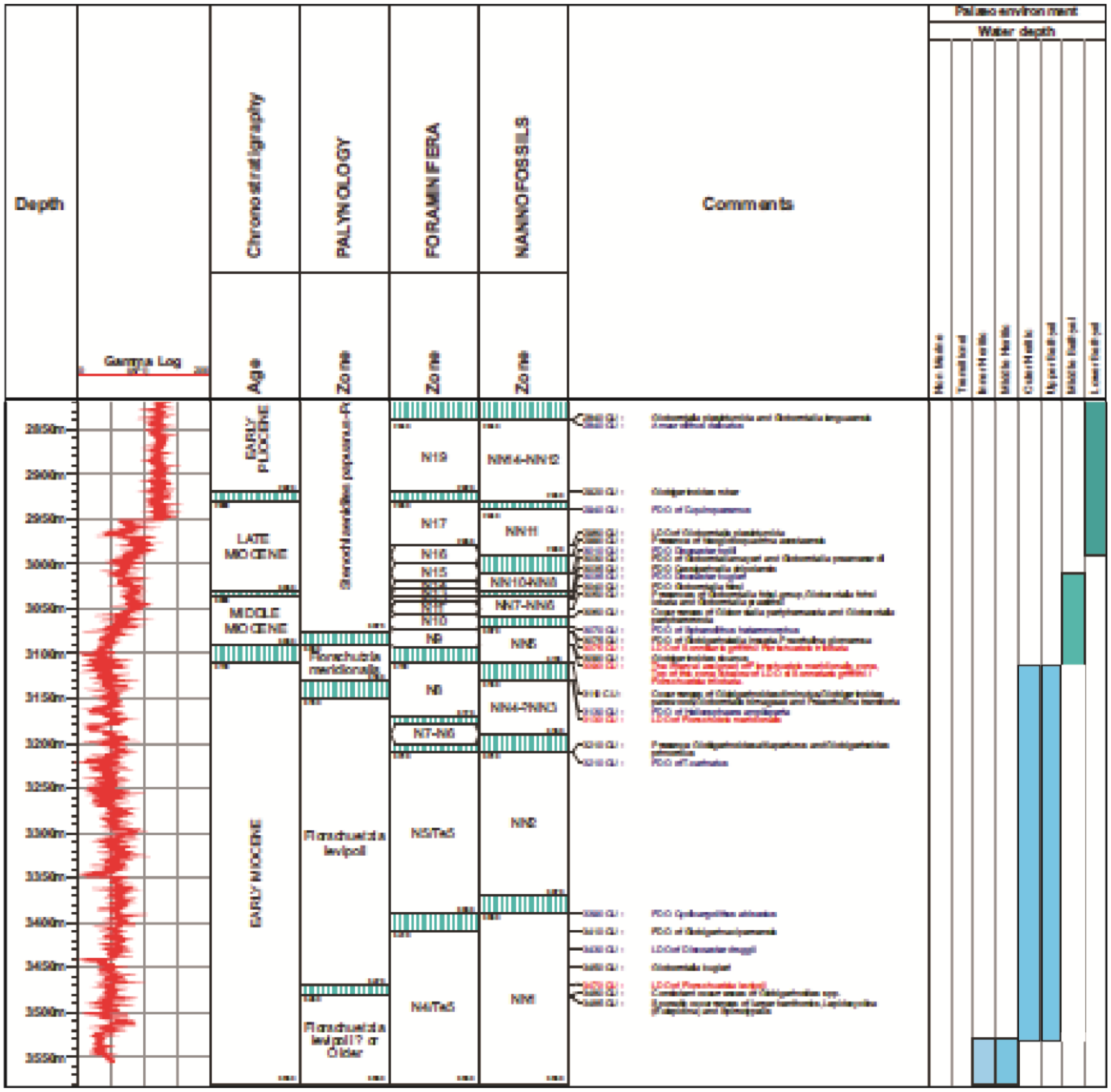

Depth
Gamma Log
Chronostratigraphy
Age
PALYNOLOGY
Zone
FORAMINIFERA
Zone
NANNOFOSSILS
Zone
Comments
Palaeo environment
Water depth
EARLY PLIOCENE
LATE MIOCENE
MIDDLE MIOCENE
EARLY MIOCENE
N19
N17
N16
N15
N10
N9
N8
N7-N6
N5/Te5
N4/Te5
NN14-NN12
NN11
NN10-NN8
NN7-NN6
NN5
NN4-?NN3
NN2
NN1
Floraschuetzia levipoli

(C)

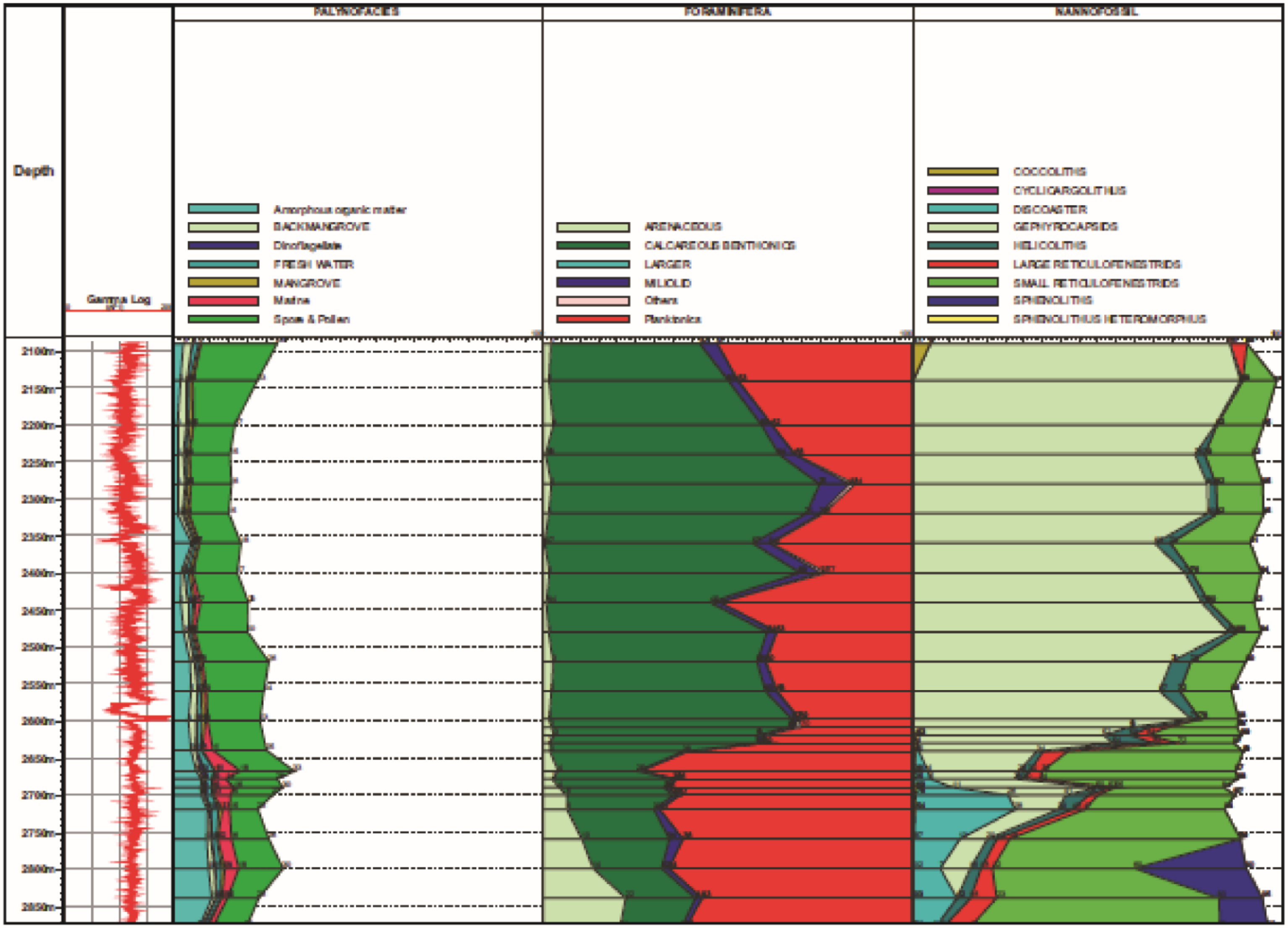

Depth
Gamma Log
PALYNOFACIES
FORAMINIFERA
NANNOFOSSIL
Amorphous organic matter
BACKMANGROVE
Dinoflagellate
FRESH WATER
MANGROVE
Marine
Spore & Pollen
ARENACEOUS
CALCAREOUS BENTHONICS
LARGER
MILIOLID
Others
Planktonics
COCCOLITHS
CYCLICARGOLITHUS
DISCOASTER
GEPHYROCAPSIDS
HELICOLITHS
LARGE RETICULOFENESTRIDS
SMALL RETICULOFENESTRIDS
SPHENOLITHS
SPHENOLITHUS HETEROMORPHUS
2100m
2150m
2200m
2250m
2300m
2350m
2400m
2450m
2500m
2550m
2600m
2650m
2700m
2750m
2800m
2850m

(D)

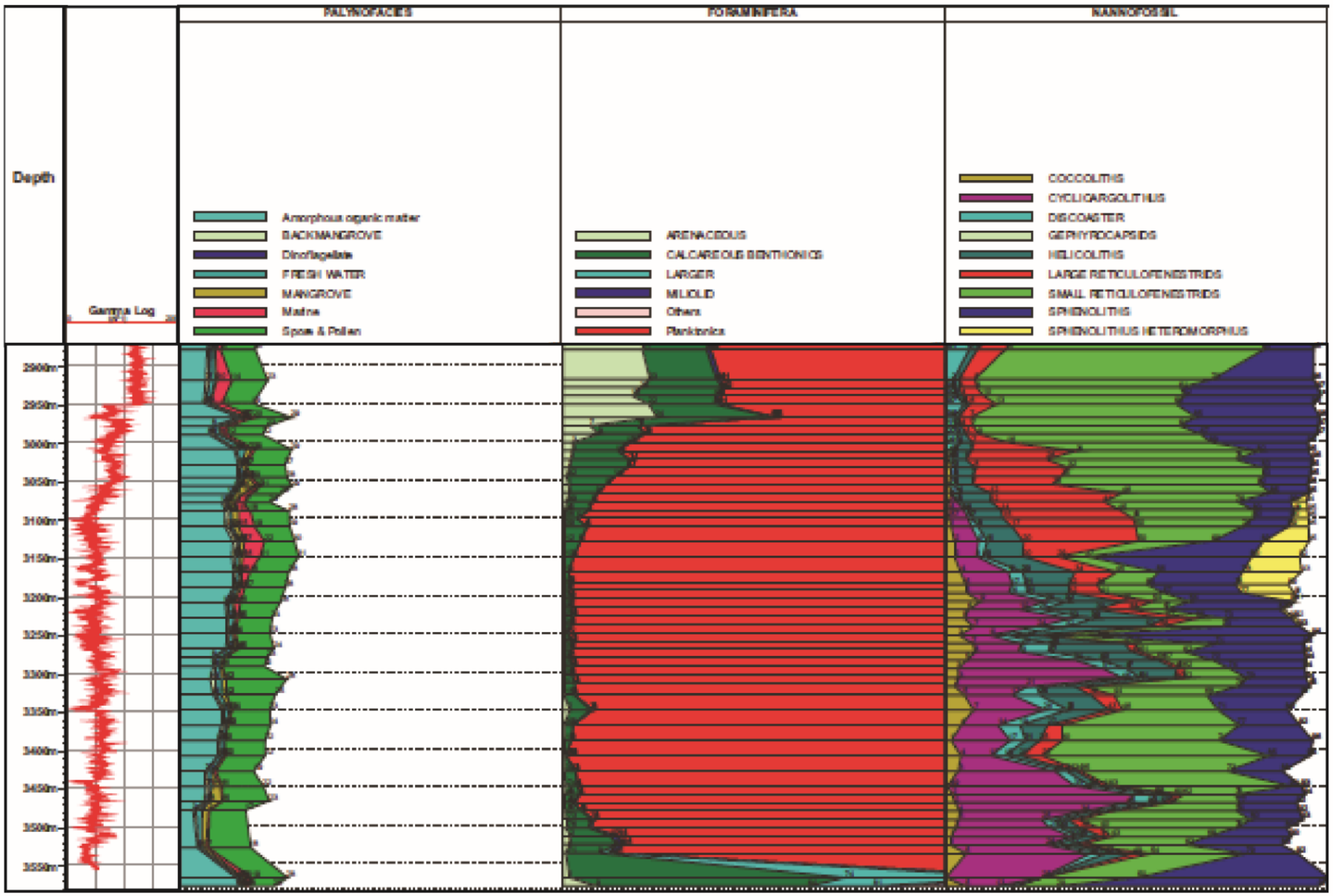

Depth
Gamma Log
PALYNOFACIES
Amorphous organic matter
BACKMANGROVE
Dinoflagellate
FRESH WATER
MANGROVE
Marine
Spore & Pollen
FORAMINIFERA
ARENACEOUS
CALCAREOUS BENTHONICS
LARGER
MILIOLID
Others
Planktonics
NANNOFOSSIL
COCCOLITHS
CYCLICARGOLITHUS
DISCOASTER
GEPHYROCAPSIDS
HELICOLITHS
LARGE RETICULOFENESTRIDS
SMALL RETICULOFENESTRIDS
SPHENOLITHS
SPHENOLITHUS HETEROMORPHUS
2900m
2950m
3000m
3050m
3100m
3150m
3200m
3250m
3300m
3350m
3400m
3450m
3500m
3550m

and calcareous nanoplankton. The biozones are shown for each taxonomic group. In addition, the relative age including of different taxa are shown in each bio group. However, one significant short coming to the report is the exact knowledge of the precise drill depths from which the cuttings were collected, because cuttings come within the circulated drilling mud.

The depositional environments and relative water depths were interpreted based on benthic foraminifera (Figure 7). Five paleoecologic zones were recognized. Overall, the upward change in paleo-ecologic zone present in the well, which represents the shallow marine carbonates, being flooded and subsiding into increasing water depths from inner to outer neritic, and lower bathyal. The shallowing near the top represents prograding of trending (Figure 7).

METHODOLOGY

The seismic data were analyzed and interpreted using IHS Kingdom, CGG InsightEarth, and Petrel E&P interpretation software packages. Significant stratigraphic surfaces were picked in IHS based on stratal terminations and were then correlated throughout the whole 2016 3D-PSTM seismic cube. In addition, some horizons were correlated into 2012 3D-PSTM seismic cube to the M1 well, where their ages of the key surfaces were established (Figure 5, 6). In total, eight megasequences were identified extending from middle (?) Miocene to the Pliocene.

The synthetic seismogram for the well was generated so that the well data (depth domain) would be tied to the seismic reflection data (time domain). Density and sonic logs were used to generate the synthetic seismogram. Once the synthetic seismogram was tied to the seismic data, then key surfaces that were identified on the seismic were tied to gamma-ray log.

Time-structure and isochron (time-thickness) maps were generated from the interpreted key surfaces to evaluate structural trends and sub-regional variations in stratigraphic thickness of each megasequence. The stacking patterns and changes in thicknesses within each megasequence have significant impact on the potential for and distribution of hydrocarbon-bearing reservoir presence.

Seismic facies maps were generated for each megasequence from the integration of the 2016 3D-PSTM seismic reflection observation and seismic reflection attributes. These maps show the spatial distribution of seismic reflections based on changes in configuration, continuity, and amplitude within the megasequence. The results were integrated with the other information to interpret the sedimentary facies.

To aid in the interpretation of seismic reflection data, particularly their lateral continuity and integrity, plots of seismic attributes were produced from the stacked seismic data (Pugin et al., 1999). Two types of seismic reflection attributes were calculated: instantaneous phase and instantaneous amplitude (or called Envelope). The instantaneous phase seismic attribute is a measure of the continuity of reflection event (Pugin et al., 1999) referring to the configuration and the continuity of seismic facies information. The instantaneous amplitude or envelope seismic attribute is measures the reflectivity strength (Pugin et al., 1999) directly showing the amplitude, part of seismic facies analysis.

The sweetness seismic attribute can be very useful for channel detection in deep-water siliclastic settings. Sweetness is derived by dividing reflection strength by the square root of instantaneous frequency, an approach first described by Radovich and Oliveros, (1998). Using this attribute, sandy intervals within shales, such as channel fills, are characterized by higher amplitude (Li et al., 2017). In addition, the coherency seismic attribute is used to distinguish structural and stratigraphic features. The sweetness and coherency attributes were used together to interpret the stratigraphy feature. By themselves, they can help to distinguish structural from stratigraphic features.

The interpretation of depositional environments was also supported from CGG InsightEarth, Stratal Transformation Calculation. The method builds the stratigraphic framework and makes the calculation of each horizon flattering to connect the horizon together. The final geological interpretation of the depositional environment was summarized based on the facies maps as well as the seismic reflection attribute analysis i.e. sweetness and coherency attributes.

REGIONAL SETTING

The M11 study area is part of a complex regional tectonic in the Martaban basin in offshore Myanmar. The structural evolution of this back-arc basin affected the evolution of the stratigraphic successions.

Regional Tectonics

Myanmar is located on the eastern edge of the zone of Himalayan convergence (Figures 8A, 9) between the Indian plate and the Burma microplate, part of the Eurasian plate (Figure 8B) (Pivnik et al., 1998). The Indian plate is subducted at a highly oblique angle, moving to the NE (Figures 8C, 9). The mountain ranges, basins, and major N-S strike-slip faults developed along the central part of the country, associated with the oblique subduction (Figures 8B, 9). The Martaban basin is one of them.

The offshore Martaban basin developed in three major phases since the late Oligocene (Figures 10, 11). A N-S rift basin developed during the late Oligocene, as the result of the plate subduction and the rotation of the Burma microplates (Figure 10A). During the middle Miocene, an extensional NE-SW growth structure formed controlled by the dextral strike-slip fault (Figure 10B). The fault has had continuous movement since then (Figures 10C, 10D). By the middle to late Miocene, the thickness of syn-rift deltaic sediments, which were derived from the north had increased markedly, causing the growth faults to develop (Figures 8, 9, 10, 11) (Racey and Ridd, 2015). During the Pleistocene, the final phase of deformation was associated with transpressional structures that were creating by NW striking thrust faults (Figure 10D).

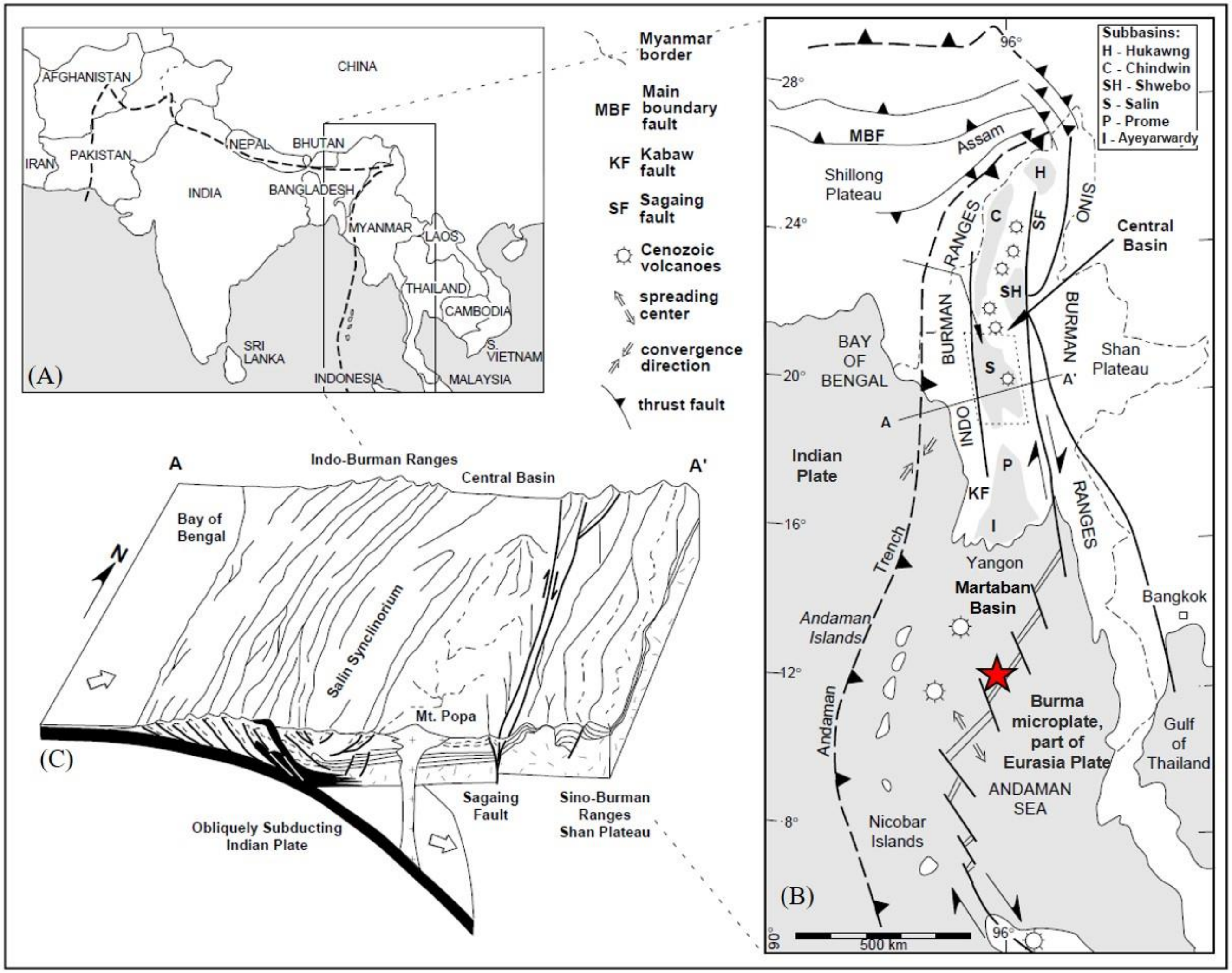

Figure 8: (A) Location of Myanmar in larger Southern Asia with tectonic schematic, which is part of Himalayan orogeny in Cenozoic is shown as the dash-line. **(B)** Map showing main structural features and onshore sub-basins. Approximate location of the study area is shown by red star. **(C)** Schematic diagram showing the oblique subduction of the Indian plate along Myanmar margin (modified from Pivnik et, al., 1998).

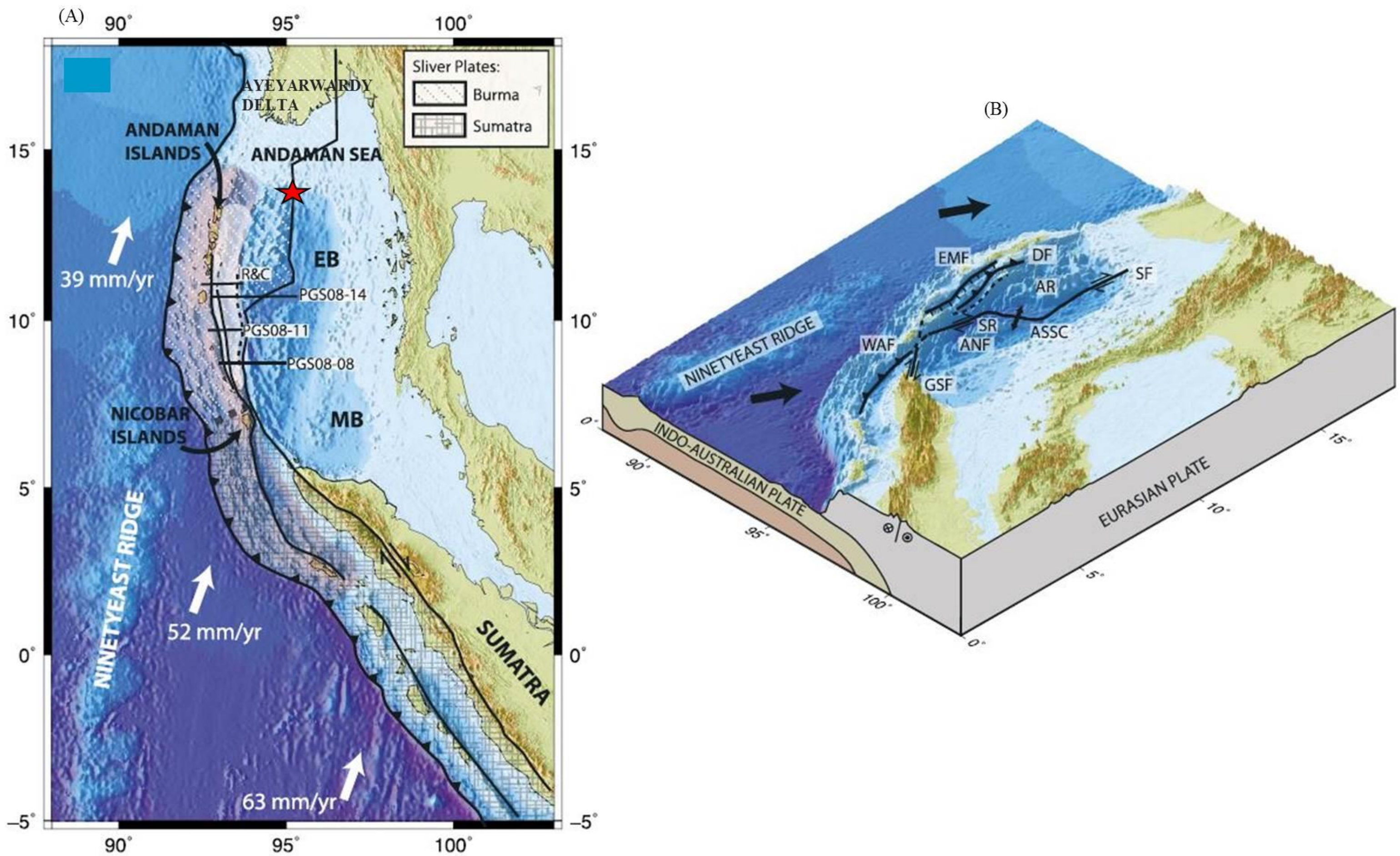

Figure 9: Topography and bathymetry maps of Myanmar and surrounding area. **(A)** Tectonic setting at offshore Myanmar, showing the oblique subduction (white arrow) with rate of movement, strike slip fault as right-lateral, the fore-arc basin as the white shade close to Andaman Island, and Back arc basins as EB = Martaban basin and MB = Mergui basin. The blue color set is representing the modern bathymetric map of this offshore area. Approximate location of the study area is shown by red star. **(B)** Block diagram of tectonic setting, note that AR = Alcock Rise, ASSC = Andaman Sea Spreading Center, GSF = Great Sumatra Fault, and SF = Sagaing Fault (modified from Moeremans and Singh, 2015).

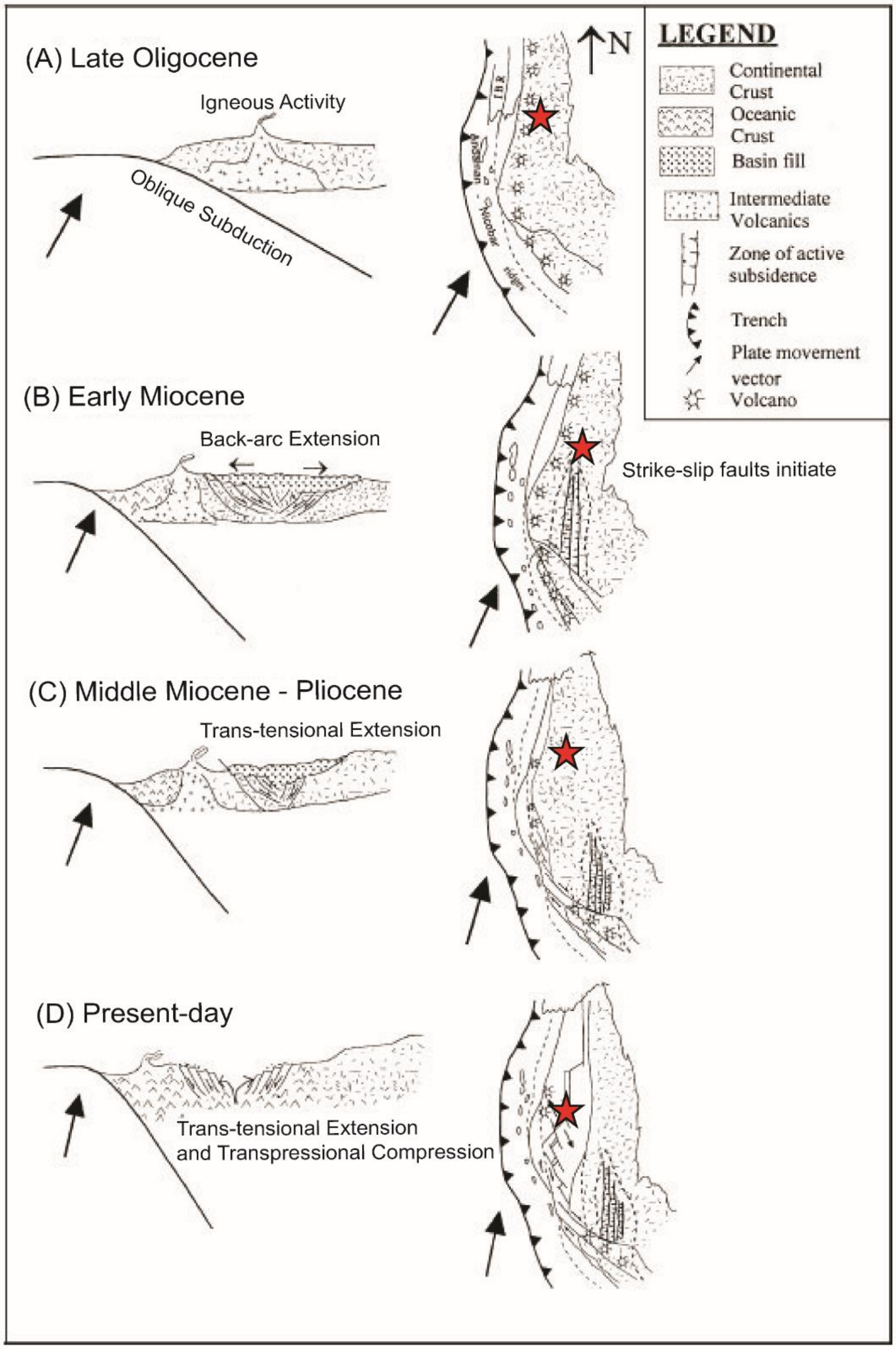

Figure 10: Schematic representation of sequential tectonic evolution of Andaman Sea including Martaban basin. Approximate location of the study area is shown by red star (modified from Khan and Chakraborty, 2005).

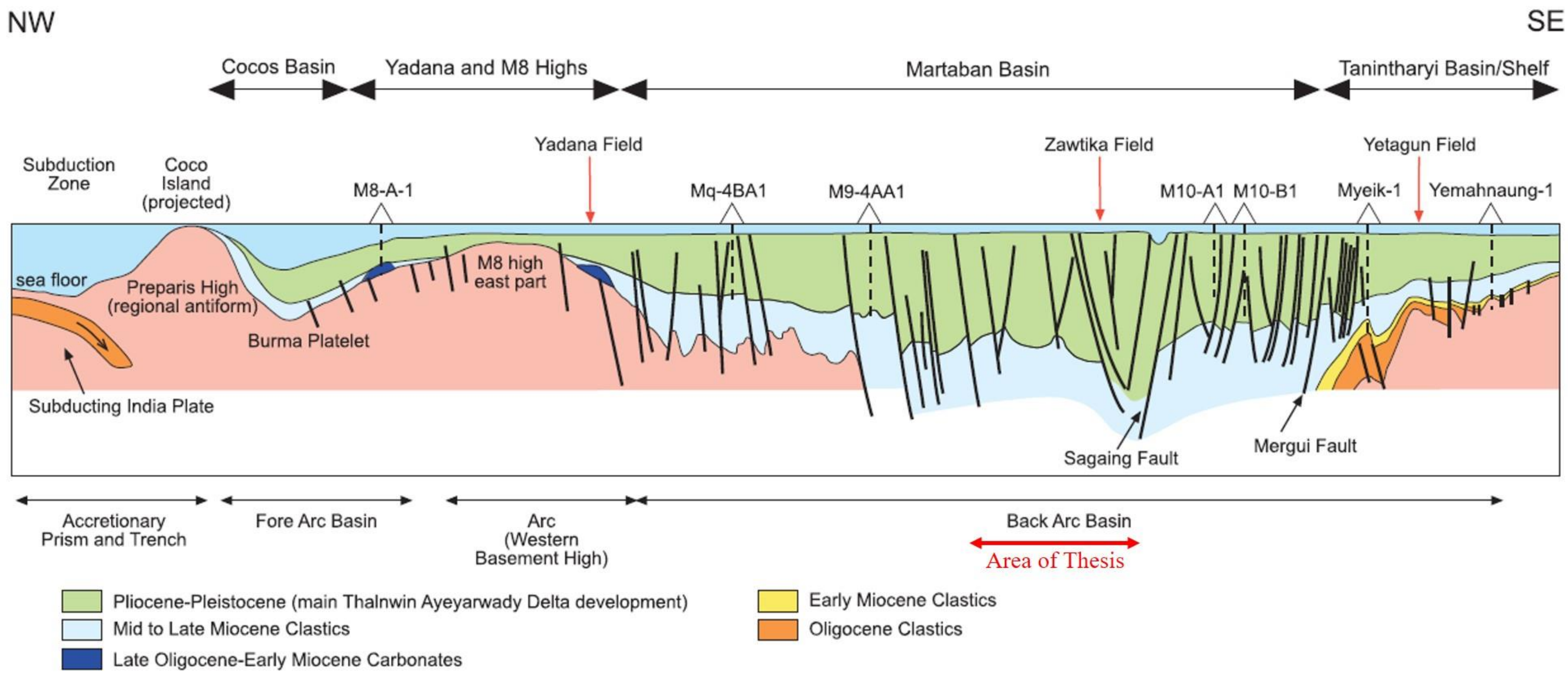

Figure 11: Regional cross-section from subduction zone (NW) to back arc basins and area of thesis, including Martaban basin to Tanintharyi basin/shelf. Sagaing and Mergui faults are two major strike-slip faults. Stratigraphy is shown color data. Main producing fields – Yadana, Zawtika, Yetagun - are also projected on this section. See Figure 1 and 3 for location of profile (modified from Racey and Ridd, 2015).

Regional Stratigraphy

The Neogene sedimentary fill of the Martaban basin ranges from 3 to 7 km in thickness (Figure 3, 5, 11, 12) (Moeremans and Singh, 2015). The thickness patterns trend north-south, and are largely controlled by the regional structural trends, which are tectonically controlled.

Basement in the western Martaban basin is believed to comprise Eocene or possibly Cretaceous volcanic rocks or accretionary complex strata (Figure 12). The overlying strata are relatively thin, compared to the other parts of the basin. To the east (east of the Sagaing Fault) in the Tanintharyi Shelf area, Mesozoic–Palaeogene granite and older meta-sediments form the basement (Figure 12). In the central part of the basin where the sedimentary package is thickest (7 km), basement rocks are considered to be Oligocene marine shale, although the oldest sediments penetrated to date are late Miocene (Figure 12) (Racey and Ridd, 2015). This area is heavily faulted and has the most subsidence.

During the first stage of the basin evolution (late Oligocene to early Miocene), the area had two depositional systems (Figures 11, 12). Carbonate platform was present to the west, overlying the volcanic basement (Racey and Ridd, 2015). In the central and eastern part of the Martaban basin, a siliciclastic succession was deposited (Figures 11, 12). These deposits thinned eastward onto the Tanintheryi shelf covering the matasediments (Figure 12). The source of siliciclastic sediments changed through time. Sediment input was mainly from the east during late Oligocene.

During the middle Miocene, the clastic sediments came from the NE and NNE, and the north from late Miocene to present. The late Miocene to recent phase of sediment input resulted in the thickest part of the basin succession, with sandstones and mudstones derived from the delta system prograding southwards (Racey and Ridd, 2015).

The back-arc setting of the Martaban Basin is a pull-apart basin resulting from middle

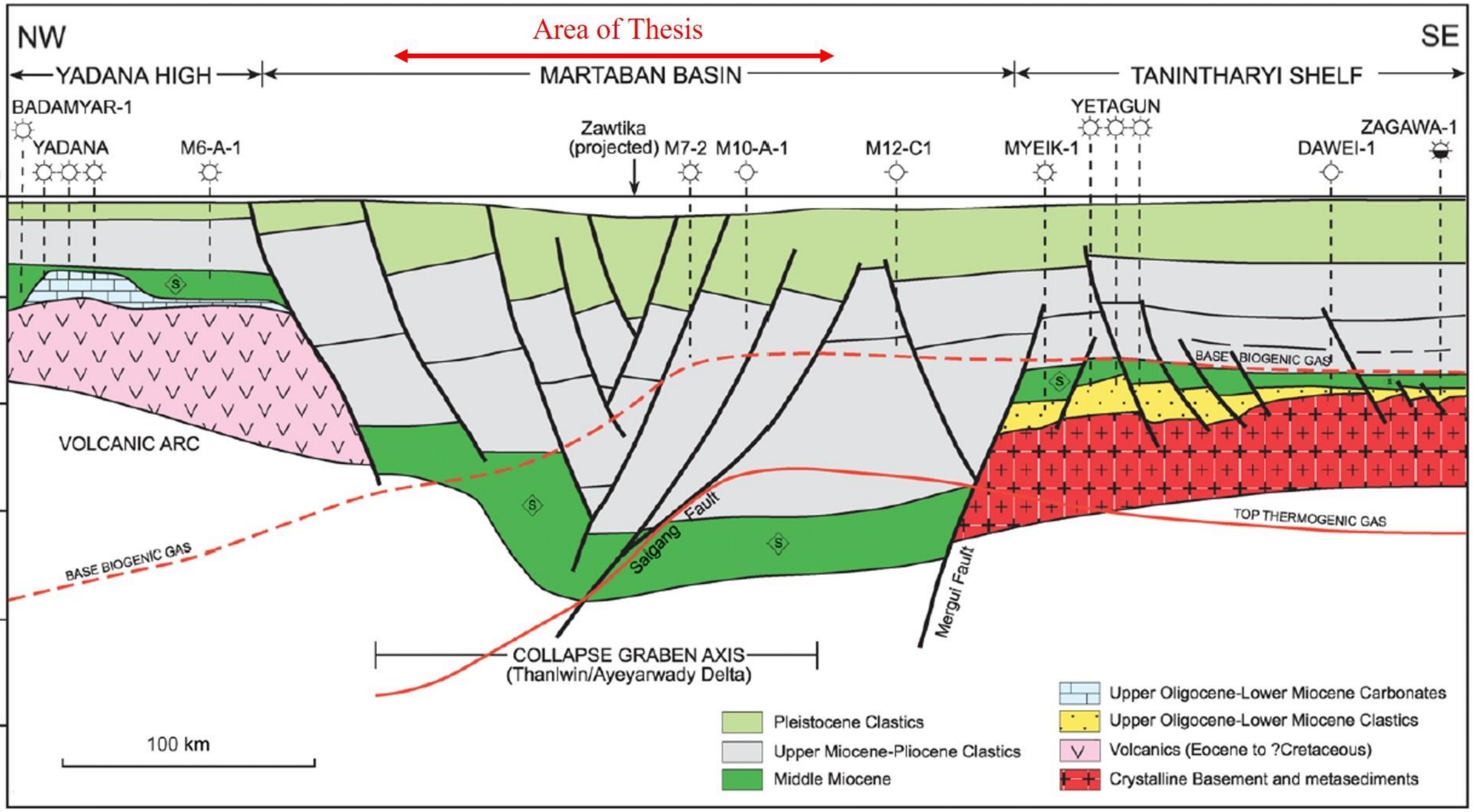

Figure 12: Cross-section across Martaban basin - from Yadana High, the depocenter of Martaban basin and Tanintharyi shelf. Strata differ in thickness each area due to different rates of accommodation, the sedimentary supply through time, and the underlying basement lithology. The structure is aligning with figure 11 as mostly about the extensional faulting system with the relationship with strike-slip faults. See Figure 1 and 3 for location of profile (After Racey and Ridd, 2015).

Miocene to Present NW–SE extension (Racey and Ridd, 2015). This extension generates major accommodation, and a complex geography from shelf through deep water during that period (Figure 10). Because of this tectonic alignment and the location of sediment source areas, sediment gravity flows moving through channel pathways of submarine canyons are the main sediments deposited in the area.

Study Area Setting

The study area, M11 block part of the Martaban Basin, is in water depth of 600 to 2,000 meters (0.8 to 2.6 seconds) (Figure 13). Overall, the seafloor dips from north to south. The shallowest part is located to the NE of the area near the modern outer shelf. The seafloor has several erosional re-entrants on the slope (Figures 13, 14), and a prominent sinuous channel is presented along the western part of the study area. These erosional and depositional channels imaged from amplitude extraction map of the seafloor (Figure 14), are aligned with the bathymetry of the seafloor time map.

Three structural zones were identified in the focusing succession in this area; (1) high structure zone, (2) extensional zone, and (3) compressional zone (Figure 15). Estimated boundaries of these zones were interpreted based on the integration of interpreted seismic sections (Figures 16 - 19) and the time slice map in middle Miocene - Pliocene section at 4.6 seconds time (Figure 15A).

The first zone, a structural high area along the western edge of the area, is recognized by the regional onlap of the relatively undeformed upper Miocene to lower Pliocene horizons onto early Miocene carbonate (Figure 16). This interpreted high area is on regional structural trend with the Yadana and Yetagun production areas (Figure 3) and the one well exploration drilled in M11 block (Figures 5, 6).

The central portion of the area consists of extensional faults at two levels (Figures 16 - 18). The older normal faults cut the lower to middle Miocene strata coeval to the carbonate build-up (Figures 16, 17). A shallower zone of normal faults cut upper Miocene to Pliocene-Pleistocene strata and detach on top of the deeper faults zone (Figures 16 - 18). These normal faults have deformed since late Miocene. Moreover, the producing Zawtika gas field is along the

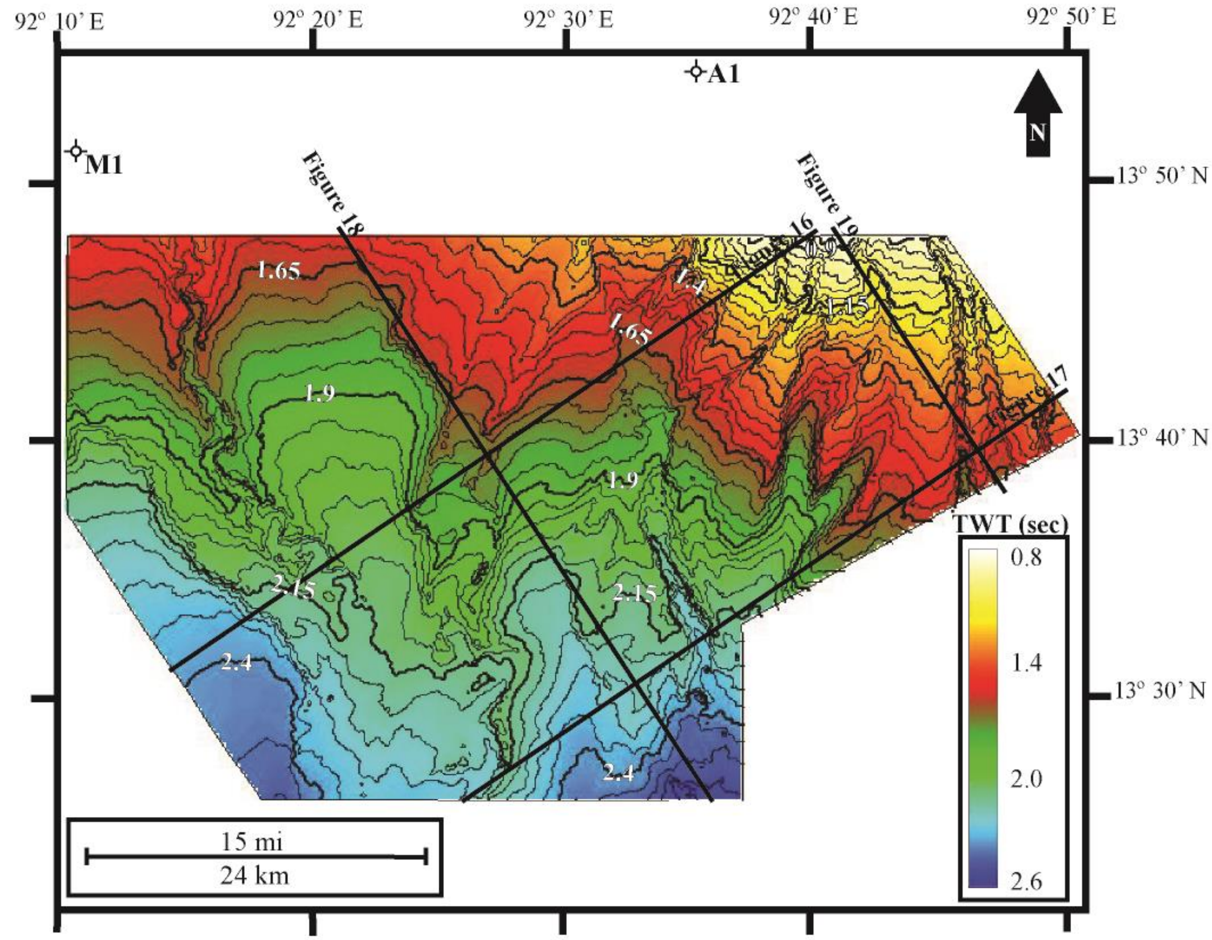

Figure 13: Seafloor time structure map (TWT). Contour interval is 50 milliseconds. The surface is dipping from north to south direction with the submarine canyon features.

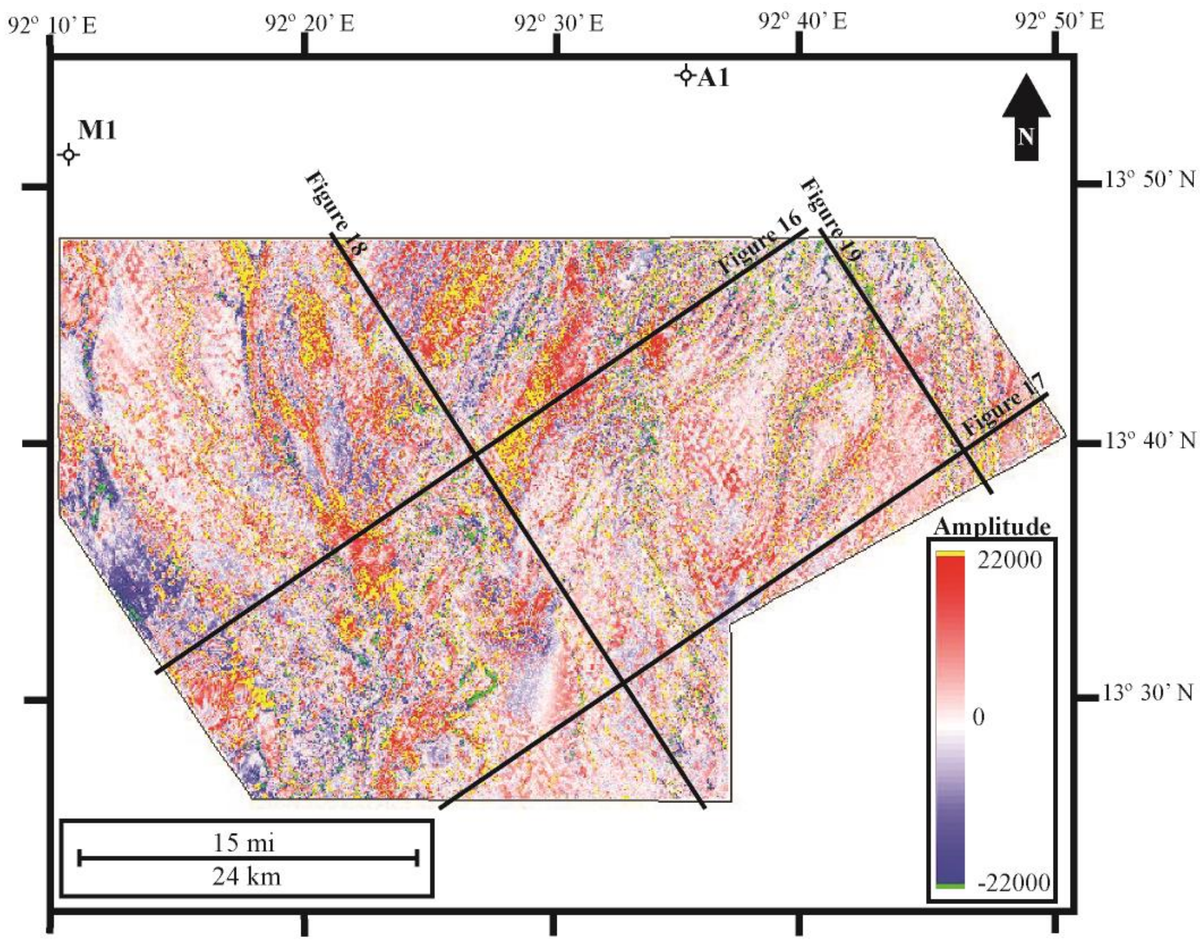

Figure 14: Seafloor amplitude extraction map (horizon slice). This was processed 10 milliseconds below the horizon.

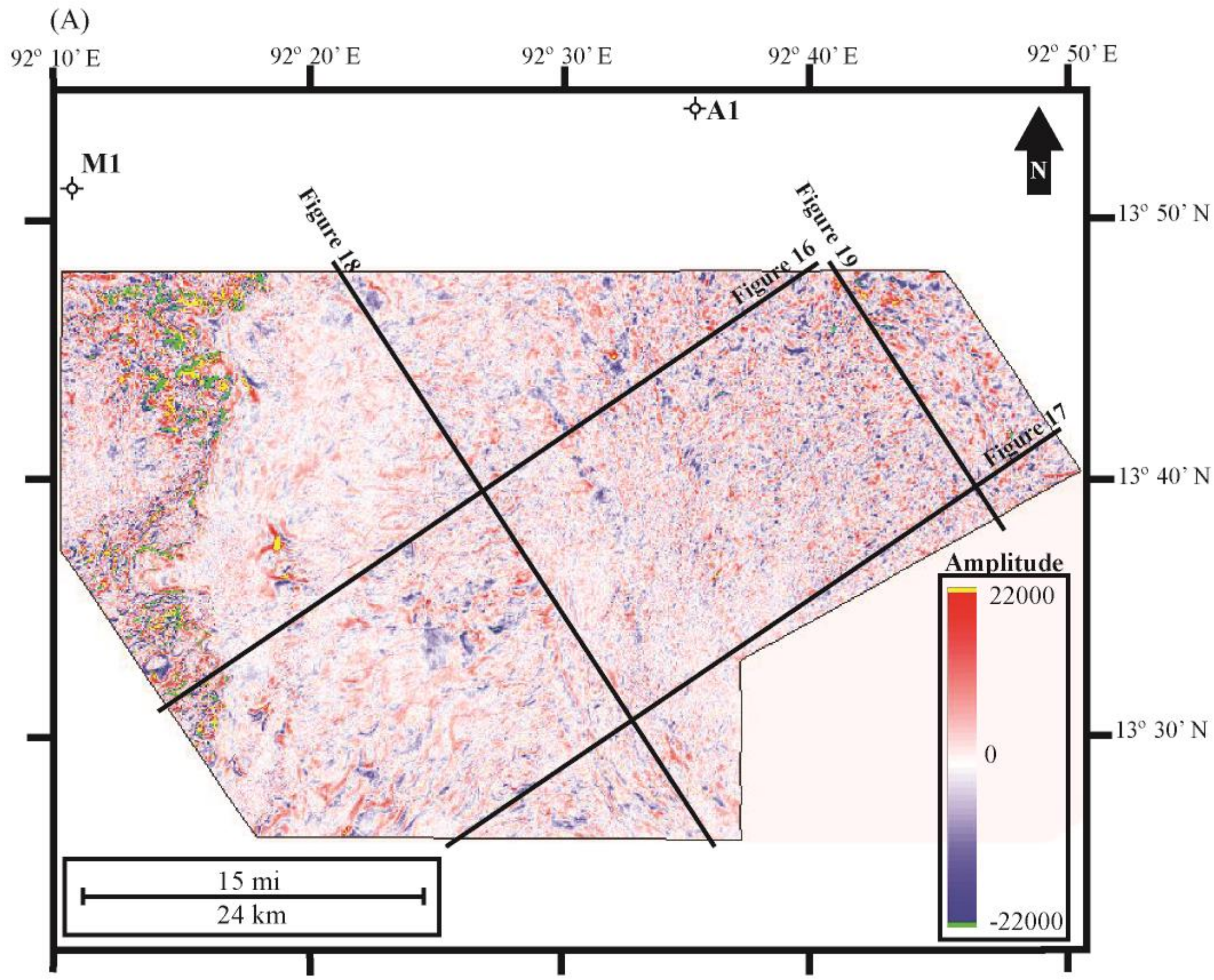

Figure 15: (A) Time slice map (Amplitude) at 4.6 seconds TWTT across the focusing stratigraphic study in middle Miocene to Pliocene section. Three structural zones are posted to Figures 16 – 19.

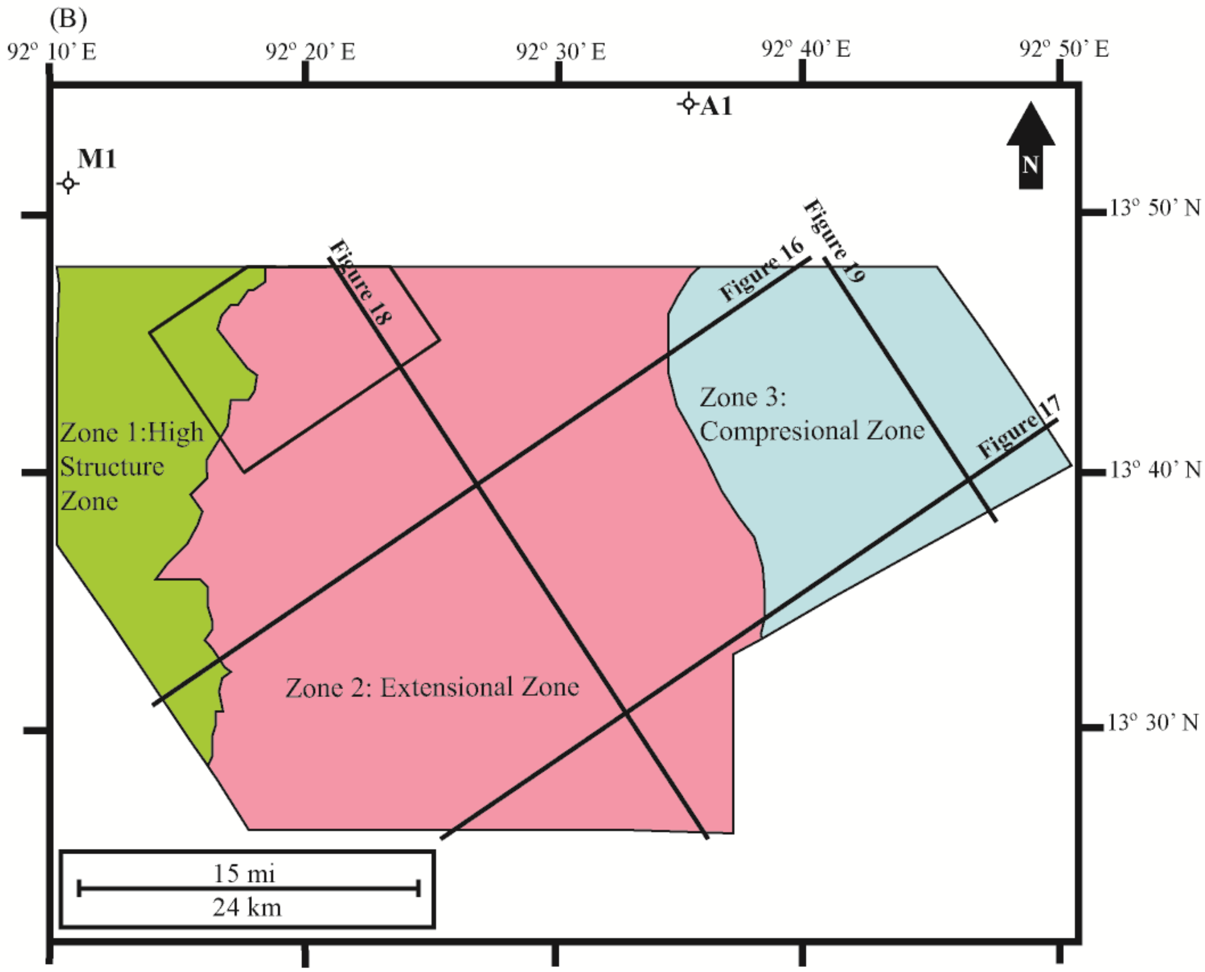

Figure 15: (B) The overall structure zone of the study area at around 4.6 seconds, which is main interval of this study. Three structural zones are presented; (1) High Structure zone, (2) Extensional zone, and (3) Compressional zone. The black area is the boundary of specific study area of geological interpretation.

(A)

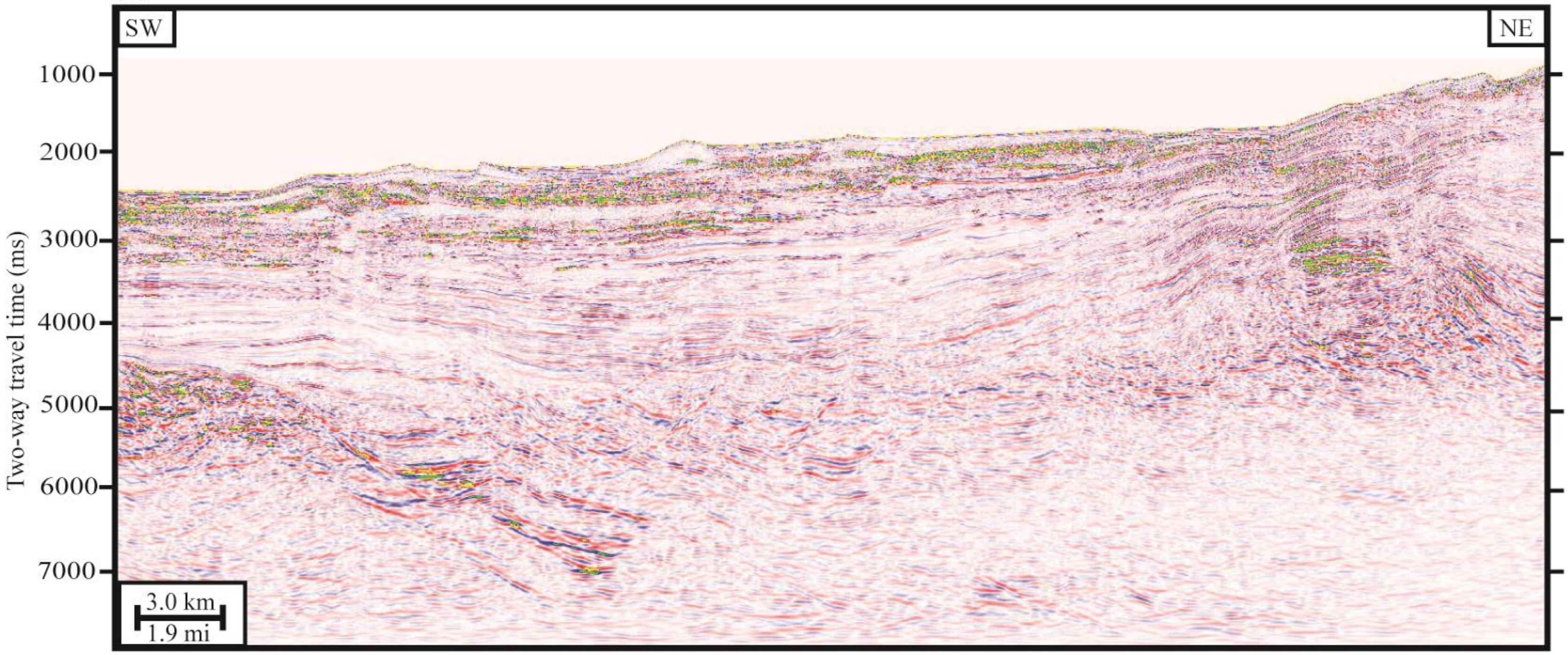

Figure 16: (A) Uninterpreted regional seismic section strike-line number 4500 from the 2016 3D-PSTM. Location of this seismic section is shown in Figures 13, 14 and 15.

(B)

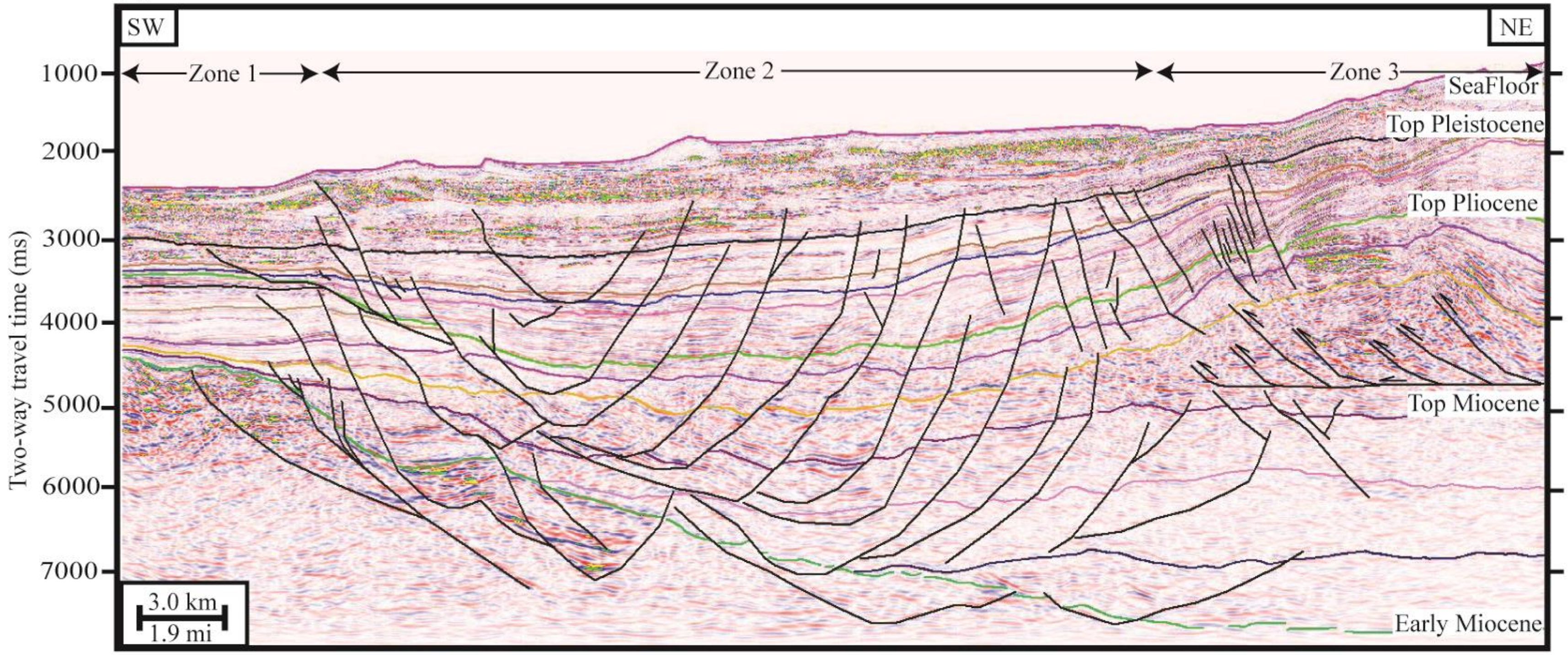

Figure 16: (B) Interpretation of regional seismic section presenting the strike line of extensional faults and the dip line of compressional faults, across structural zones 1 to 3. The fault presented as black line. The thrust fault marked specifically as the black one-side arrow. The color lines interpreted to stratigraphic horizon.
Location of this seismic section is shown in Figures 13, 14, and 15.

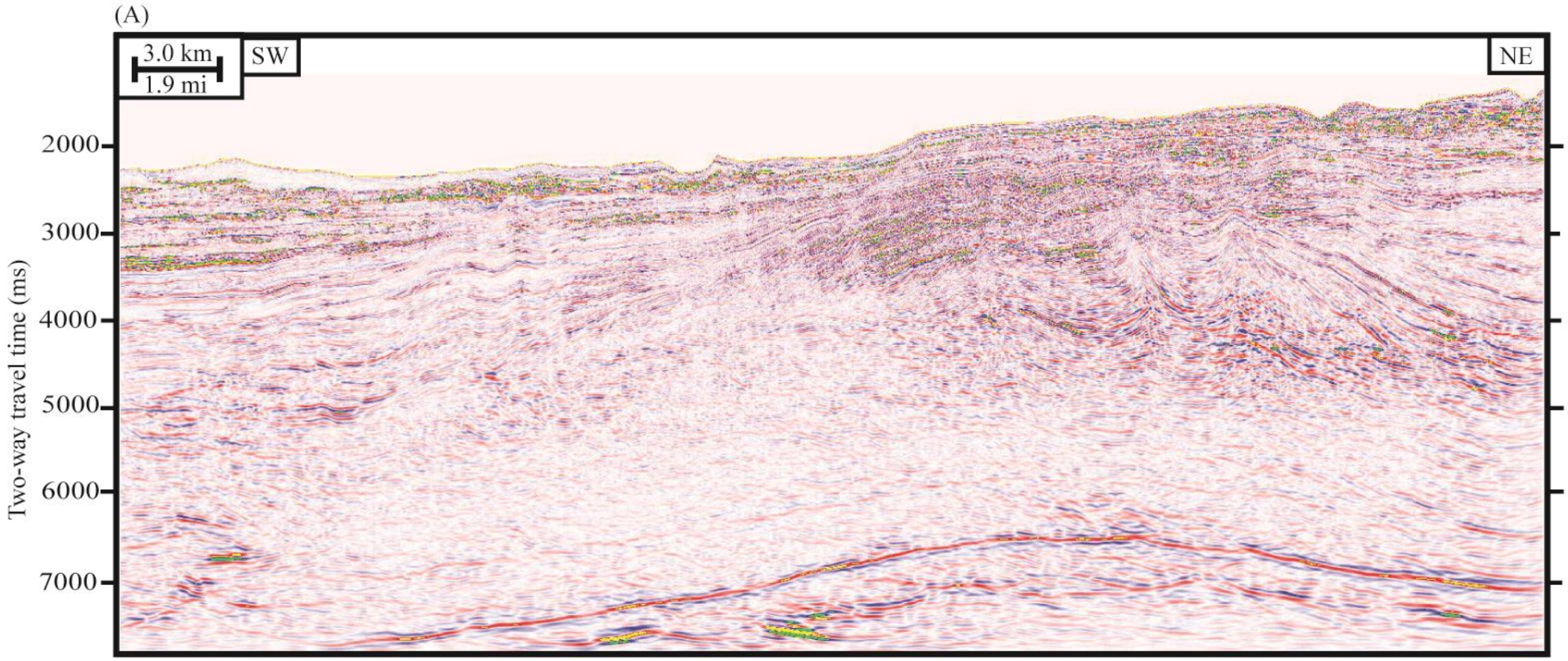

Figure 17: (A) Uninterpreted regional seismic section strike-line number 2900 from the 2016 3D-PSTM. Location of this seismic section is shown in Figures 13, 14, and 15.

(B)

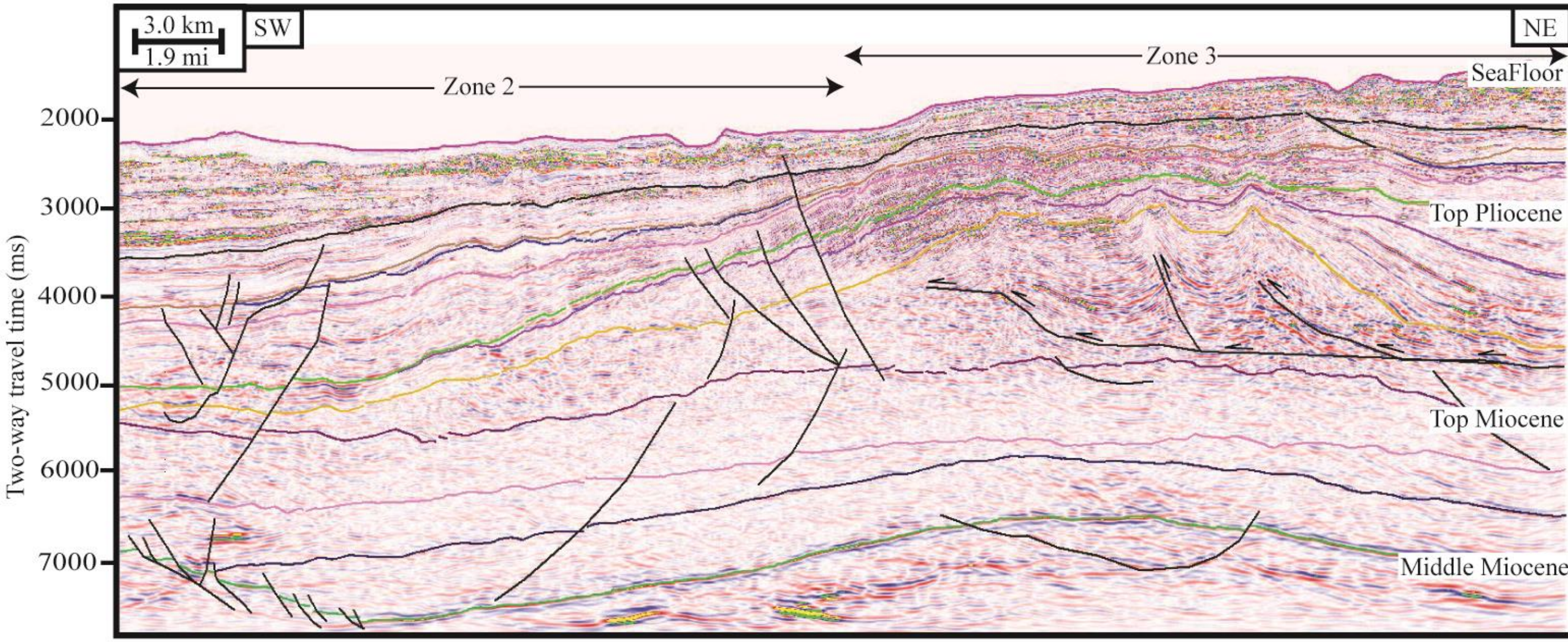

Figure 17: (B) Interpretation of regional seismic section presenting the strike line of extensional faults and the dip line of compressional faults, across structural zones 2 to 3. The fault presented as black line. The thrust fault marked specifically as the black one-side arrow. The color lines interpreted to stratigraphic horizon.
Location of this seismic section is shown in Figures 13, 14, and 15.

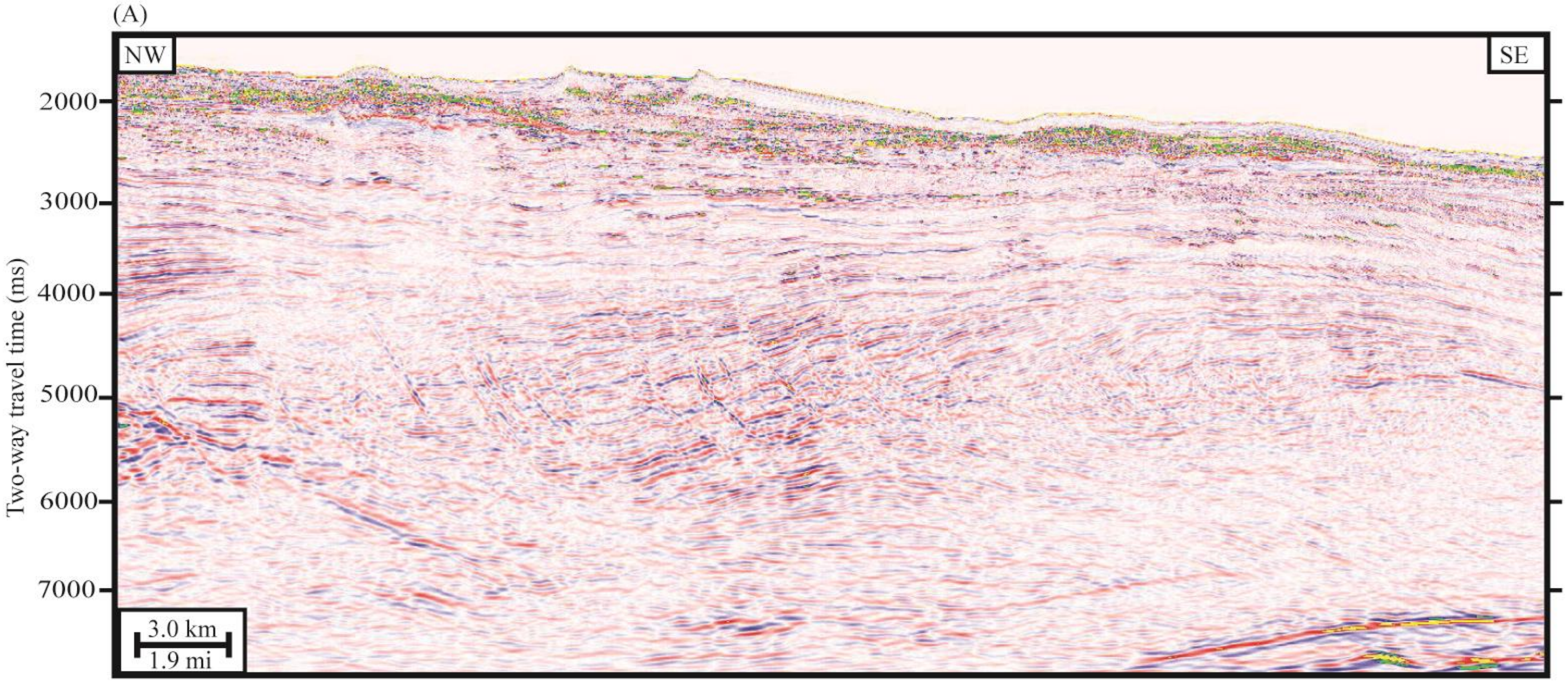

Figure 18: (A) Uninterpreted regional seismic section dip-line number 4140 from the 2016 3D-PSTM. Location of this seismic section is shown in Figures 13, 14, and 16.

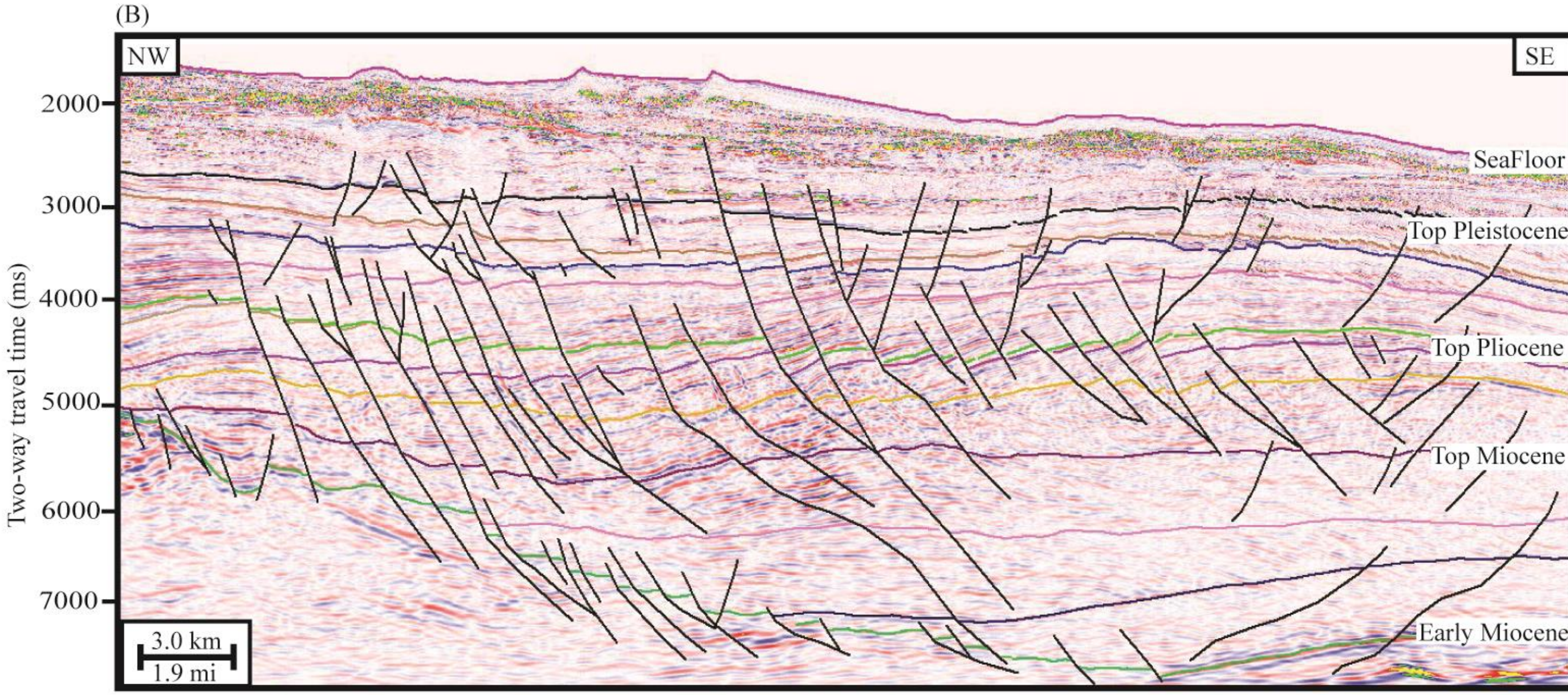

Figure 18: (B) Interpretation of regional seismic section presenting the dip line of extensional faults across structural zone 2. The fault presented as black line. The color lines interpreted to stratigraphic horizon.
Location of this seismic section is shown in Figures 13, 14, and 16.

(A)

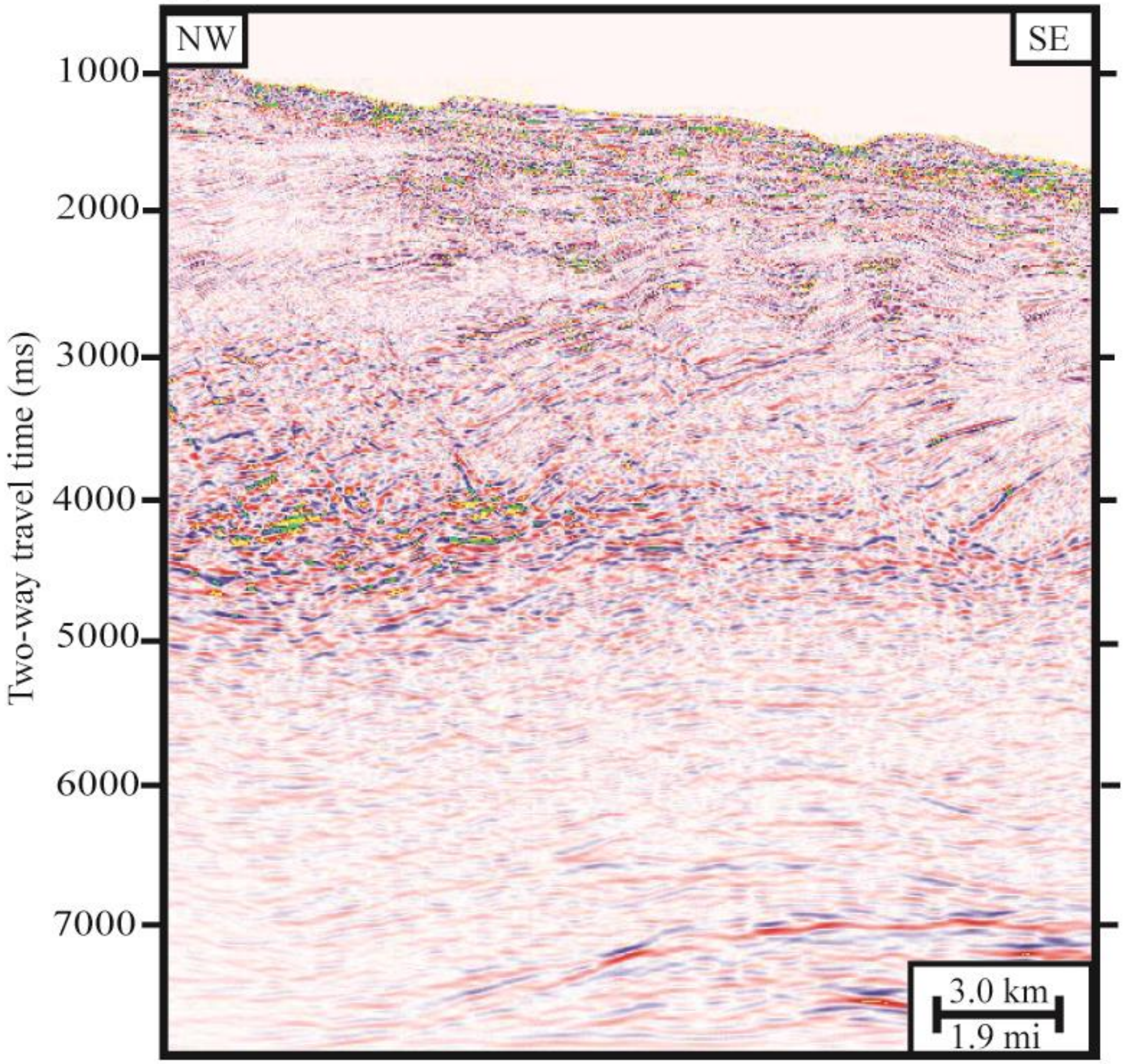

Figure 19: (A) Uninterpreted regional seismic section dip-line number 6580 from the 2016 3D-PSTM.
Location of this seismic section is shown in Figures 13, 14, and 19.

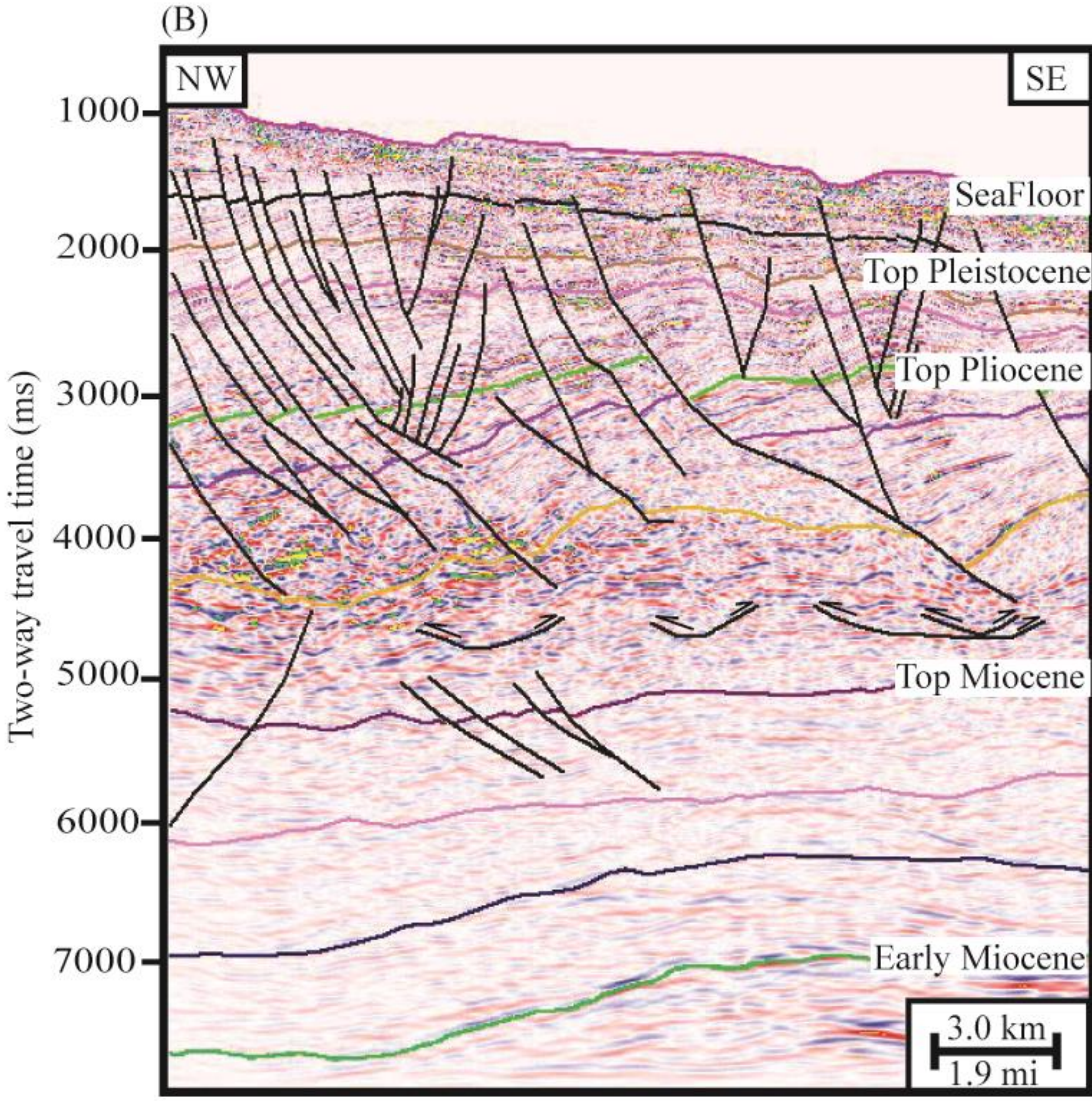

Figure 19: (B) Interpretation of regional seismic section presenting the dip line of extensional faults and the strike line of compressional faults across structural zone 3. The fault presented as black line. The thrust fault marked specifically as the black one-side arrow. The color lines interpreted to horizon stratigraphy.
Location of this seismic section is shown in Figures 13, 14, and 19.

extension of this fault zone (Figure 3).

To the east, third zone consists of shallow thrust faults that cut Pliocene sediment above the relatively undeformed Miocene sediment (Figures 16, 17, 19). This NW-SE trending structural zone consists of fault-bend and fault propagation folds as part of a thrust fault system. This zone developed during the Pleistocene due the reactivated oblique subduction. Syndepositional growth sediments are variable in thickness in early Pleistocene due ongoing detachment.

SEQUENCE STRATIGRAPHY

Overview of Megasequences

Nine key surfaces, sequence boundaries bounding megasequences, were interpreted through the 2016 3D-PSTM (Figures 16 – 23). Onlap and truncation seismic terminations are mainly recognized above and below of the horizon, respectively (Figures 20 – 23). Some downlap can also be seen. The seismic reflection at of each surface horizon is mostly peak association. The exception is the shallowest surface, top Pliocene, which is trough association due to the obvious erosional feature cut into the surface below, separating coarser siliciclastic sediments above from finer-grained strata below.

Eight megasequences were defined from the middle Miocene to Pliocene section (Figures 20 – 23). The sequence stratigraphy of this area consists of mostly aggradation developing in deepwater setting, as part of bottomset beds geometry. The complex structure is captured in megasequences 4-8, which are thick sedimentary successions reactivated by the compressional regime (Figures 15B, 23). However, higher-frequency, internal sequences typically cannot be easily correlated across the study area due to decreases in megasequence thickness, lack of seismic resolution, and extensive faulting.

The 2012 3D-PSTM Seismic at cube was interpreted and tied to the 2016 3D-PSTM cube; key surfaces were correlated at the crossing between two seismic cubes (Figure 24). Only seven key horizons were correlated (Figure 24), with eight of them were present in both dip-line and strike-line correlations (Figures 25, 26) due to the pinch-out of some key surfaces onto the underlying horizon, related to high structural zone in this study area (Figure 15B).

The M1 well provides information that allows for a tie between the well data and the 2012 3D-PSTM seismic interpretation. The synthetic seismogram allows correlation of only five key markers (Figures 25, 26). The synthetic seismogram generated for the M1 well resulted in a

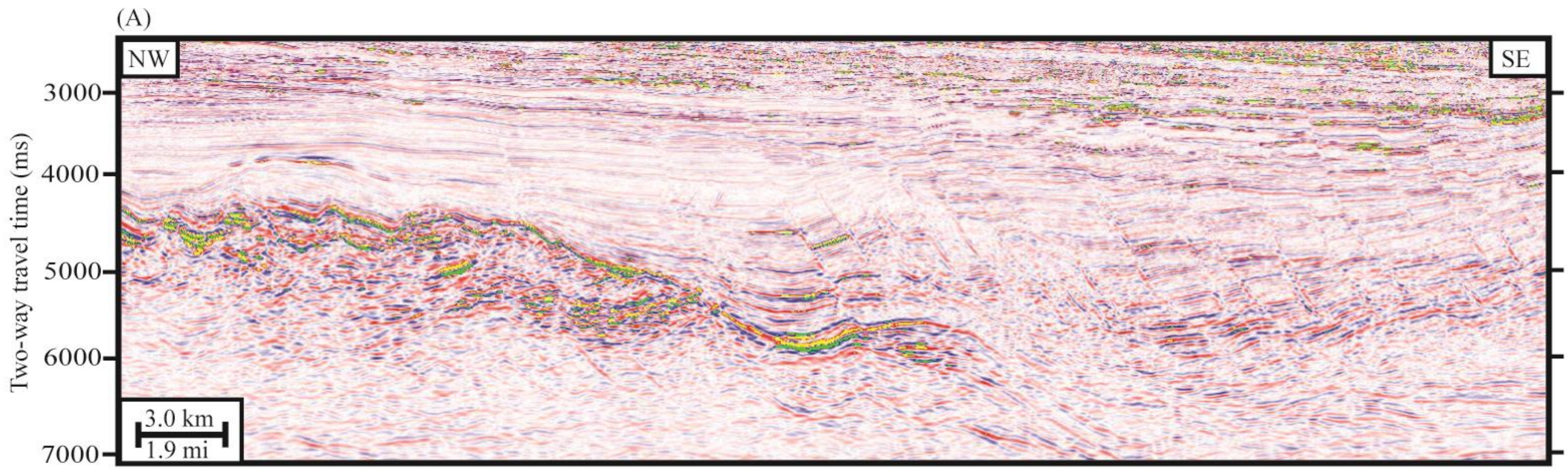

Figure 20: (A) Uninterpreted regional seismic section dip-line number 3100 from the 2016 3D-PSTM. **(B)** Interpreted seven megasequences were shaded with internal features as highlighted black line interpretation. 2 = Tortonian (?), 3 = Messinian (?), 4-5-6 = early-middle-late Zanclean, and 7-8 = early-late Piacenzian. **(C)** Interpretation emphasizing to extensional faults.
Location of this seismic section is shown in Figures 32 and 69.

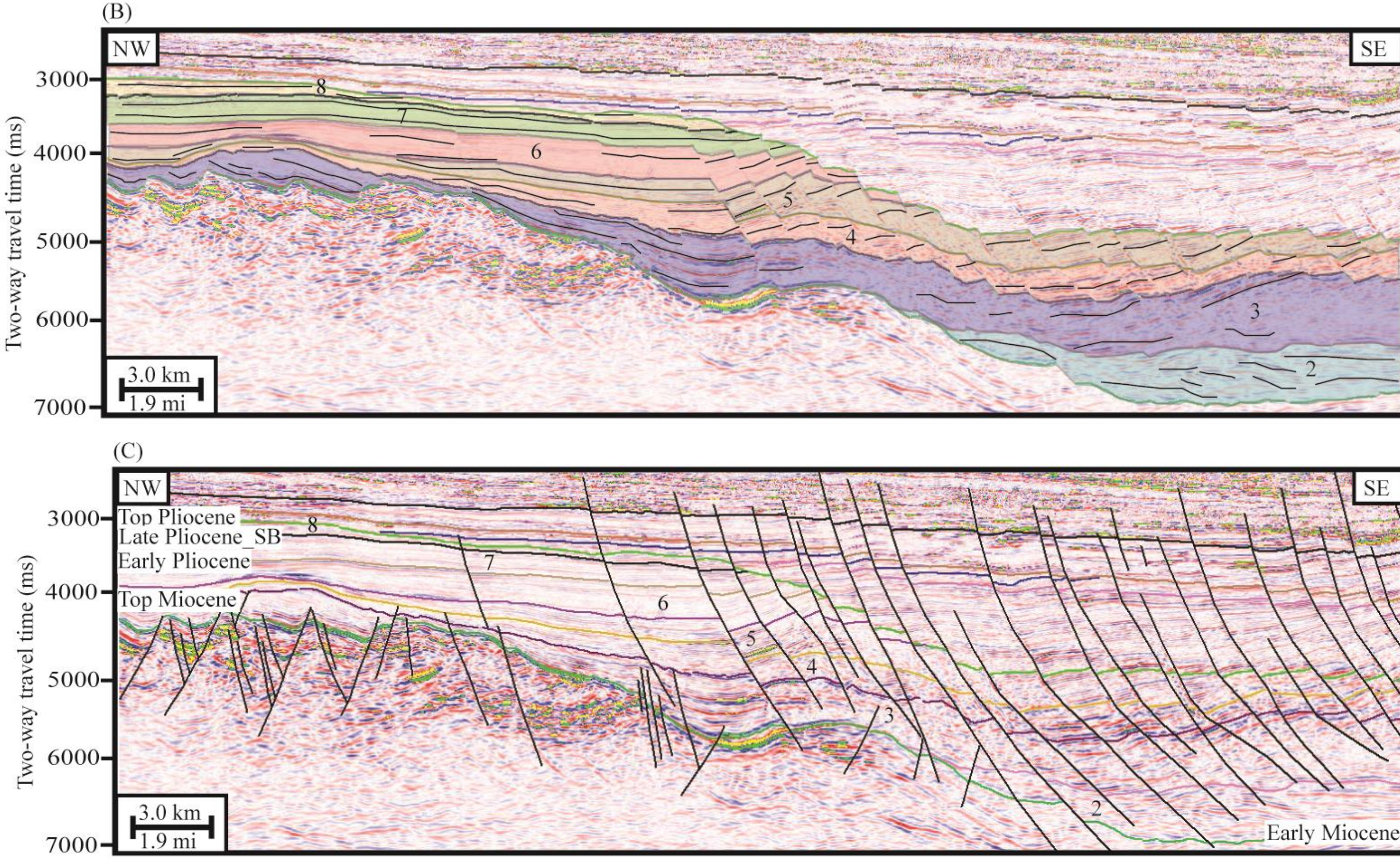
(B)
NW
SE
Two-way travel time (ms)
3000
4000
5000
6000
7000
8
7
6
5
4
3
2
3.0 km
1.9 mi
(C)
NW
SE
Top Pliocene
Late Pliocene_SB
Early Pliocene
Top Miocene
Early Miocene
3.0 km
1.9 mi

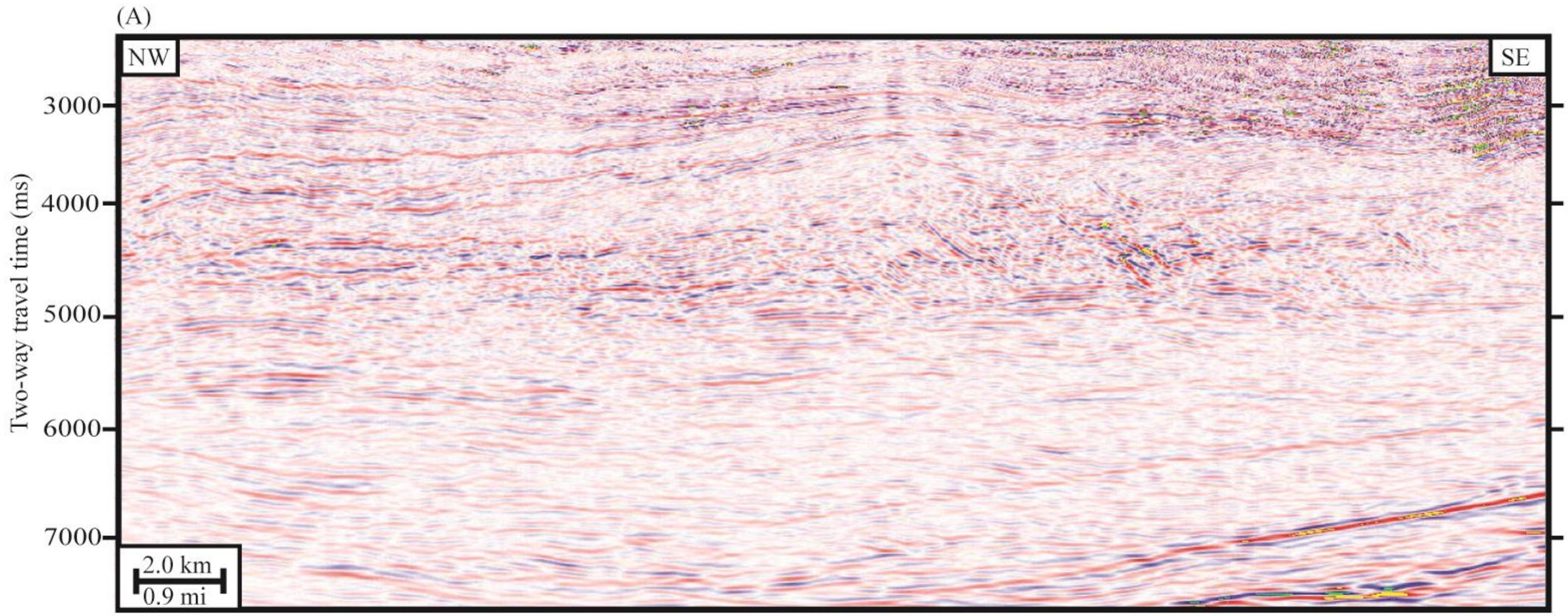

Figure 21: (A) Uninterpreted regional seismic section dip-line number 5180 from the 2016 3D-PSTM. Location of this seismic section is shown in Figures 32 and 69.

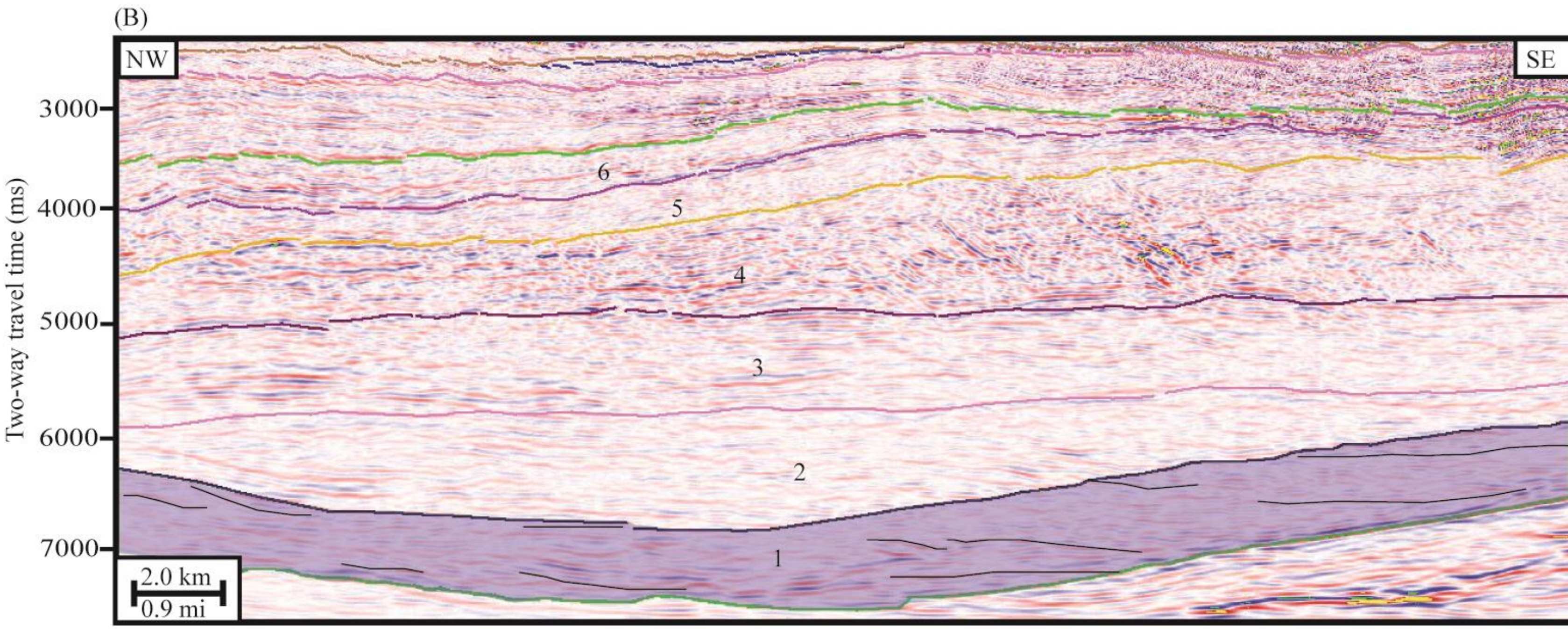

Figure 21: (B) Interpreted only megasequence 1 was shaded with internal features as highlighted black line interpretation. 1 = Langhian – Serravallian (?), 2 = Totonian (?), 3 = Messinian (?), and 4-5-6 = Early-Middle-Late Zanclean.

(C)

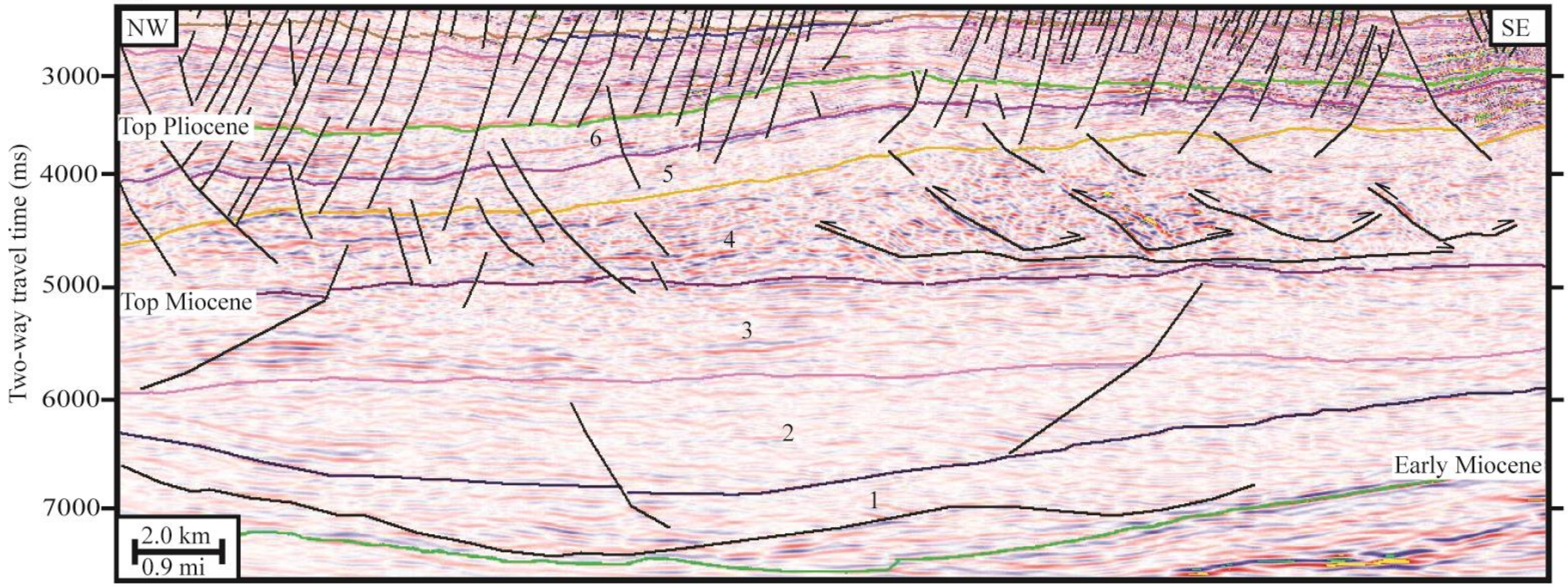

Figure 21: (C) Interpretation emphasizing to the dip line of extensional faults.

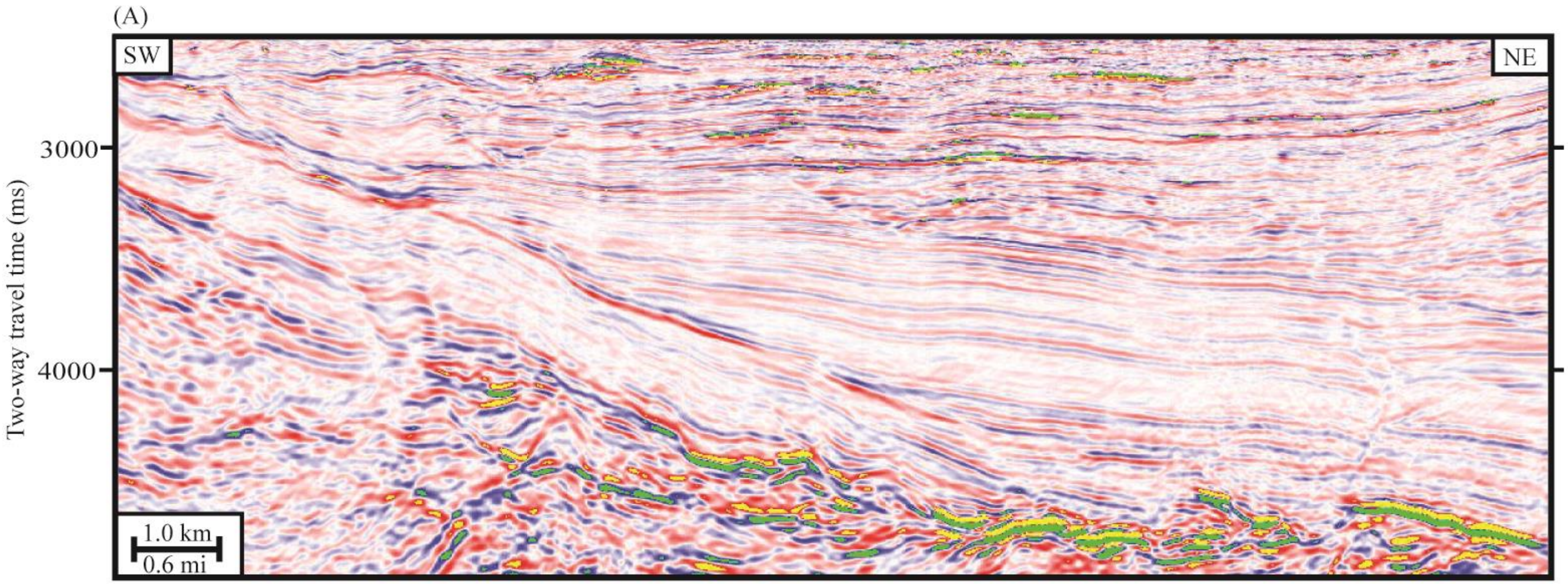

Figure 22: (A) Uninterpreted regional seismic section strike-line number 6100 from the 2016 3D-PSTM. Location of this seismic section is shown in Figures 32 and 69.

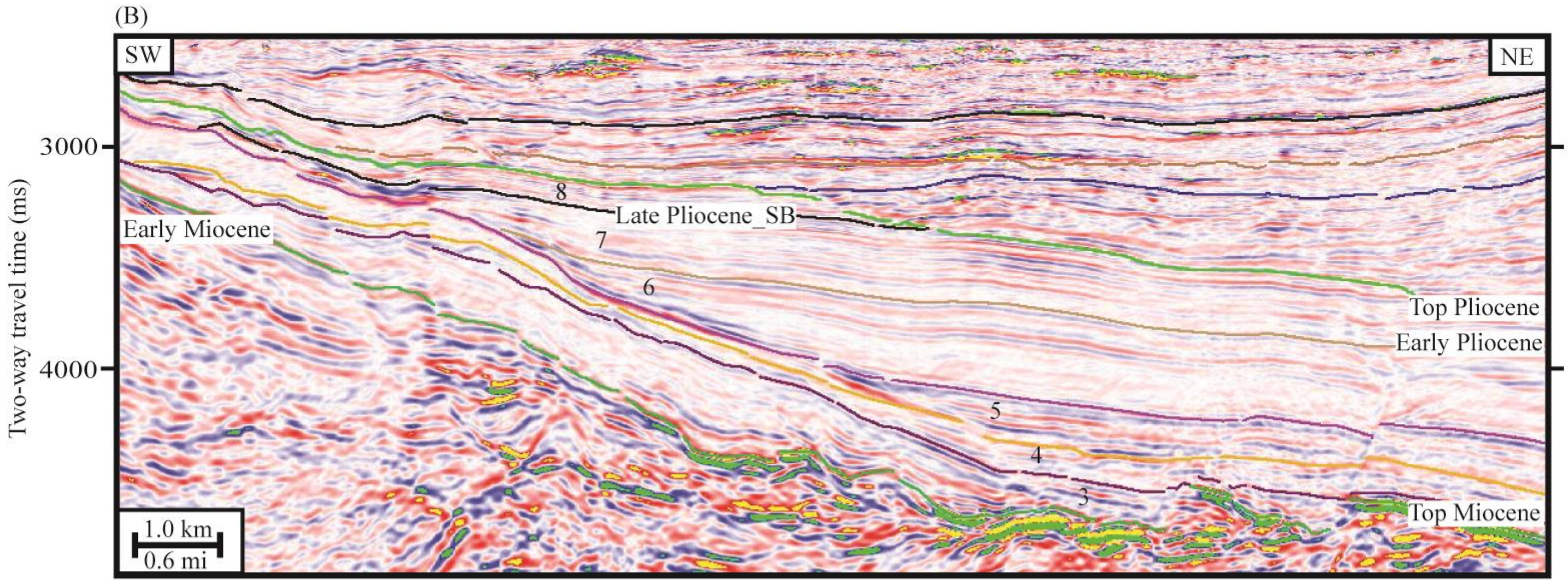

Figure 22: (B) Stratigraphic interpretation including 3 = Messinia, 4-5-6 = Early-Middle-Late Zanclean, and 7-8 = Early-Late Piacenzian.

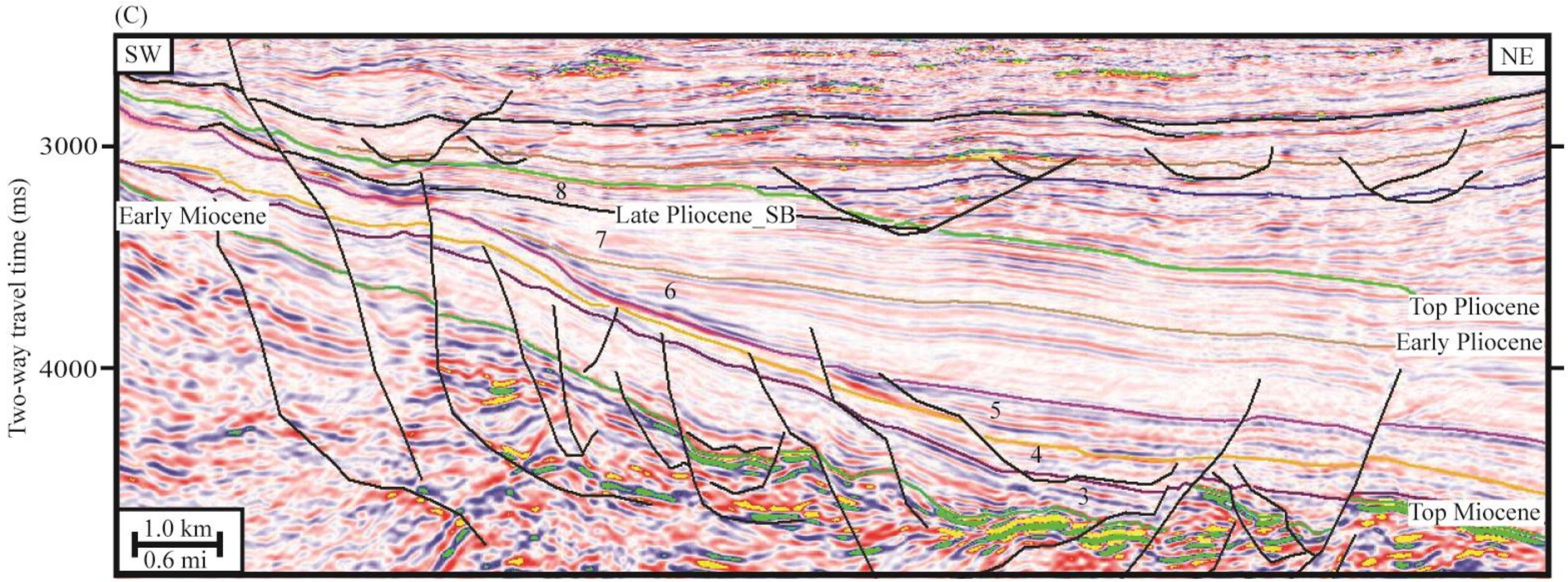

Figure 22: (C) Interpretation emphasizing to the strike line of extensional faults.

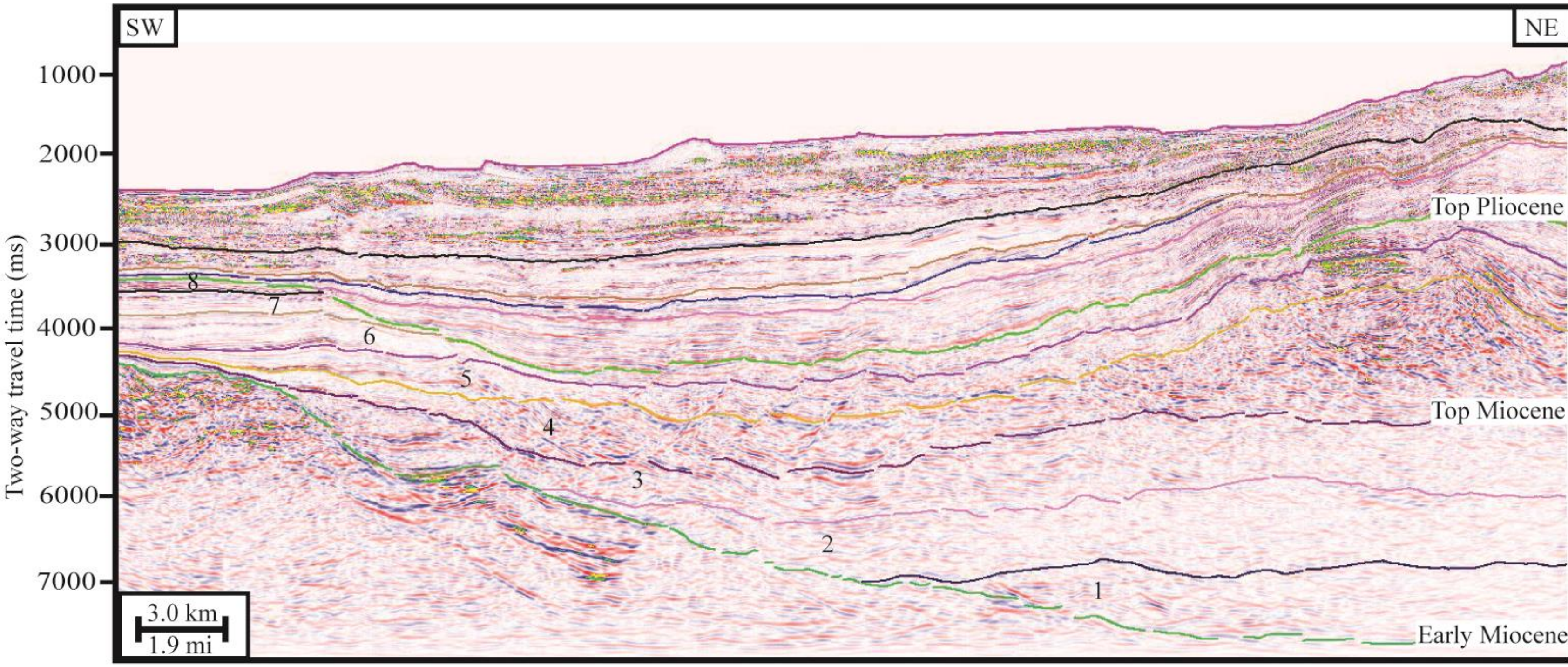

Figure 23: Part of figure 15, Stratigraphic interpretation including 1 = Langhian – Serravallian (?), 2 = Totonian, 3 = Messinia, 4-5-6 = Early-Middle-Late Zanclean, and 7-8 = Early-Late Piacenzian.
The adjacent information is shown in Figure 16 and location of this seismic section is shown in Figures 32 and 69.

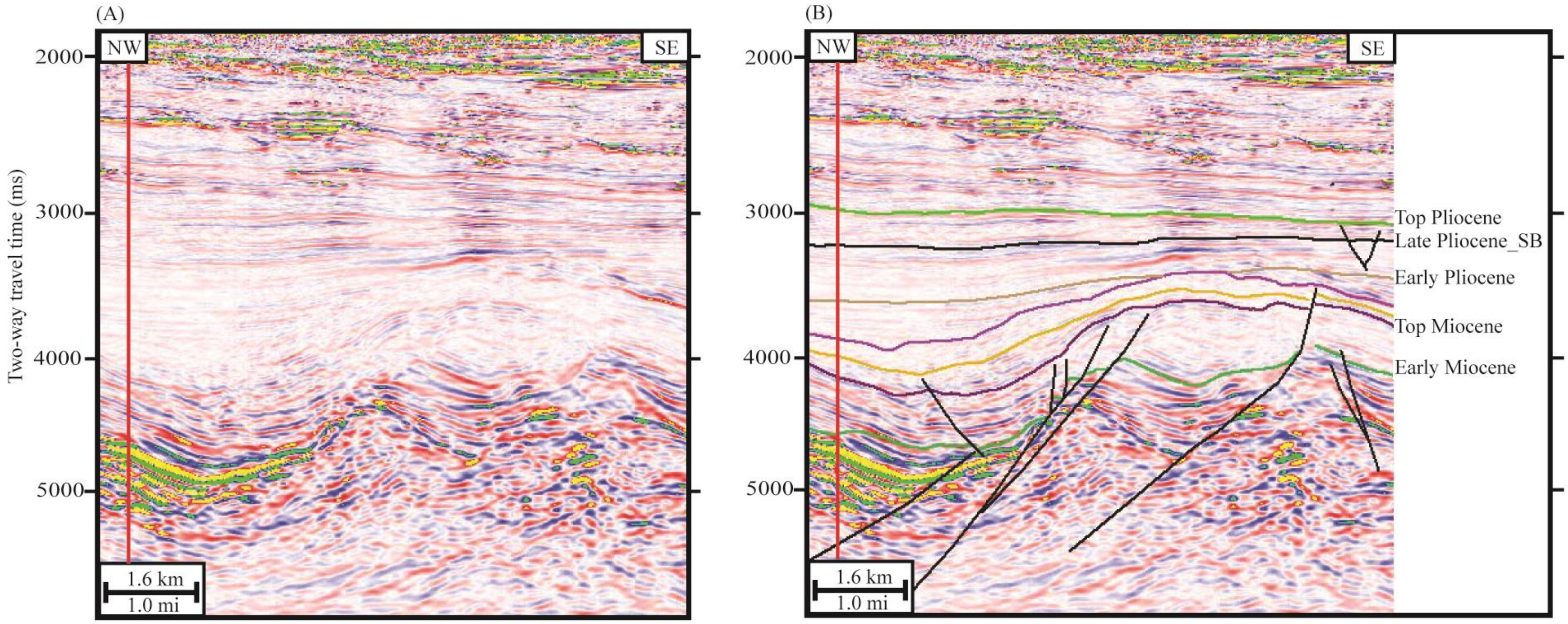

Figure 24: (A) Uninterpreted seismic section dip-line number 2900 from the 2016 3D-PSTM. The red line on the seismic section is the tie point between the 2012 3D-PSTM and the 2016 3D-PSTM. **(B)** Interpretation of key horizons: seven horizons were interpreted. Location of this seismic section is shown in Figures 32 and 69.

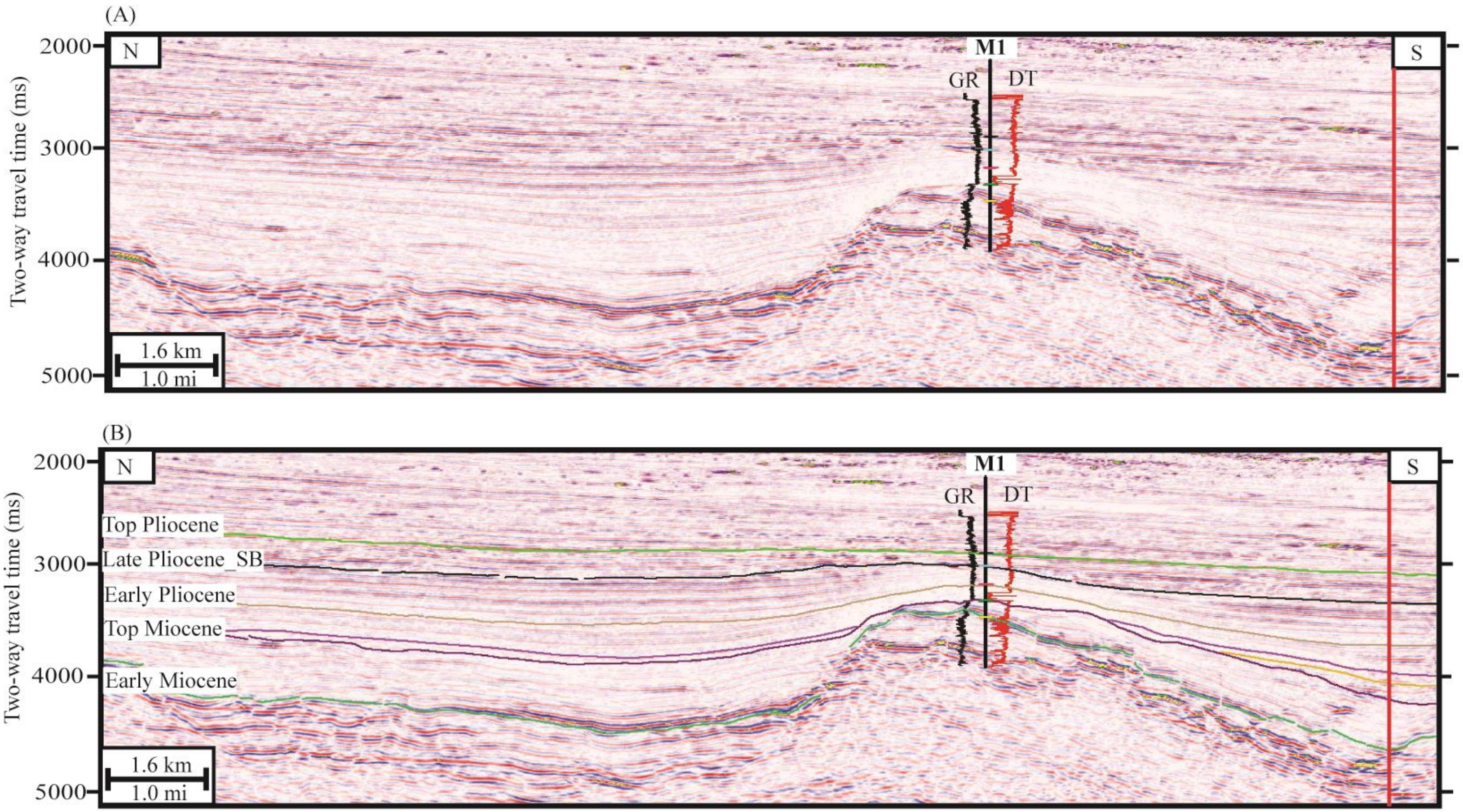

Figure 25: (A) Uninterpreted regional seismic section strike-line number 1592 from the 2012 3D-PSTM at the well location. See figure 26 for the description. The red line on the seismic section is the tie point between the 2012 3D-PSTM and the 2016 3D-PSTM. **(B)** Stratigraphic interpretation of key horizons; five horizons were interpreted with additional two horizons that represent the pinch-out features in early Pliocene.
Location of this seismic section is shown in Figures 32 and 69.

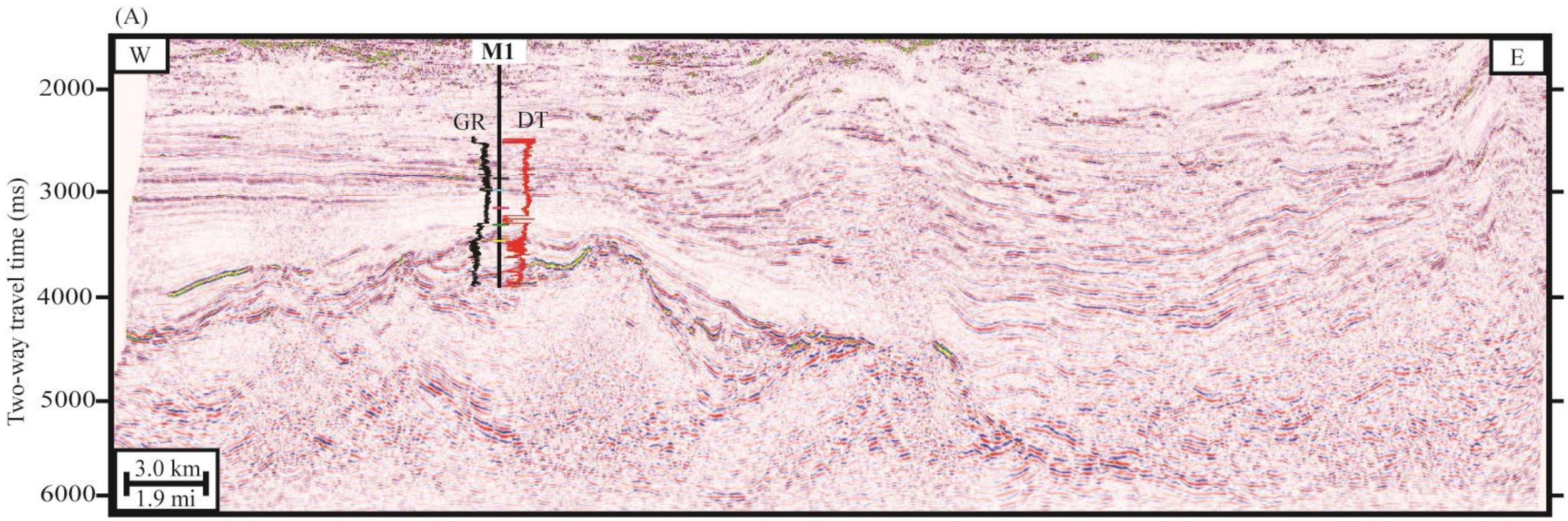

Figure 26: (A) Uninterpreted regional seismic section dip-line number 978 from the 2012 3D-PSTM at the well location. GR = gamma-ray log (scale 0 -200 GAPI), and DT = sonic log (scale 60 -160 ms/ft). Black marker = Top Pliocene, Blue marker = late Pliocene sequence boundary (SB), Pink marker = early Pliocene, Green marker = Top Miocene, and Yellow marker = early Miocene. Location of this seismic section is shown in Figures 32 and 69.

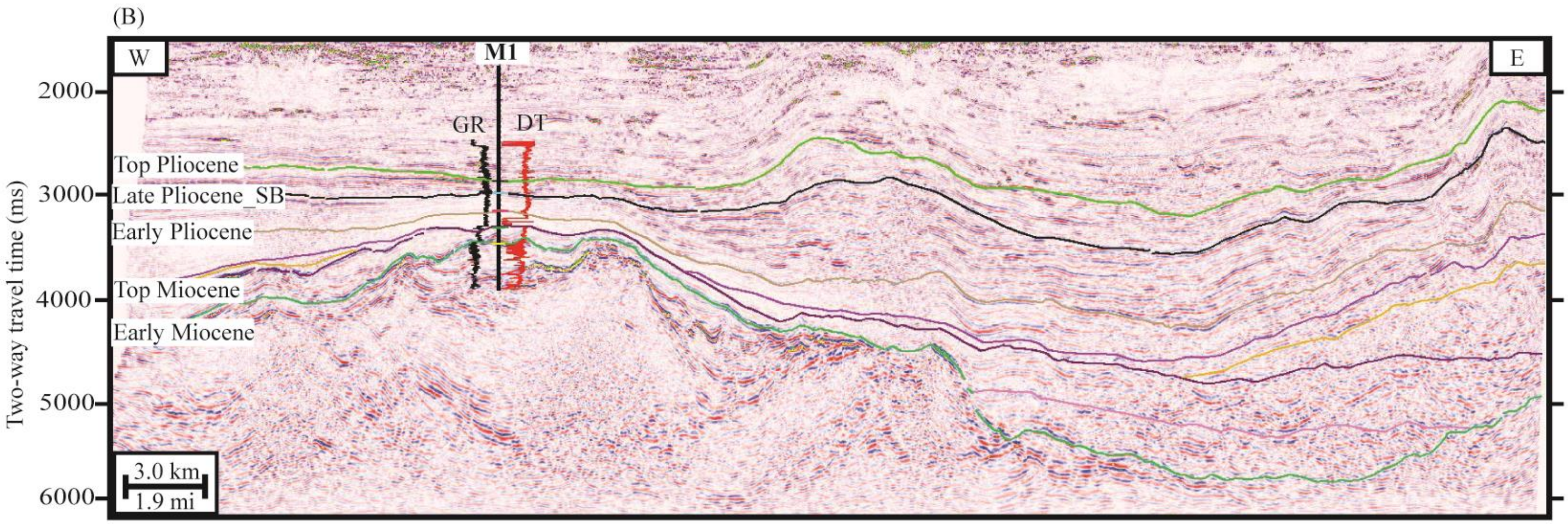

Figure 26: (B) Stratigraphic interpretation of key horizons; five horizons were interpreted with additional three horizons that represent the pinch-out features. One horizon is in late Miocene, another two horizons are in early Pliocene.

good correlation between the synthetic trace comparing to 2012 3D-PSTM seismic reflection (Figure 27). The checkshot data, the sonic, and the density logs were used to calculate the acoustic impedance and reflection coefficient convolution with positive zero phase wavelet, which was extracted from the whole seismic cube. The result showed 68% correlation matching in 2.8 – 3.5 seconds window.

Five key surfaces and four intervals were identified primarily based on the wireline log and biostratigraphic data (Figures 7, 28): (1) early Miocene (part of Kwingyang Formation), (2) Top Miocene (part of Kathabaung Formation), (3) early Pliocene, (4) late Pliocene sequence boundary (SB), and (5) Top Pliocene (part of Ayeyarwardy group).

Early Miocene: This marker was picked based on the shallowest or first occurrence of carbonate cuttings from the M-1 well that matched the gamma-ray log response. This marker marks a shift between carbonate rock and overlying shale (Figure 28). An abrupt change in the interval velocity, derived from the checkshot data of this well, was also recognized this marker (depth 3,070.51 mMD / 3,038.93 mTVDSS). This marker is the lower boundary of the interval in this thesis.

Top Miocene: This marker is a clear shift of gamma-ray log response based on Miocene-Pliocene boundary, which represents a changing of the depositional environment from higher N/G to the lower (Figure 28). The biomarker from the biostratigraphic report (Figure 7) was integrated to this marker defining (depth 2,969.96 mMD / 2,938.38 mTVDSS).

Early Pliocene: This key marker was picked by the interfacing of the interval velocity derived from sonic log in shale section (Figure 28) (depth 2,808.58 mMD / 2,775.00 mTVDSS).

System / Period	Series / Epoch	Stage / Age	Age (Ma)
Neogene	Pliocene	Piacenzian	2.58 - 3.60
		Zanclean	3.60 - 5.33
	Late Miocene	Messinian	5.33 - 7.24
		Tortonian	7.24 - 11.63
	Middle Miocene	Serravallian	11.63 - 13.82
		Langhian	13.82 - 15.97
	Early Miocene	Burdigalian	15.97 - 20.44
		Aquitanian	20.44 - 23.03

Table 2: The reference table of Neogene system and megasequences, as defined by the stage name (GSA, 2017).

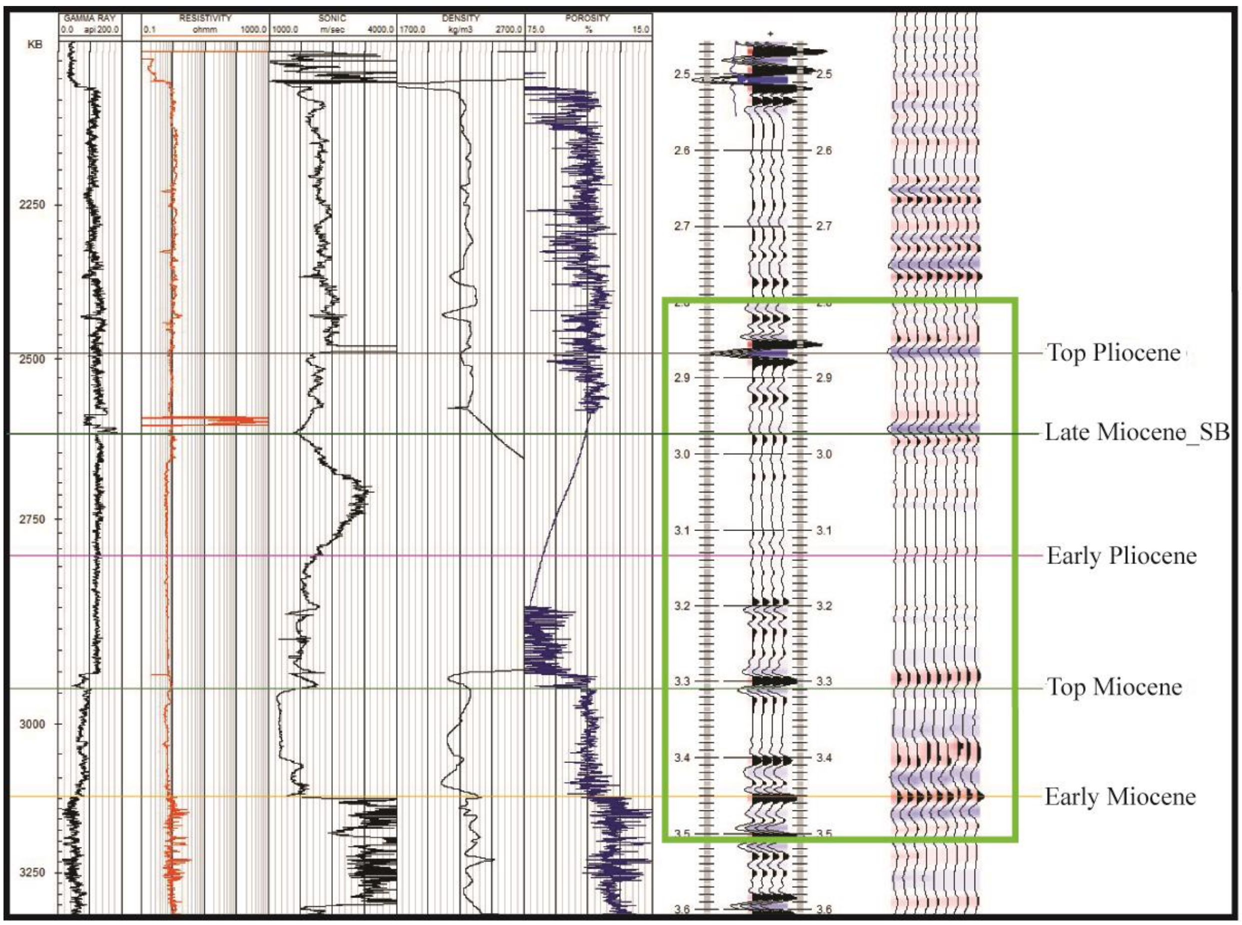

Figure 27: Synthetic seismogram displayed with the wireline log data, sonic log and density Log were used to generate the synthetic tract. The green zone shows the correlation window as 2.8 – 3.5 seconds.

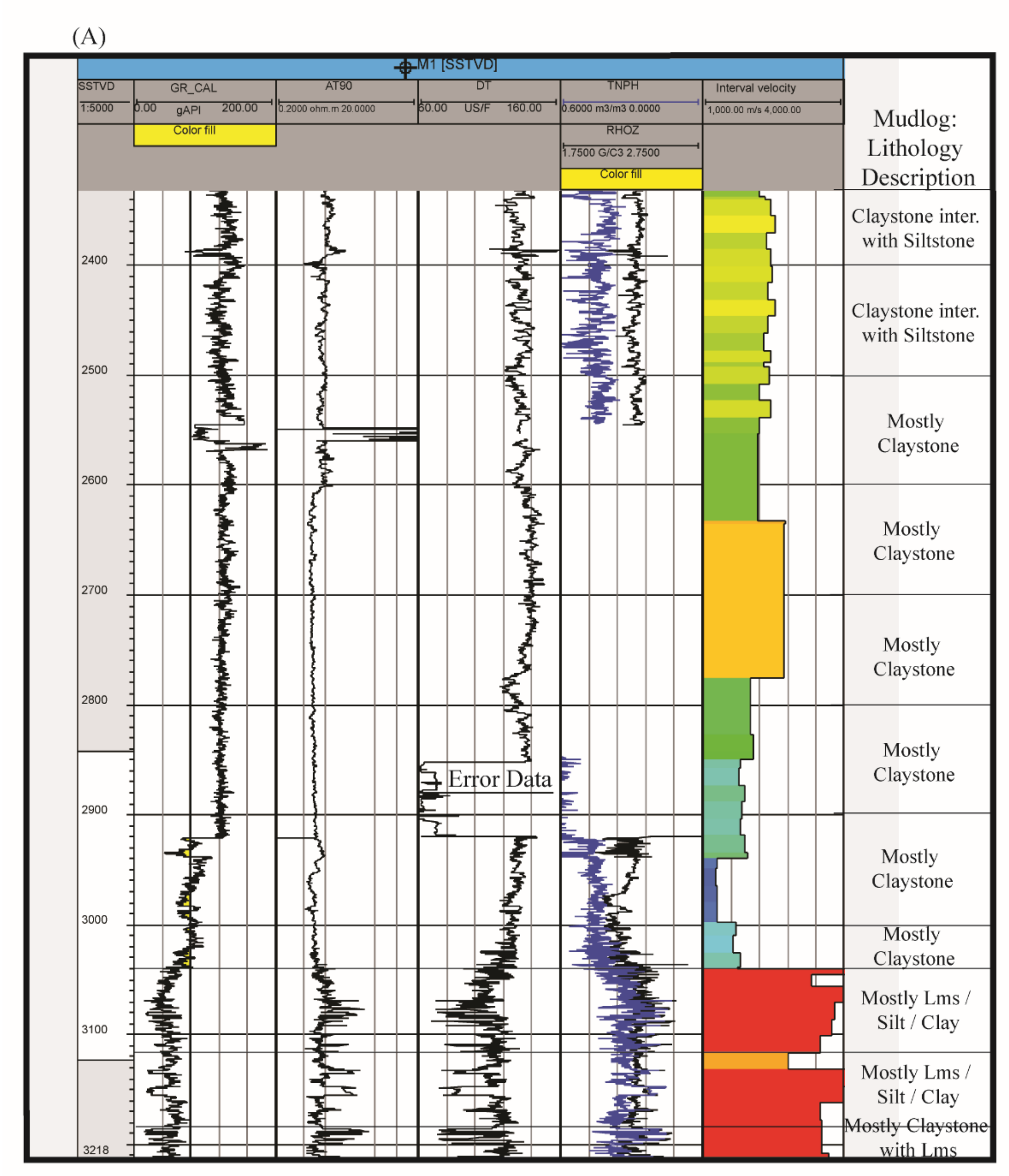

Figure 28: Wireline log data of the M1 exploration well, including gamma-ray log, resistivity log, sonic log, crossover of porosity log and density log, and the derivative of Checkshot as interval velocity. **(A)** uninterpreted overall data in the studied succession, including mudlog lithology description.
Location of this exploration well is shown in Figure 5.

(B)

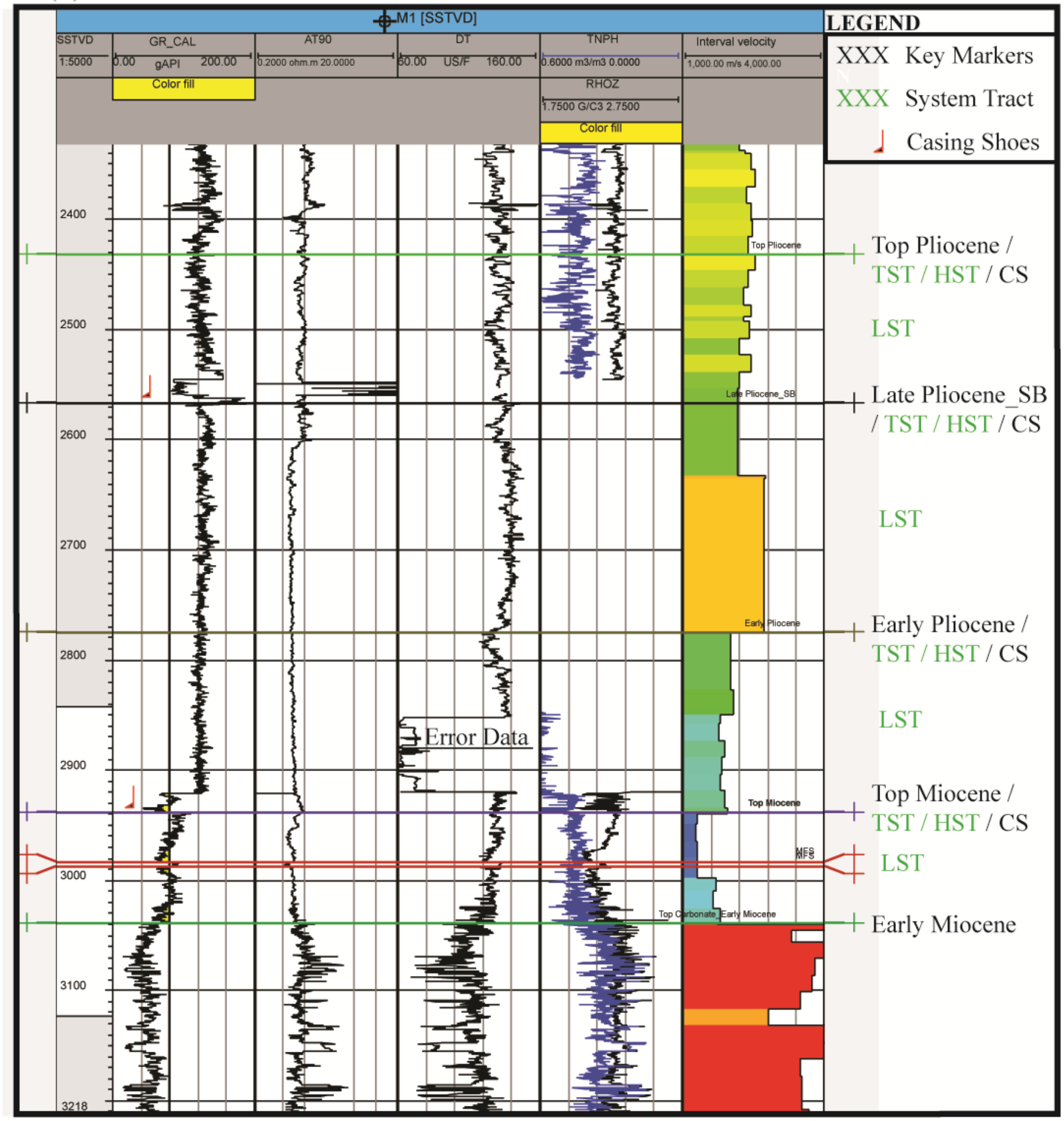

Figure 28: (B) interpreted log showing five key markers, four intervals, key surfaces (MFS = Maximum Flooding Surface, CS = Condensed Section and systems tracts, TST = Transgressive system tract, LST = Low Stand system tract, and HST = High Stand system tract.

(C)

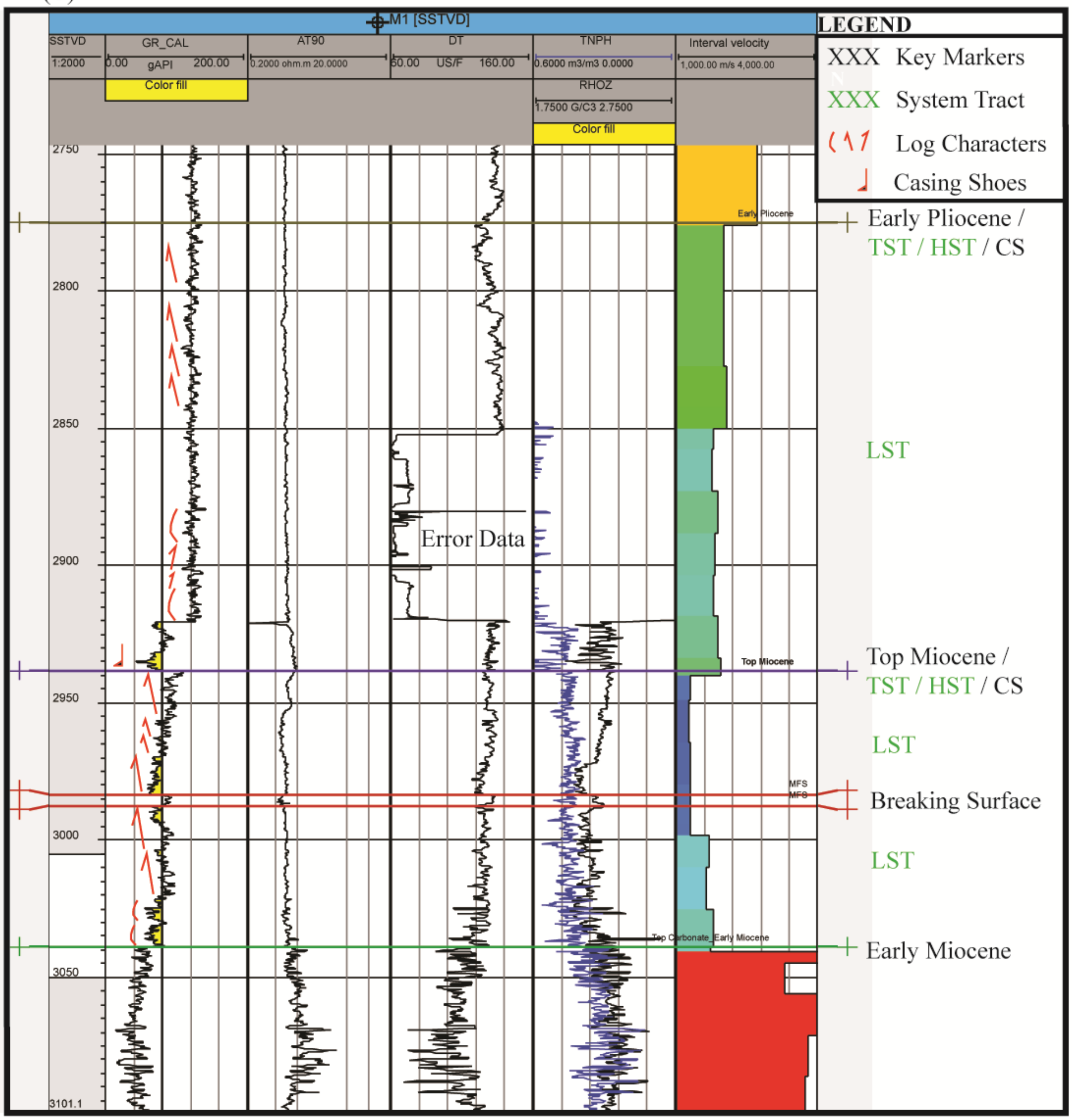

Figure 28: (C) The detail interpretation from early Miocene to early Pliocene. Partial circle = symmetrical shape, Left-tilted arrow = Coarsening upward, and Right-tilted arrow = Fining upward**.**

(D)

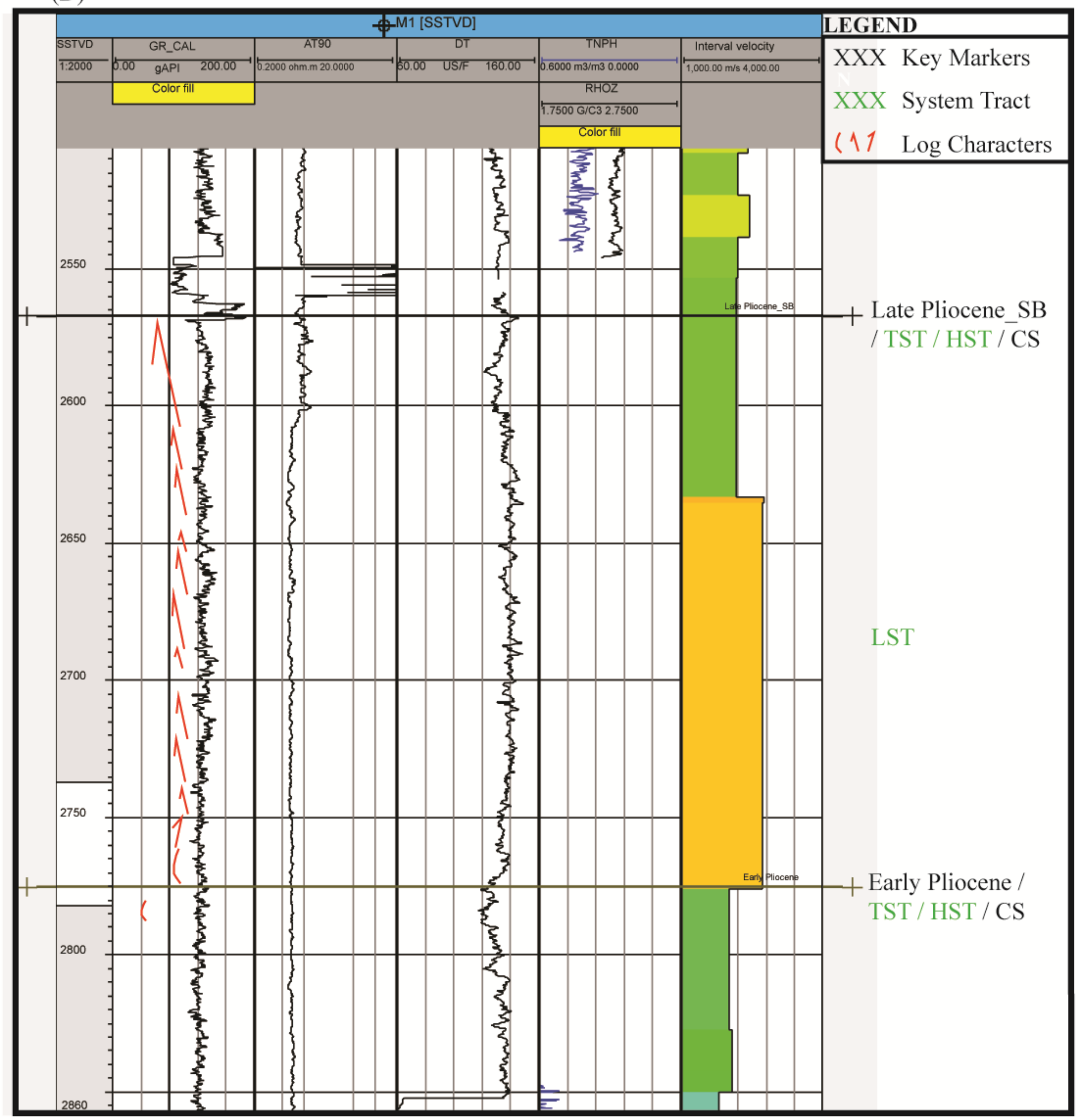

Figure 28: (D) From early Pliocene to late Pliocene sequence boundary (SB).

(E)

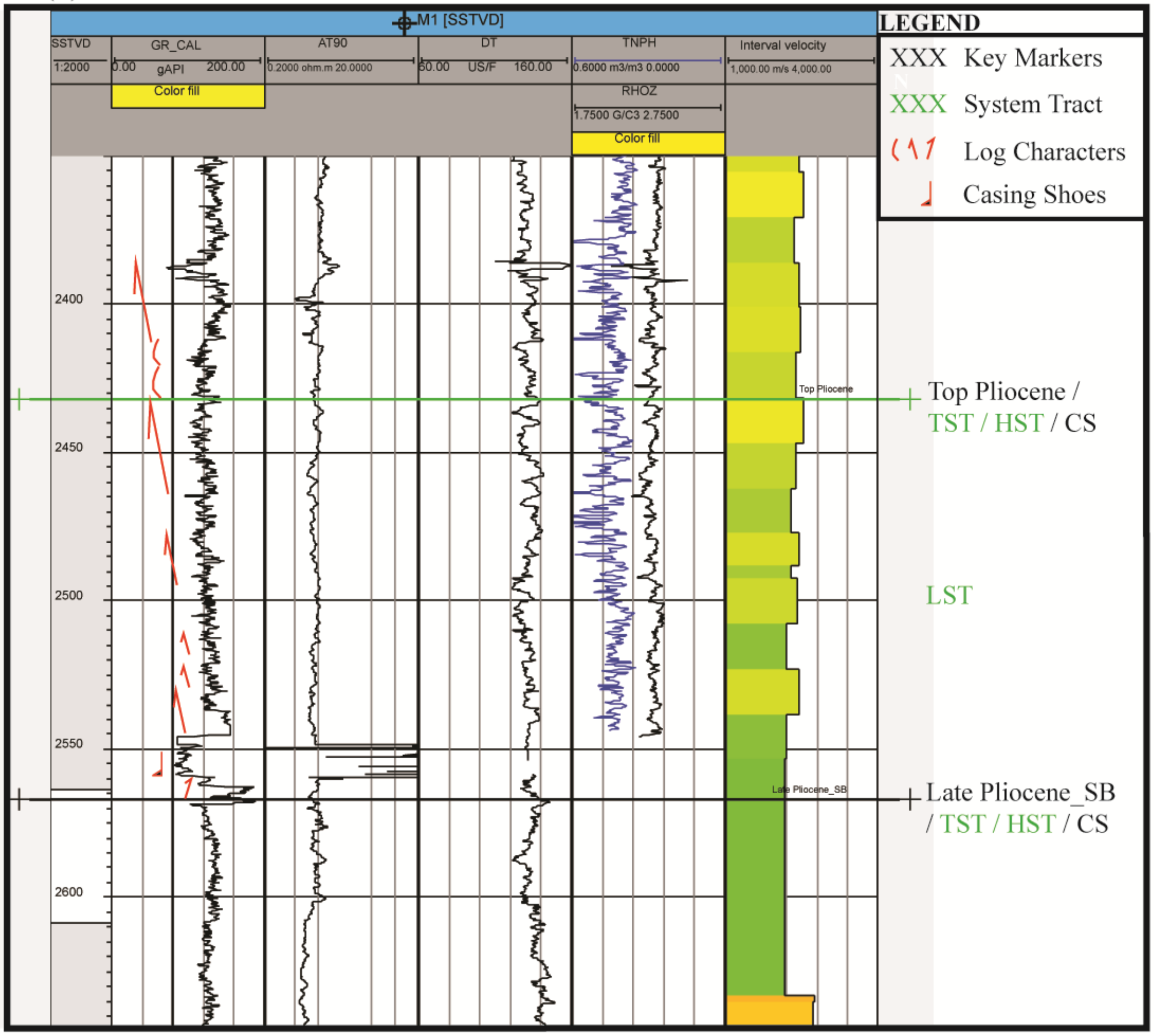

Figure 28: (E) From late Pliocene sequence boundary (SB) to Top Pliocene.

Late Pliocene sequence boundary (SB): This key marker is part of upper Pliocene succession, which was picked by the change in gamma-ray log in shale section (Figure 28) (depth 2,598.57 mMD / 2,567.00 mTVDSS).

Top Pliocene: The key marker was picked based on another shift of gamma-ray log, in which the Pleistocene section has an increase in N/G siliciclastic sediments (Figure 28) (depth 2,464.00 mMD / 2,432.43 mTVDSS). Moreover, the coarser siliciclastic sediment package on top of this marker also presents. This marker is the upper boundary of the interval in this thesis.

The ages of key markers and megasequences were derived from the well interpretation (Table 2), (Figures 7, 20 – 26, 28). Because the well was drilled on a structural high, the ages in the deeper part of the basin have high uncertainty. However, the estimation ages of each megasequence was constrained by early Miocene and Top Pliocene.

The lowest part of megasequences, overlying early Miocene to Top Miocene has three megasequceses, which are defined as Megasequence 1 is Langhian-Serravallian (?), Megasequence 2 is Tortonian (?), and Megasequence 3 is Messinian (?) (Figures 20 – 26, 28). Megasequences 4-6 are part of the Pliocene section as specific to early, middle, and late Zanclean, respectively (Figures 20 – 26, 28). The two yonger megasequences were identified by the well interpretation: Megasequence 7 is early Piacenzian, and Megasequence 8 is late Piacenzian (Figures 20 – 26, 28).

The detail, which is including their structure, isochron, seismic facies, and system tracts, is described later. The geological interpretation is the main focus as one of the important objectives to understand the uncertainties of petroleum exploration in this area related to potential reservoir presence and quality. In addition, the detail geological interpretation was performed in specific area (figure 15B), due to the limitation of computer tool in case of high-resolution seismic data handling. The area was chosen from the interesting high structure area, potential hydrocarbon accumulation trap, and the obvious features in sweetness seismic attribute interpretation. The area was scoped in the 2016 3D-PSTM seismic between inline (dip-line) 3001 to 4401 and crossline (strike-line) 5300 to 6300, which is covering Megasequence 3 to 7.

Megasequence 1: Langhian-Serravallian (?)

Key Surfaces: The lower sequence boundary (early Miocene) was defined by clear onlap and truncation features overlying and below the horizon, respectively (Figures 21, 29 – 31). The seismic reflection corresponds to a high amplitude peak association. The surface is onlapped by several overlying sequences. Therefore, this surface merges several of the younger sequence boundaries (Figures 20, 22, 23). In the M1 well, this surface correlates to the distinct change from carbonate to overlying siliciclastic rocks (Figure 28).

The upper sequence boundary (Langhian-Serravallian (?)) was identified by extensive onlap and downlap onto the top of disconformity, with some local erosional truncation below this horizon (Figures 29 – 31). This is a regional erosional surface within the bottomset beds, and this upper boundary is parallel to the basal surface, both surfaces merge towards the west (Figures 29, 31). Clear high amplitude peak seismic reflection can be marked for this sequence boundary.

Time-Structure Map: The time structure map of the lower boundary shows north-trending structural high to the west (at 2.6 sec TWT) (Figure 32). The surface dips to the east, and a north trending synclinal is present in the central part of the area. A structural high is present to the far east, i.e. the eastern limb of the syncline.

The structure of the upper sequence boundary, (Langhian-Serravallian (?)) indicates a portion of the syncline and the structural high to the east are presented, which have a similar geometry to the lower sequence boundary (Figure 33). Due to the pinch-out of the surface against the lower boundary, the upper sequence boundary is only present in the east of the area.

Isochron Map: The isochron values of this megasequence range from 0.04 to 1.14 seconds (TWT), and trend NNE-SW (Figure 34). Most of values are between 0.57 to 0.87 seconds

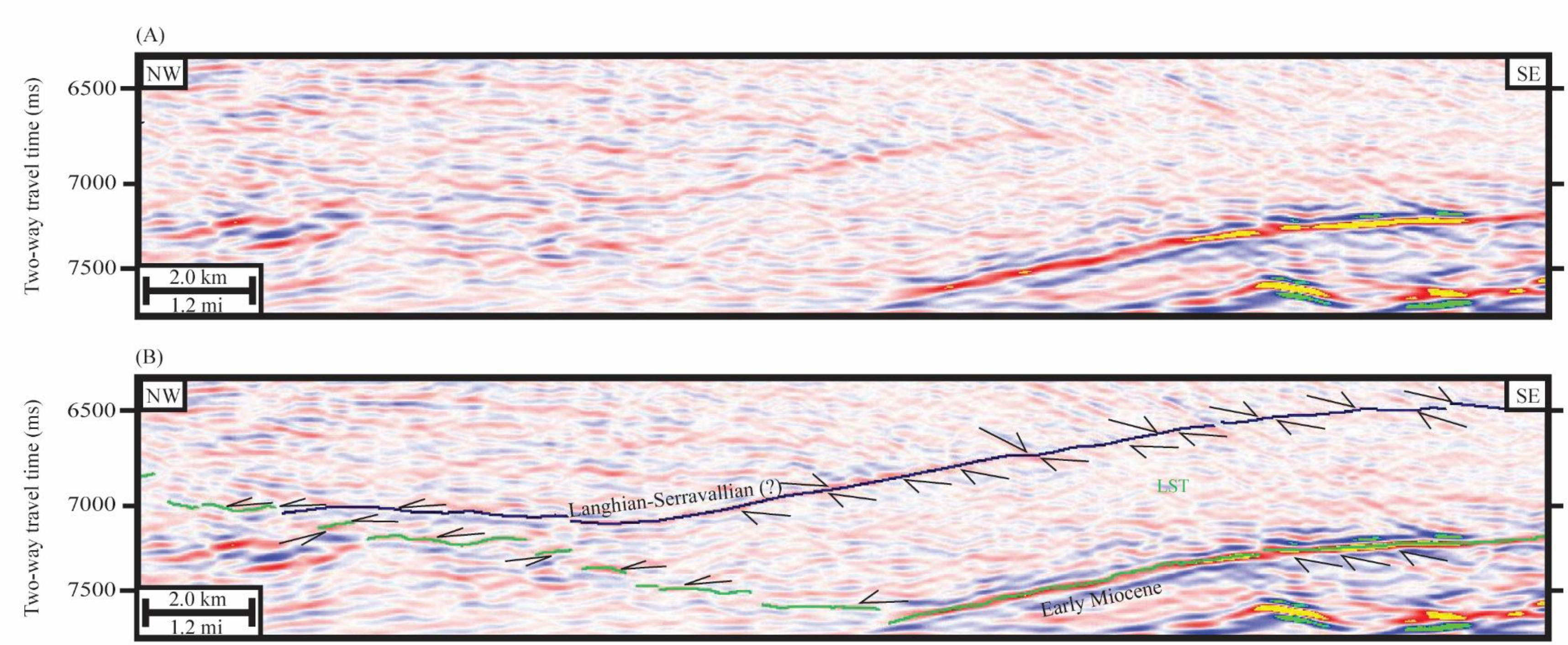

Figure 29: Seismic profile showing megasequence 1 across the 2016 3D-PSTM, dip-line number 4140. **(A)** uninterpreted **(B)** interpreted including sequence boundaries and stratal terminations. LST = Low-Stand system tract.

Location of this seismic section is shown in Figures 33 - 36.

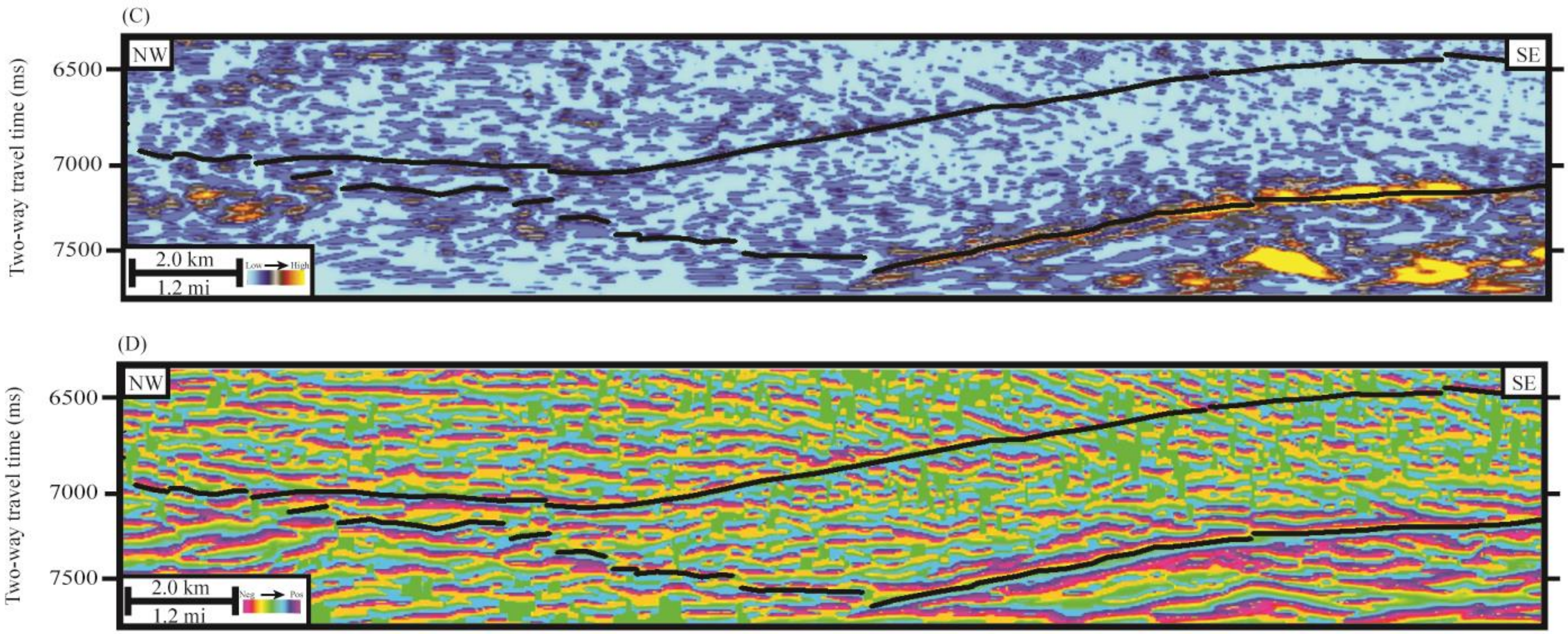

Figure 29: (C) Envelope seismic attribute **(D)** Instantaneous Phase seismic attribute.

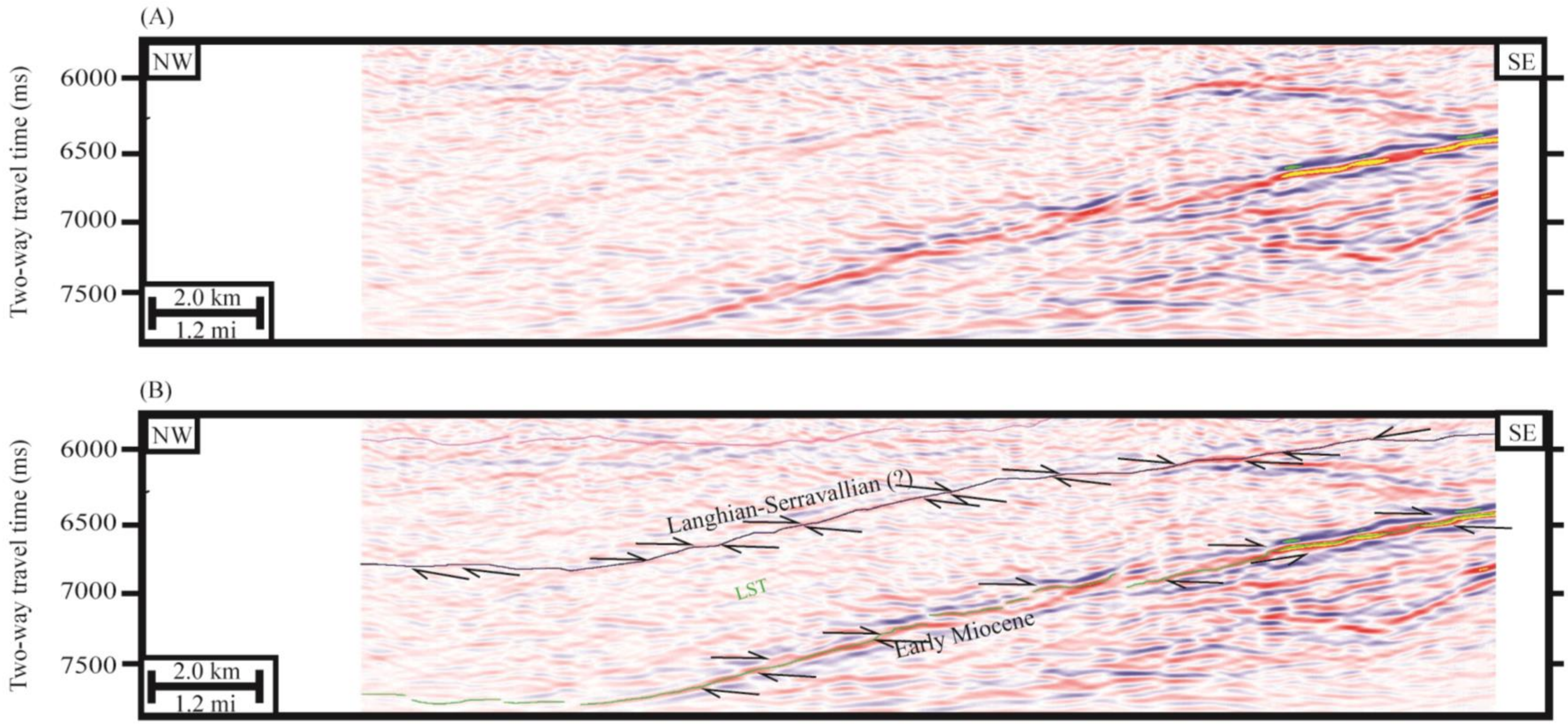

Figure 30: Seismic profile showing megasequence 1 across the 2016 3D-PSTM, dip-line number 5900. **(A)** uninterpreted **(B)** interpreted including sequence boundaries and stratal terminations. LST = Low-Stand system tract.

Location of this seismic section is shown in Figures 33 - 36.

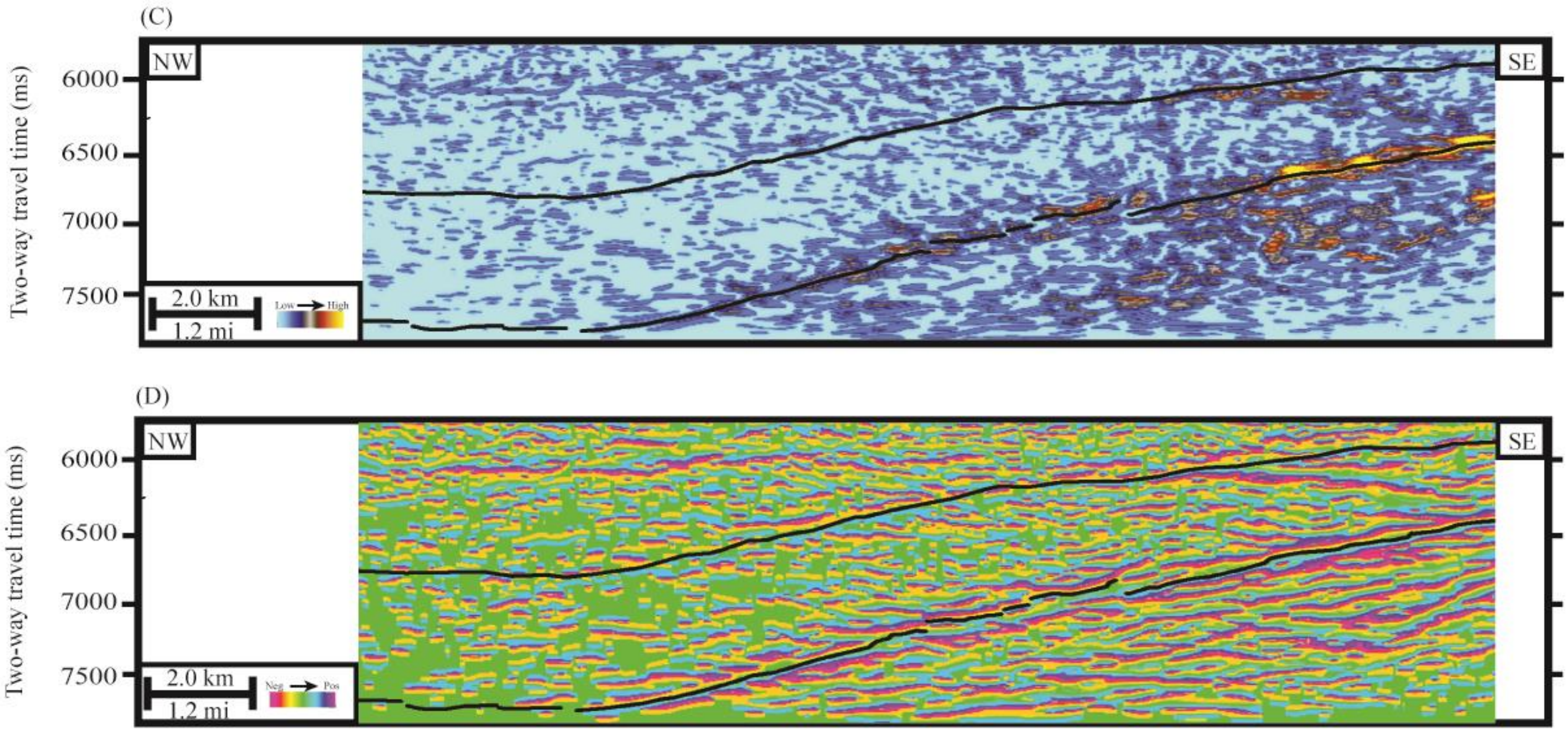

Figure 30: (C) Envelope seismic attribute **(D)** Instantaneous Phase seismic attribute.

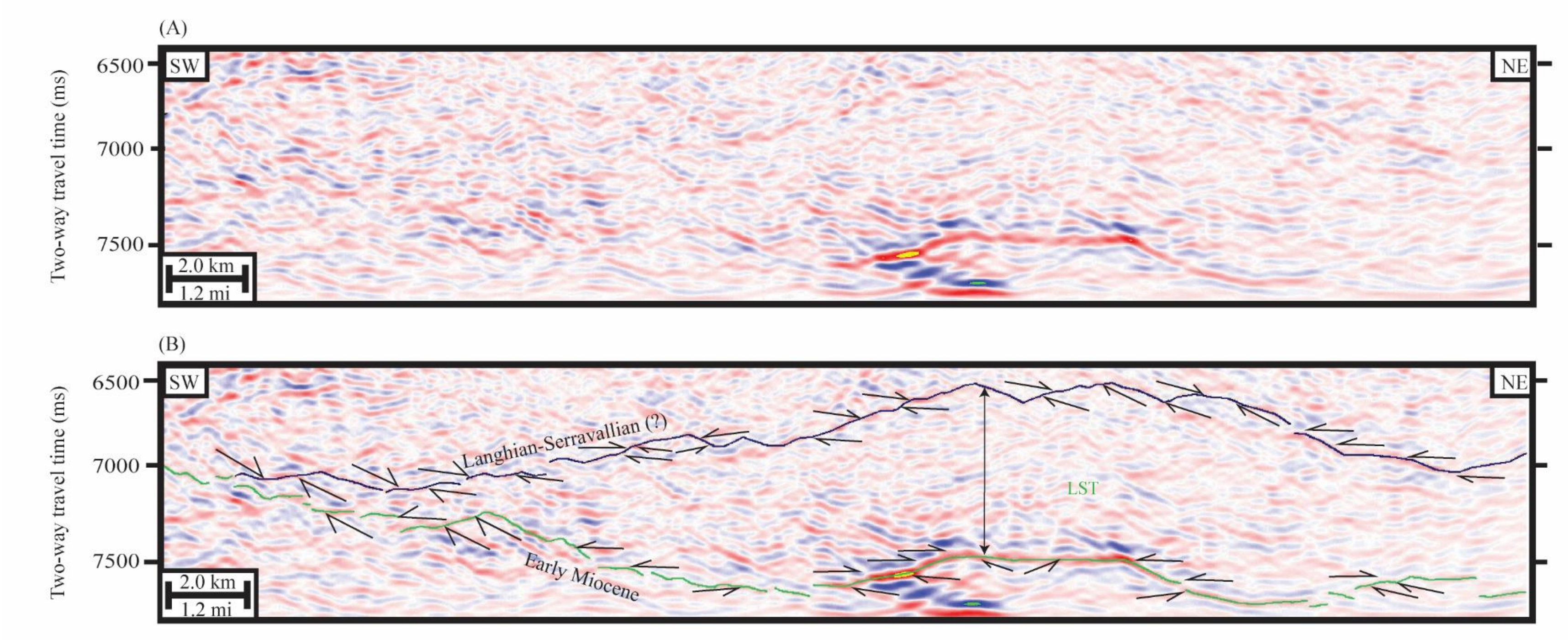

Figure 31: Seismic profile showing megasequence 1 across the 2016 3D-PSTM, strike-line number 4100. **(A)** uninterpreted **(B)** interpreted including sequence boundaries and stratal terminations. LST = Low-Stand system tract. Double-arrow indicates the thickest zone of this megasequence.

Location of this seismic section is shown in Figures 33 - 36.

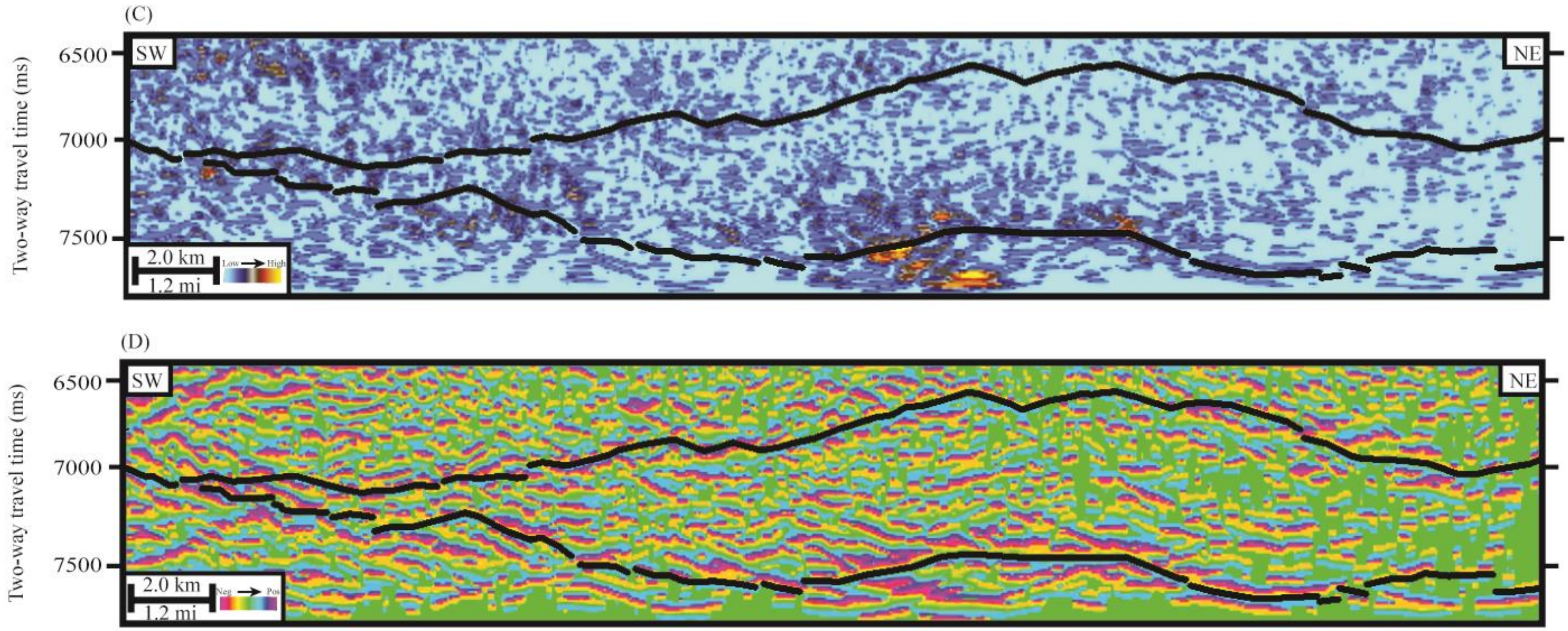

Figure 31: (C) Envelope seismic attribute **(D)** Instantaneous Phase seismic attribute.

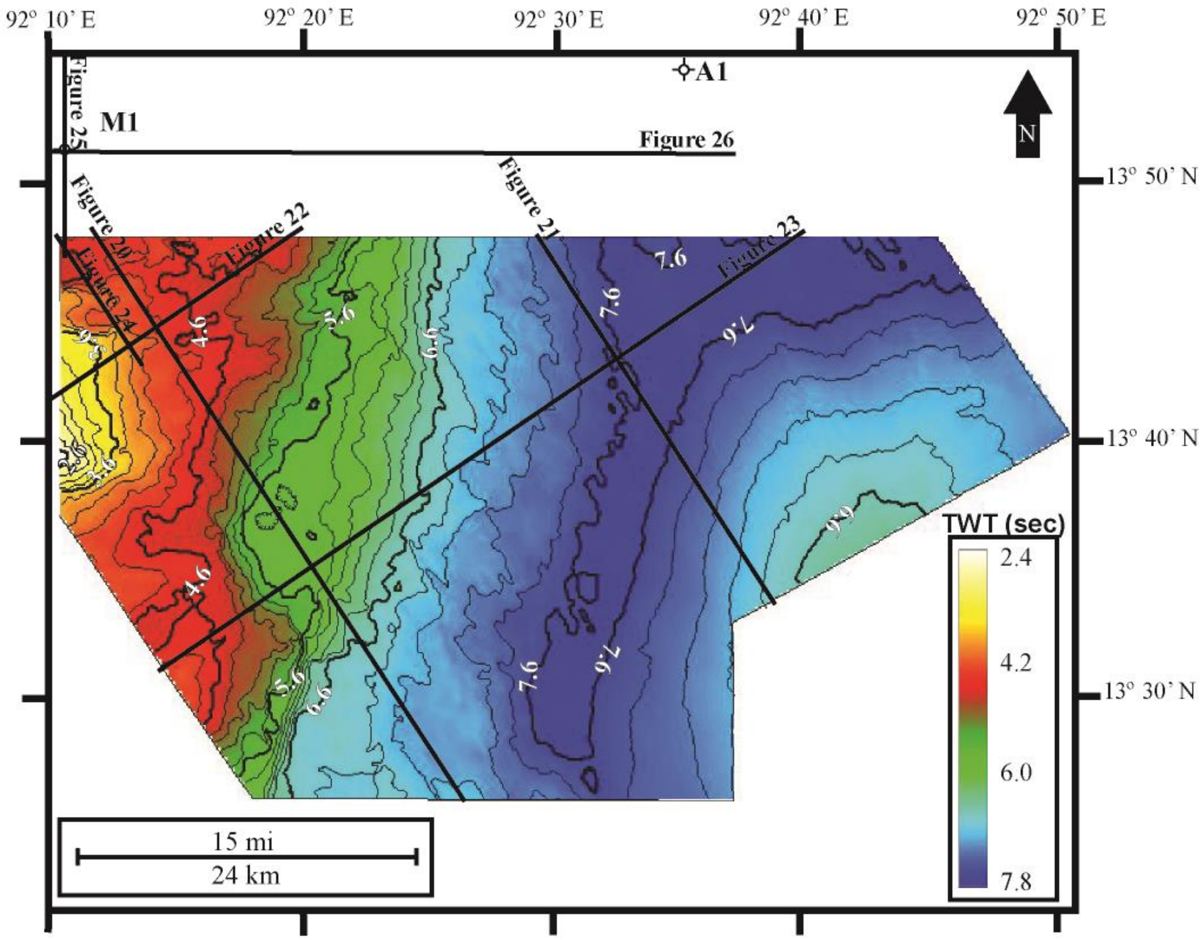

Figure 32: Time structure map of early Miocene (TWT). Contour interval is 200 milliseconds with bold contour in every one second.

Locations of Figures 20 – 26 are shown.

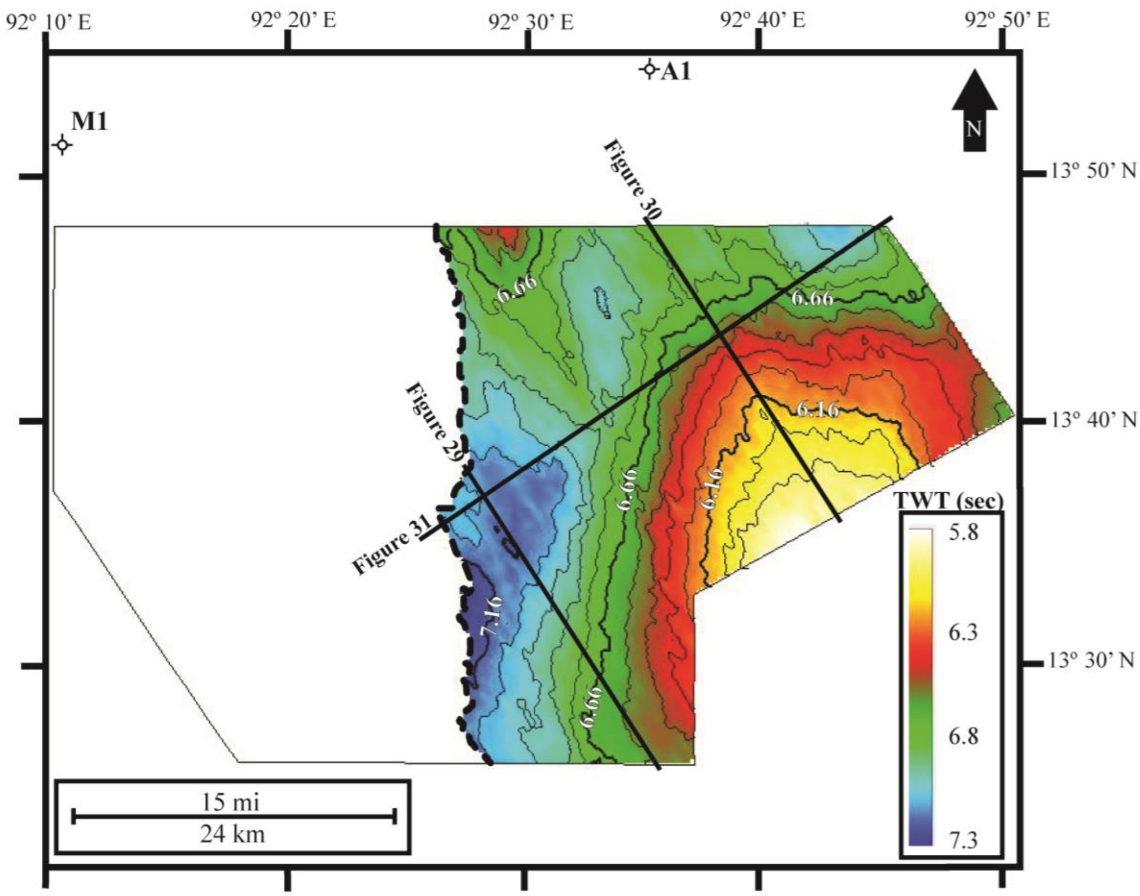

Figure 33: Time structure map of Langhian-Serravallian (?) (TWT). Contour interval is 100 milliseconds with bold contour in every 500 milliseconds. Dashed line is onlap edge.

Locations of Figures 29 – 31 are shown.

(TWT) (Figures 30, 31). The thickest part, between 0.83 to 1.10 seconds (TWT) (Figure 31), is located in the middle part of the map. The greatest time thickness is to the NE with thinning to the east and west. Abrupt thinning of the megasequence to the west is due to the onlap onto the top carbonate (Figure 29, 31). The main accommodation for this megasequence was controlled by the initial stage of NE-SW trans-tensional extension structure and associated subsidence.

Seismic Facies: Two seismic and geological facies were interpreted based, on the seismic attributes, i.e. instantaneous phase and envelope (Figure 35). The facies make trend NNE-SSW. Facies 1 is a series of hummocky and sub-parallel reflections, high amplitude with moderate to poor continuity (Figures 29 – 31). Facies 2 is a series of sub-parallel reflections with low amplitude and poor continuity (Figures 30, 31).

Geological Interpretation: The depositional environment map (Figure 36) was based on interpretation of seismic facies (Figure 35) and seismic attributes (Figure 36). The hummocky and sup-parallel reflection configuration with an elongated trend is interpreted as a submarine channel system, which includes muddy and sandy channel belts and levees. The distinguishing features of each part are recognized by the sweetness seismic attribute (Figure 36). The lower value of sweetness is indicates muddy channel fill as well as levee deposits. On the other hand, facies 2 is interpreted as muddy levees and distal overbank packages, which are separated by the sweetness seismic attribute as well. The higher value of sweetness of facies 2 is part of the muddy levees that were deposited from mud-rich channels or part of between levees and distal of overbanks. The channel belts have an overall N-S trend, with both NNE-SSW and NNW-SSE directions (Figure 35, 36).

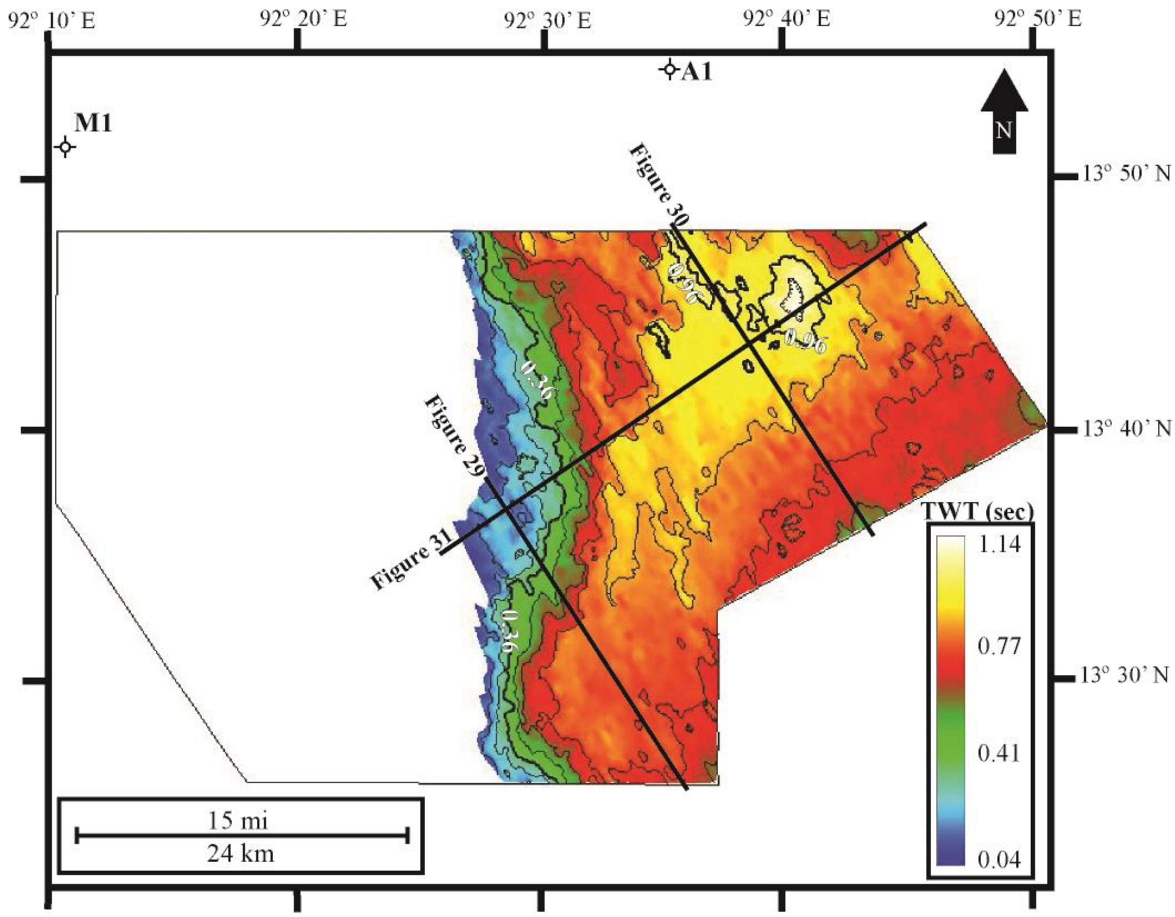

Figure 34: Isochron map of Langhian-Serravallian (?) megasequence (TWT). Contour interval is 120 milliseconds with bold contours every 600 milliseconds.

Locations of Figures 29 – 31 are shown.

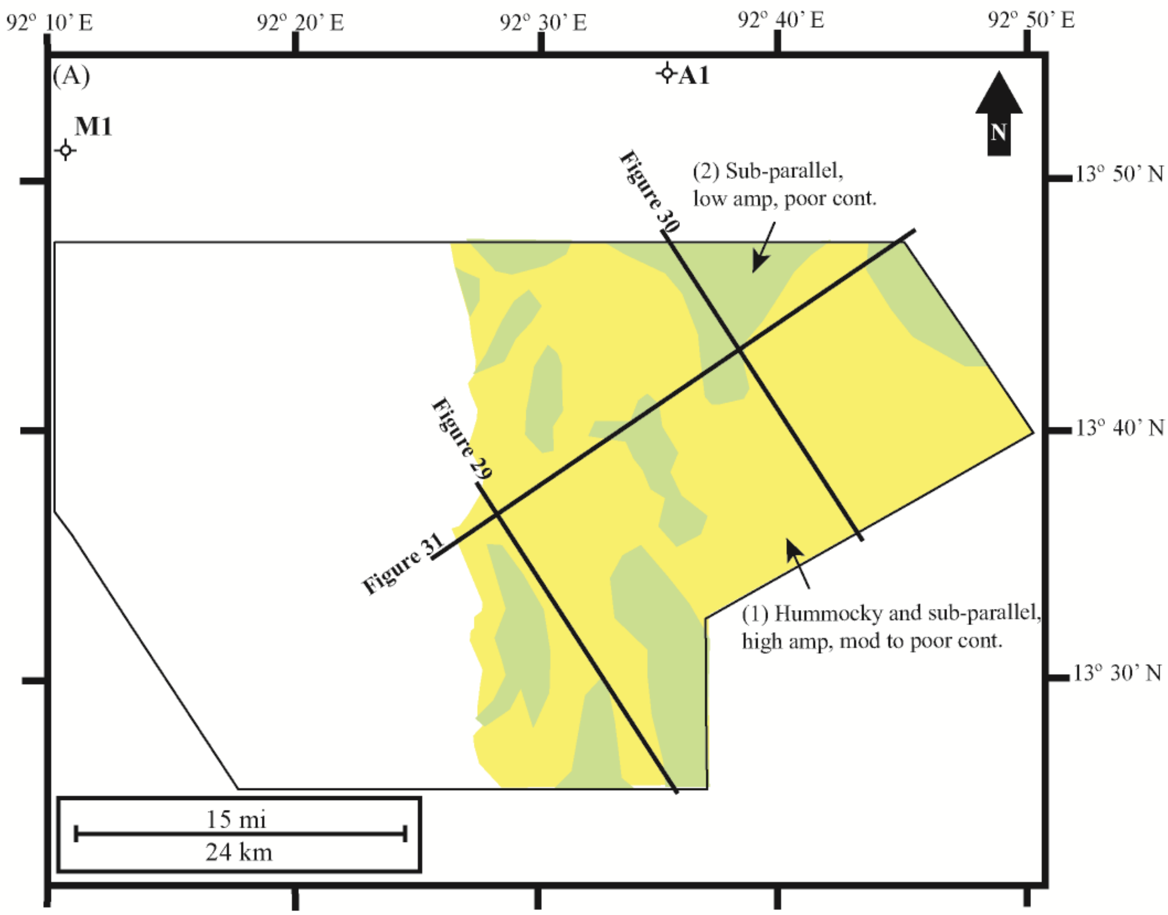

Figure 35: (A) Interpreted seismic facies map as yellow color is facies 1 and green color is facies 2. Each facies is listed by reflection configuration, following by amplitude (amp.) and continuity (cont.) classifications. **(B)** Envelope attribute map, calculated at 30 milliseconds below Langhian-Serravallian (?) surface. Map is twt unit. **(C)** Instantaneous Phase attribute map, calculated at 30 milliseconds below Langhian-Serravallian (?) surface. Map is degree of phase unit.

Locations of Figures 29 – 31 are shown.

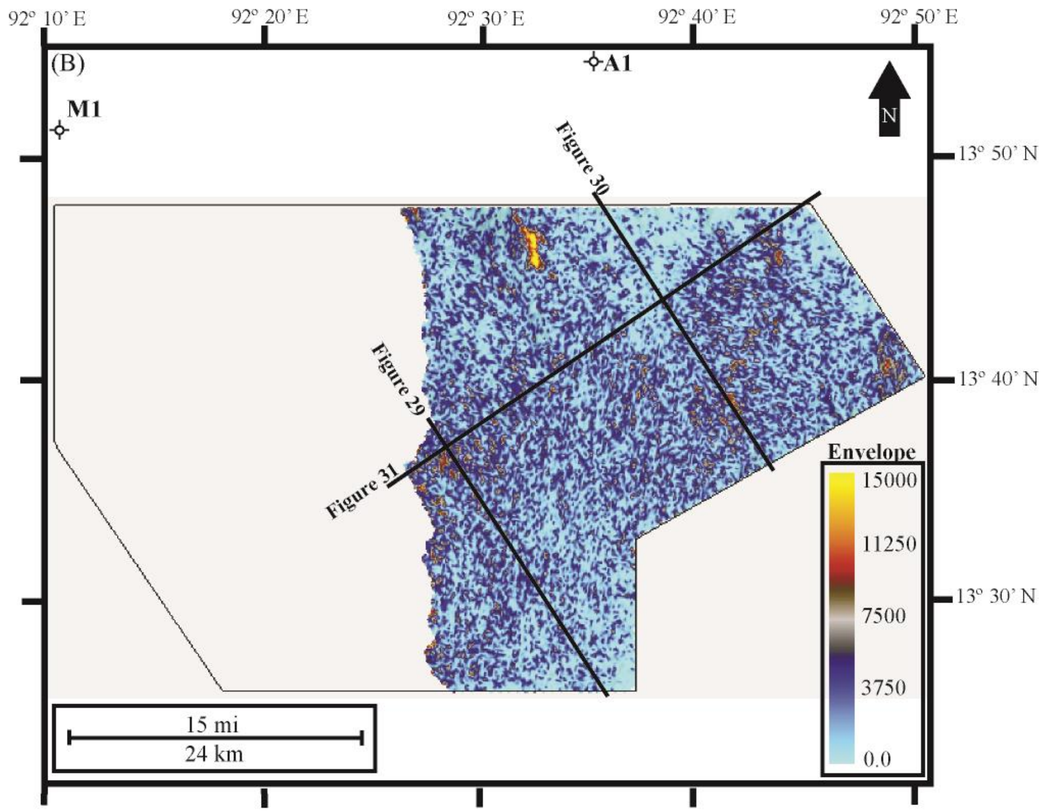
92° 10' E
92° 20' E
92° 30' E
92° 40' E
92° 50' E
(B)
A1
M1
N
13° 50' N
13° 40' N
13° 30' N
Figure 30
Figure 29
Figure 31
Envelope
15000
11250
7500
3750
0.0
15 mi
24 km

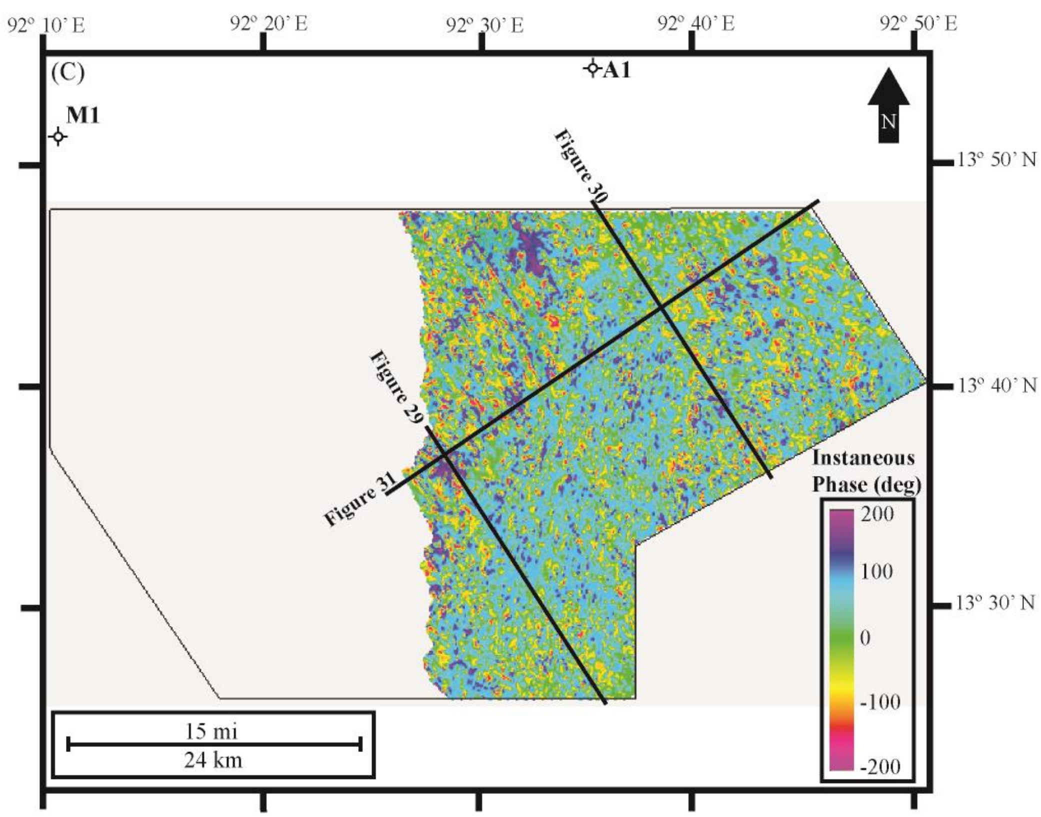
92° 10' E
92° 20' E
92° 30' E
92° 40' E
92° 50' E
(C)
A1
M1
N
13° 50' N
13° 40' N
13° 30' N
Figure 30
Figure 29
Figure 31
Instaneous
Phase (deg)
200
100
0
-100
-200
15 mi
24 km

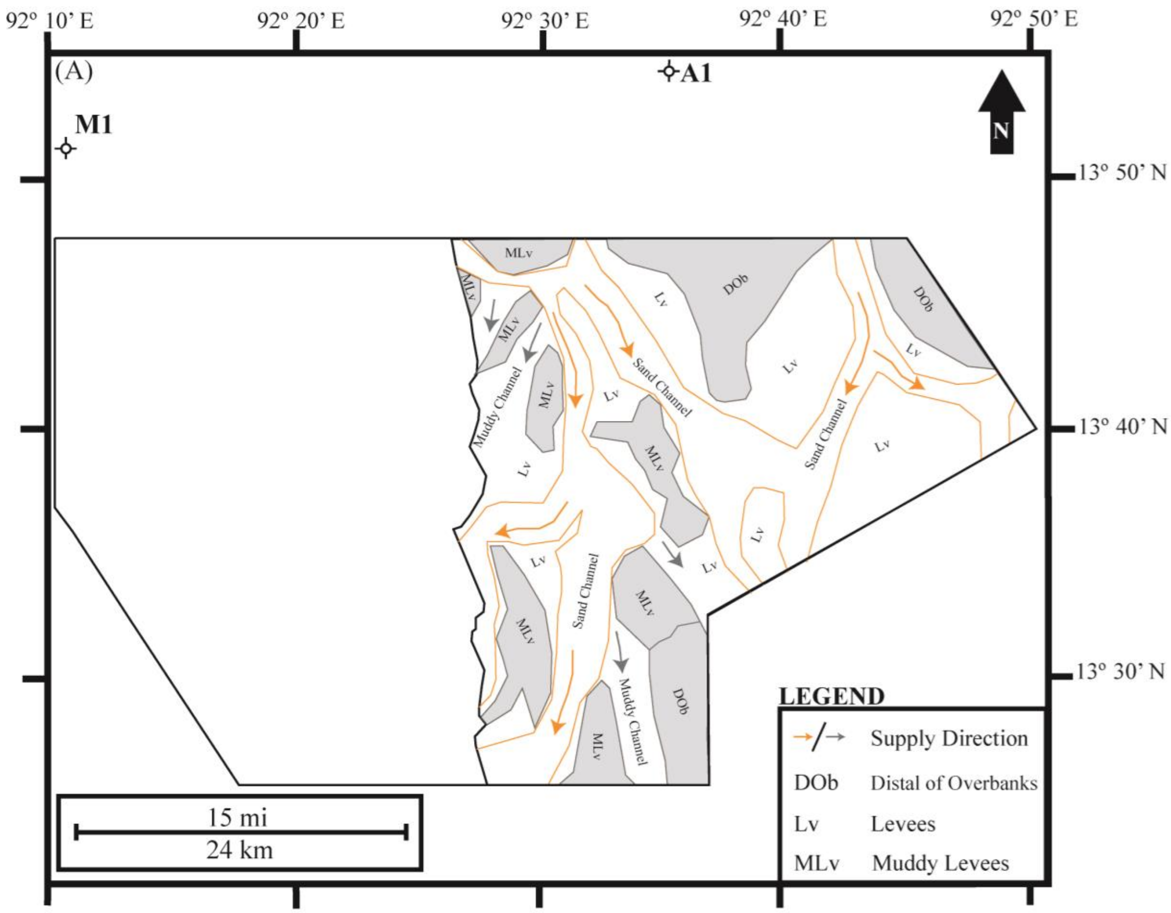

Figure 36: (A) Depositional setting map **(B)** Sweetness attribute map, calculated at 30 milliseconds below Langhian-Serravallian (?) surface. Map is absolute amplitude value in twt unit. **(C)** Coherency attribute map, calculated at 30 milliseconds below Langhian-Serravallian (?) surface.

Locations of Figures 29 – 31 are shown.

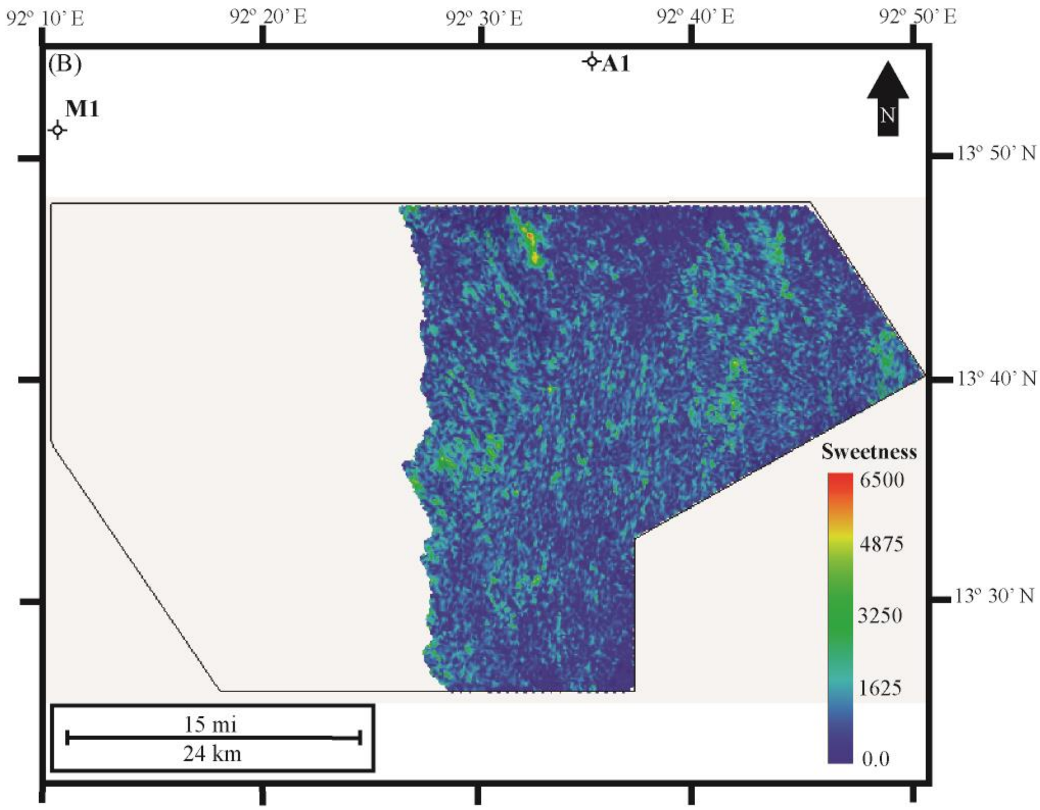
92° 10' E
92° 20' E
92° 30' E
92° 40' E
92° 50' E
(B)
A1
M1
N
13° 50' N
13° 40' N
13° 30' N
Sweetness
6500
4875
3250
1625
0.0
15 mi
24 km

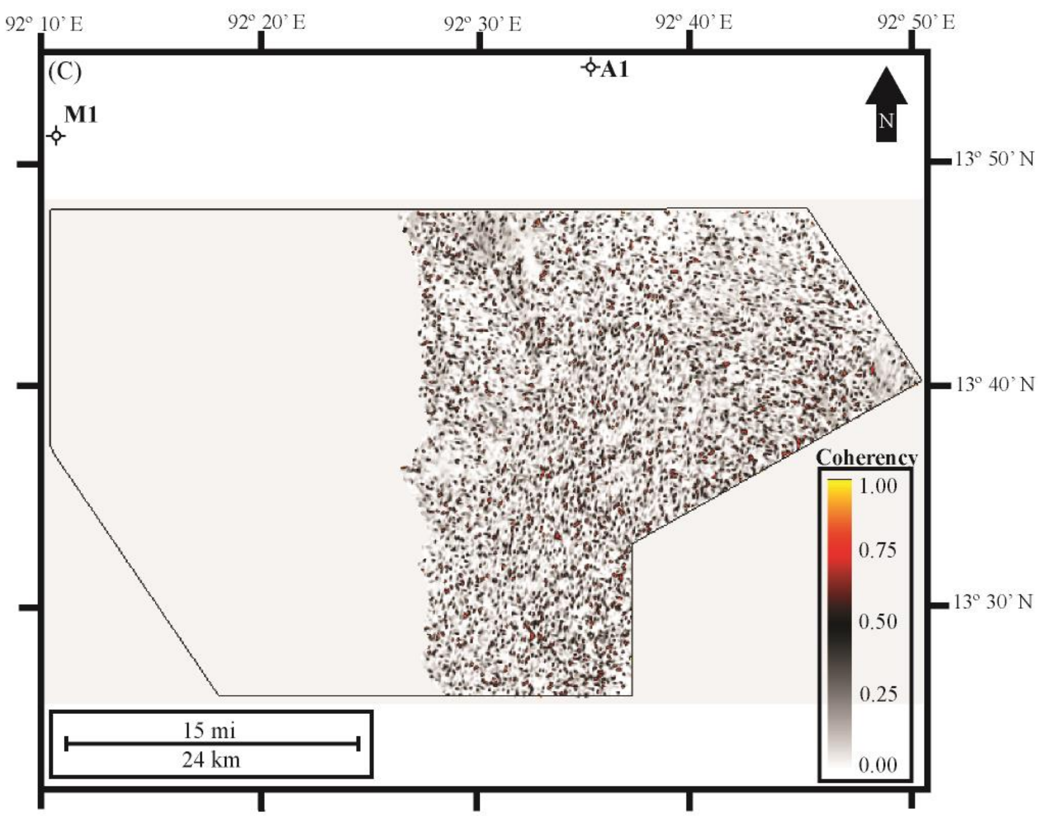
92° 10' E
92° 20' E
92° 30' E
92° 40' E
92° 50' E
(C)
A1
M1
N
13° 50' N
13° 40' N
13° 30' N
Coherency
1.00
0.75
0.50
0.25
0.00
15 mi
24 km

Megasequence 2: Tortonian (?)

Key Surfaces: The lower sequence boundary was defined by the merged surface consisting of early Miocene horizon and the upper sequence boundary of megasequence 1 (Figures 20, 37 - 40). The main criteria for defining the horizon is onlap onto both two horizons (Figures 37 - 40). Truncation is present underlying the surface. Moderate to high amplitude peak seismic reflector can be picked for this sequence boundary.

The upper sequence boundary (Tortonian (?)) was identified by a prominent erosional surface within the bottomset of clinoforms. Onlap and downlap reflections were defined overlying horizon (Figures 37 - 40). The seismic reflection has a moderate amplitude peak association. This sequence boundary onlaps onto early Miocene key surface (Figure 38).

Time-Structure Map: The structure map of the upper sequence boundary (Tortonian (?)) showing a north-trending syncline in the central part of the study area with two-way travel time value from 5.55 to 6.60 seconds (Figure 41). An anticlinal nose is present to the east that plunges to the north. The horizon shallows to the west, where it onlaps onto the early Miocene surface (Figure 38).

Isochron Map: The Tortonain (?) megasequence has two-way travel time values ranging from 0.01 to 1.18 seconds interval (Figure 42). Most of this megasequence is between 0.45 to 0.95 seconds twt (Figures 38, 39). The thickest part is located in the middle part of the area (0.64 to 1.18 seconds twt) (Figures 39, 42). The megasequence thins is to the west and east due to the onlap onto carbonate and the beneath structure high, respectively (Figures 37, 38 and 40).

Seismic Facies: Three seismic and geological facies were interpreted based on the seismic attributes, i.e. instantaneous phase and envelope (Figure 43). Facies 1 is a series of hummocky and sub-parallel reflections, moderate to high amplitude with moderate to poor continuity

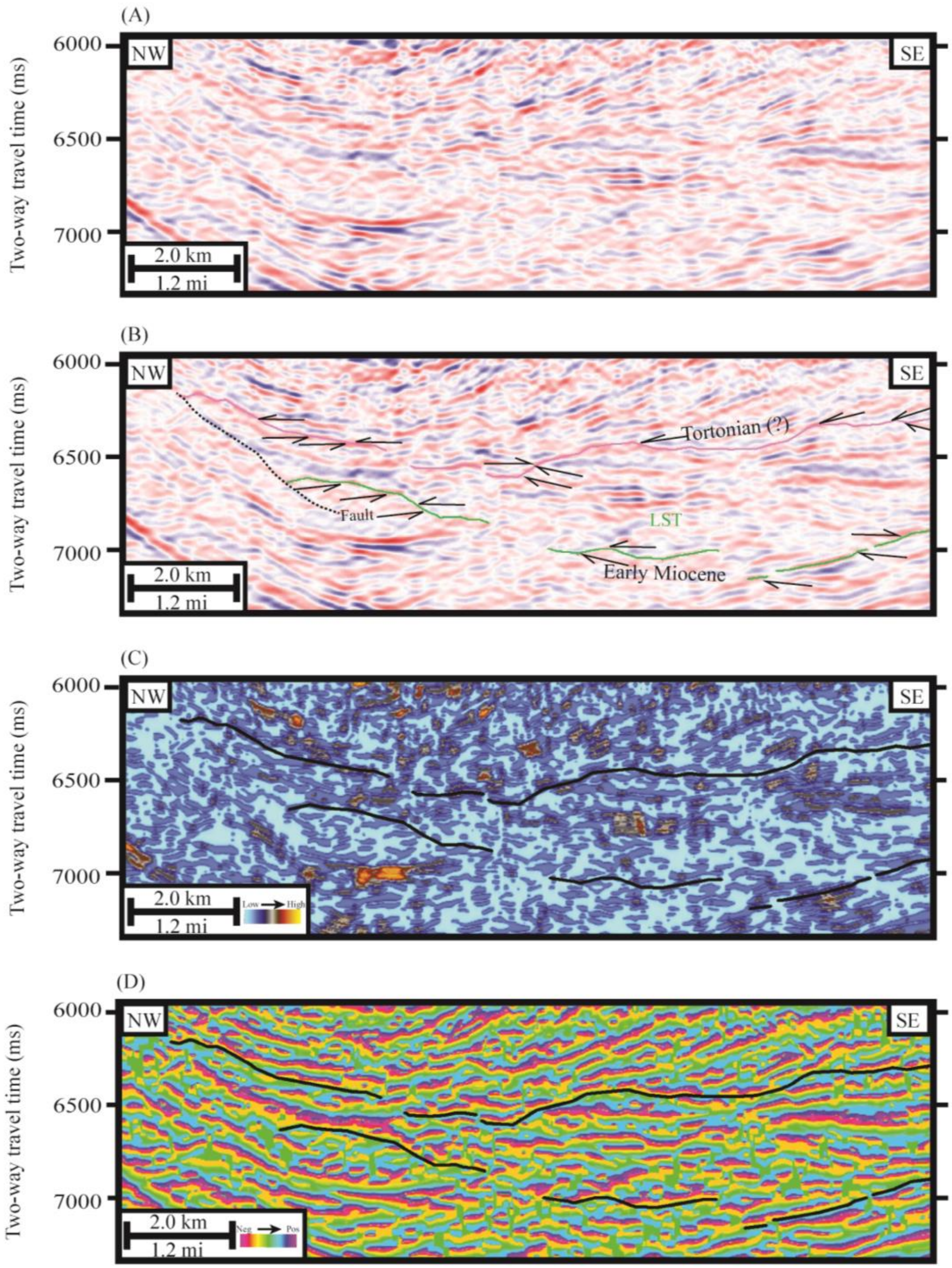

Figure 37: Seismic profile showing megasequence 2 across the 2016 3D-PSTM, dip-line number 2980. **(A)** uninterpreted **(B)** interpreted including sequence boundaries and stratal terminations. LST = Low-Stand system tract. **(C)** Envelope seismic attribute **(D)** Instantaneous Phase seismic attribute.

Location of this seismic section is shown in Figures 41 - 43.

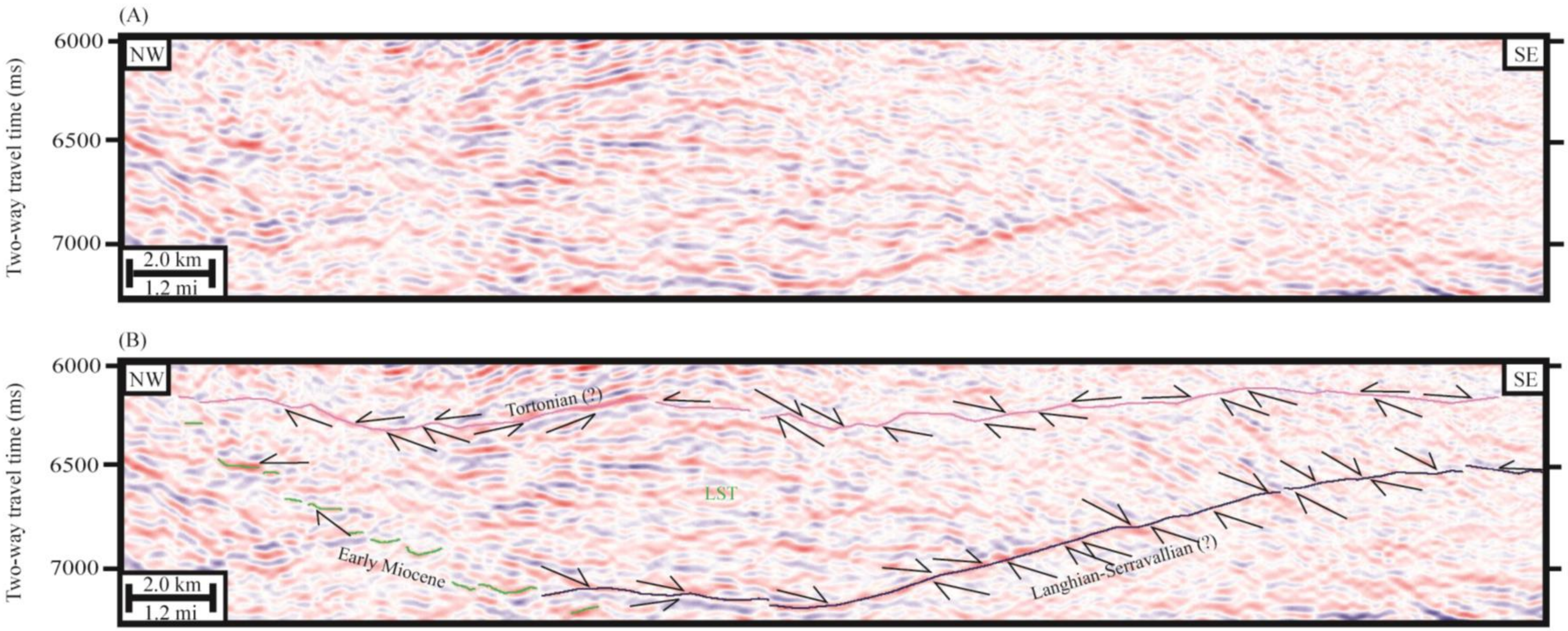

Figure 38: Seismic profile showing megasequence 2 across the 2016 3D-PSTM, dip-line number 4140. **(A)** uninterpreted **(B)** interpreted including sequence boundaries and stratal terminations. LST = Low-Stand system tract.

Location of this seismic section is shown in Figures 41 - 43.

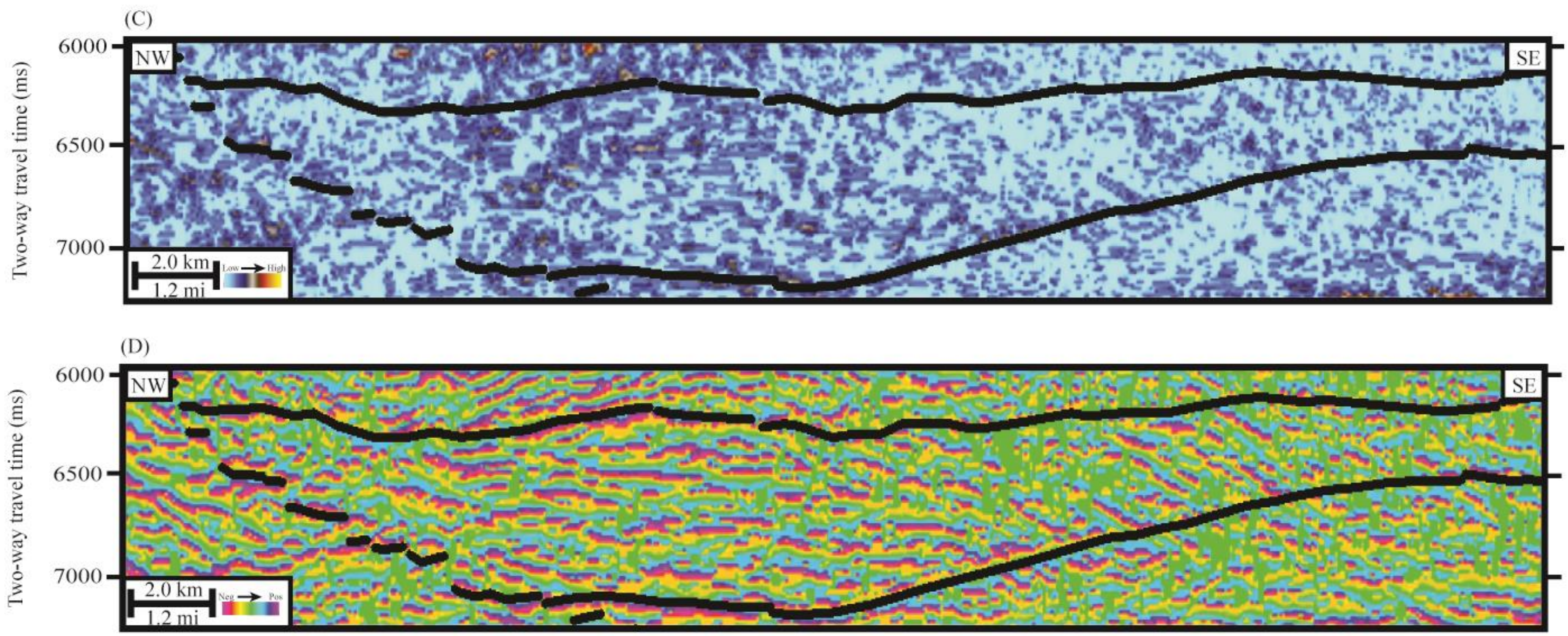

Figure 38: (C) Envelope seismic attribute **(D)** Instantaneous Phase seismic attribute.

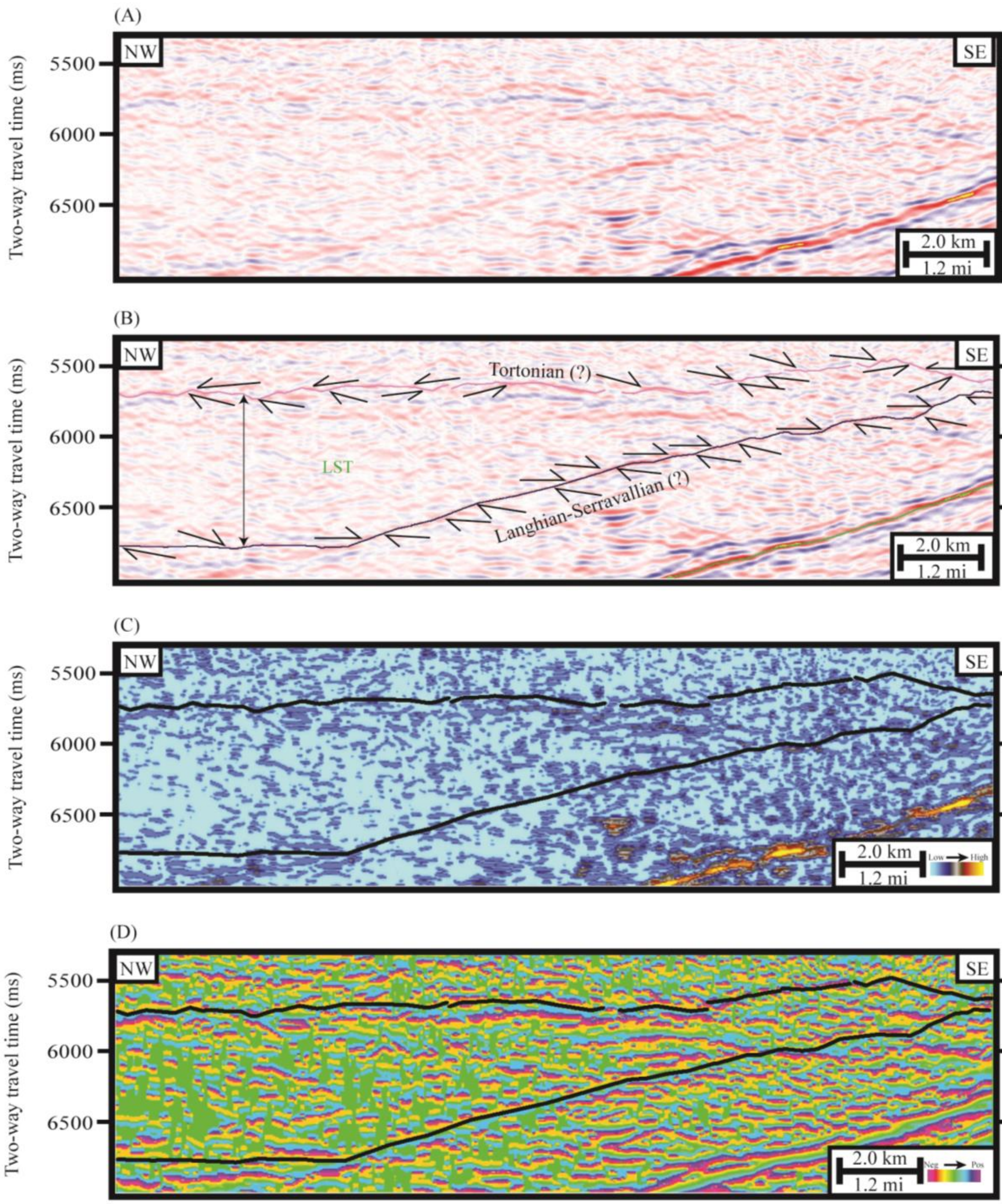

Figure 39: Seismic profile showing megasequence 2 across the 2016 3D-PSTM, dip-line number 5620. **(A)** uninterpreted **(B)** interpreted including sequence boundaries and stratal terminations. LST = Low-Stand system tract. Double-arrow indicates the thickest zone of this megasequence. **(C)** Envelope seismic attribute **(D)** Instantaneous Phase seismic attribute.

Location of this seismic section is shown in Figures 41 - 43.

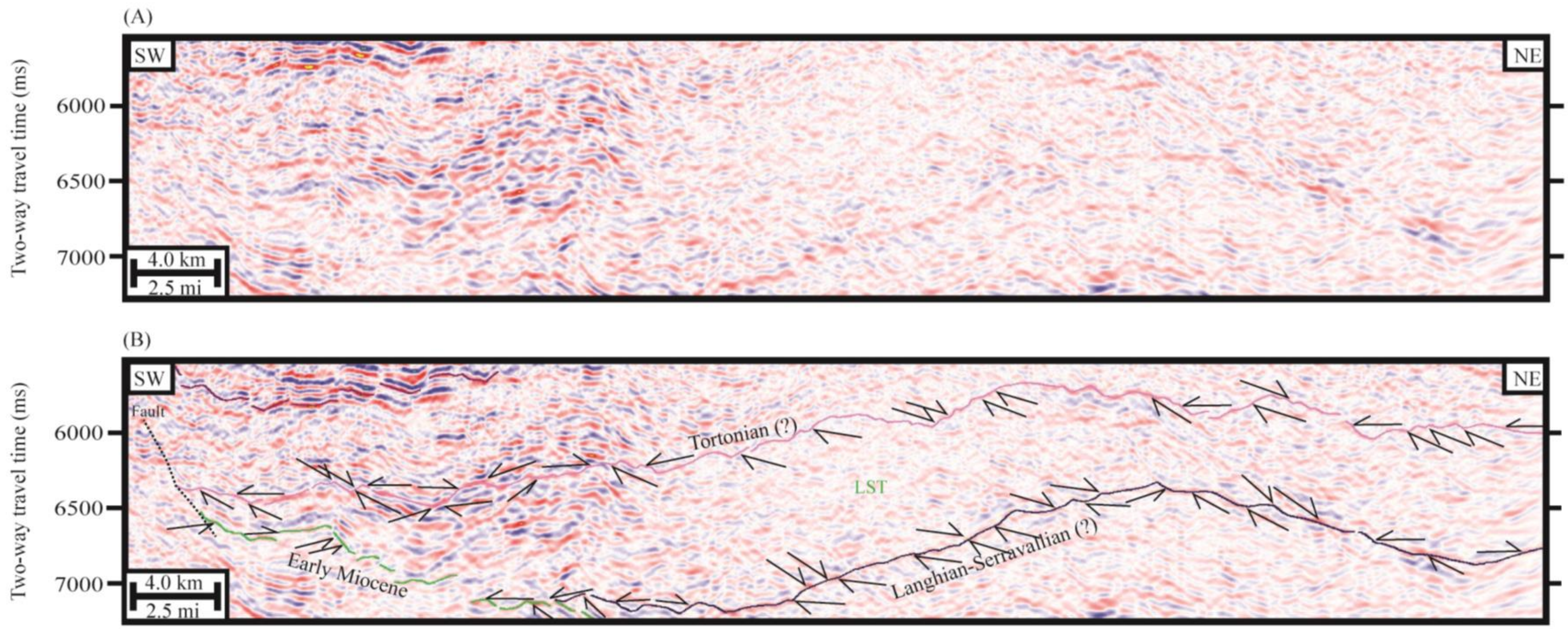

Figure 40: Seismic profile showing megasequence 2 across the 2016 3D-PSTM, strike-line number 3900. **(A)** uninterpreted **(B)** interpreted including sequence boundaries and stratal terminations. LST = Low-Stand system tract.

Location of this seismic section is shown in Figures 41 - 43.

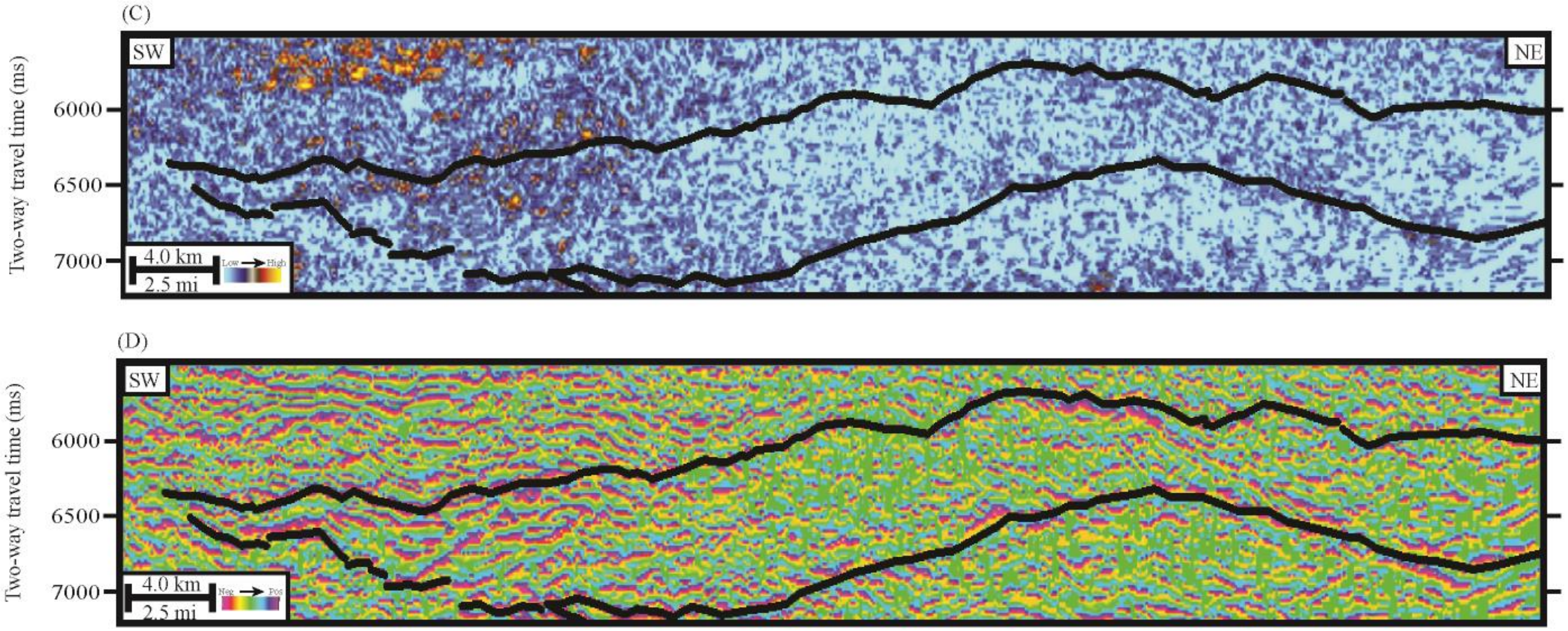

Figure 40: (C) Envelope seismic attribute **(D)** Instantaneous Phase seismic attribute.

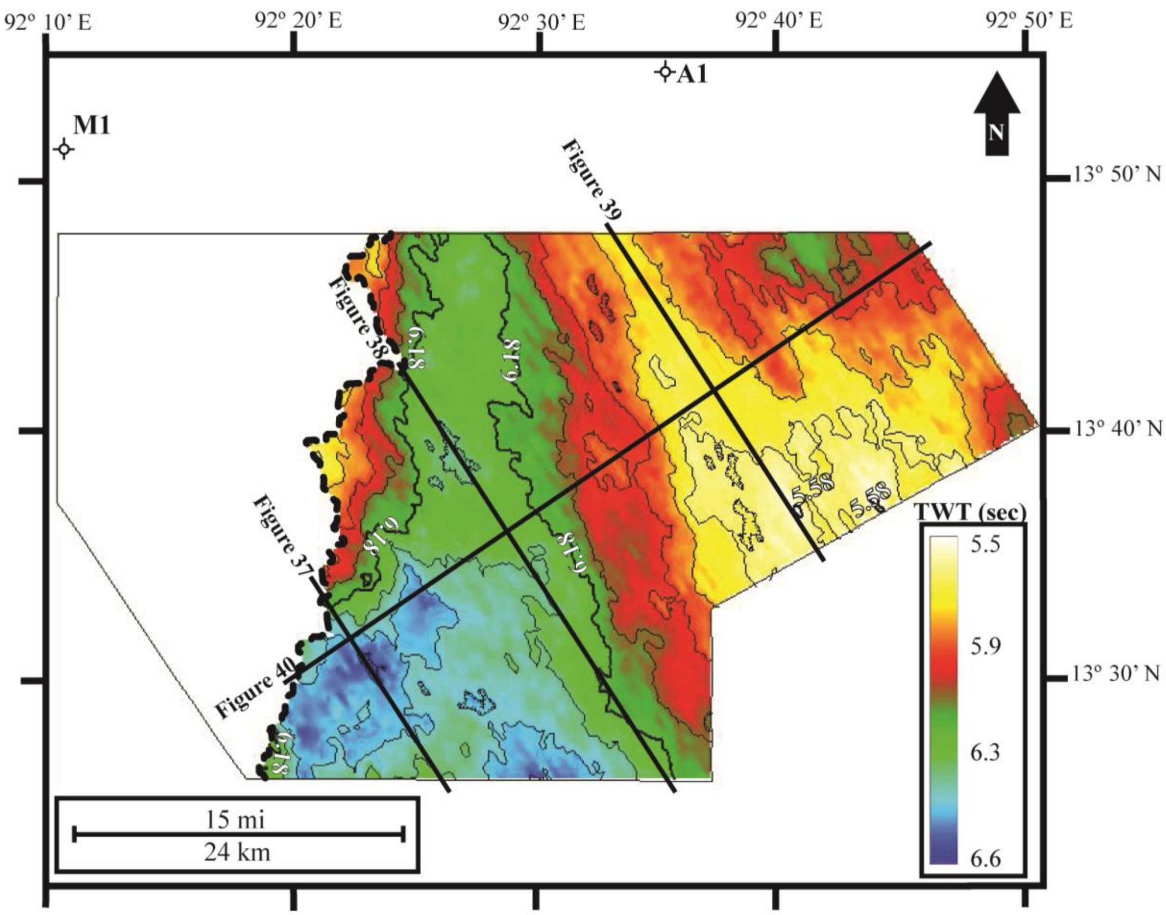

Figure 41: Time structure map of Tortonian (?) (TWT). Contour interval is 120 milliseconds with bold contour in every 600 milliseconds. Dashed line is onlap edge.

Locations of Figures 37 – 40 are shown.

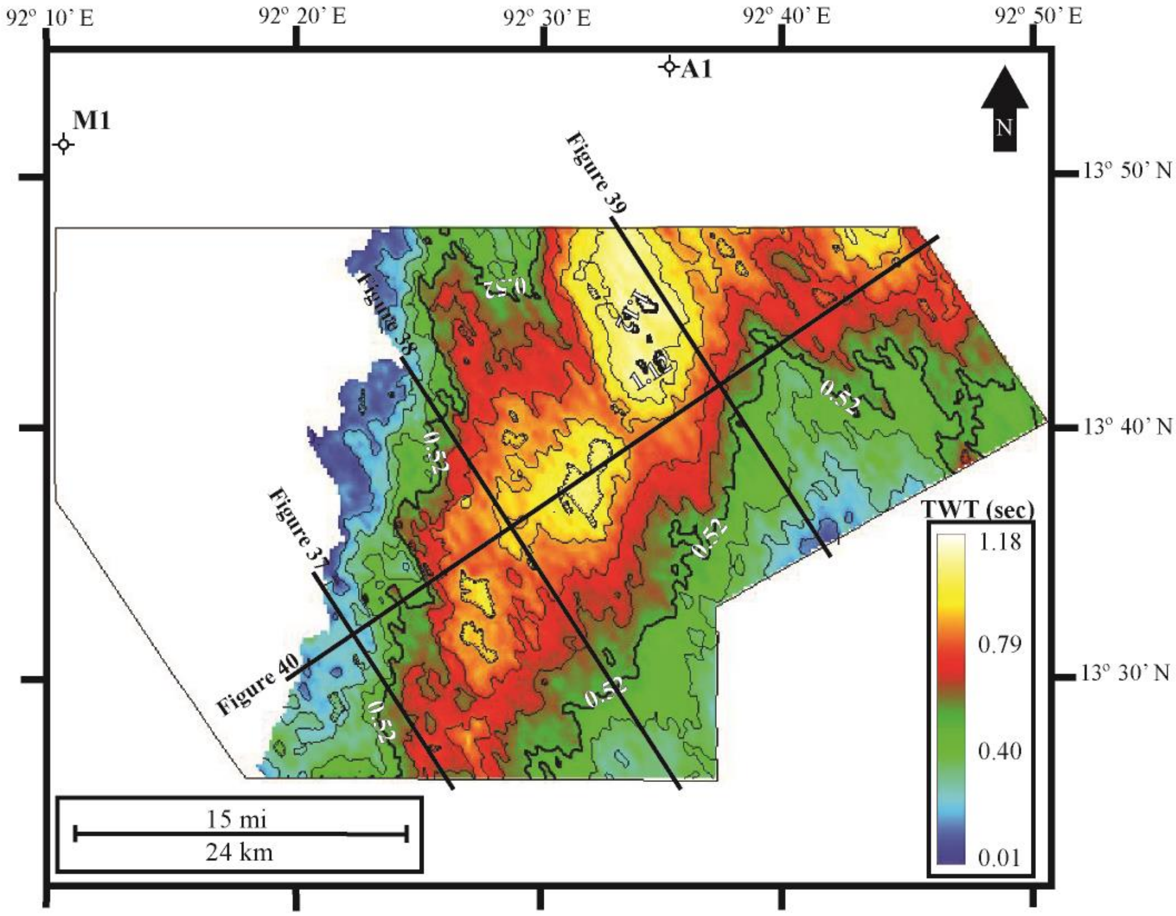

Figure 42: Isochron map of Tortonian (?) megasequence (TWT). Contour interval is 120 milliseconds with bold contour in every 600 milliseconds.

Locations of Figures 37 – 40 are shown.

(Figures 37, 40). Facies 2 is a series of hummocky, low amplitude with moderate to good continuity. This facies covers most of the area (Figures 38, 40). Facies 3 is a series of parallel reflections overlying hummocky, moderate amplitude with poor to good continuity (Figures 39, 40).

Geological Interpretation: The depositional environment map (Figure 44) was interpreted based on seismic facies (Figure 43) and seismic attributes (Figure 44). Two of three facies in this megasequence had hummocky seismic reflections with different amplitude value (Figures 37, 38, 40, 43), suggesting the same depositional environment in different parts of depositional lobes. Facies 1 was part of a proximal lobe with higher amplitude of seismic reflection and higher value of sweetness attribute. The middle lobe is assigned as part of facies 2. Sediment supply is interpreted as coming from West to East direction, aligned to proximal and middle lobes. Channel belts trend in NNW-SSE direction are part of facies 3 (Figures 43, 44).

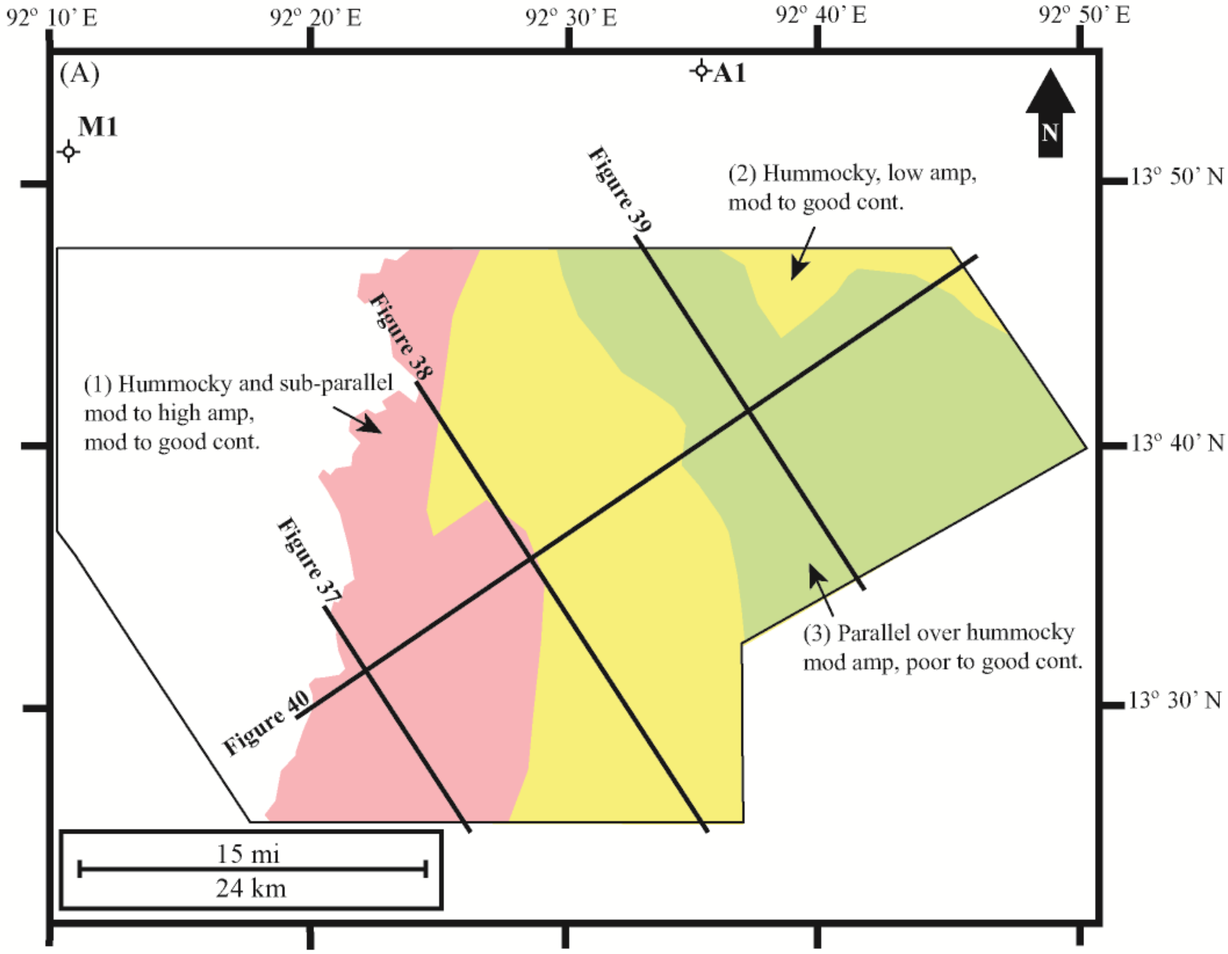

Figure 43: (A) Interpreted seismic facies map as pink color is facies 1, yellow color is facies 2 and green color is facies 3. Each facies is listed by reflection configuration, following by amplitude (amp.) and continuity (cont.) classifications. **(B)** Envelope attribute map, calculated at 30 milliseconds below Tortonian (?) surface. Map is twt unit. **(C)** Instantaneous Phase attribute map, calculated at 30 milliseconds below Tortonian (?) surface. Map is degree of phase unit.

Locations of Figures 37 – 40 are shown.

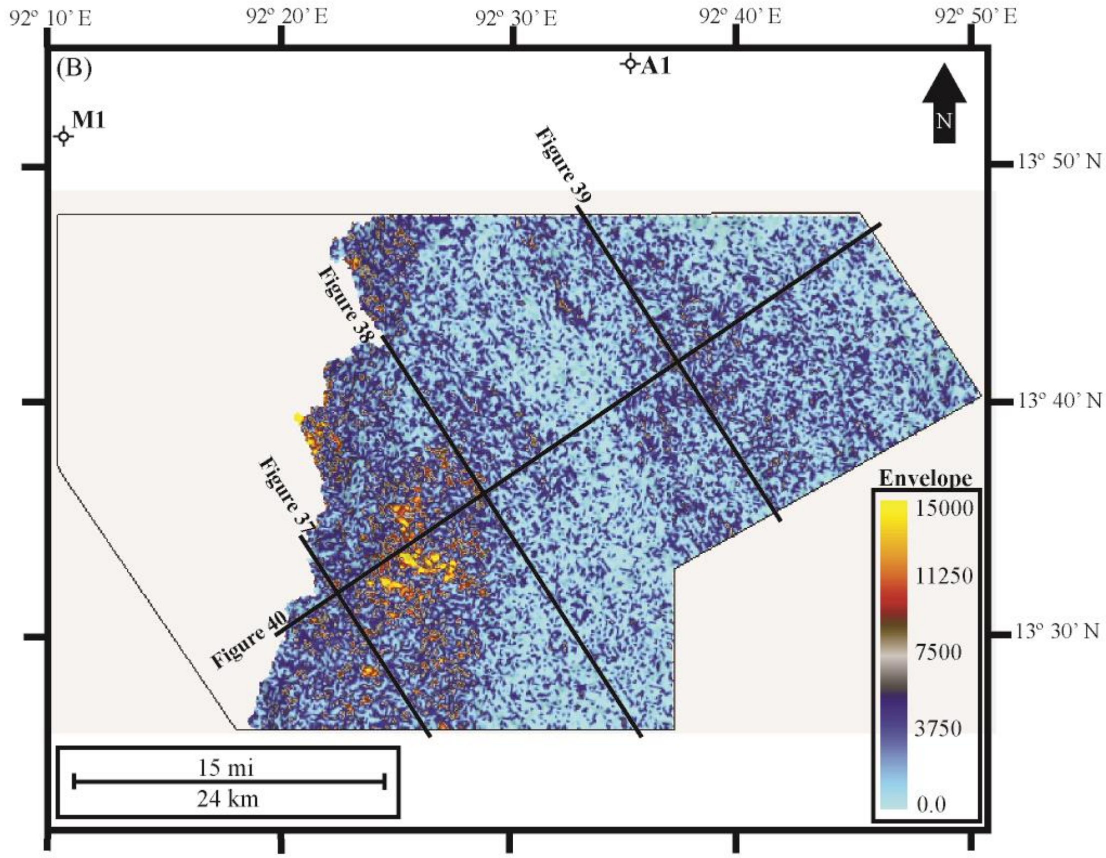

92º 10' E
92º 20' E
92º 30' E
92º 40' E
92º 50' E
(B)
A1
M1
N
13º 50' N
13º 40' N
13º 30' N
Figure 39
Figure 38
Figure 37
Figure 40
Envelope
15000
11250
7500
3750
0.0
15 mi
24 km

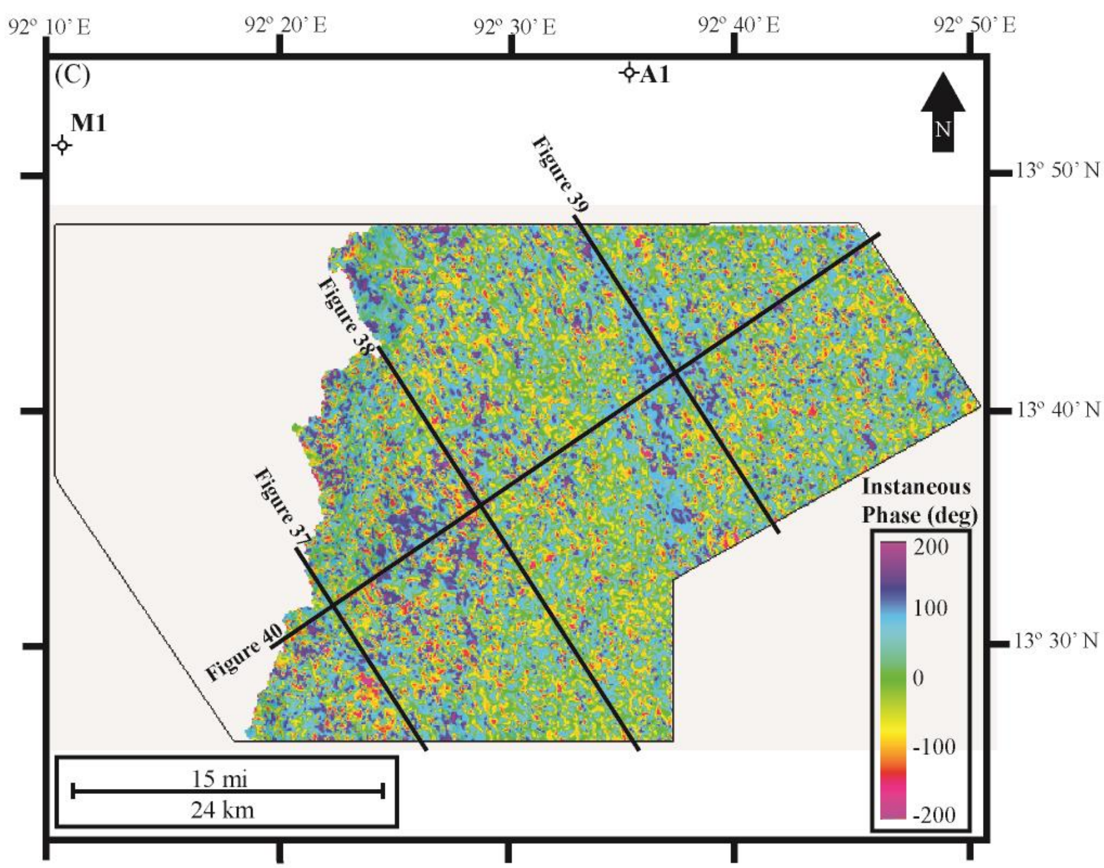

92º 10' E
92º 20' E
92º 30' E
92º 40' E
92º 50' E
(C)
A1
M1
N
13º 50' N
13º 40' N
13º 30' N
Figure 39
Figure 38
Figure 37
Figure 40
Instaneous
Phase (deg)
200
100
0
-100
-200
15 mi
24 km

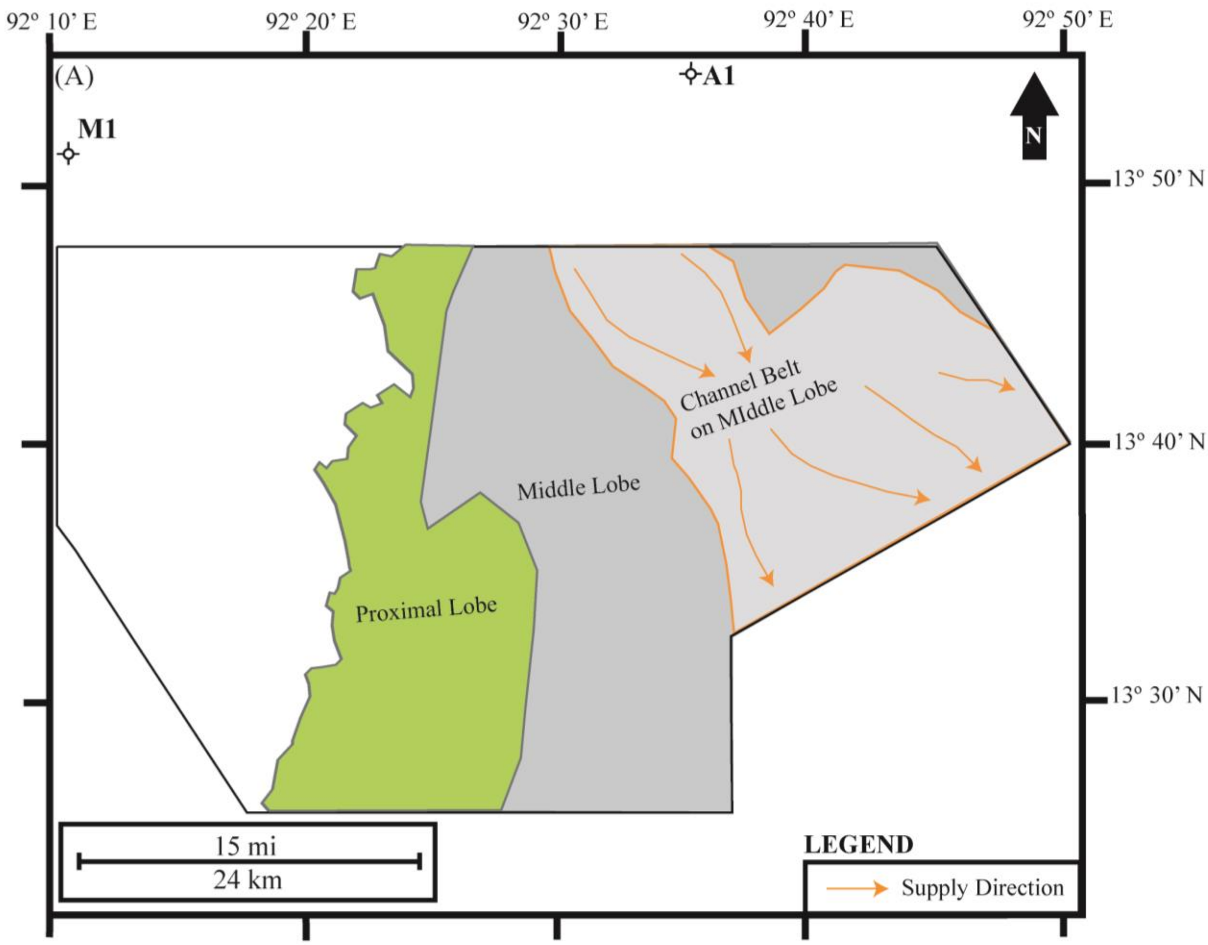

Figure 44: (A) Depositional setting map **(B)** Sweetness attribute map, calculated at 30 milliseconds below Tortonian (?) surface. Map is absolute amplitude value in twt unit. **(C)** Coherency attribute map, calculated at 30 milliseconds below Tortonian (?) surface.

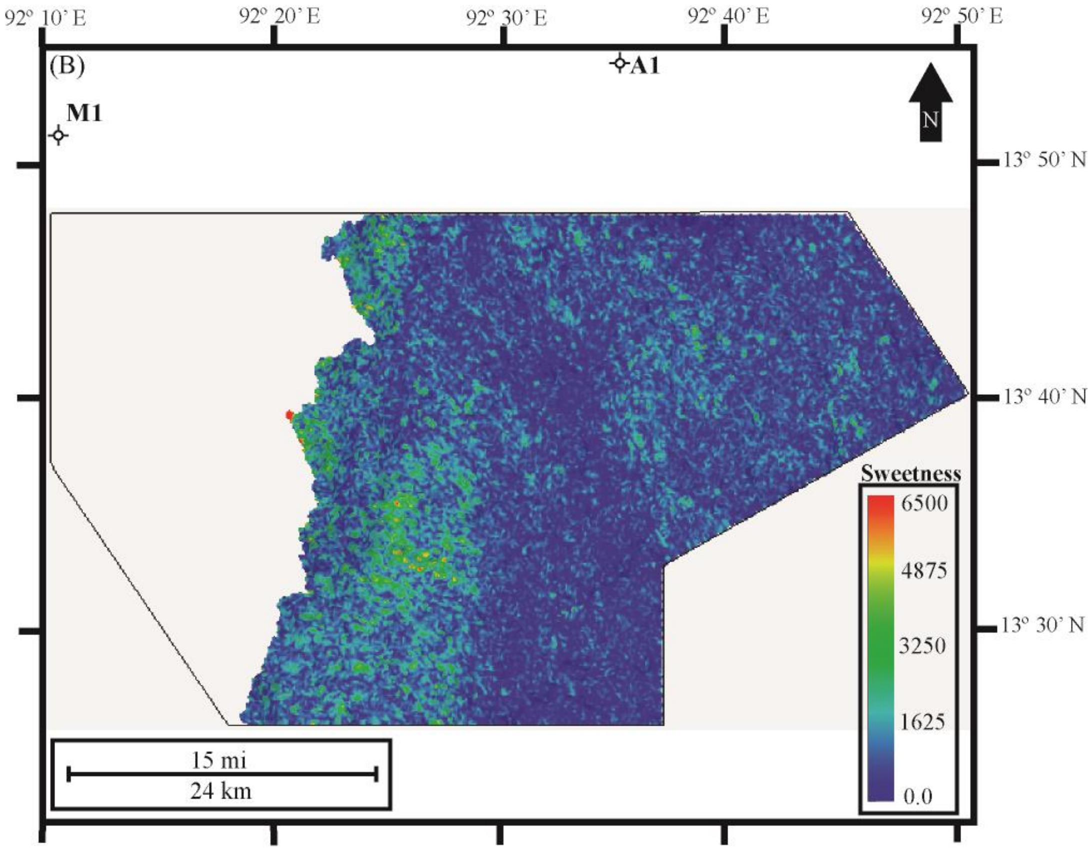

92° 10' E
92° 20' E
92° 30' E
92° 40' E
92° 50' E
(B)
A1
M1
N
13° 50' N
13° 40' N
13° 30' N
Sweetness
6500
4875
3250
1625
0.0
15 mi
24 km

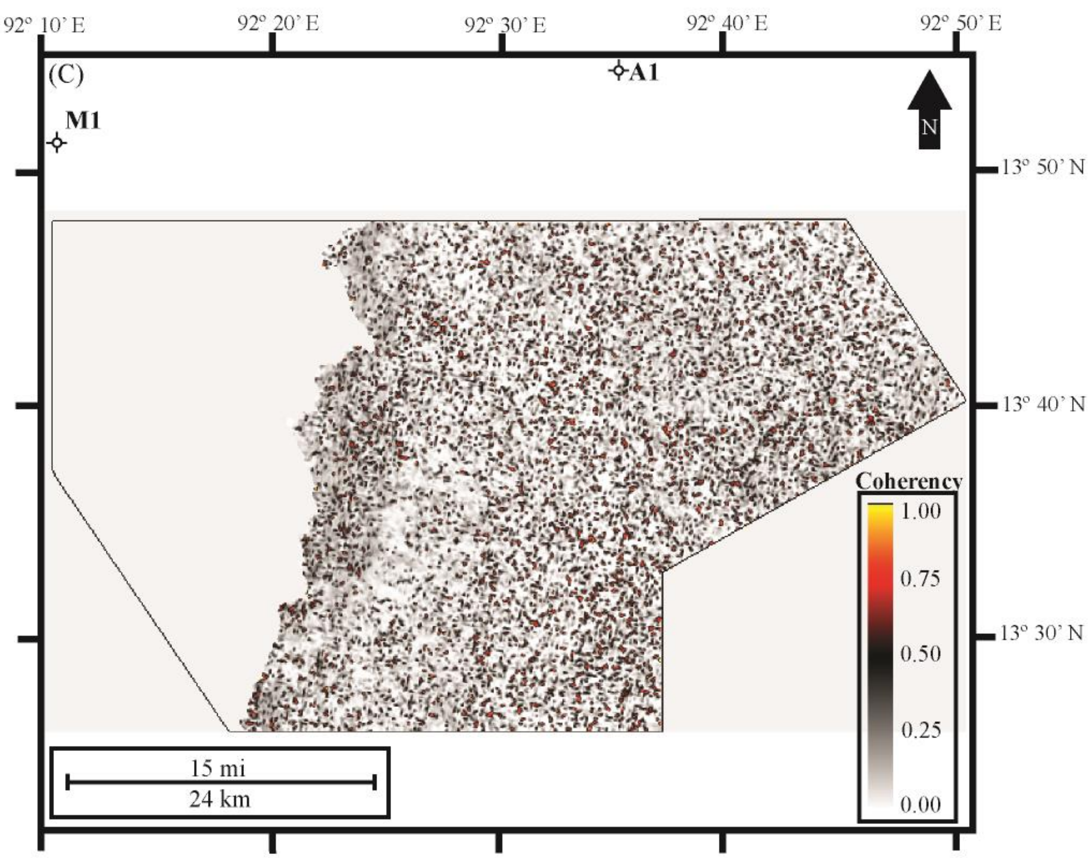

92° 10' E
92° 20' E
92° 30' E
92° 40' E
92° 50' E
(C)
A1
M1
N
13° 50' N
13° 40' N
13° 30' N
Coherency
1.00
0.75
0.50
0.25
0.00
15 mi
24 km

Megasequence 3: Messinian (?)

Key Surfaces: The lower sequence boundary corresponds to the upper sequence boundary of megasequence 2 (Tortonian (?)) and early Miocene surface (Figures 20, 45 - 48). Onlap and truncation features are used to define the surface (Figures 45 - 48). Moderate to high amplitude peak seismic reflector can be picked as this sequence boundary.

The upper sequence boundary (Top Miocene) was identified by the unconformity using clear onlap and truncation at above and below the horizon, respectively (Figures 45 – 48). The seismic reflection is pick on a high amplitude peak association. In the M1 well, this surface correlates to the distinct change between Miocene to Pliocene section (Figure 28).

Time-Structure Map: The structure map of the upper sequence boundary (Top Miocene) is showing a syncline in the central part of the study area in north trending with two-way travel time value from 5.55 to 6.60 seconds (Figure 49). An anticlinal nose is present to the east that plunges to the north. The horizon shallows to the west, where it onlaps onto the early Miocene surface (Figure 48).

Isochron Map: The Messinian (?) megasequence has the two-way travel time values ranging from 0.01 to 1.17 seconds interval (Figure 50). Most of area has an isothick between 0.54 to 0.99 seconds twt (Figures 46, 47). The thickest part is located in the middle part of the area (0.63 to 1.17 seconds twt) (Figure 47). The megasequence thins is to the west due to onlap onto carbonate buildup and underlying structural high (Figures 45 and 48).

Seismic Facies: Four seismic and geological facies that were interpreted based on the seismic attributes, i.e. instantaneous phase and envelope (Figure 51). Overall, the facies trend N-S and partially NW-SE and NE-SW direction. Facies 1 is a series of parallel reflections with some hummocky mounded; they have high amplitude with moderate continuity. This facies is mainly

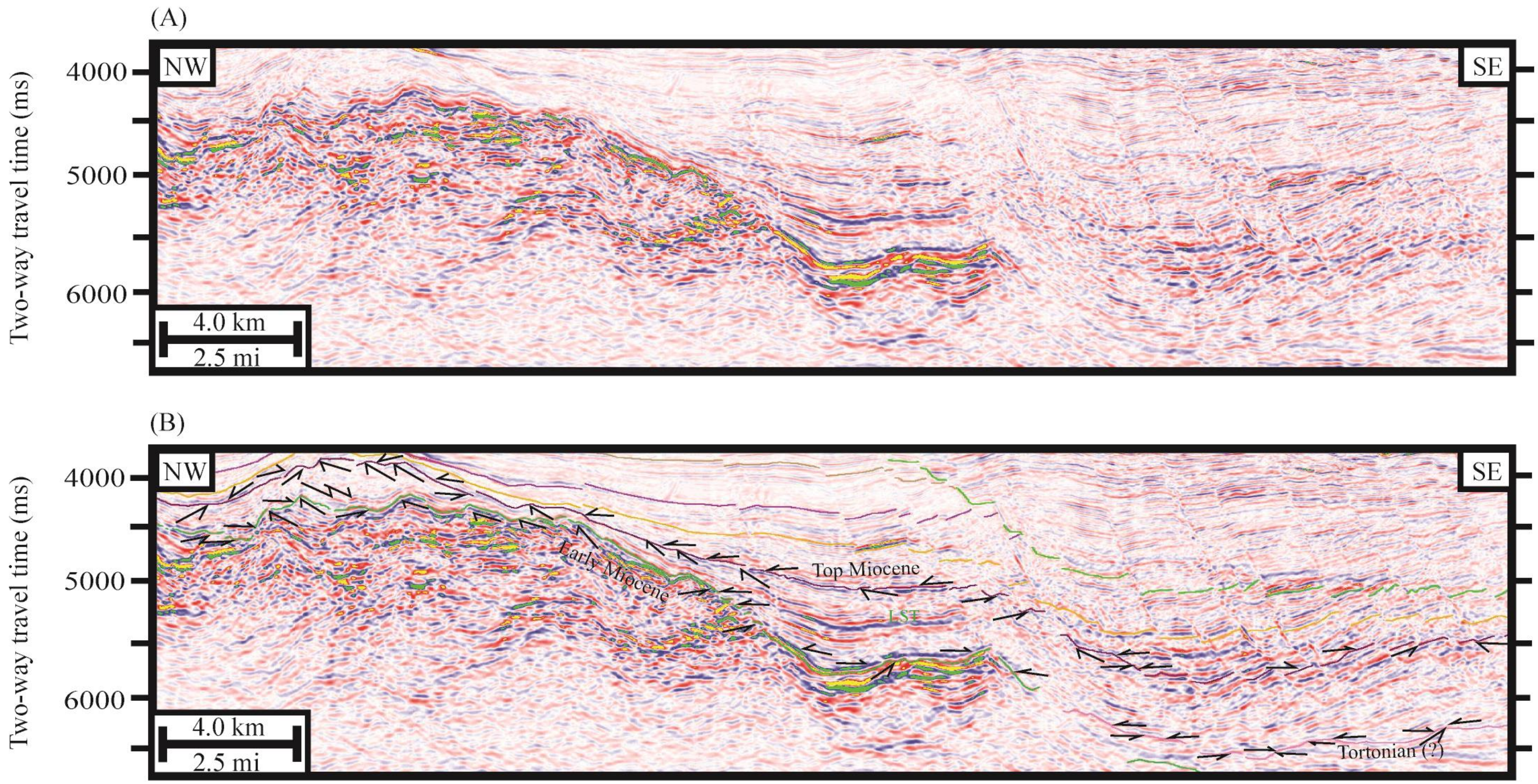

Figure 45: Seismic profile showing megasequence 3 across the 2016 3D-PSTM, dip-line number 2980. **(A)** uninterpreted **(B)** interpreted including sequence boundaries and stratal terminations. LST = Low-Stand system tract.

Location of this seismic section is shown in Figures 49 - 51.

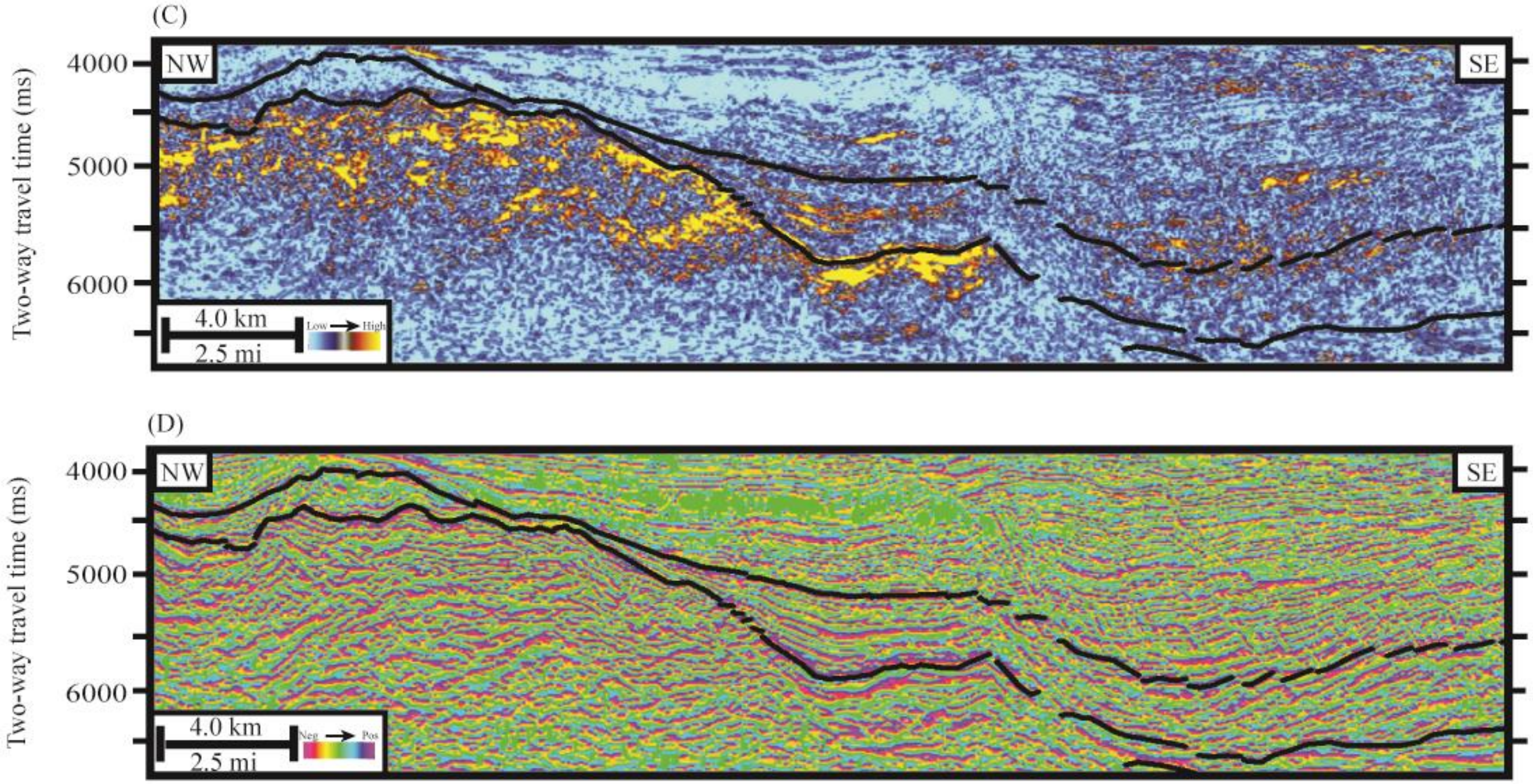

Figure 45: (C) Envelope seismic attribute **(D)** Instantaneous Phase seismic attribute.

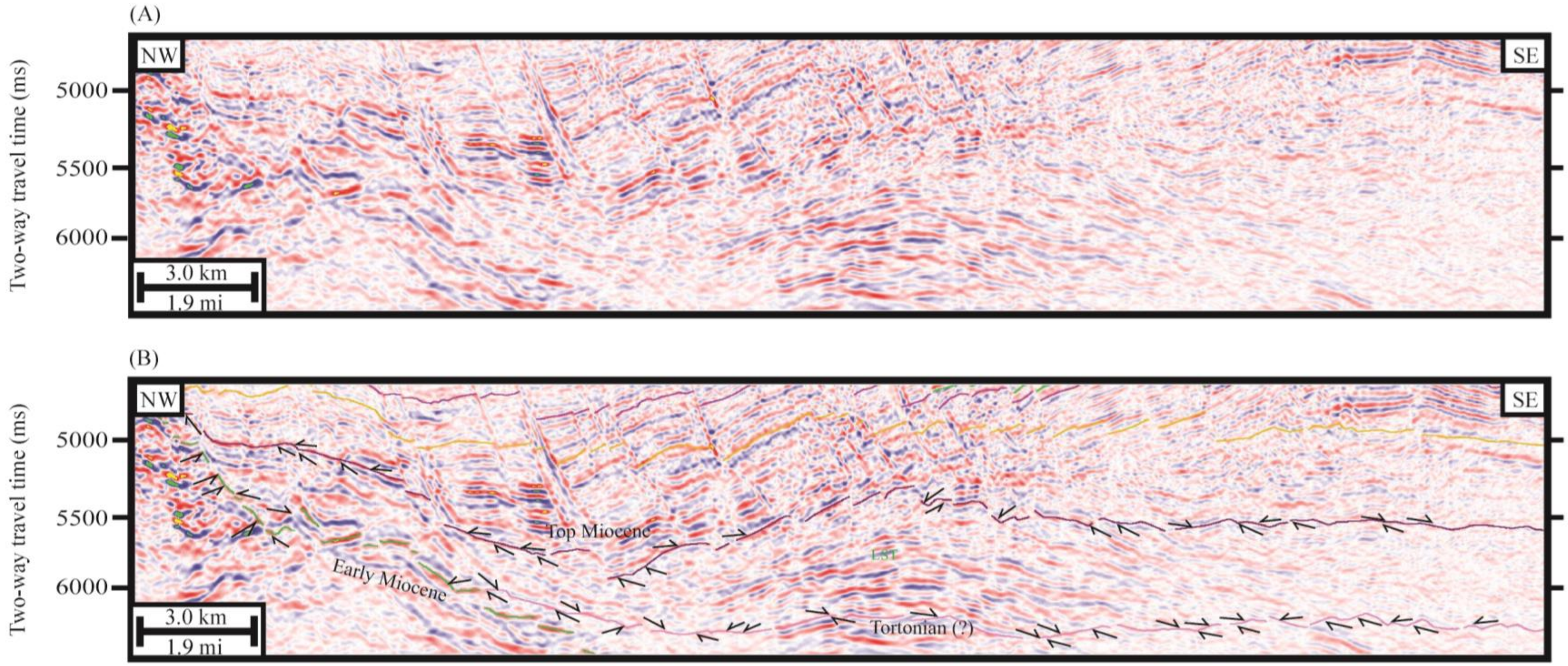

Figure 46: Seismic profile showing megasequence 3 across the 2016 3D-PSTM, dip-line number 4020. **(A)** uninterpreted **(B)** interpreted including sequence boundaries and stratal terminations. LST = Low-Stand system tract.

Location of this seismic section is shown in Figures 49 - 51.

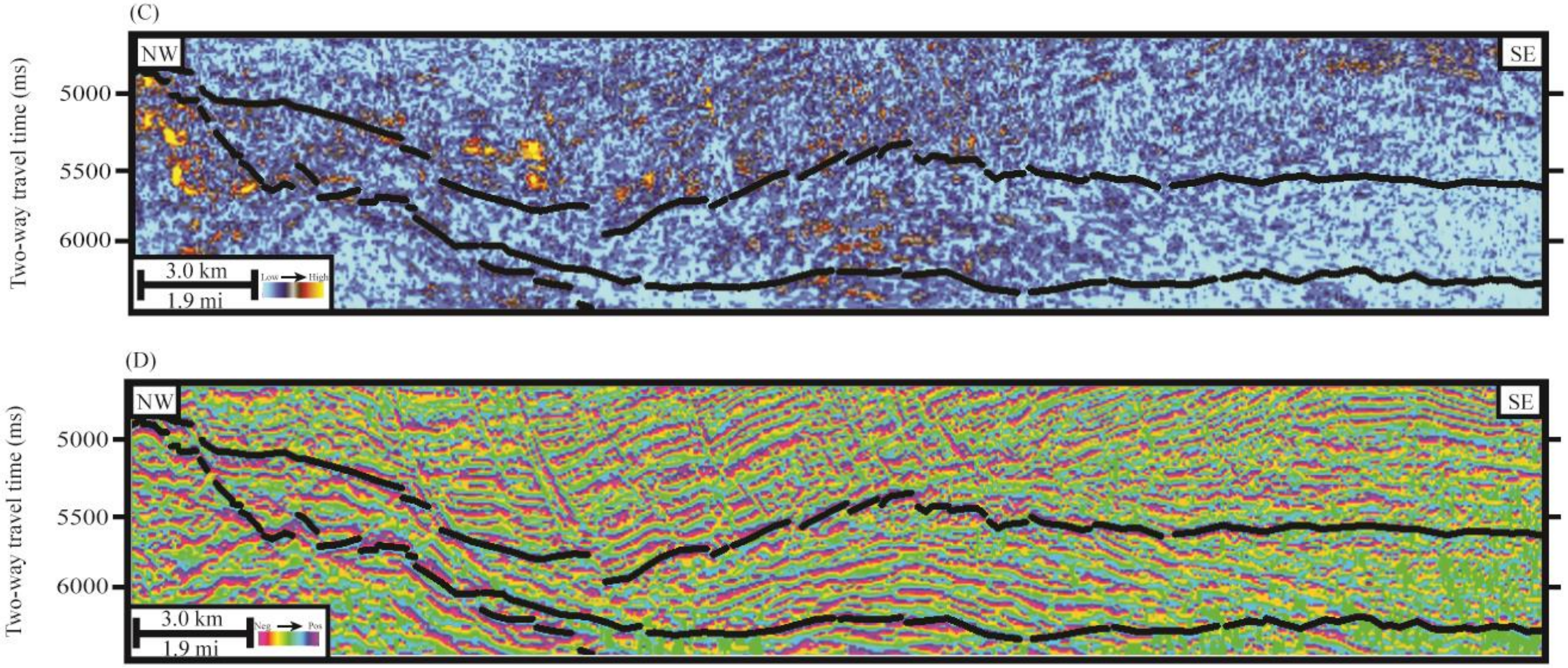

Figure 46: (C) Envelope seismic attribute **(D)** Instantaneous Phase seismic attribute.

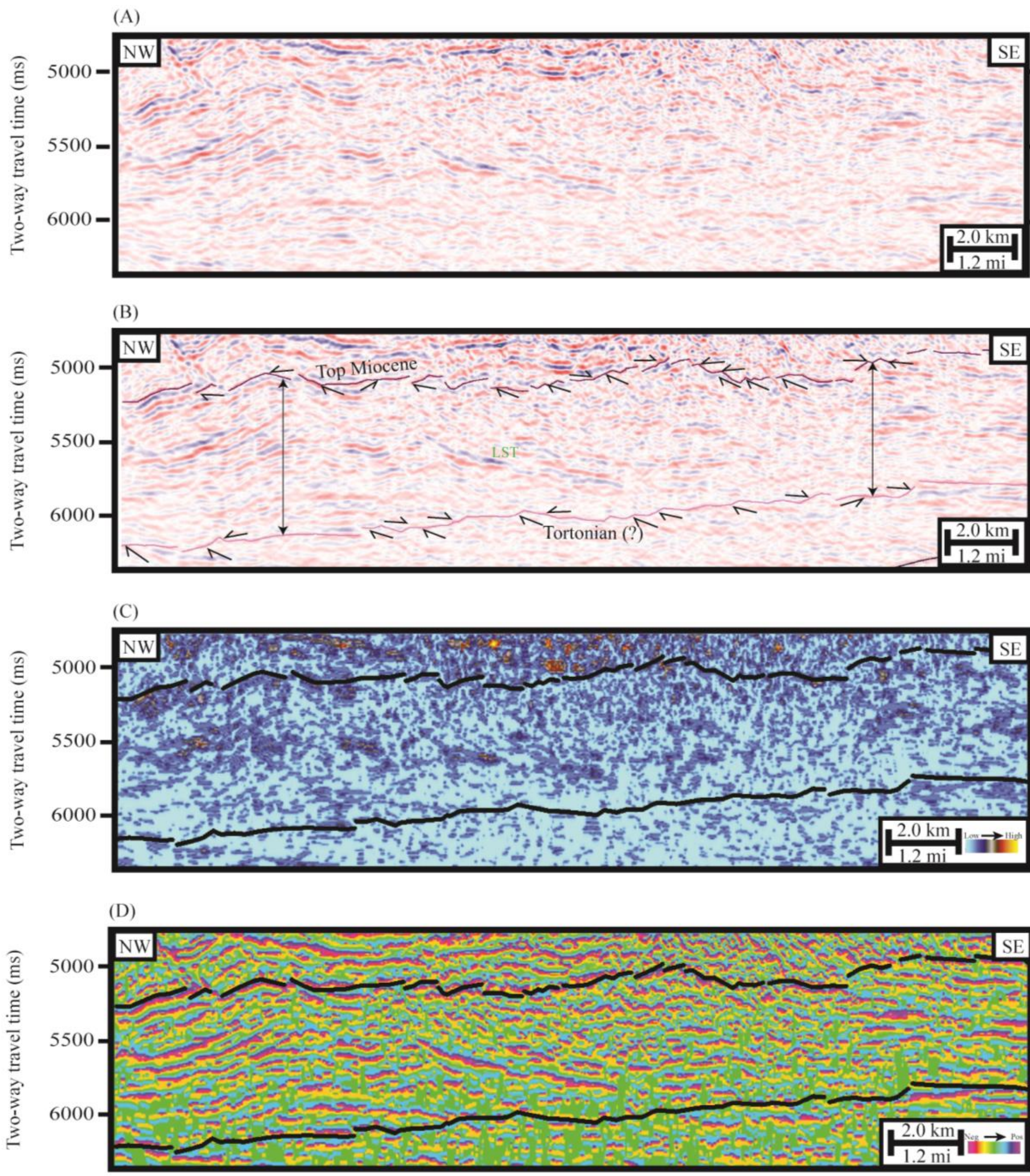

Figure 47: Seismic profile showing megasequence 3 across the 2016 3D-PSTM, dip-line number 4980. **(A)** uninterpreted **(B)** interpreted including sequence boundaries and stratal terminations. LST = Low-Stand system tract. Double-arrow indicates the thickest zone of this megasequence. **(C)** Envelope seismic attribute **(D)** Instantaneous Phase seismic attribute.

Location of this seismic section is shown in Figures 49 - 51.

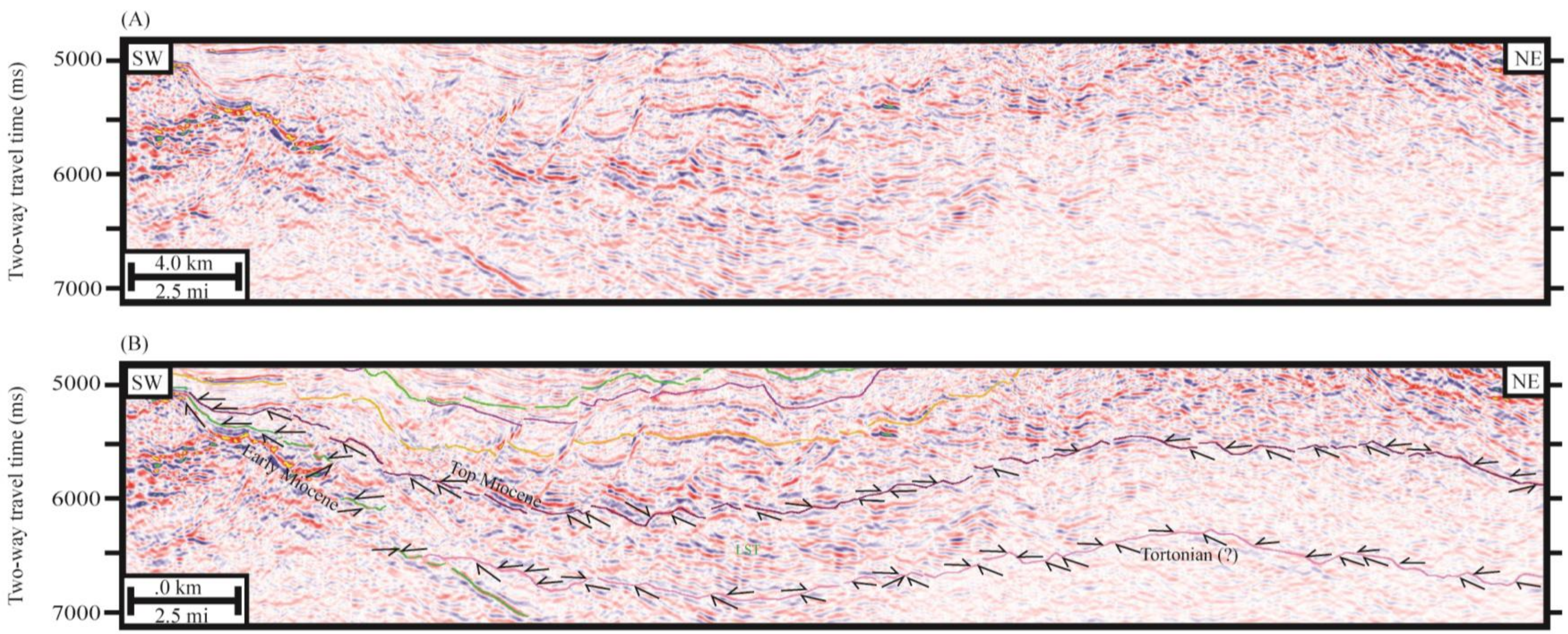

Figure 48: Seismic profile showing megasequence 3 across the 2016 3D-PSTM, strike-line number 4300. **(A)** uninterpreted **(B)** interpreted including sequence boundaries and stratal terminations. LST = Low-Stand system tract.

Location of this seismic section is shown in Figures 49 - 51.

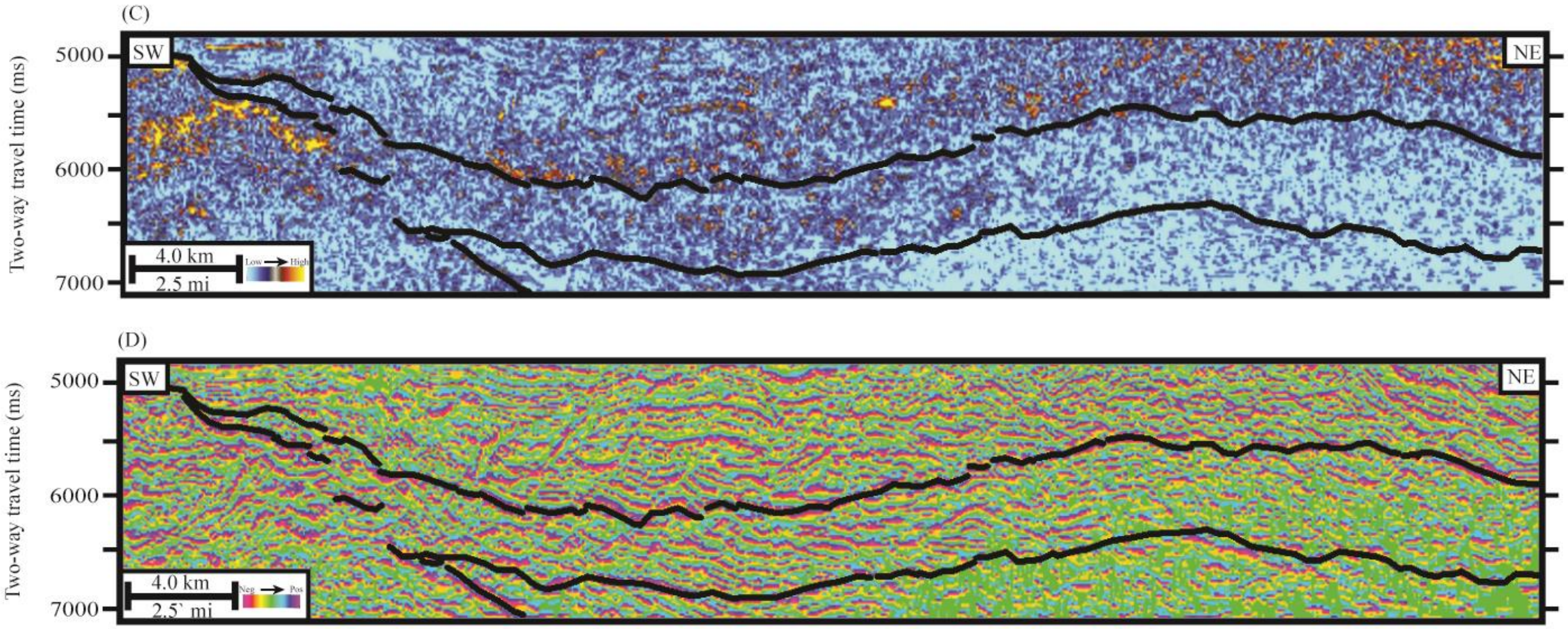

Figure 48: (C) Envelope seismic attribute **(D)** Instantaneous Phase seismic attribute.

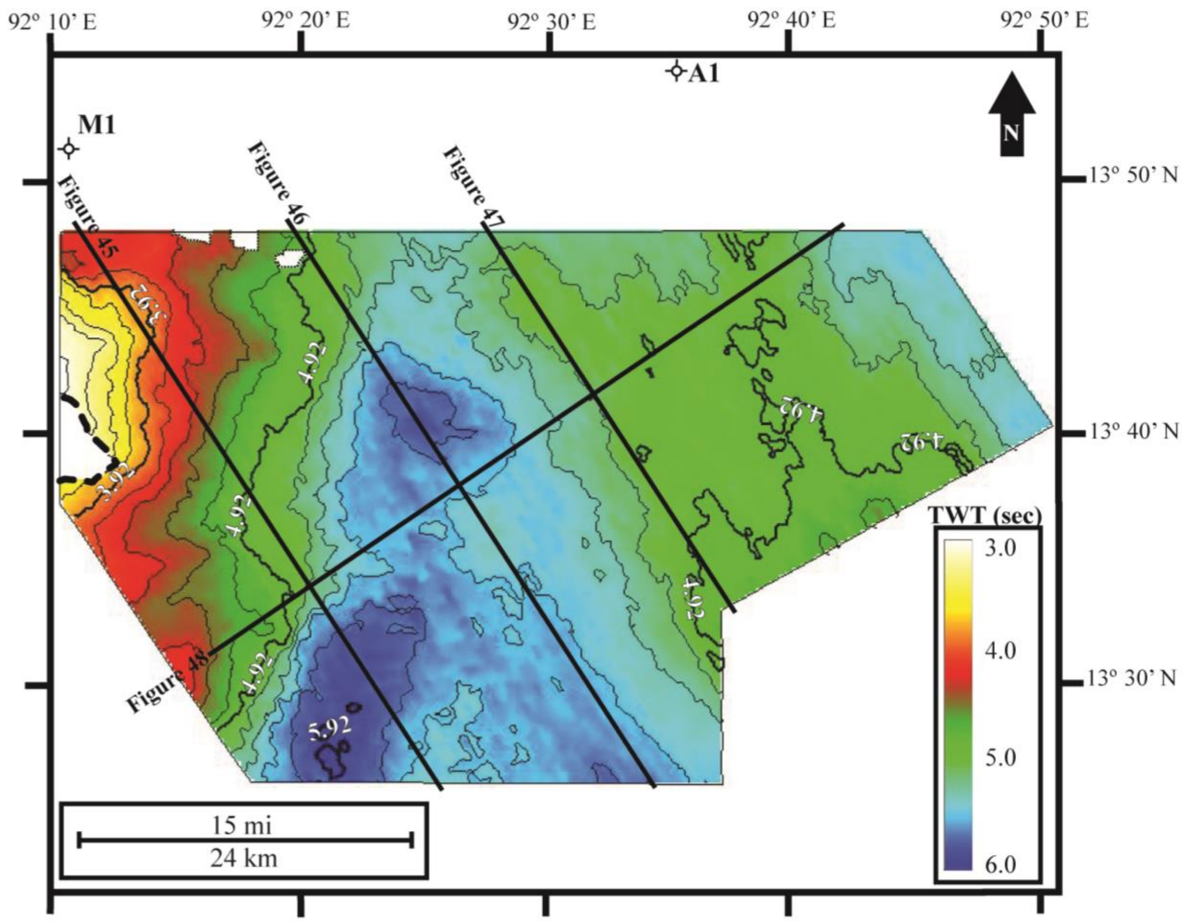

Figure 49: Time structure map of Top Miocene (TWT). Contour interval is 200 milliseconds with bold contour in every 500 milliseconds. Dash-line is onlap edge.

Locations of Figures 45 – 48 are shown.

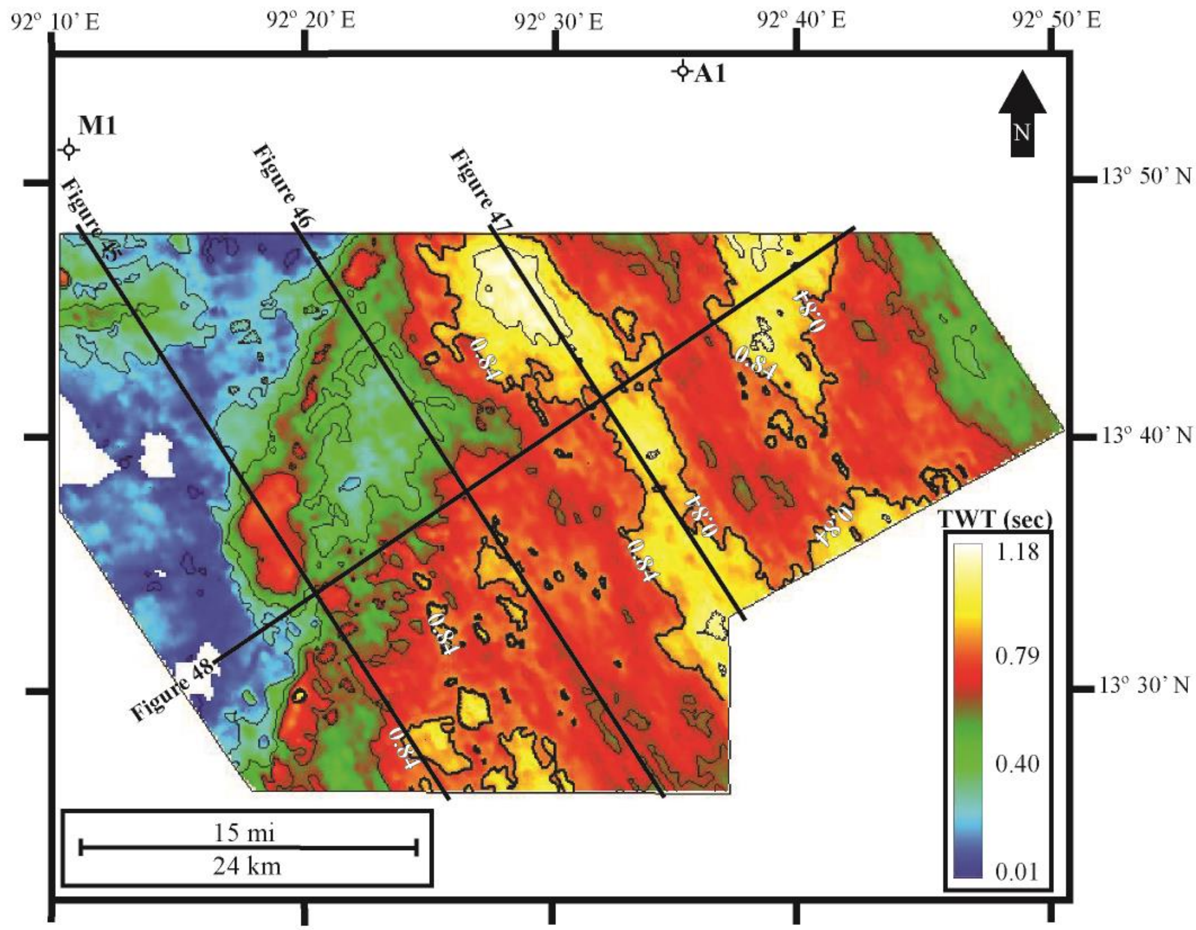

Figure 50: Isochron map of Messinian (?) megasequence (TWT). Contour interval is 200 milliseconds with bold contour in every second.

Locations of Figures 45 – 48 are shown.

elongated shape (Figures 45, 46, 48). Facies 2 is a series of hummocky and sub-parallel reflections, moderate amplitude with moderate to good continuity (Figures 45 – 48). Facies 3 is a series of parallel to sub-parallel reflections, with low amplitude with poor to moderate continuity (figures 45 – 48). Facies 4 are oblique clinoforms with low amplitude and poor continuity (Figure 45).

Geological Interpretation: The depositional environment map (Figure 52) was interpreted based on seismic facies (Figure 51) and seismic attributes (Figures 52, 53). Facies 1 consists of channel-fill belts and levees that form parallel to sub-parallel reflections. Levees have lower values on the sweetness attribute. Facies 2 includes muddy levees, crevasse splay, and muddy channel-fill belts based on hummocky geometries. Crevasse splay deposits are related to the channel-fill belt geometry. Facies 3 consists of the distal overbanks deposits and muddy levees, which has higher value in sweetness amplitude. Facies 4 are prograding clinoforms associated with a carbonate buildup (Figure 45). The facies overall trend N-S, specifically in both NNE-SSW and NNW-SSE directions. Likewise, the depositional interpretation based on the stratal transformation in the specific area (Figure 52) shows channel features with NNW-SSE trend as well (Figure 53).

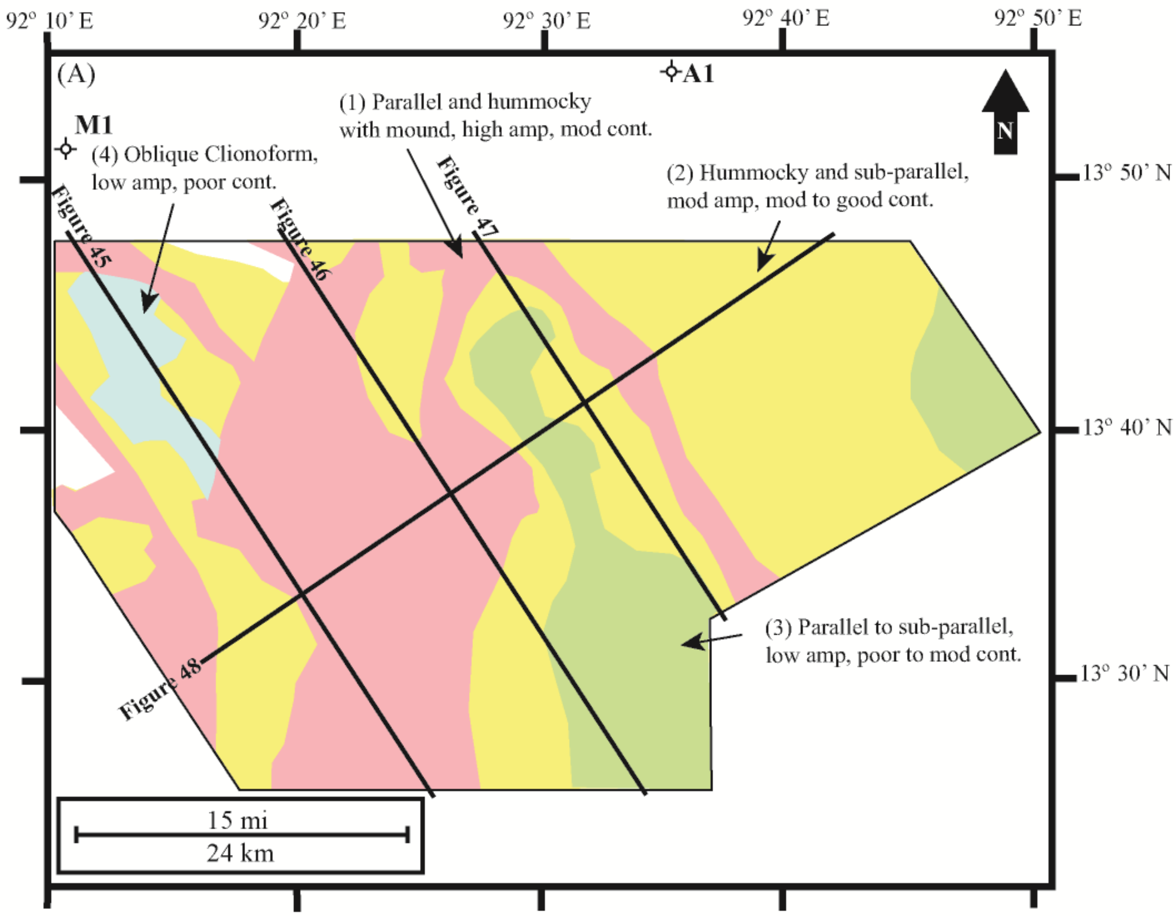

Figure 51: (A) Interpreted seismic facies map as pink color is facies 1, yellow color is facies 2, green color is facies 3 and blue color is facies 4. Each facies is listed by reflection configuration, following by amplitude (amp.) and continuity (cont.) classifications. **(B)** Envelope attribute map, calculated at 30 milliseconds below Top Miocene surface. Map is twt unit. **(C)** Instantaneous Phase attribute map, calculated at 30 milliseconds below Top Miocene surface. Map is degree of phase unit.

Locations of Figures 45 – 48 are shown.

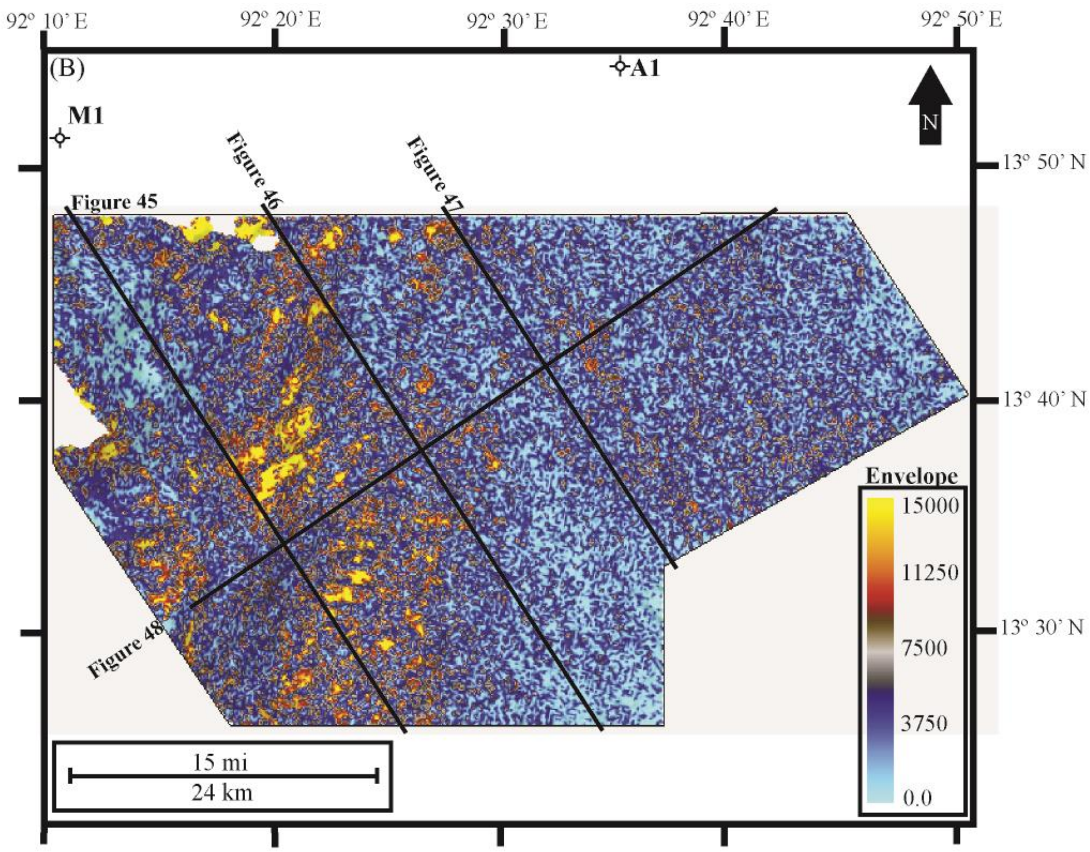

92º 10' E
92º 20' E
92º 30' E
92º 40' E
92º 50' E
(B)
A1
M1
N
Figure 45
Figure 46
Figure 47
Figure 48
13º 50' N
13º 40' N
13º 30' N
Envelope
15000
11250
7500
3750
0.0
15 mi
24 km

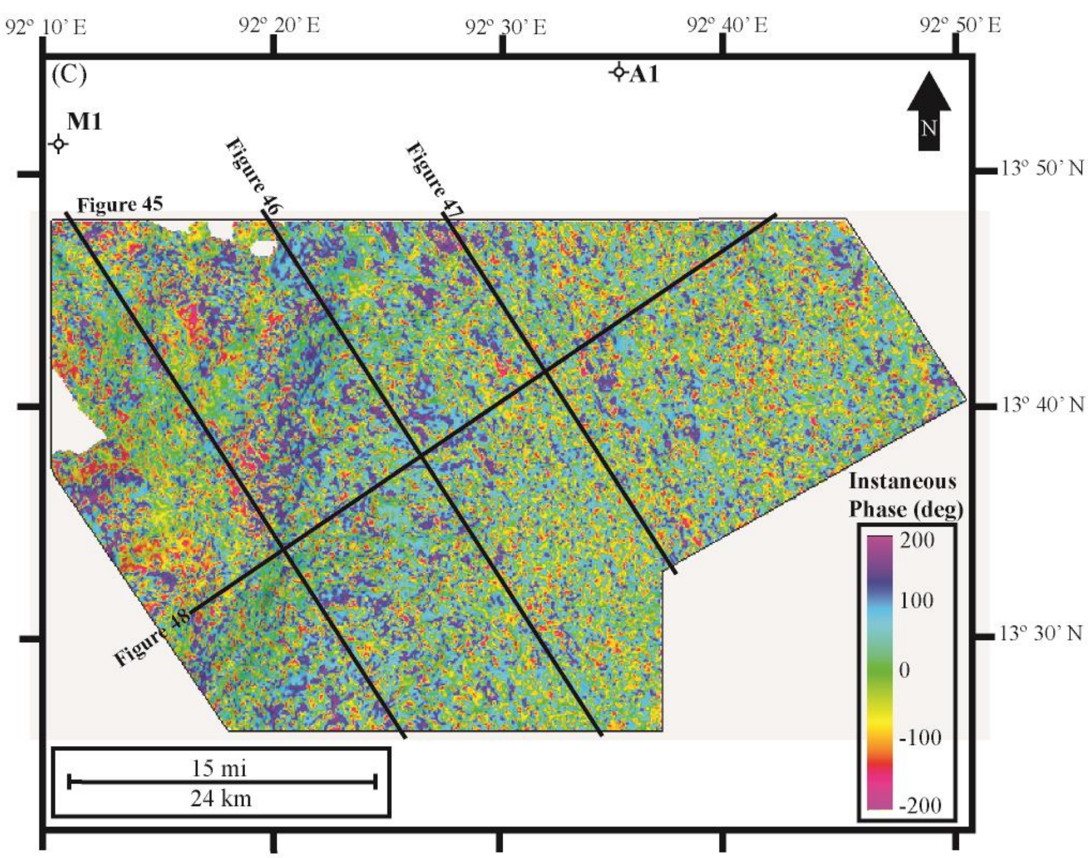

92º 10' E
92º 20' E
92º 30' E
92º 40' E
92º 50' E
(C)
A1
M1
N
Figure 45
Figure 46
Figure 47
Figure 48
13º 50' N
13º 40' N
13º 30' N
Instaneous
Phase (deg)
200
100
0
-100
-200
15 mi
24 km

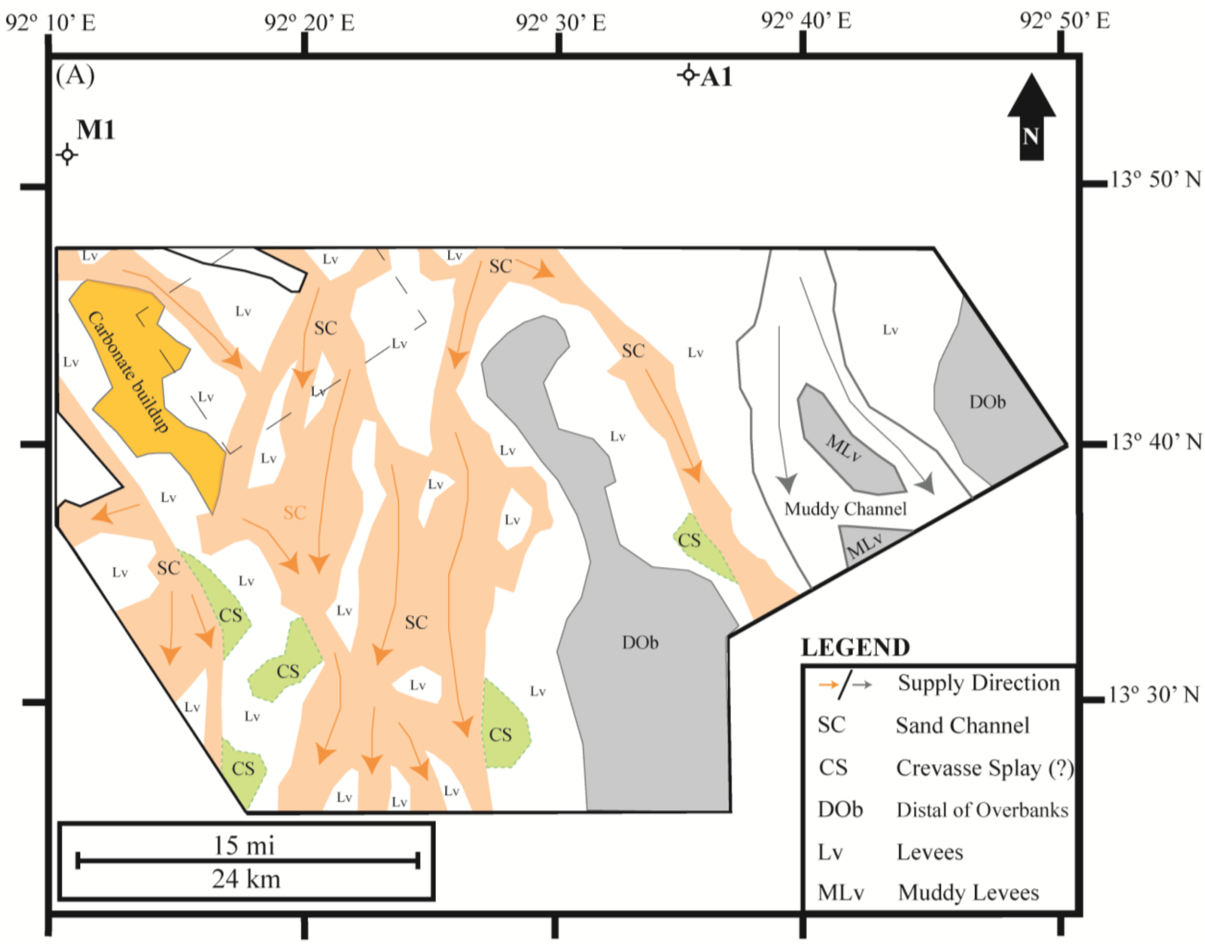

Figure 52: (A) Depositional setting map **(B)** Sweetness attribute map, calculated at 30 milliseconds below top Miocene surface. Map is absolute amplitude value in twt unit. **(C)** Coherency attribute map, calculated at 30 milliseconds below Top Miocene surface.

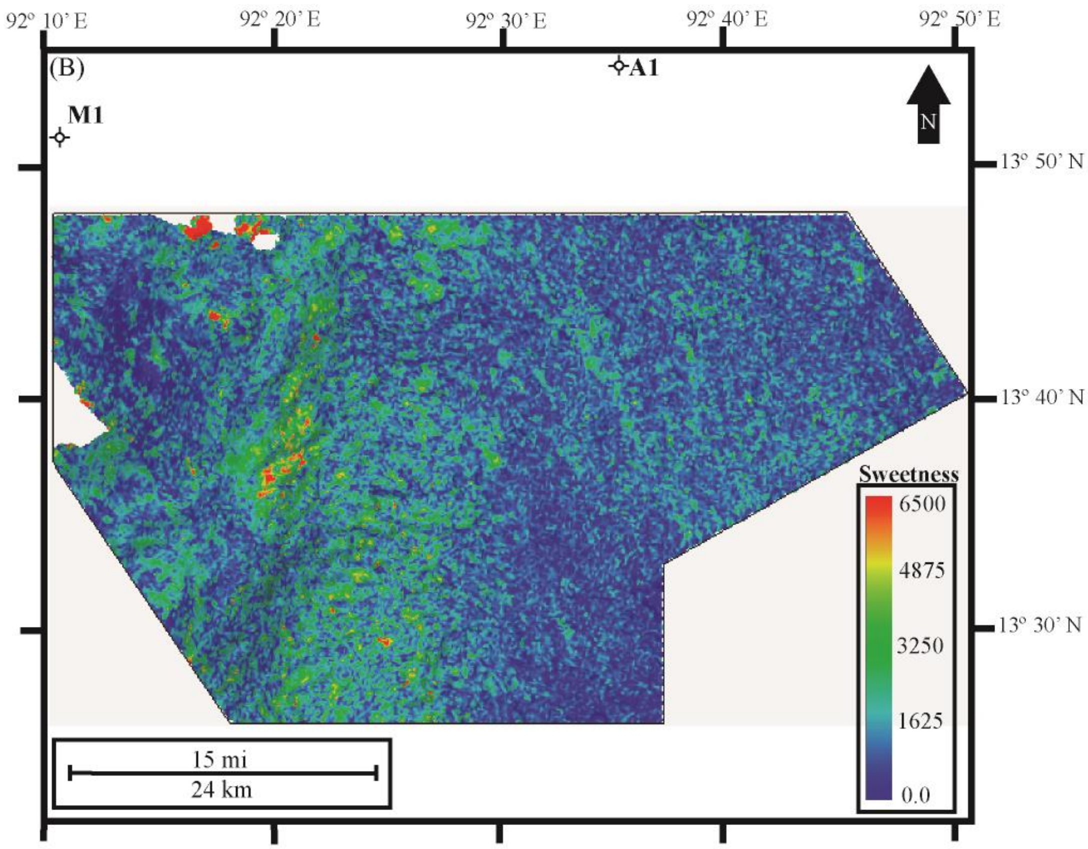

92º 10' E
92º 20' E
92º 30' E
92º 40' E
92º 50' E
(B)
A1
M1
N
13º 50' N
13º 40' N
13º 30' N
Sweetness
6500
4875
3250
1625
0.0
15 mi
24 km

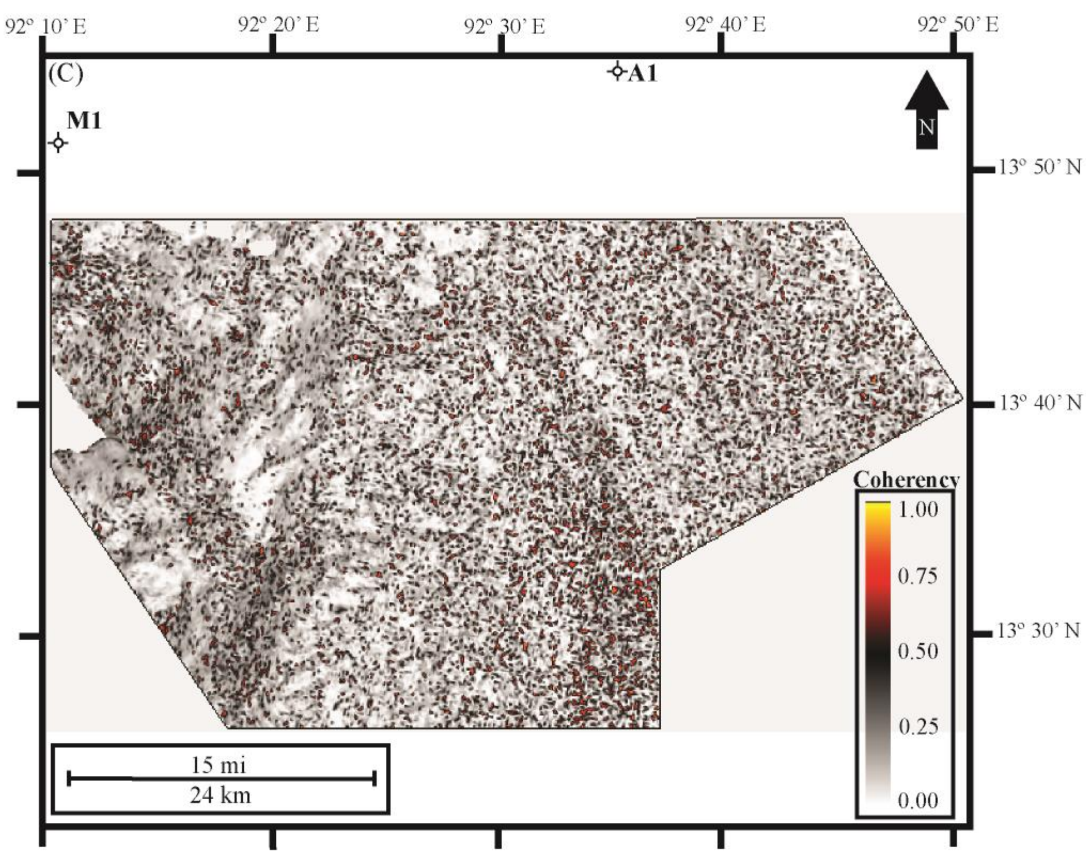

92º 10' E
92º 20' E
92º 30' E
92º 40' E
92º 50' E
(C)
A1
M1
N
13º 50' N
13º 40' N
13º 30' N
Coherency
1.00
0.75
0.50
0.25
0.00
15 mi
24 km

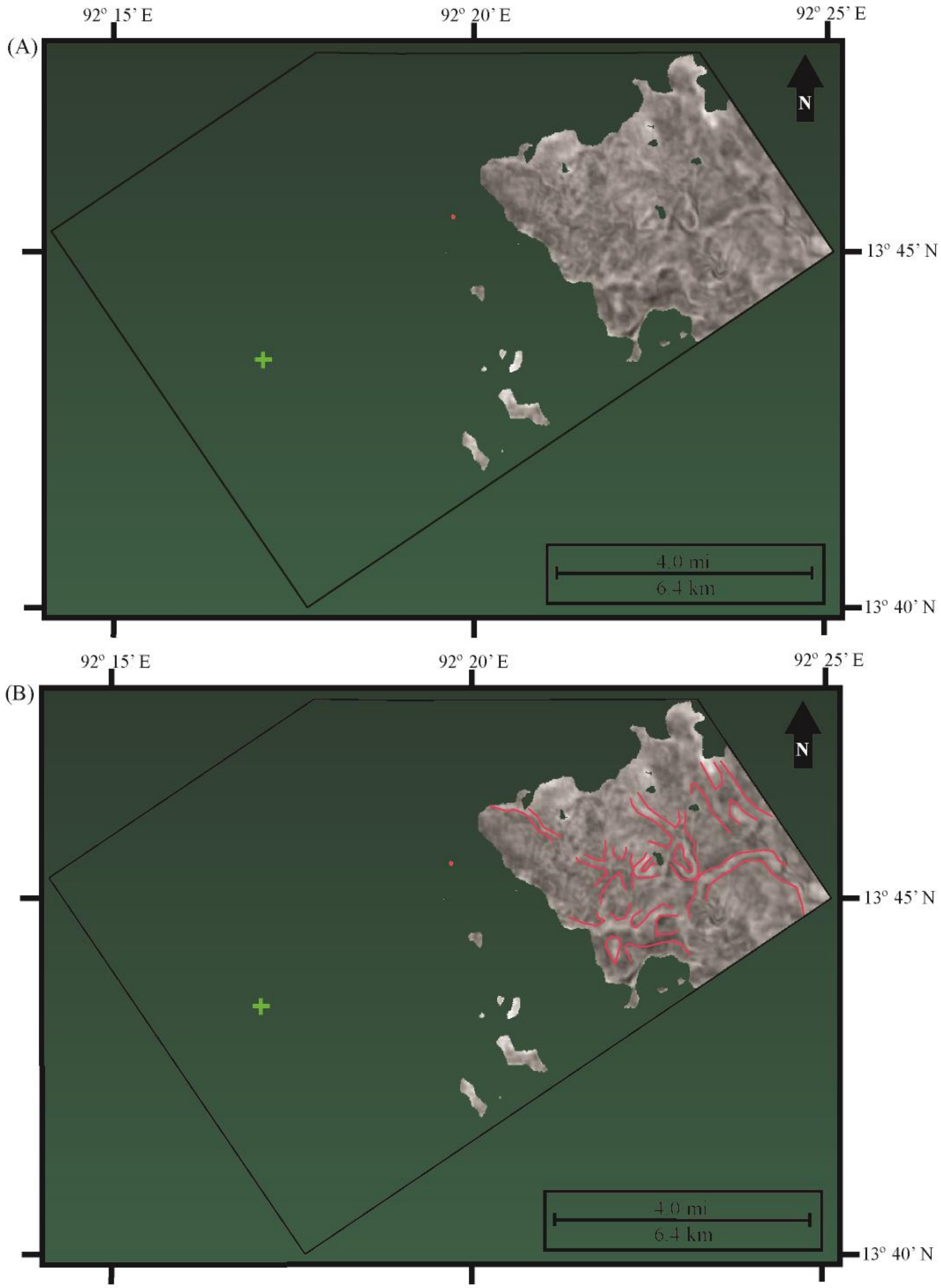

Figure 53: Strata transformation calculation horizon map about 30 milliseconds below Top Miocene surface. **(A)** Uninterpreted **(B)** Interpreted depositional environment showing possible channel features. For location, see in figure 15B and 52.

Megasequence 4: early Zanclean

Key Surfaces: The lower sequence boundary was defined by the merged surface consisting of early Miocene horizon and the upper sequence boundary of megasequence 3 (Top Miocene) (Figures 20, 57). Startal onlap is extensive at the lower boundary, as well as erosional truncation below the horizon (Figures 54 – 57). A high amplitude peak seismic reflection can be picked as this sequence boundary.

The upper sequence boundary (early Zanclean) was identified by an erosional surface within the bottomset, which present as aggradation sets (Figures 54 - 58). Onlap and local truncation are recognized above and below the surface. The seismic reflection is moderate amplitude peak association. Similar to the basal sequence boundary, this sequence boundary onlaps onto early Miocene key surface (Figures 54, 57).

Time-Structure Map: The structure map of the upper sequence boundary (early Zanclean) shows a syncline in the central part of the study area that trends north, with two-way travel time value from 2.88 to 5.60 seconds (Figure 58). An anticlinal nose is present to the east that plunges to the north. The horizon shallows to the west, where it onlaps onto the early Miocene surface (Figure 58).

Isochron Map: The early Zanclean megasequence has the two-way travel time values ranging from 0.05 to 2.06 seconds (Figure 59), with most of this megasequence is between 0.29 to 0.77 seconds twt (Figures 55, 57). Two overall isochron trends are present: NE-SW (to the west of the studay area) and NE-SE (to the east).The thickest part is located to the east (1.09 to 2.06 seconds twt) (Figure 56). The megasequence thins to the west due to the onlap onto carbonate buildup (Figure 54).

Seismic Facies: Four seismic and geological facies were interpreted based on the seismic attributes, i.e. instantaneous phase and envelope (Figure 60). Facies 1 is a series of parallel to

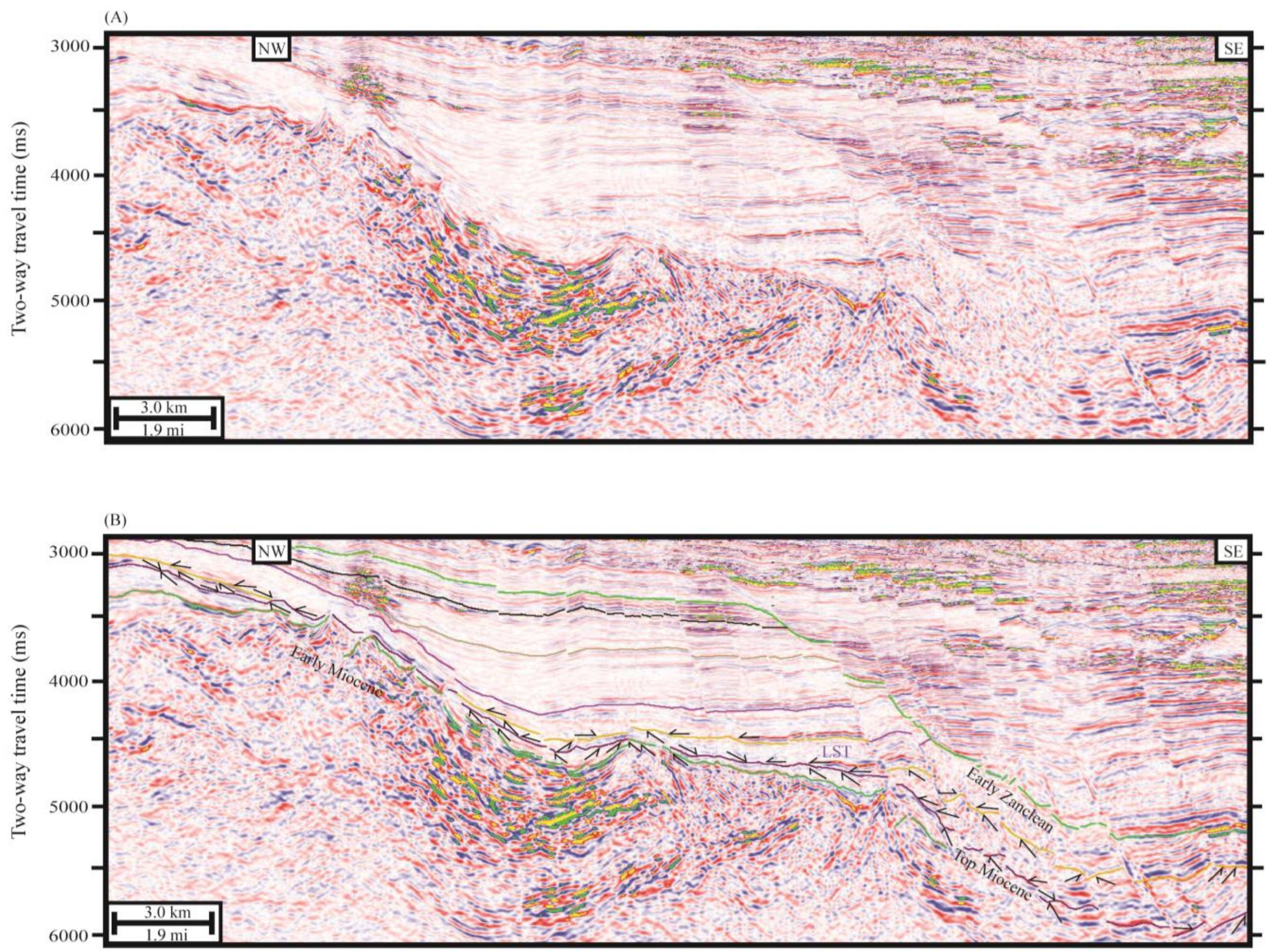

Figure 54: Seismic profile showing megasequence 4 across the 2016 3D-PSTM, dip-line number 2500. **(A)** uninterpreted **(B)** interpreted including sequence boundaries and stratal terminations. LST = Low-Stand system tract.

Location of this seismic section is shown in Figures 58 - 61.

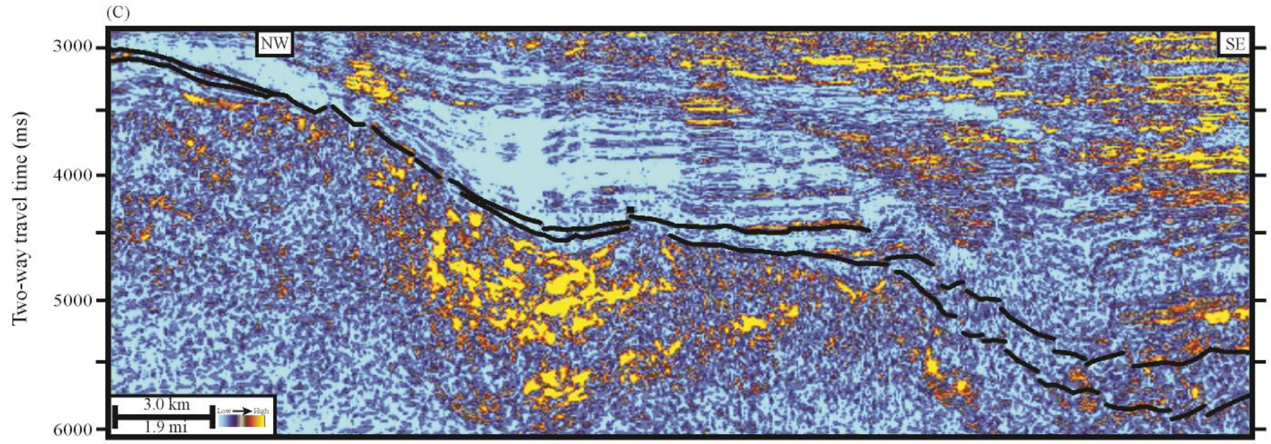

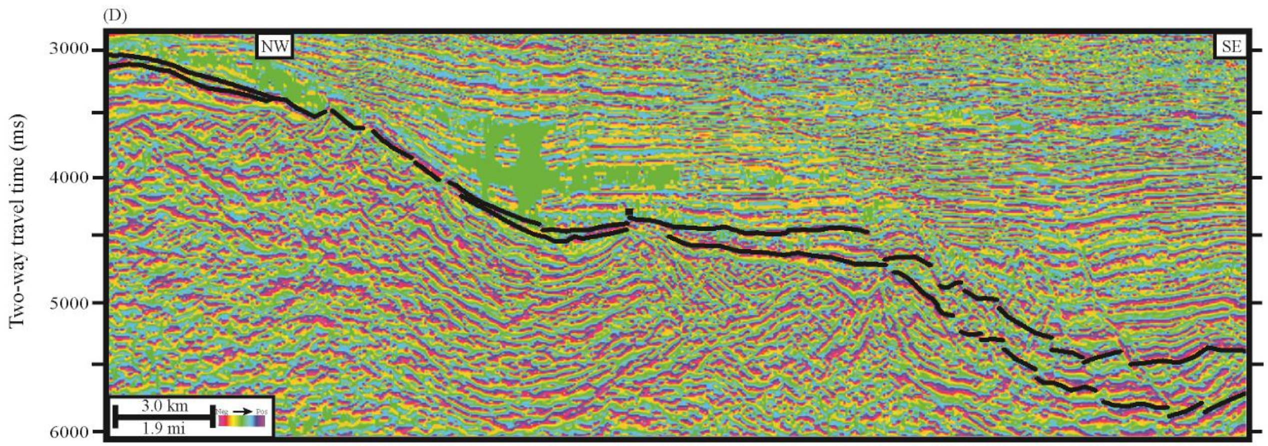

Figure 54: (C) Envelope seismic attribute **(D)** Instantaneous Phase seismic attribute.

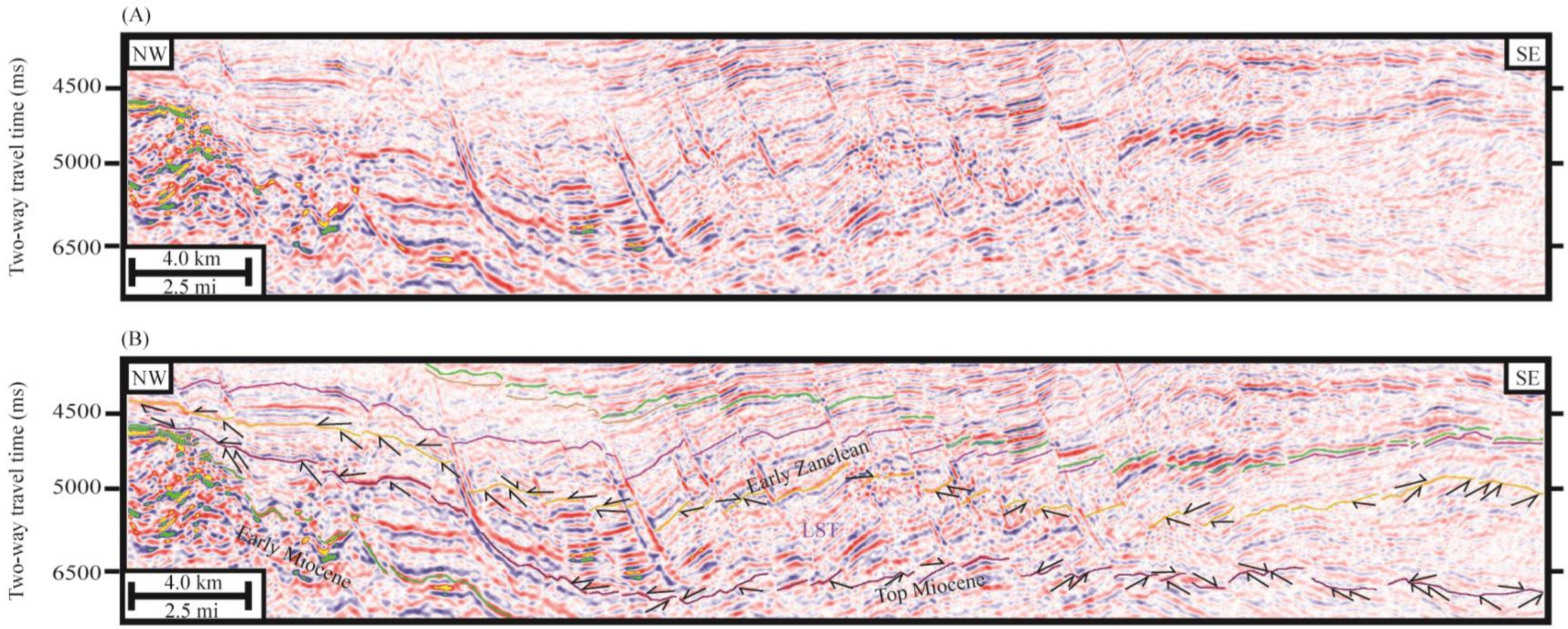

Figure 55: Seismic profile showing megasequence 4 across the 2016 3D-PSTM, dip-line number 3820. **(A)** uninterpreted **(B)** interpreted including sequence boundaries and stratal terminations. LST = Low-Stand system tract.

Location of this seismic section is shown in Figures 58 - 61.

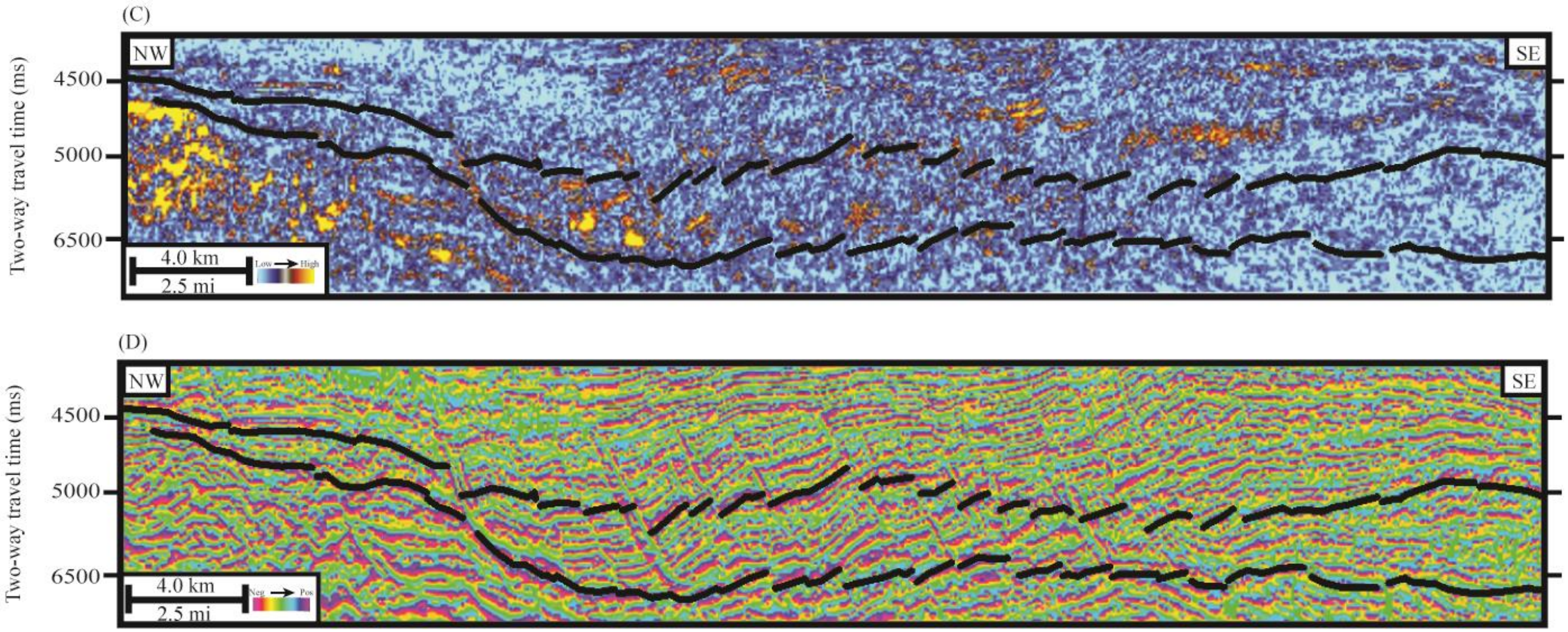

Figure 55: (C) Envelope seismic attribute **(D)** Instantaneous Phase seismic attribute.

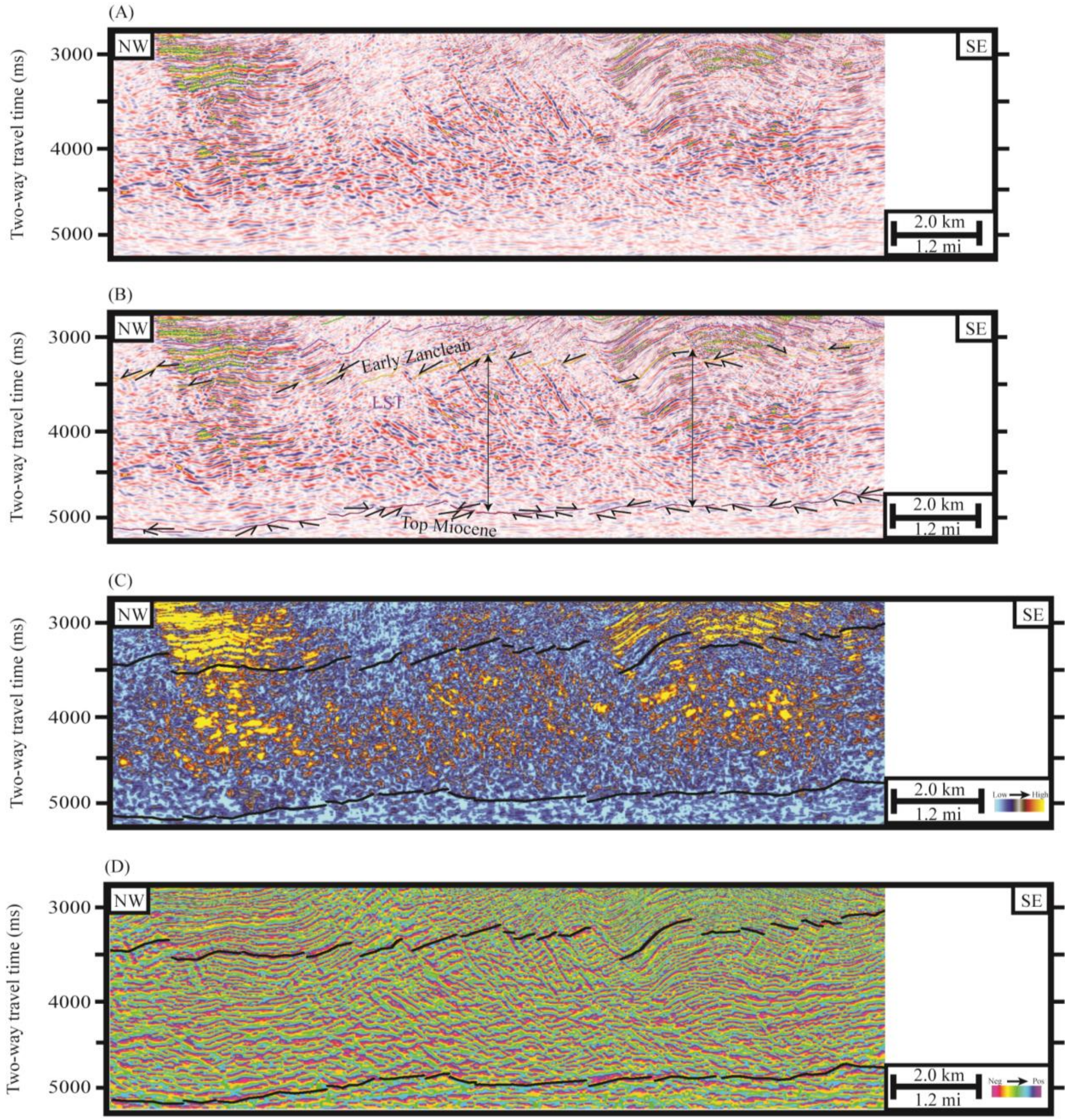

Figure 56: Seismic profile showing megasequence 4 across the 2016 3D-PSTM, dip-line number 5820. **(A)** uninterpreted **(B)** interpreted including sequence boundaries and stratal terminations. LST = Low-Stand system tract. Double-arrow indicates the thickest zone of this megasequence. **(C)** Envelope seismic attribute **(D)** Instantaneous Phase seismic attribute.

Location of this seismic section is shown in Figures 58 - 61.

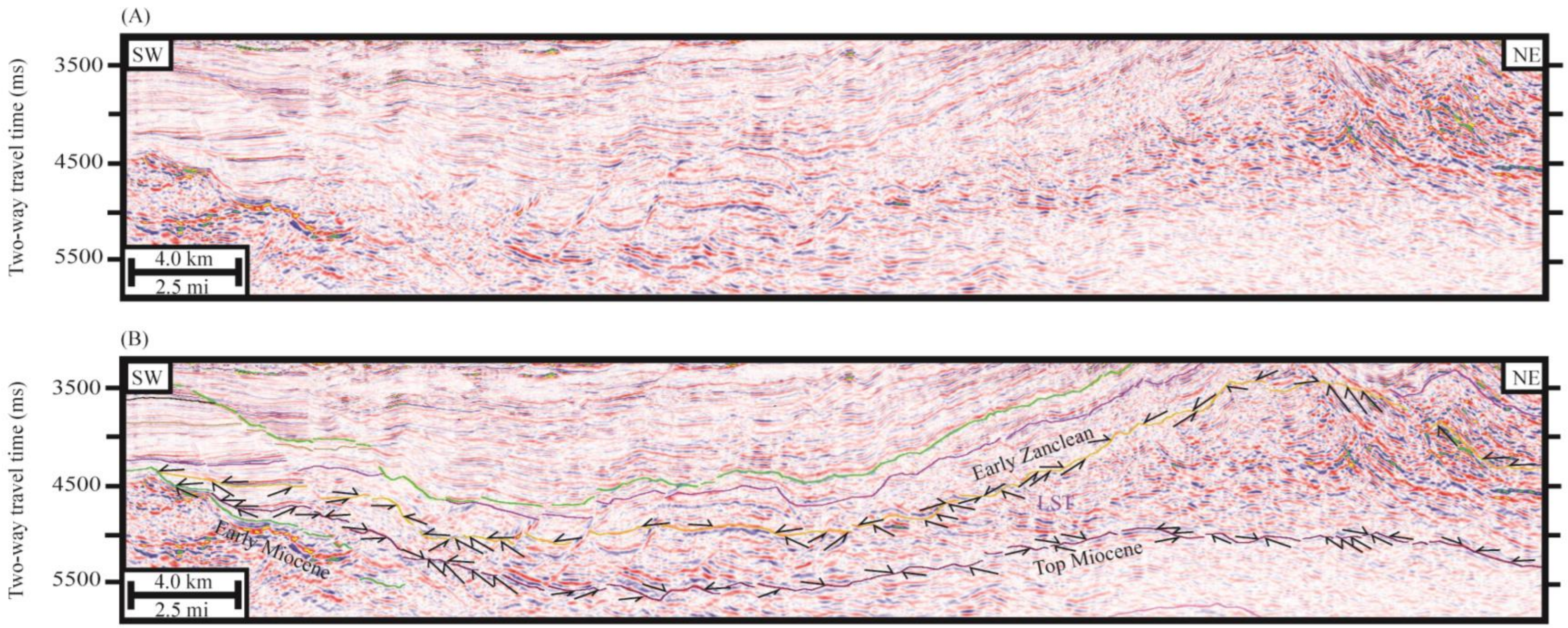

Figure 57: Seismic profile showing megasequence 4 across the 2016 3D-PSTM, strike-line number 4300. **(A)** uninterpreted **(B)** interpreted including sequence boundaries and stratal terminations. LST = Low-Stand system tract.

Location of this seismic section is shown in Figures 58 - 61.

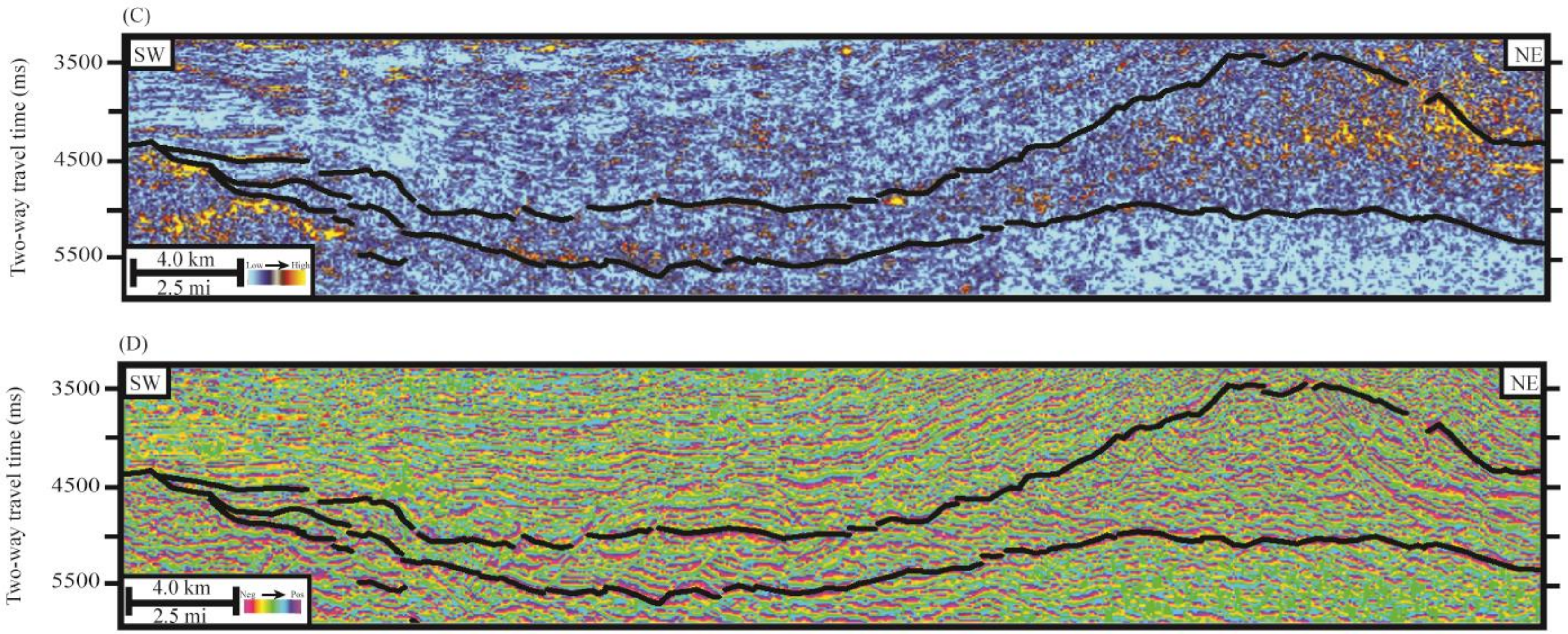

Figure 57: (C) Envelope seismic attribute **(D)** Instantaneous Phase seismic attribute.

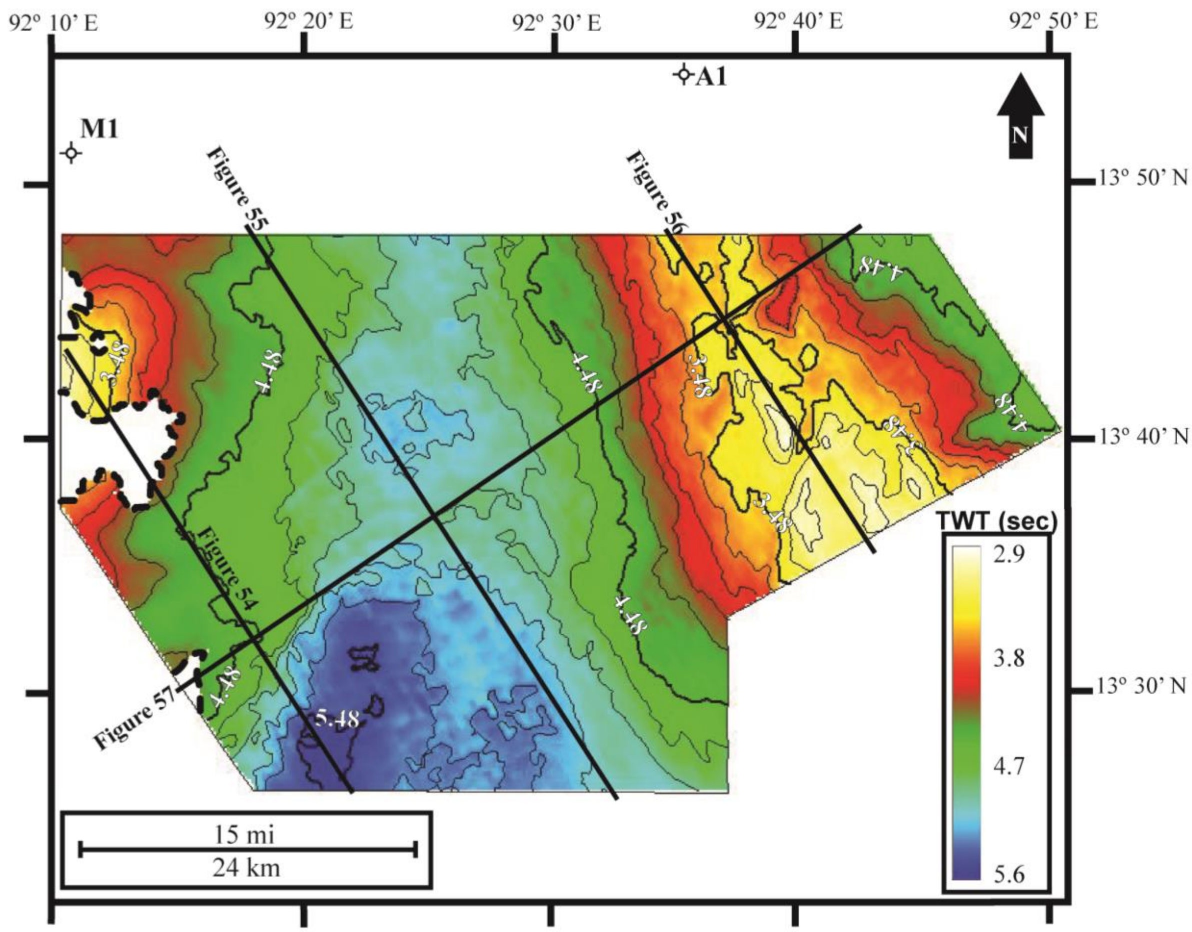

Figure 58: Time structure map of early Zanclean (TWT). Contour interval is 200 milliseconds with bold contour in every second. Dash-line is onlap edge.

Locations of Figures 54 – 57 are shown.

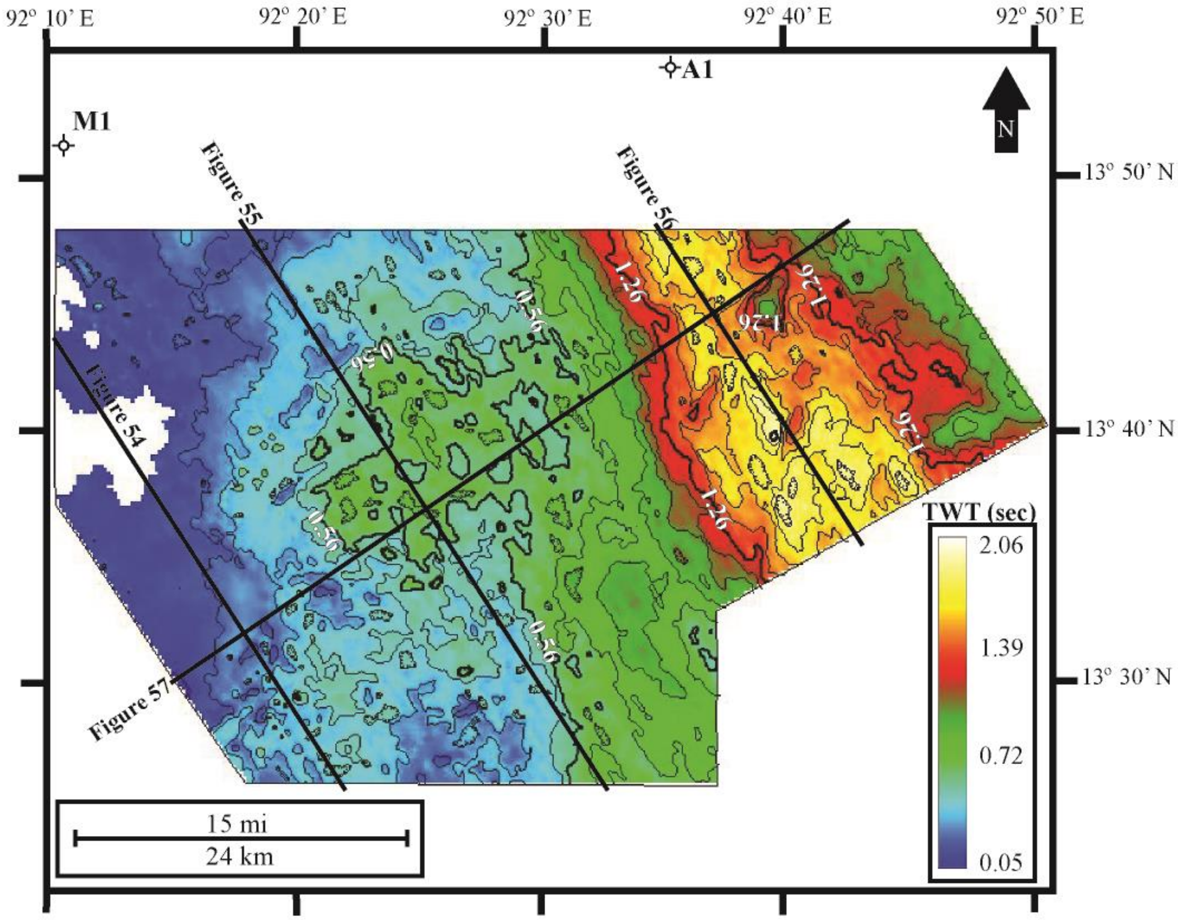

Figure 59: Isochron map of early Zanclean megasequence (TWT). Contour interval is 200 milliseconds with bold contour in every second.

Locations of Figures 54 – 57 are shown.

sub-parallel, with moderate to high amplitude and good continuity (Figures 54, 55, and 57). Facies 2 is a series of sub-parallel to hummocky reflections with high amplitude and poor to moderate continuity (Figures 57, 58). The facies was deformed by the reverse faults near compressional zones to the east (Figure 15). Facies 3 is a series of parallel reflections and hummocky, low to moderate amplitude with moderate to good continuity (Figures 55 - 57). Facies 4 is a series of parallel to sub-parallel reflections with low amplitude and moderate to good continuity (Figures 55 and 57).

Geological Interpretation: The depositional environment map (Figure 61) was interpreting based on the seismic facies (Figure 60) and the seismic attributes (Figure 61). All facies configurations consists of parallel, sub-parallel with partial hummocky reflections (Figures 54 – 57). Sand channel belts are interpreted in facies 2 and facies 1, based on the higher values in the sweetness attribute (Figure 61). Levees that are associated with the channel are interpreted in facies 1 and facies 3. The lower sweetness values in facies 3 are interpreted as distal overbanks. Facies 3 is also included muddy channel belts. The overall channel belts trend N-S direction (Figures 60, 61). The stratal transformation calculation also suggests channelized features that trend N-S (Figure 62).

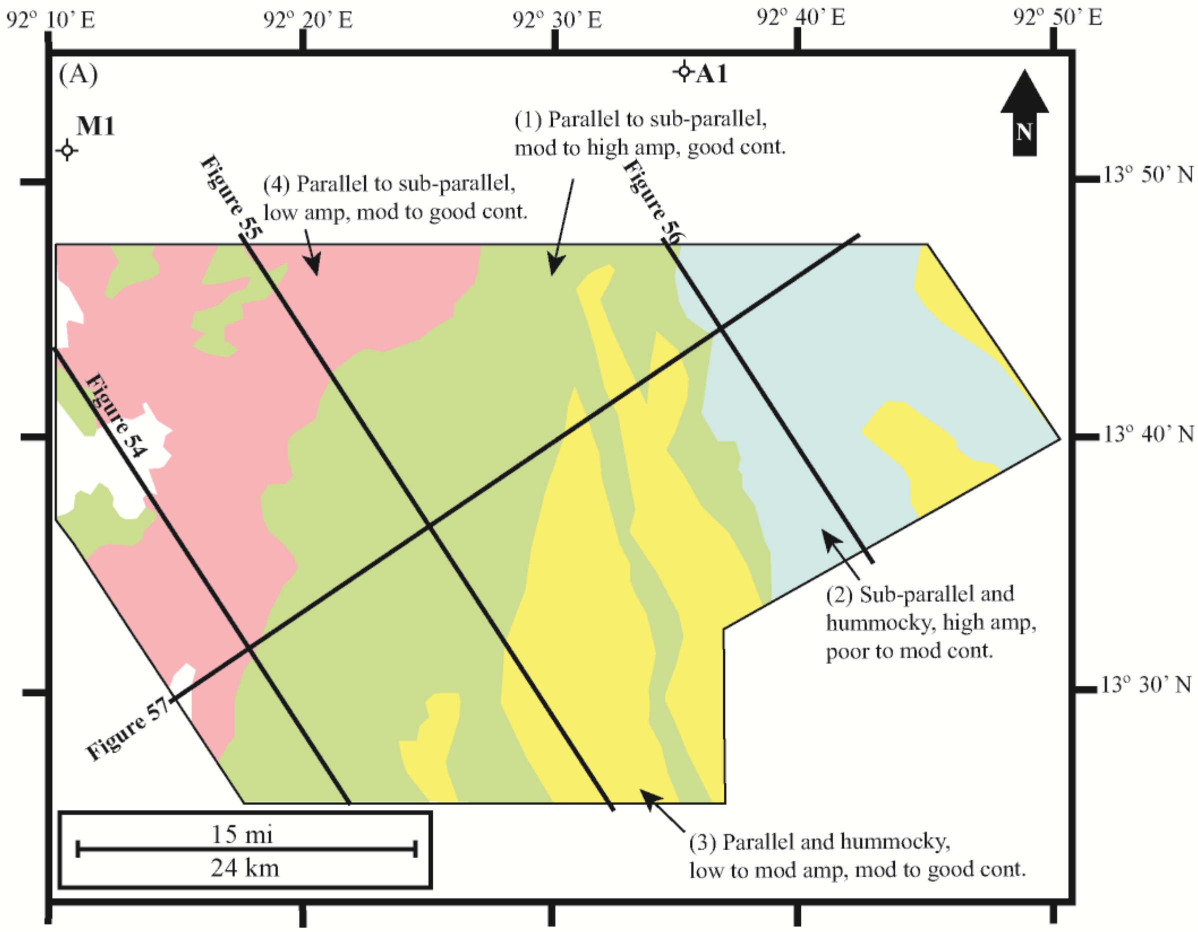

Figure 60: (A) Interpreted seismic facies map as green color is facies 1, blue color is facies 2, yellow color is facies 3 and pink color is facies 4. Each facies is listed by reflection configuration, following by amplitude (amp.) and continuity (cont.) classifications. **(B)** Envelope attribute map, calculated at 30 milliseconds below early Zanclean surface. Map is twt unit. **(C)** Instantaneous Phase attribute map, calculated at 30 milliseconds below early Zanclean surface. Map is degree of phase unit.

Locations of Figures 54 – 57 are shown.

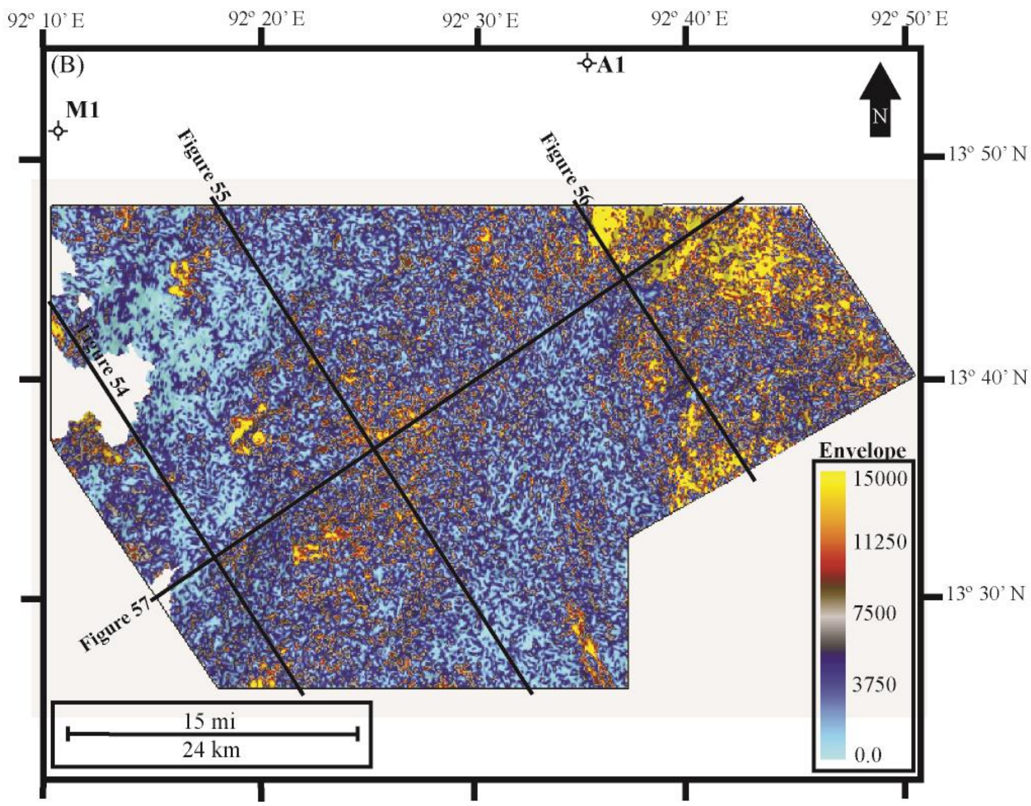

92° 10' E
92° 20' E
92° 30' E
92° 40' E
92° 50' E
(B)
A1
M1
N
13° 50' N
13° 40' N
13° 30' N
Figure 55
Figure 56
Figure 54
Figure 57
Envelope
15000
11250
7500
3750
0.0
15 mi
24 km

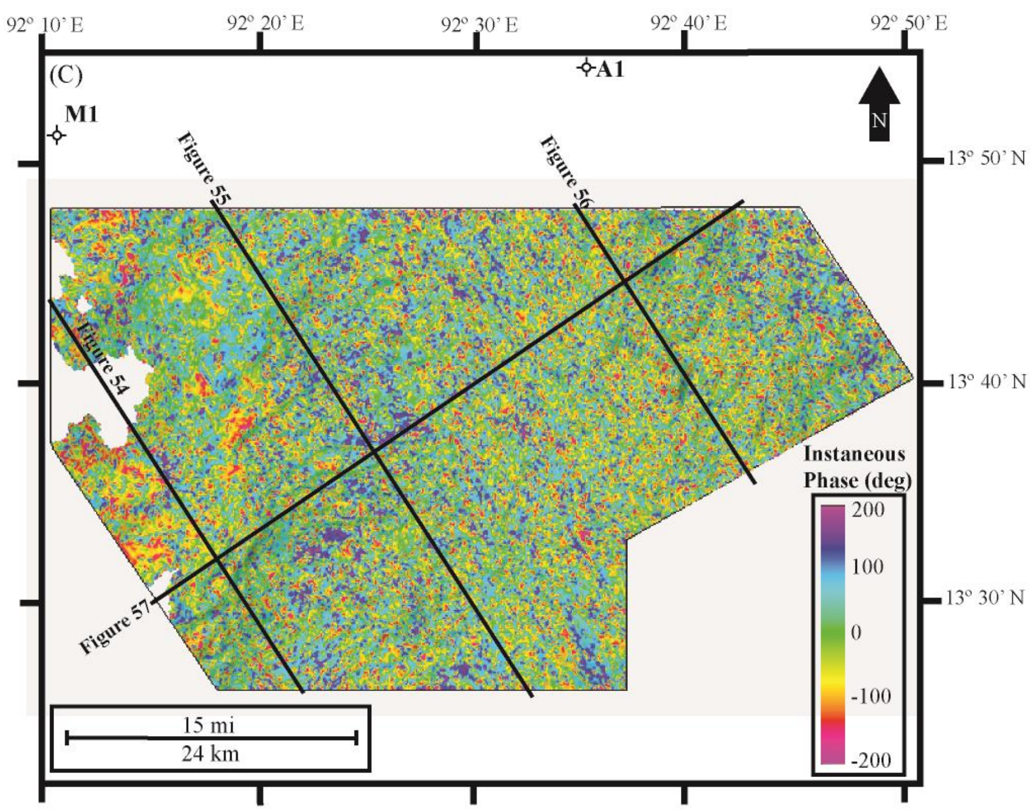

92° 10' E
92° 20' E
92° 30' E
92° 40' E
92° 50' E
(C)
A1
M1
N
13° 50' N
13° 40' N
13° 30' N
Figure 55
Figure 56
Figure 54
Figure 57
Instaneous
Phase (deg)
200
100
0
-100
-200
15 mi
24 km

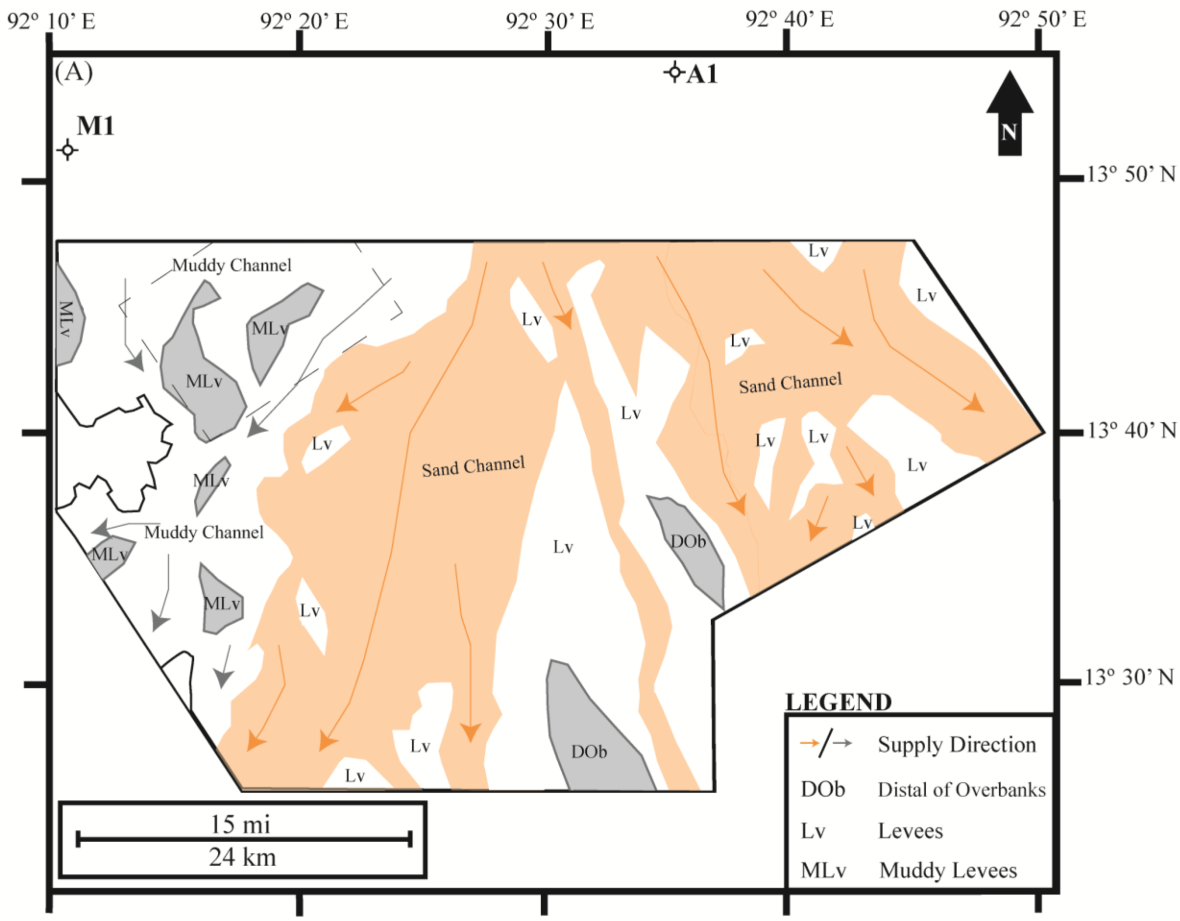

Figure 61: (A) Depositional setting map **(B)** Sweetness attribute map, calculated at 30 milliseconds below early Zanclean surface. Map is absolute amplitude value in twt unit. **(C)** Coherency attribute map, calculated at 30 milliseconds below early Zanclean surface.

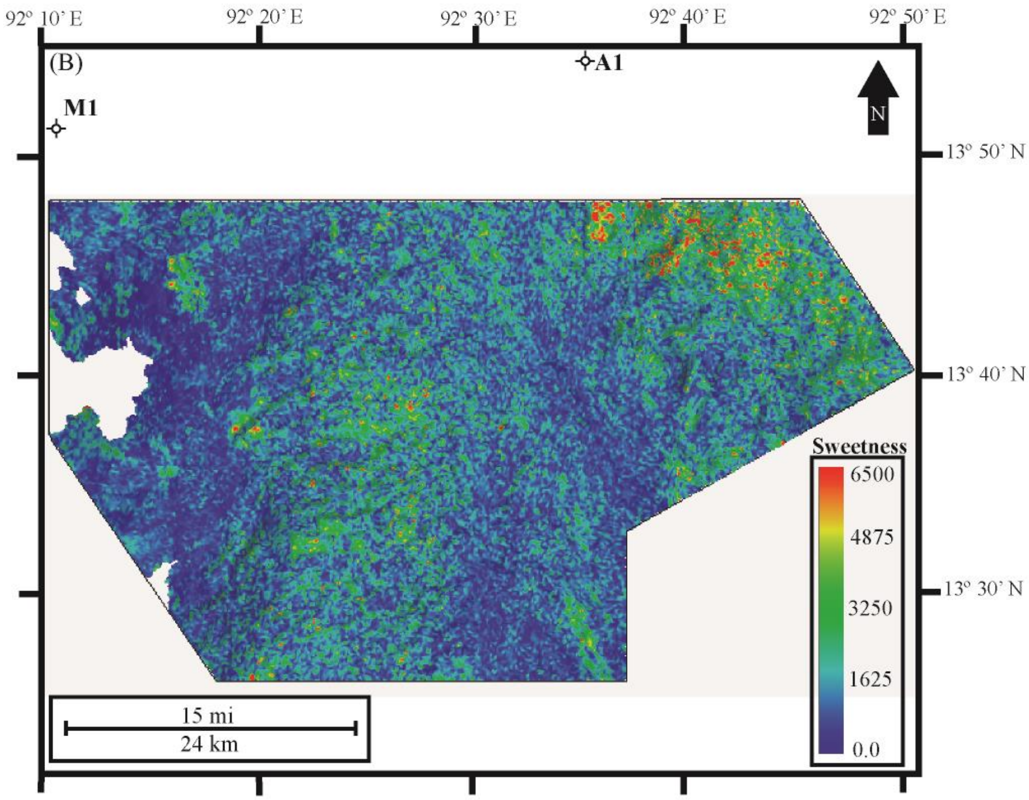
92° 10' E
92° 20' E
92° 30' E
92° 40' E
92° 50' E
(B)
A1
M1
N
13° 50' N
13° 40' N
13° 30' N
Sweetness
6500
4875
3250
1625
0.0
15 mi
24 km

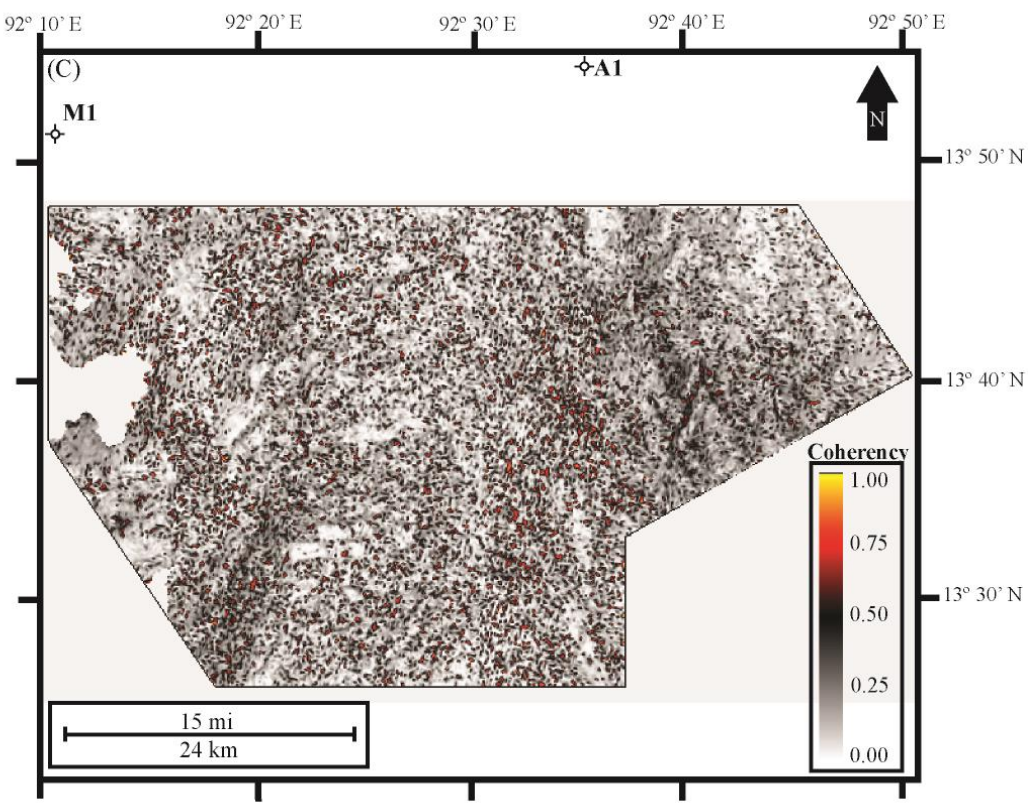
92° 10' E
92° 20' E
92° 30' E
92° 40' E
92° 50' E
(C)
A1
M1
N
13° 50' N
13° 40' N
13° 30' N
Coherency
1.00
0.75
0.50
0.25
0.00
15 mi
24 km

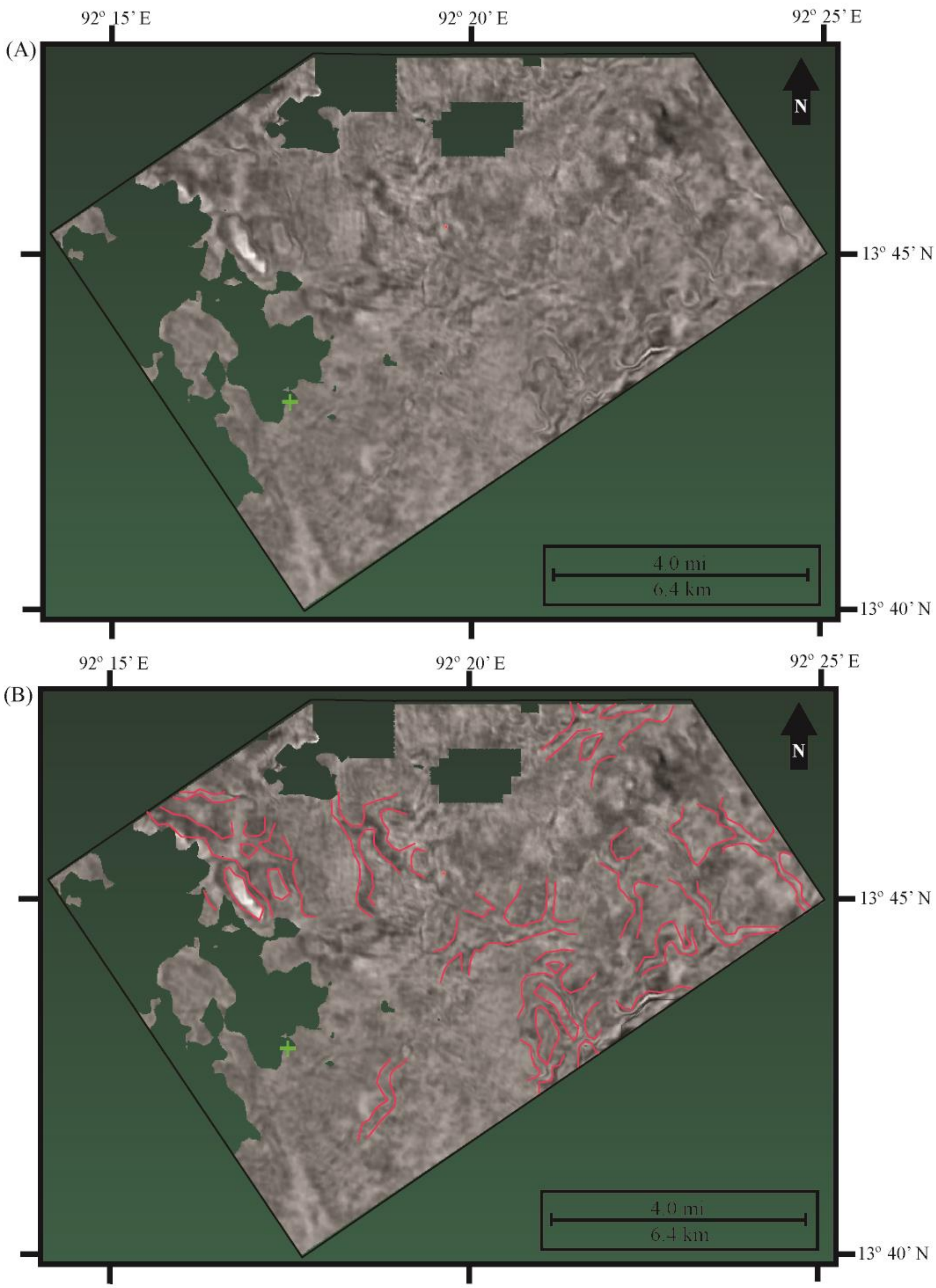

Figure 62: Strata transformation calculation horizon map about 30 milliseconds below early Zanclean surface. **(A)** Uninterpreted **(B)** Interpreted depositional environment showing possible channel features. For location, see in figure 15B and 61.

Megasequence 5: middle Zanclean

Key Surfaces: The lower sequence boundary of megasequence 5 comprise three surfaces, which are the upper sequence boundary of megasequence 4 (early Zanclean), early Miocene and Top Miocene surfaces (Figures 20, 63). Both onlap and truncating reflections are present along the surface (Figures 63 - 66). A moderate to high amplitude peak seismic reflection can be picked at this sequence boundary.

The upper sequence boundary was identified by two merged surfaces (middle Zanclean and Top Pliocene surfaces) with obvious onlap and truncation above and below the horizon, respectively (Figures 63 – 66). The seismic reflection corresponds to a moderate to high amplitude peak association together with high amplitude trough association, which corresponds to Top Pliocene surface.

Time-Structure Map: The structure map of the first surface of upper sequence boundary (middle Zanclean) has a north-trending syncline in the central part of the study, with two-way travel time values ranging from 2.57 to 4.95 seconds (Figure 67). An anticlinal nose is present to the east that plunges to the north. The horizon was eroded to the south Top Pliocene surface (Figure 63).

The structure map of the second surface of upper sequence boundary (Top Pliocene) shows the same a north-trending syncline in the central part with two-way travel time values ranging from 2.26 to 5.31 seconds (Figure 68). The same anticlinal nose is present to the east that plunges to the north. In the M1 well, this surface correlates to the distinct lithological change between Pliocene to Pleistocene section (Figure 28).

Isochron Map: The middle Zanclean megasequence has two-way travel time values ranging from 0.03 to 1.44 seconds (Figure 69). Most of this megasequence is between 0.30 to 0.57 seconds twt (Figures 63, 64, 66). The thickest part is located to the east of the area (0.84 to 1.06 seconds twt)

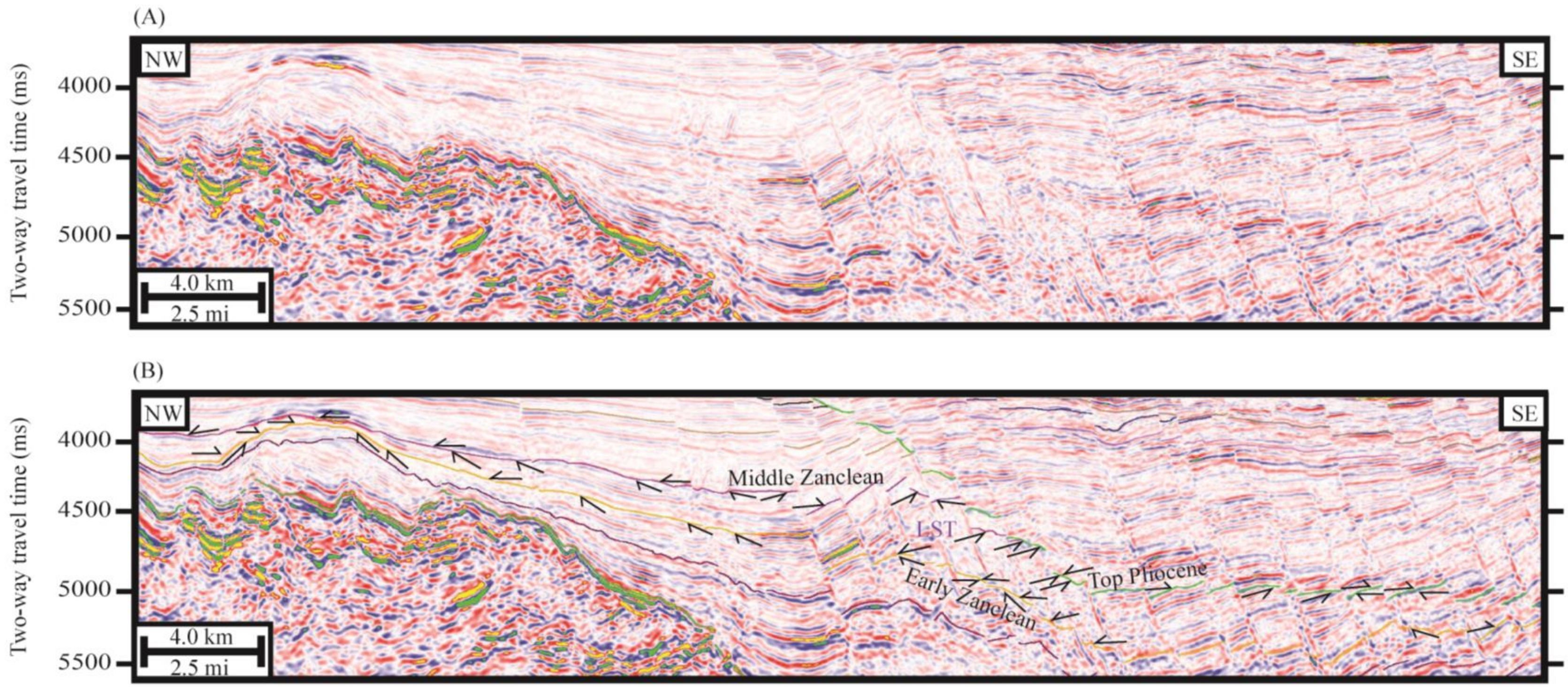

Figure 63: Seismic profile showing megasequence 5 across the 2016 3D-PSTM, dip-line number 3100. **(A)** uninterpreted **(B)** interpreted including sequence boundaries and stratal terminations. LST = Low-Stand system tract.

Location of this seismic section is shown in Figures 67, 69 - 70.

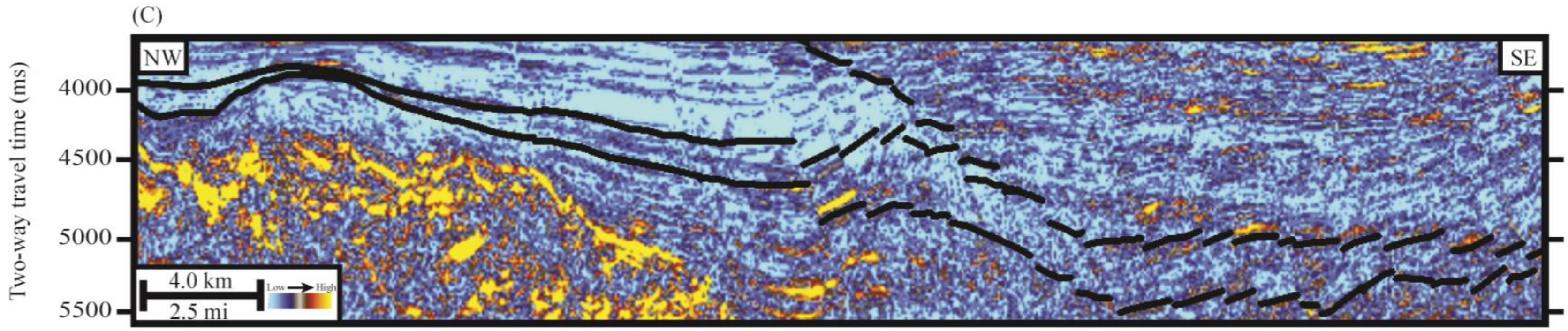

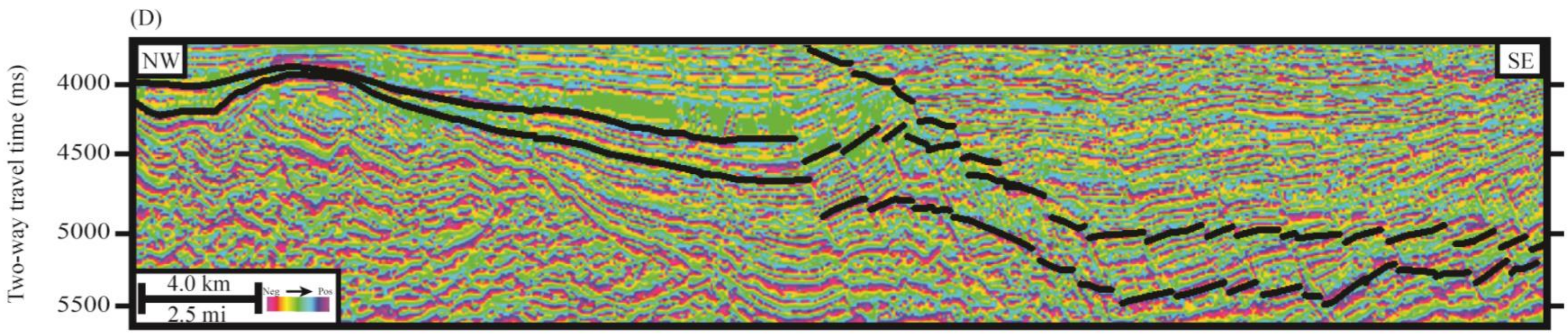

Figure 63: (C) Envelope seismic attribute **(D)** Instantaneous Phase seismic attribute.

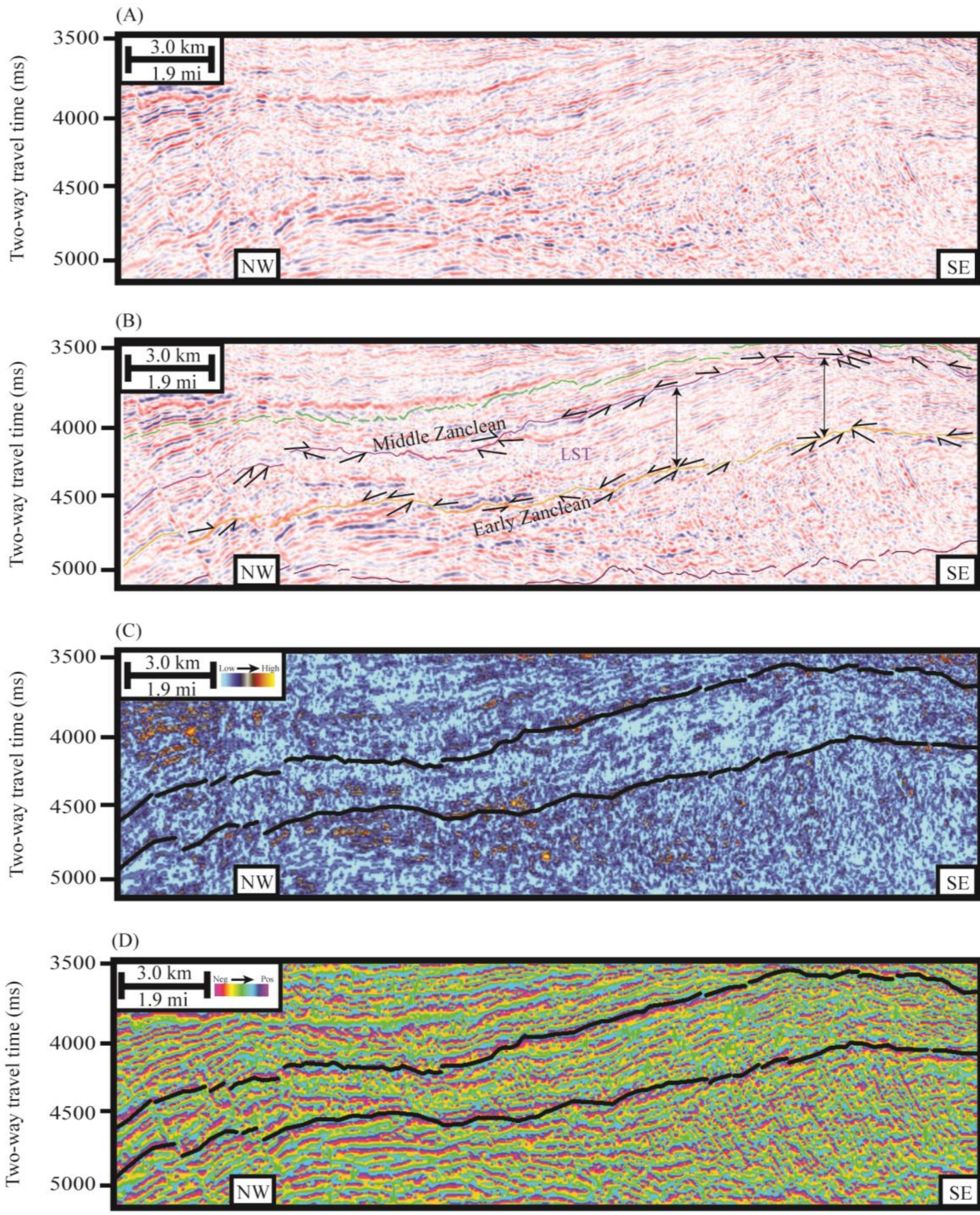

Figure 64: Seismic profile showing megasequence 5 across the 2016 3D-PSTM, dip-line number 4860. **(A)** uninterpreted **(B)** interpreted including sequence boundaries and stratal terminations. LST = Low-Stand system tract. Double-arrow indicates the thickest zone of this megasequence. **(C)** Envelope seismic attribute **(D)** Instantaneous Phase seismic attribute.

Location of this seismic section is shown in Figures 67, 69 - 70.

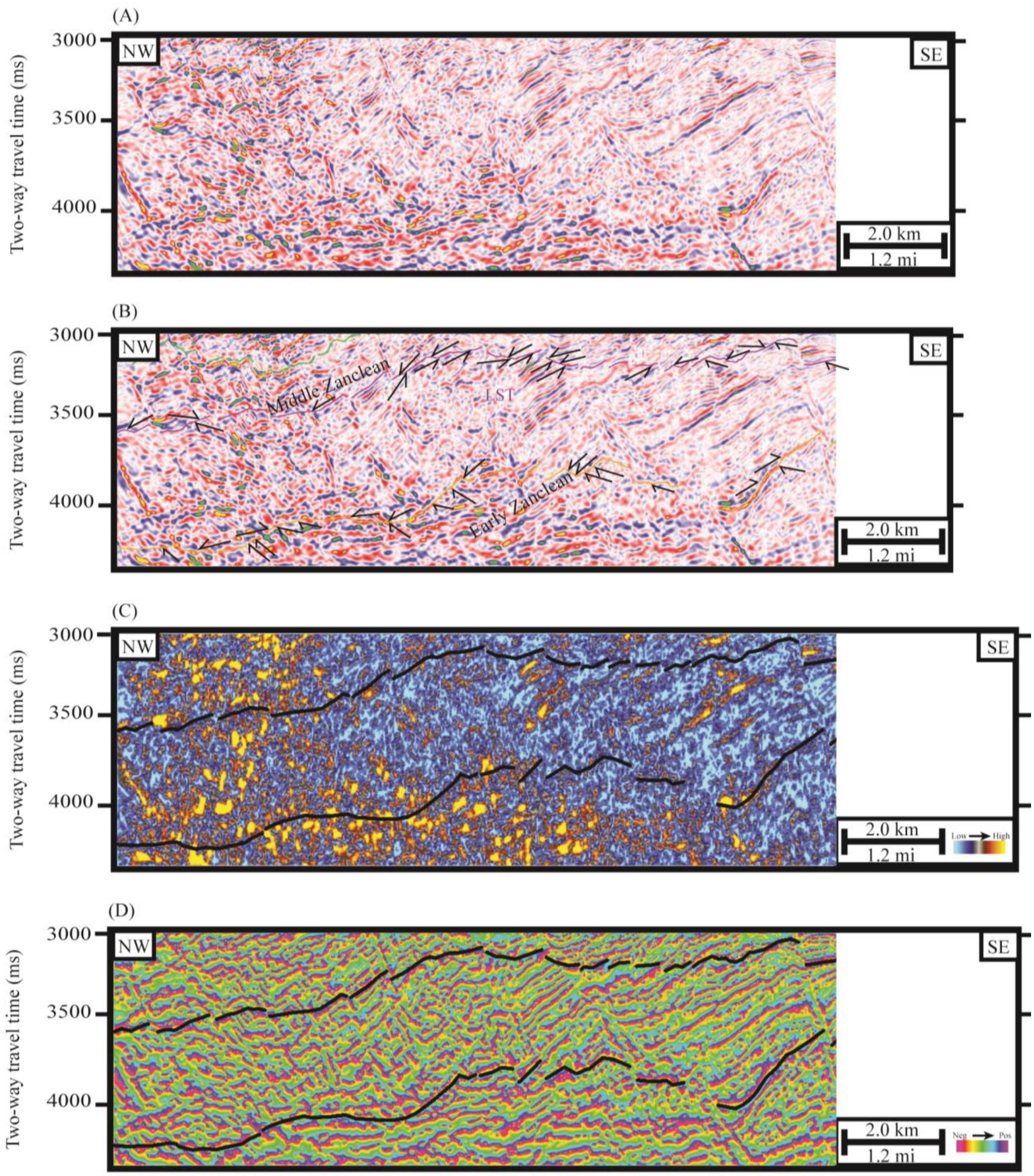

Figure 65: Seismic profile showing megasequence 5 across the 2016 3D-PSTM, dip-line number 6500. **(A)** uninterpreted **(B)** interpreted including sequence boundaries and stratal terminations. LST = Low-Stand system tract. Double-arrow is meaning to the thickest zone of this megasequence. **(C)** Envelope seismic attribute **(D)** Instantaneous Phase seismic attribute.

Location of this seismic section is shown in Figures 67, 69 - 70.

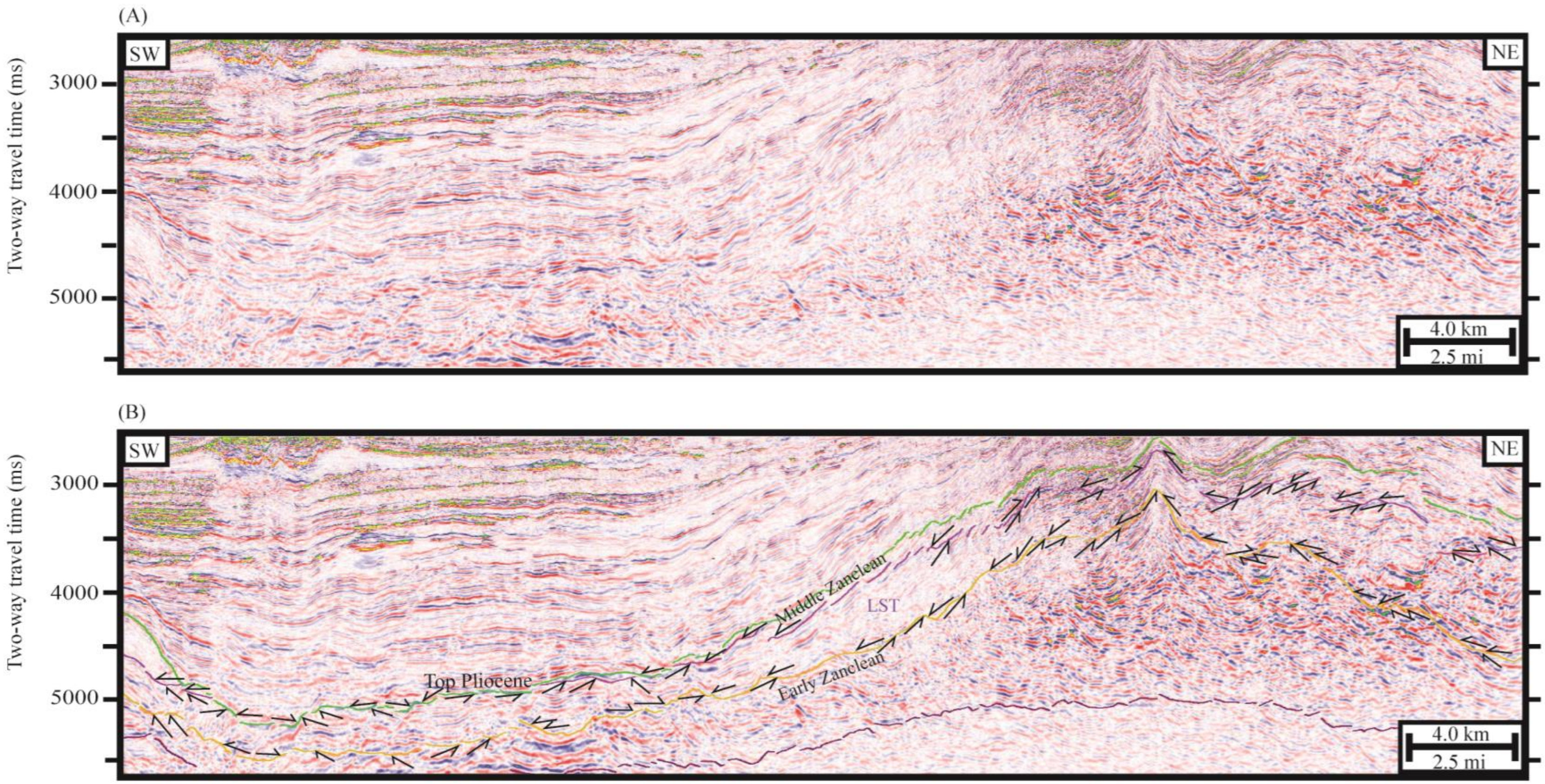

Figure 66: Seismic profile showing megasequence 5 across the 2016 3D-PSTM, strike-line number 3700. **(A)** uninterpreted **(B)** interpreted including sequence boundaries and stratal terminations. LST = Low-Stand system tract.

Location of this seismic section is shown in Figures 67, 69 - 70.

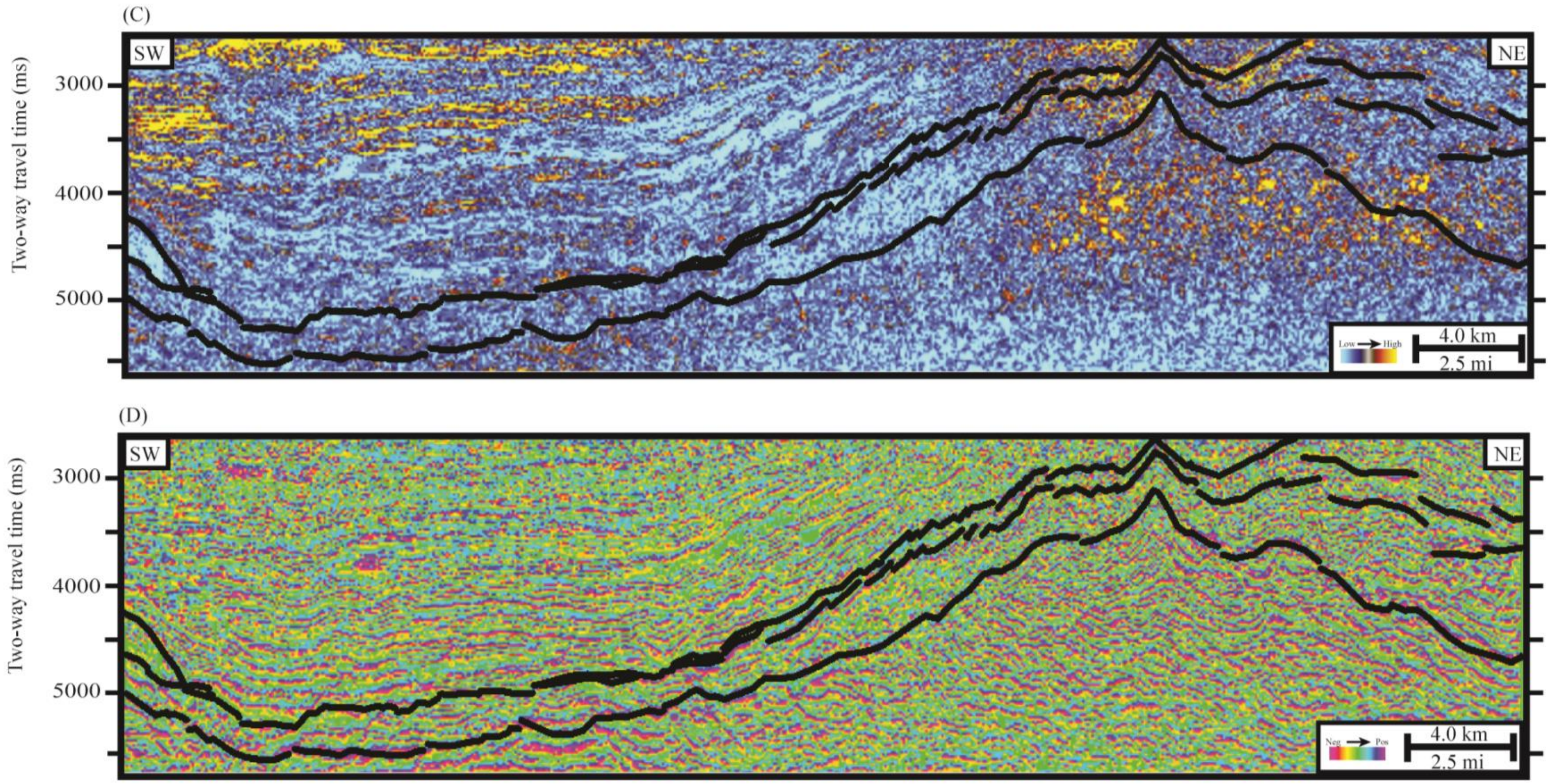

Figure 66: (C) Envelope seismic attribute **(D)** Instantaneous Phase seismic attribute.

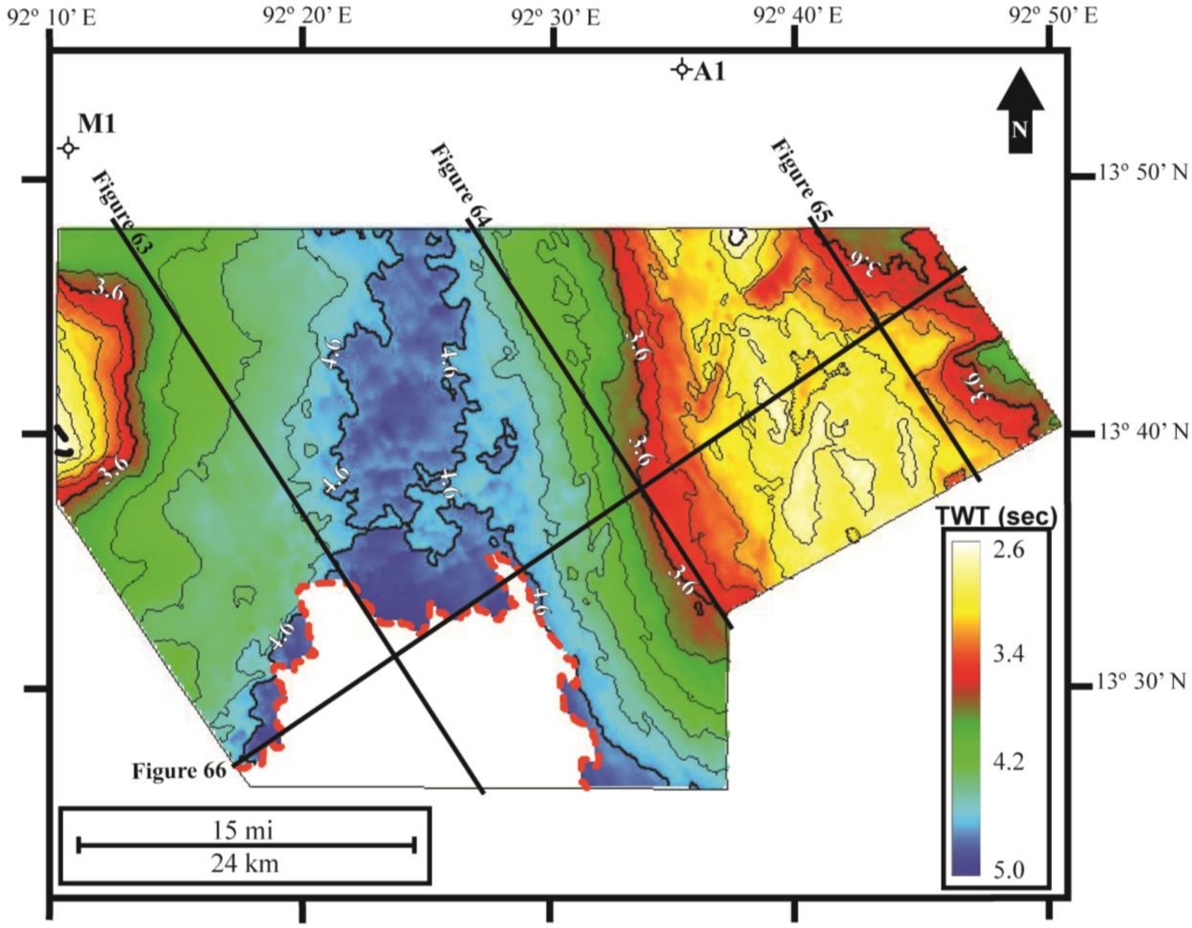

Figure 67: Time structure map of middle Zanclean (TWT). Contour interval is 200 milliseconds with bold contour in every second. Black dash-line is onlap edge and red dash-line is truncation edge.

Locations of Figures 63 – 66 are shown.

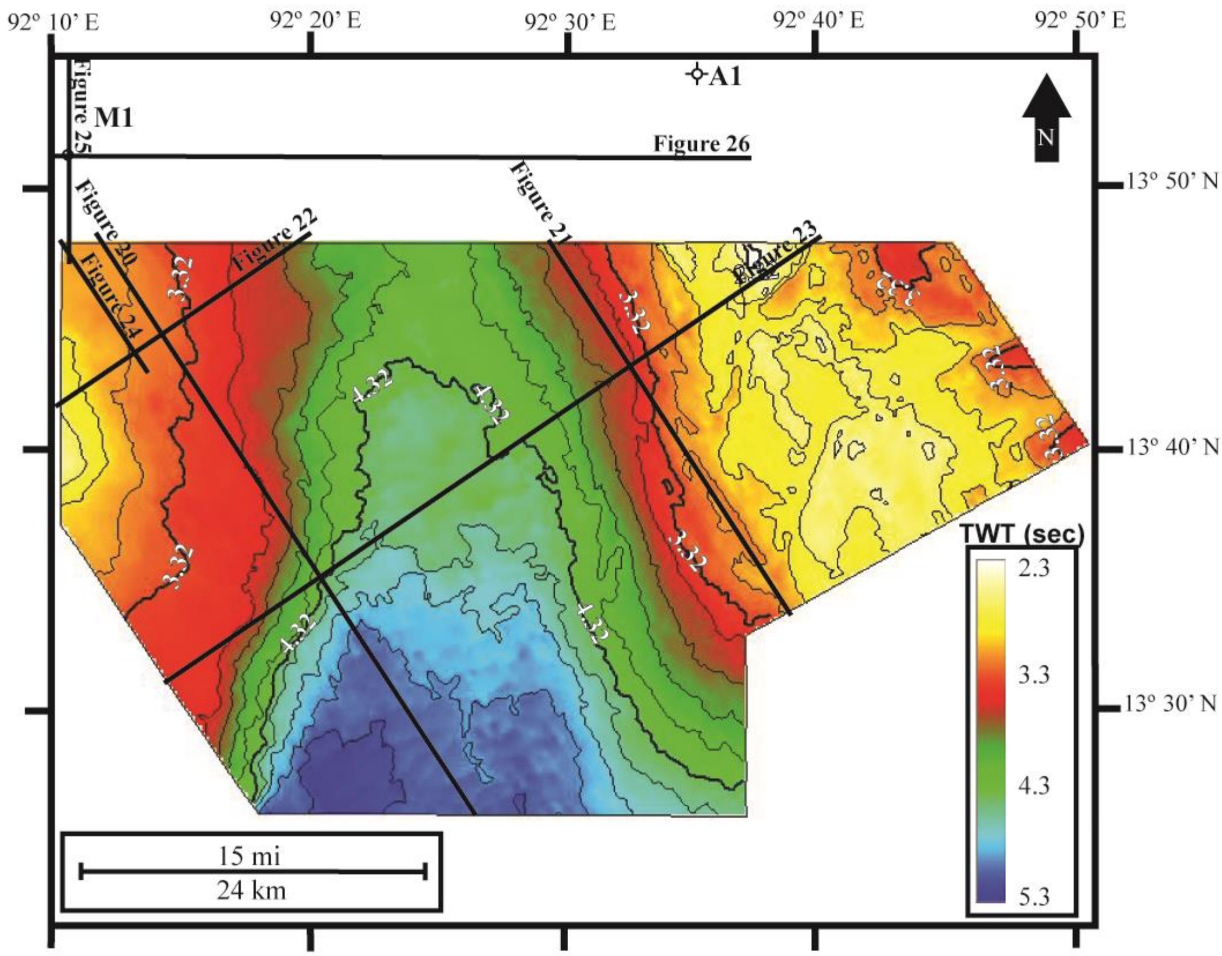

Figure 68: Time structure map of Top Pliocene (TWT). Contour interval is 200 milliseconds with bold contour in every second.

Locations of Figures 20 – 26 are shown.

(Figure 65). The megasequence thins to the west due to the onlap onto shallow carbonate buildup and to the south from erosional truncation (Figures 63, 66).

Seismic Facies: Four seismic and geological facies that were interpreted based on the seismic attributes, i.e. instantaneous phase and envelope (Figure 70). The oveall trend of the facies is N-S. Facies 1 is a series of parallel reflections, with moderate to high amplitude with good continuity (Figures 63, 64 and 66). Facies 2 is a series of hummocky, high amplitude with moderate continuity (Figures 65 and 66), which was affected by thrust faults. Facies 3 and 4 are a series of parallel to sub-parallel reflections, with low to moderate and low amplitude, respectively (Figures 63 - 66).

Geological Interpretation: The depositional environment map (Figure 71) was interpreted based on seismic facies (Figure 70) and seismic attributes (Figures 70, 71). All facies configurations consist of parallel, sub-parallel with partial hummocky reflections (Figures 63 – 66). Sand channel belts are interpreted in facies 2 and facies 1 based on the higher values of sweetness attribute (Figure 71). Levees that are associated with the channels are interpreted in facies 1 and facies 3. The lower sweetness value of facies 3 is interpreted as distal overbank sediments. Facies 3 is also included muddy channel belts. The overall channel belts trend N-S direction (Figures 70, 71); the stratal transformation calculation also suggests-S trending channel features (Figure 72).

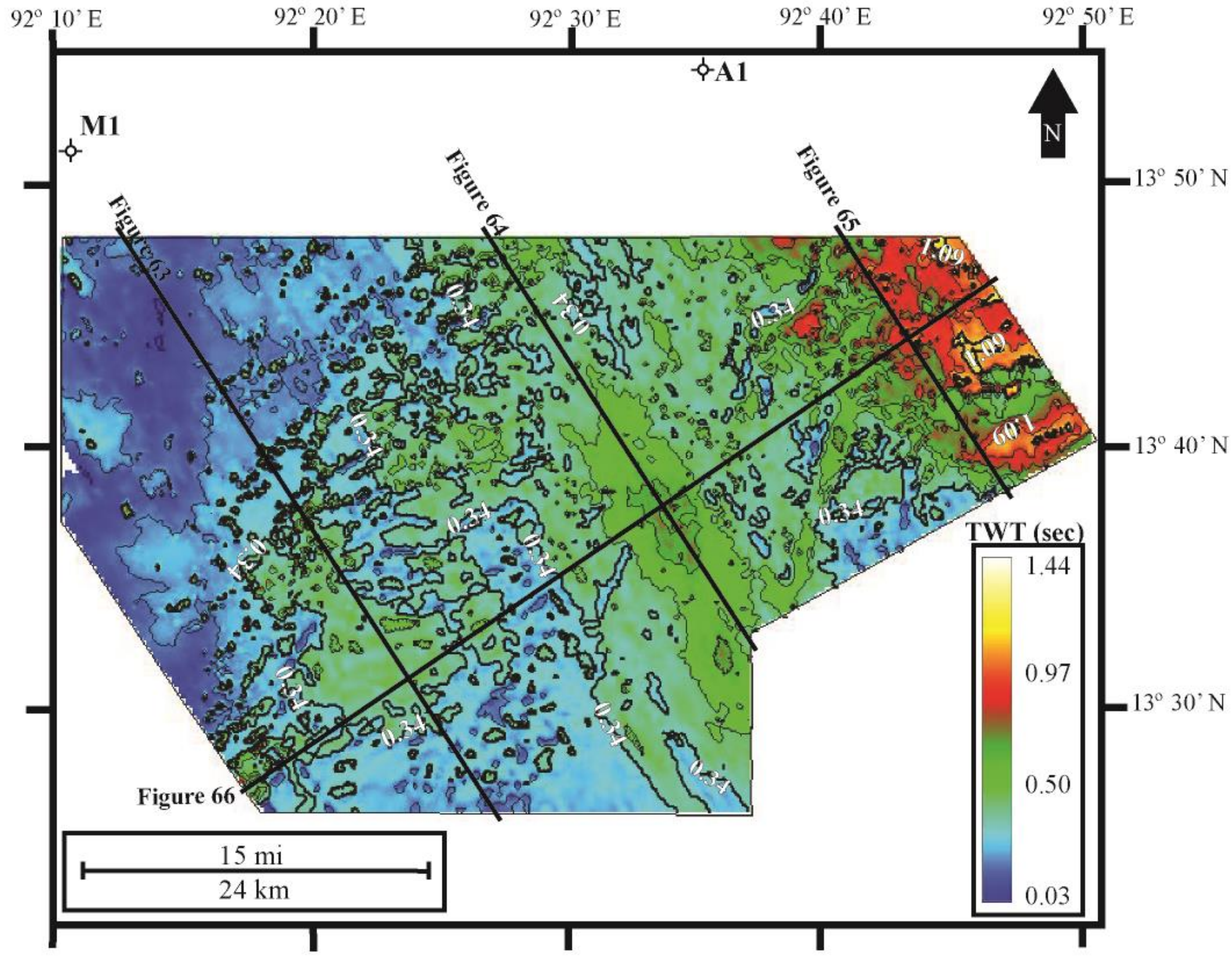

Figure 69: Isochron map of middle Zanclean megasequence (TWT). Contour interval is 200 milliseconds with bold contour in every second.

Locations of Figures 63 – 66 are shown.

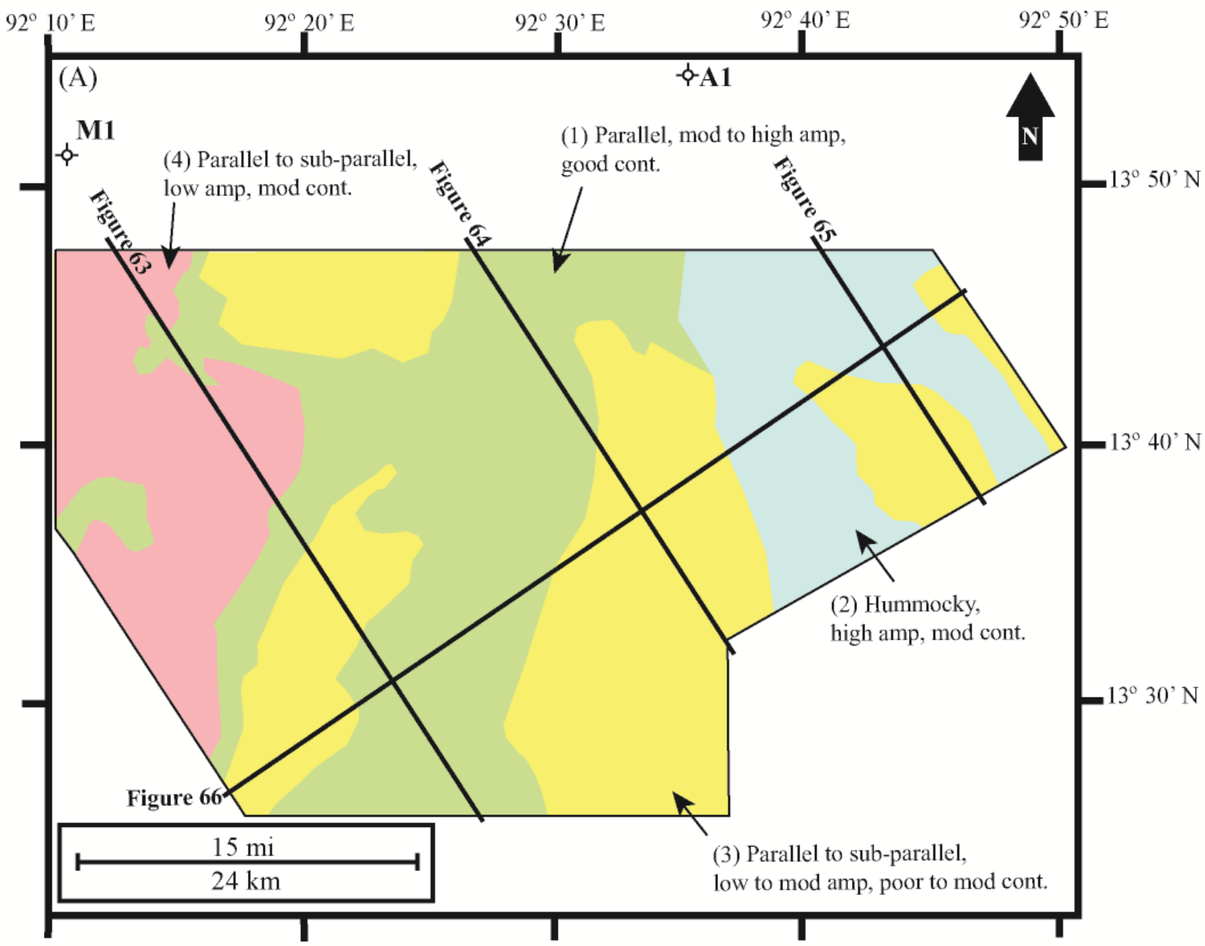

Figure 70: (A) Interpreted seismic facies map as green color is facies 1, blue color is facies 2, yellow color is facies 3 and pink color is facies 4. Each facies is listed by reflection configuration, following by amplitude (amp.) and continuity (cont.) classifications. **(B)** Envelope attribute map, calculated at 30 milliseconds above early Zanclean surface. Map is twt unit. **(C)** Instantaneous Phase attribute map, calculated at 30 milliseconds above early Zanclean surface. Map is degree of phase unit.

Locations of Figures 63 – 66 are shown.

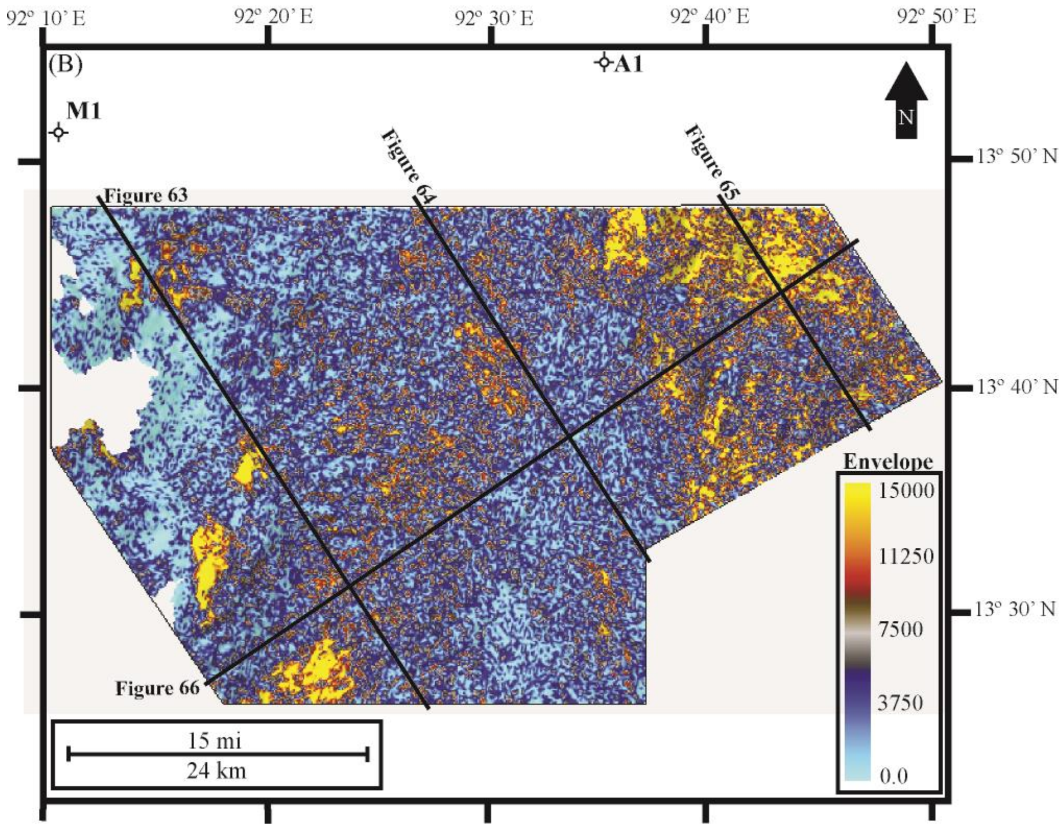
92° 10' E
92° 20' E
92° 30' E
92° 40' E
92° 50' E
(B)
A1
M1
N
13° 50' N
13° 40' N
13° 30' N
Figure 63
Figure 64
Figure 65
Figure 66
Envelope
15000
11250
7500
3750
0.0
15 mi
24 km

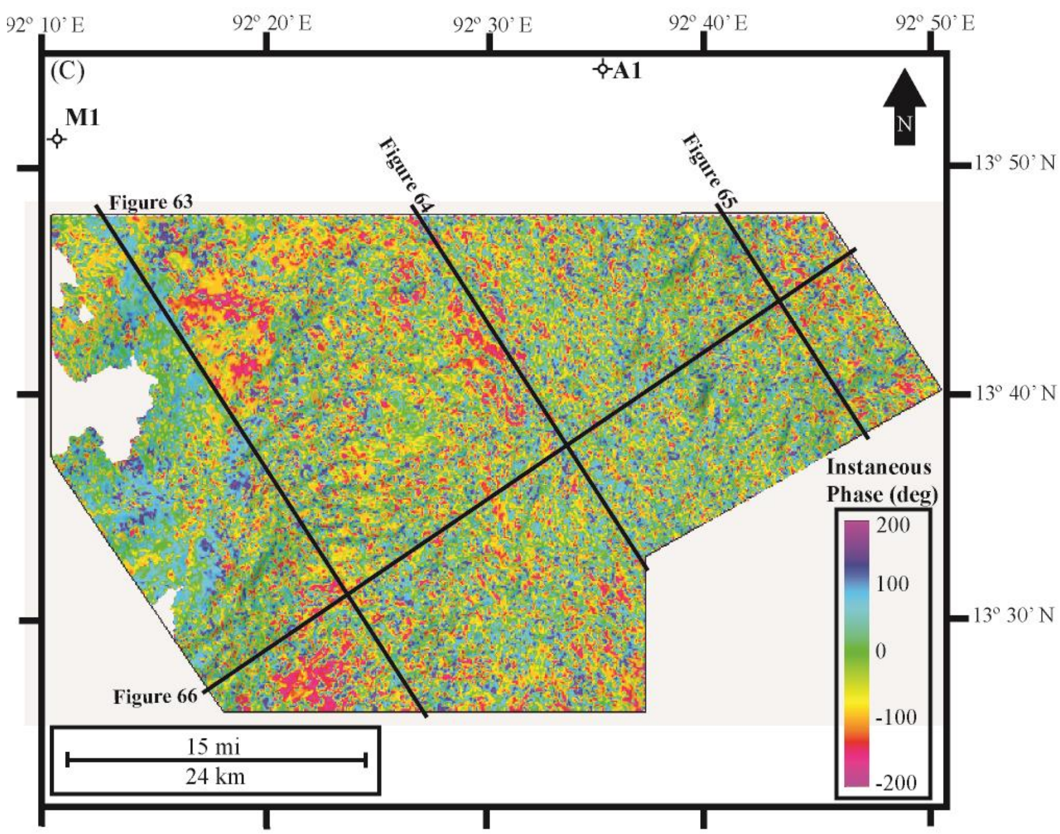
92° 10' E
92° 20' E
92° 30' E
92° 40' E
92° 50' E
(C)
A1
M1
N
13° 50' N
13° 40' N
13° 30' N
Figure 63
Figure 64
Figure 65
Figure 66
Instaneous
Phase (deg)
200
100
0
-100
-200
15 mi
24 km

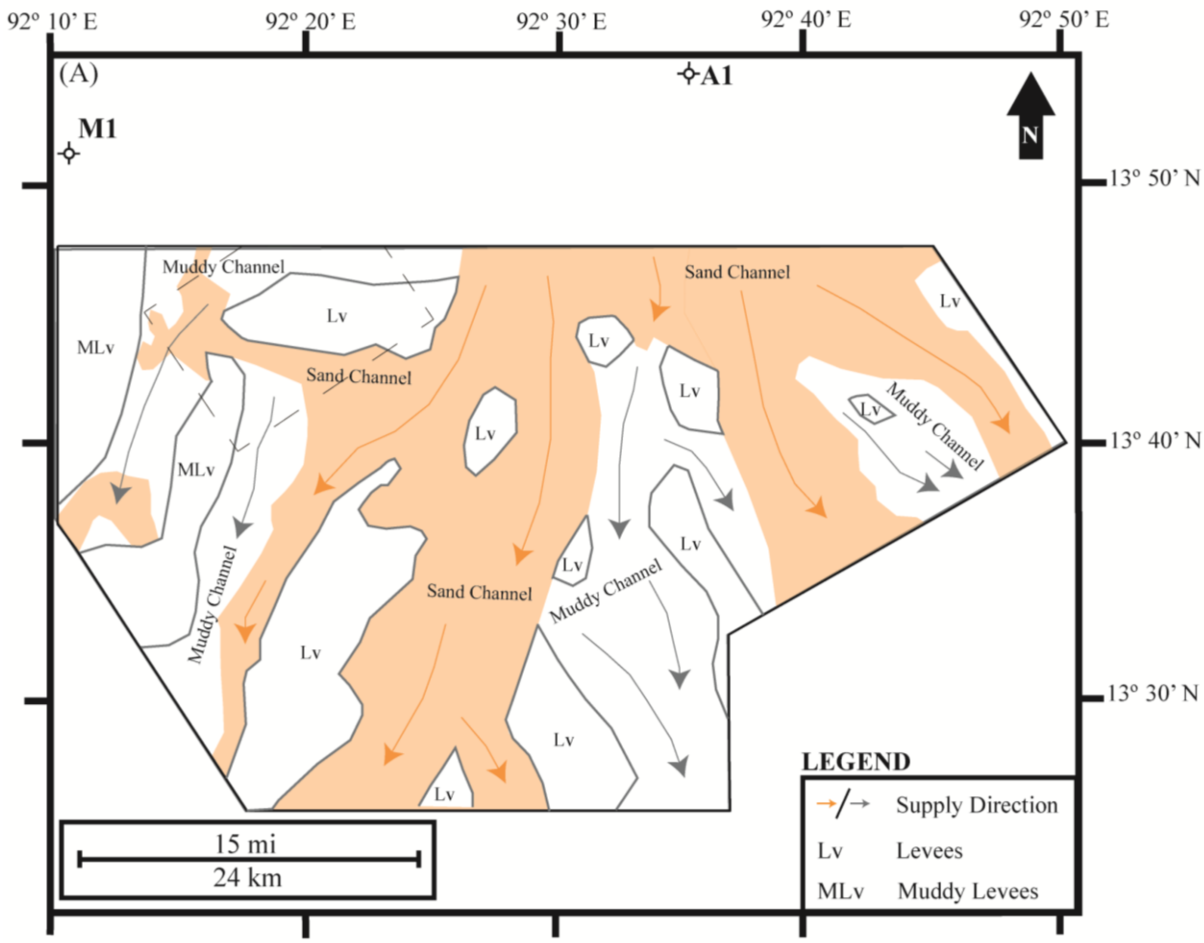

Figure 71: (A) Depositional setting map **(B)** Sweetness attribute map, calculated at 30 milliseconds above early Zanclean surface. Map is absolute amplitude value in twt unit. **(C)** Coherency attribute map, calculated at 30 milliseconds above early Zanclean surface.

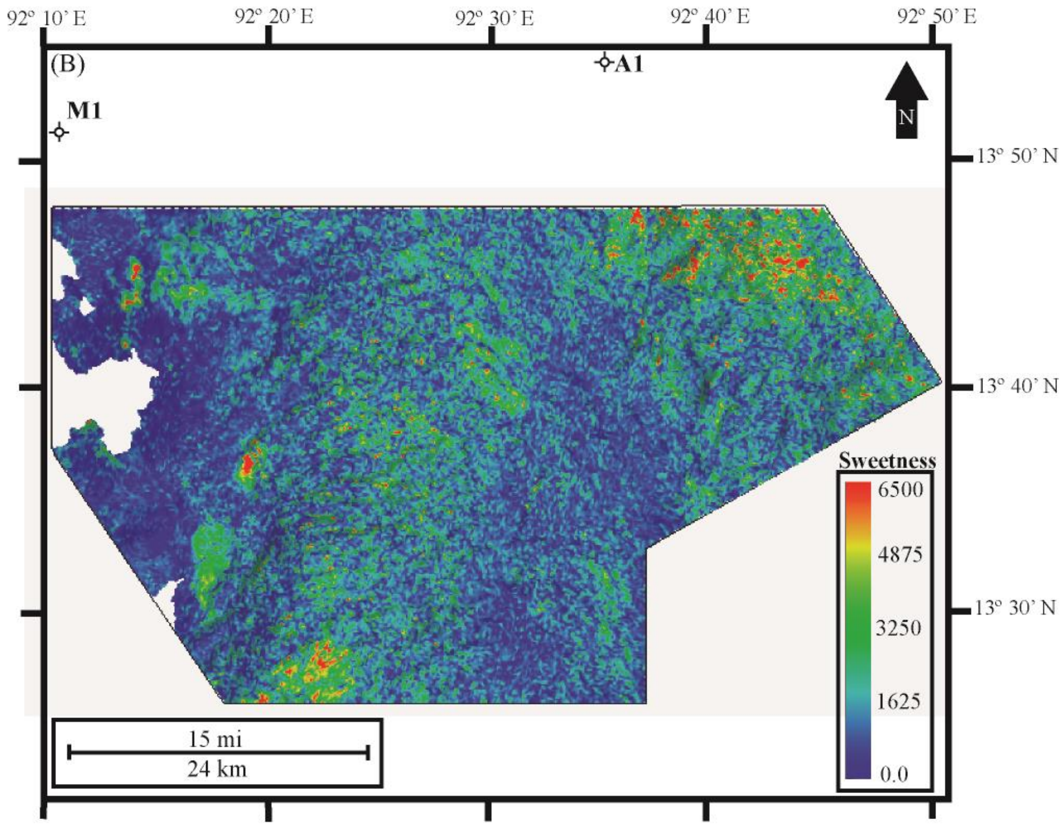

92º 10' E
92º 20' E
92º 30' E
92º 40' E
92º 50' E
(B)
A1
M1
N
13º 50' N
13º 40' N
13º 30' N
Sweetness
6500
4875
3250
1625
0.0
15 mi
24 km

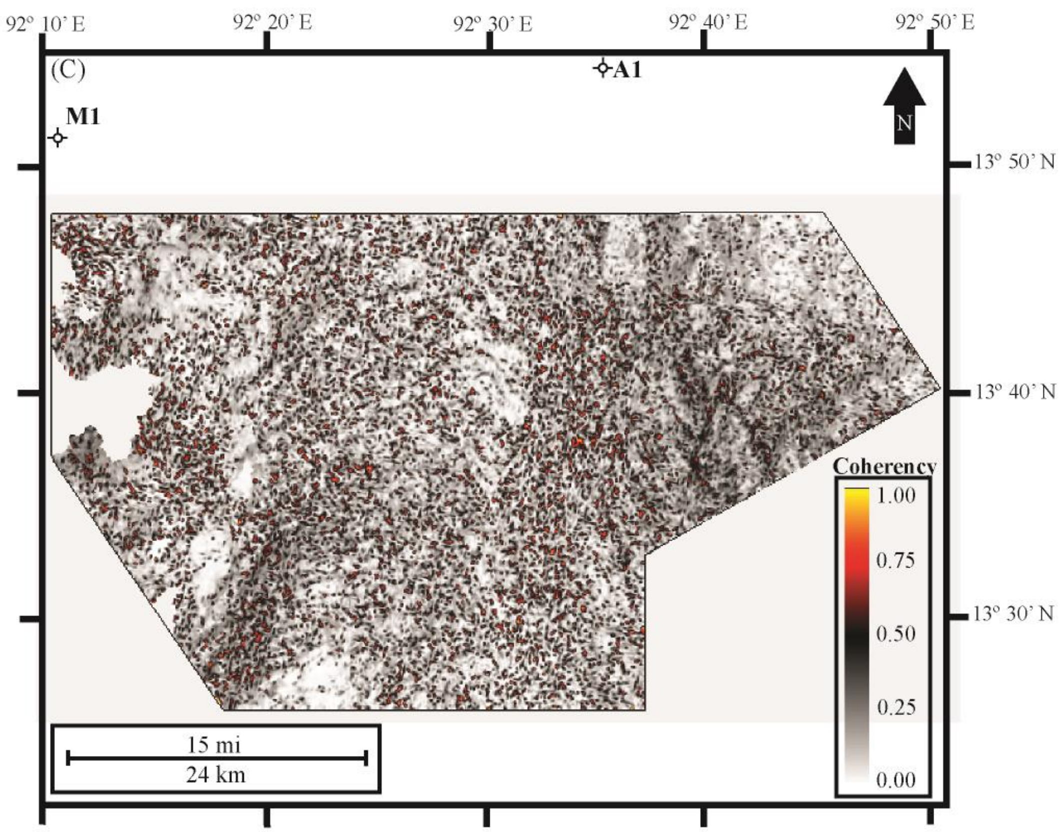

92º 10' E
92º 20' E
92º 30' E
92º 40' E
92º 50' E
(C)
A1
M1
N
13º 50' N
13º 40' N
13º 30' N
Coherency
1.00
0.75
0.50
0.25
0.00
15 mi
24 km

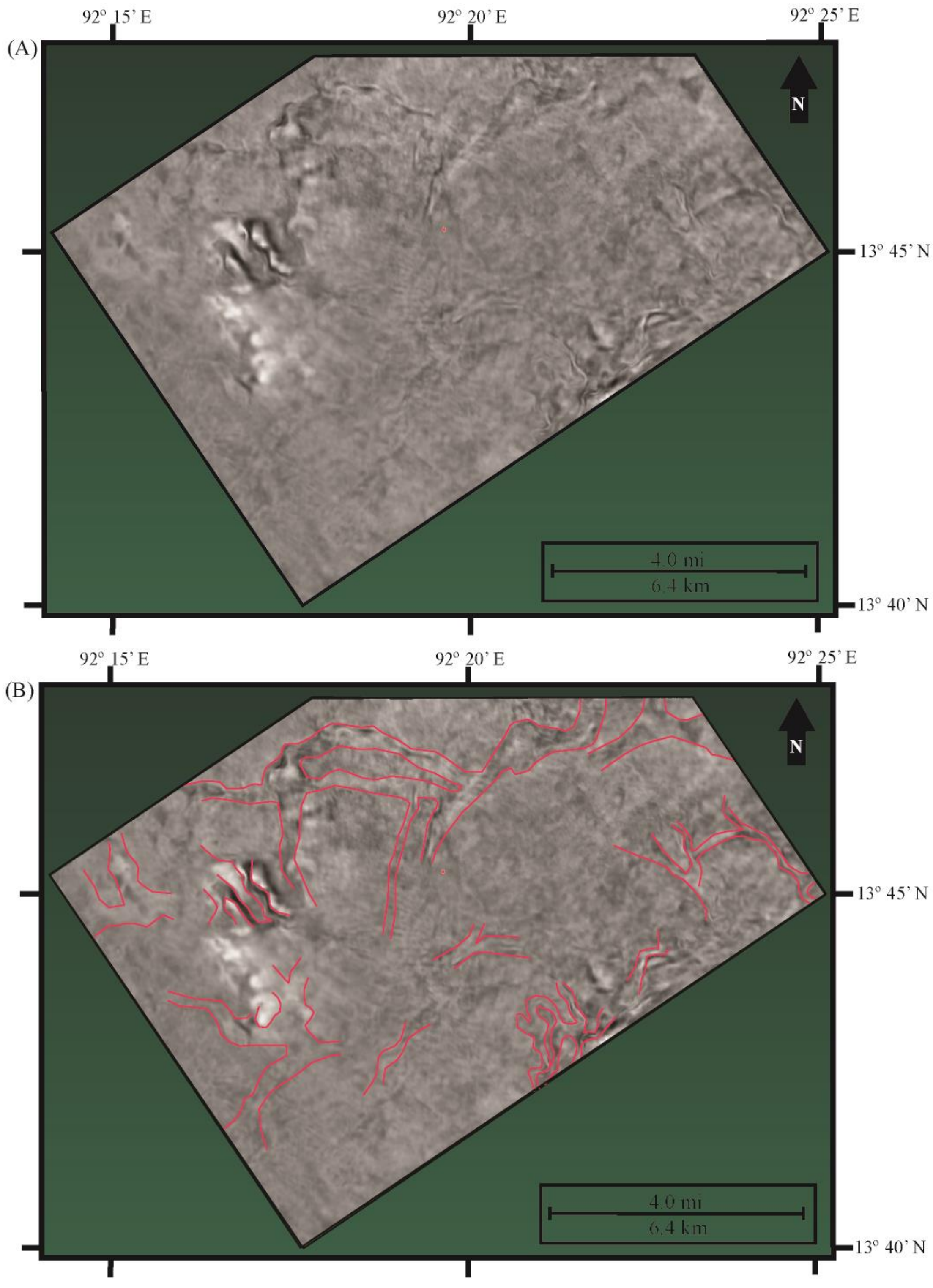

Figure 72: Strata transformation calculation horizon map about 30 milliseconds above early Zanclean surface. **(A)** Uninterpreted **(B)** Interpreted depositional environment showing possible channel features. For location, see in figure 15B and 71.

Megasequence 6: late Zanclean

Key Surfaces: The lower sequence boundary was defined by the merged surface consisting of early Miocene and middle Zanclean horizons (Figures 20, 73 - 76). Startal onlap is extensive at the lower boundary, as well as erosional truncation below the horizon (Figures 73 – 76). The moderate to high amplitude peak seismic reflection corresponds to this sequence boundary.

The upper sequence boundary was identified by two merged surfaces merging (early Pliocene and Top Pliocene surfaces) with onlap and truncation at above and below the horizon, respectively (Figures 73 – 76). The seismic reflection picked as the moderate amplitude peak association together with high amplitude trough association, which responses to Top Pliocene surface.

Time-Structure Map: The structure map of one of the upper sequence boundary (early Pliocene) shows a homoclinal structure dipping to the east, with two-way travel time values ranging from 2.49 to 4.58 seconds (Figure 77). The horizon pinch-outs to the west. (Figures 73, 74, 77).

Isochron Map: The late Zanclean megasequence has two-way travel time values that range from 0.03 to 0.84 seconds interval (Figure 79), with most of this megasequence ranging between 0.23 to 0.42 seconds twt (Figures 73 - 76). Three thick zones are present in this megasequence (0.49 to 0.55 seconds twt) (Figure 56). The megasequence thins to the west and to the south due to sediment deposit onto the high structure area and the erosional feature, respectively (Figures 76, 78).

Age: This megasequence is penetrated by the M11 well (Figure 28), where the megasequence is relatively thin. The age is interpreted as late Zanclean, (lower Pliocene) (Table 2).

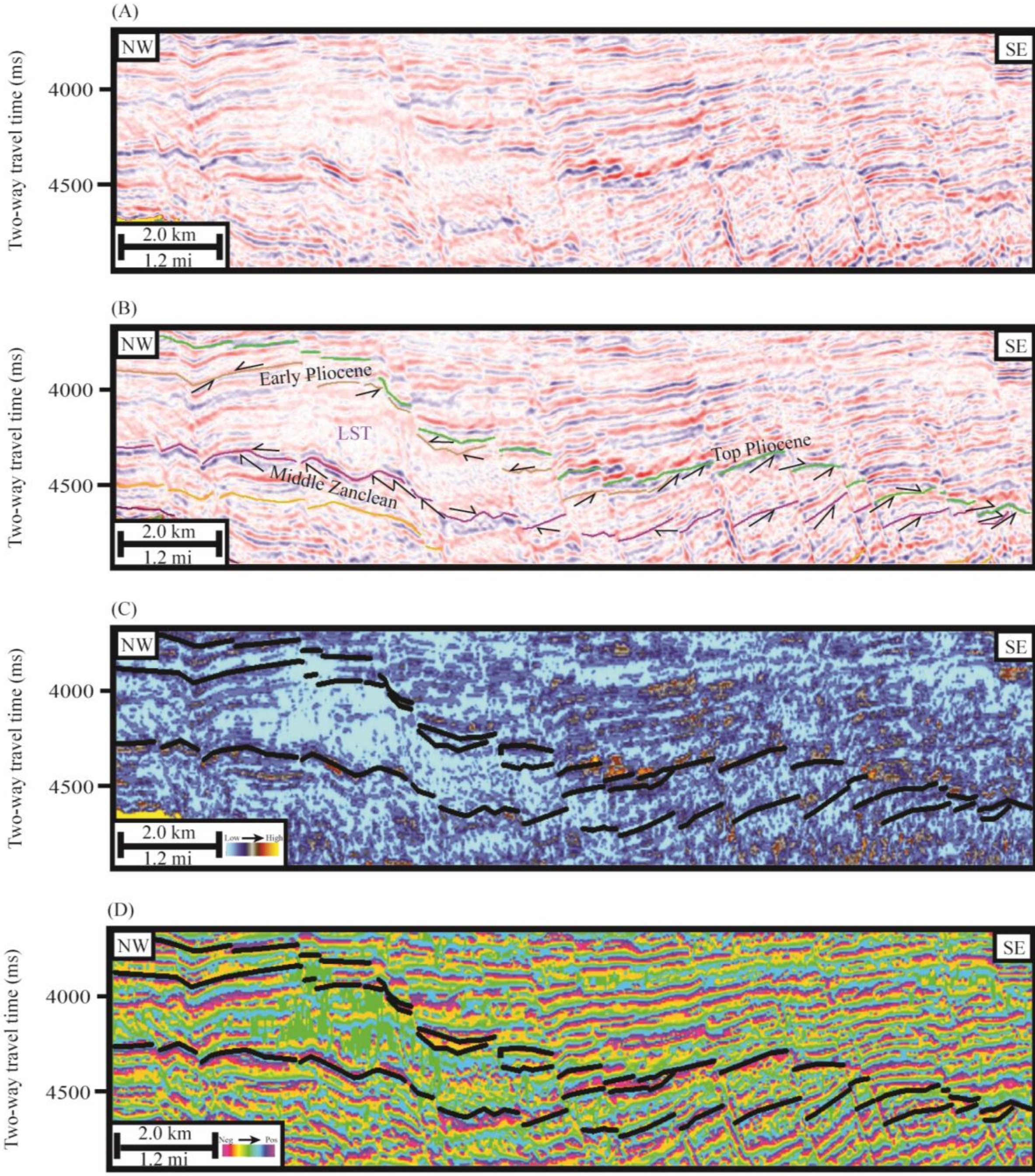

Figure 73: Seismic profile showing megasequence 6 across the 2016 3D-PSTM, dip-line number 2700. **(A)** uninterpreted **(B) i**nterpreted including sequence boundaries and stratal terminations. LST = Low-Stand system tract. Double-arrow indicates the thickest zone of this megasequence. **(C)** Envelope seismic attribute **(D)** Instantaneous Phase seismic attribute.

Location of this seismic section is shown in Figures 77 - 79.

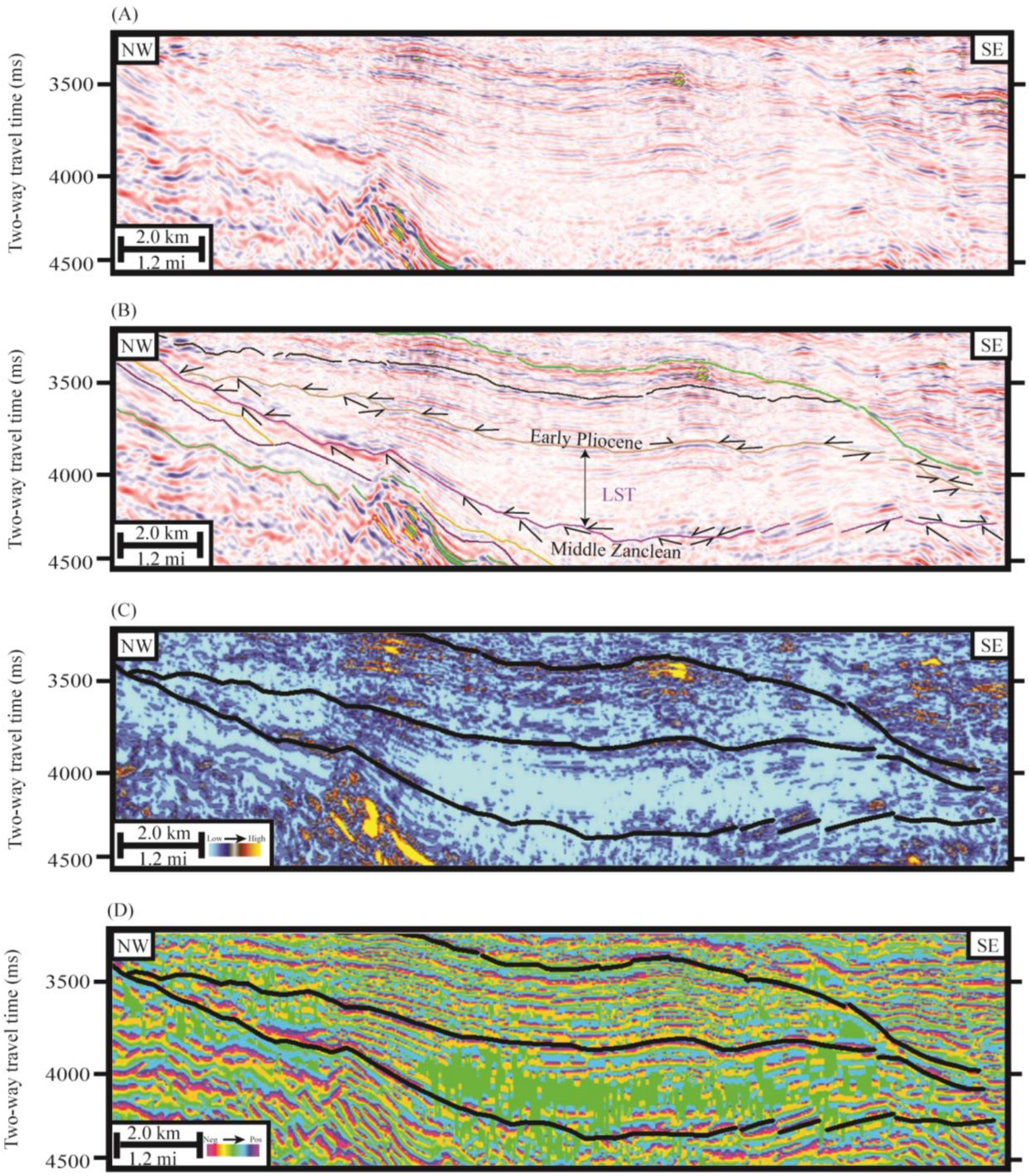

Figure 74: Seismic profile showing megasequence 6 across the 2016 3D-PSTM, dip-line number 3900. **(A)** uninterpreted **(B)** interpreted including sequence boundaries and stratal terminations. LST = Low-Stand system tract. **(C)** Envelope seismic attribute **(D)** Instantaneous Phase seismic attribute.

Location of this seismic section is shown in Figures 77 - 79.

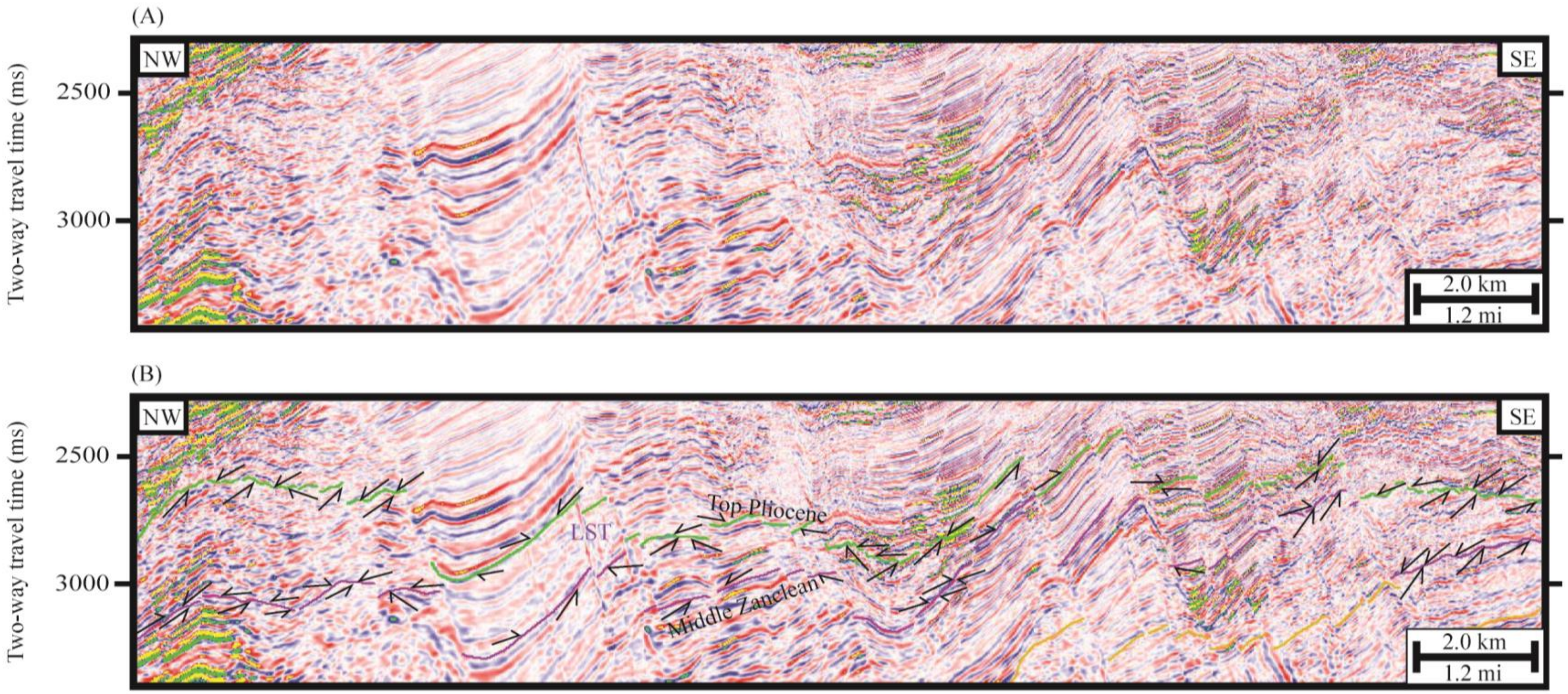

Figure 75: Seismic profile showing megasequence 6 across the 2016 3D-PSTM, dip-line number 5980. **(A)** uninterpreted **(B)** interpreted including sequence boundaries and stratal terminations. LST = Low-Stand system tract.

Location of this seismic section is shown in Figures 77 - 79.

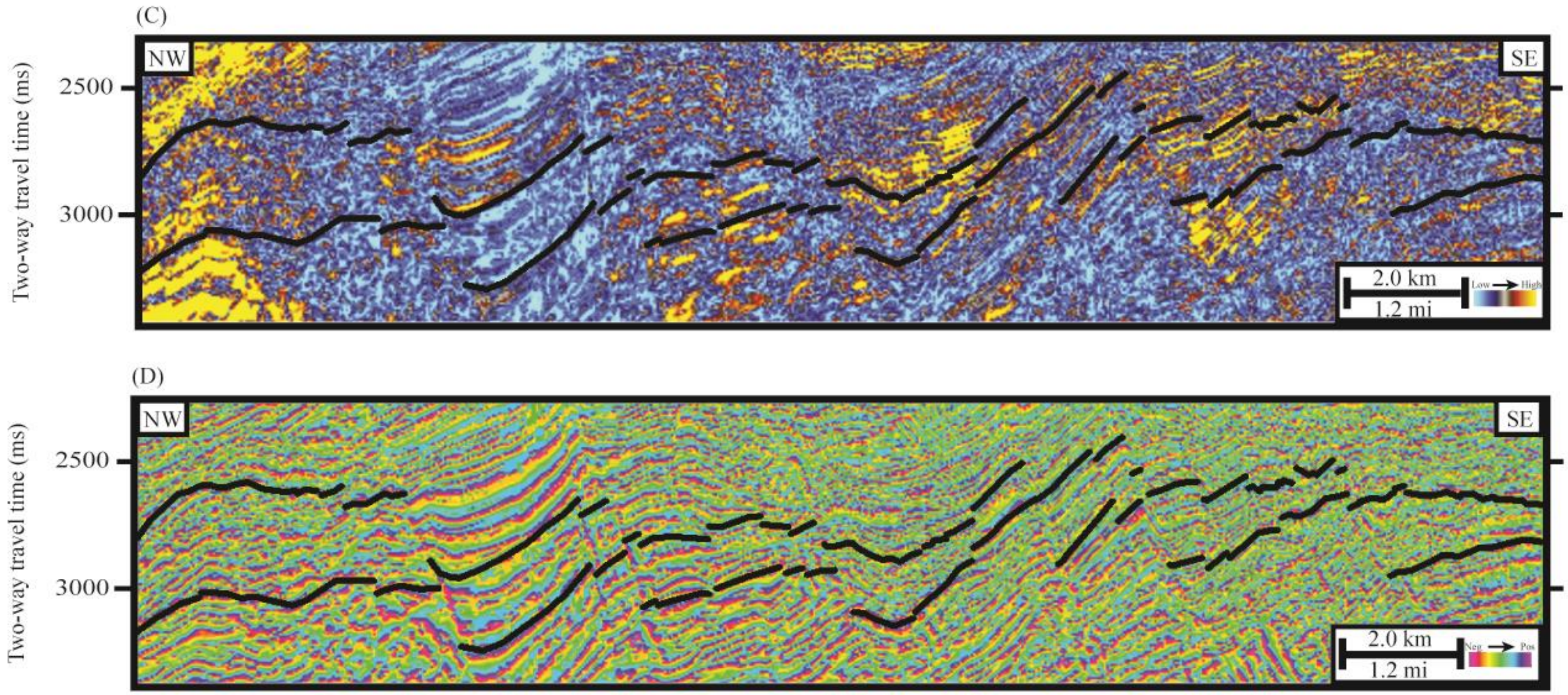

Figure 75: (C) Envelope seismic attribute **(D)** Instantaneous Phase seismic attribute.

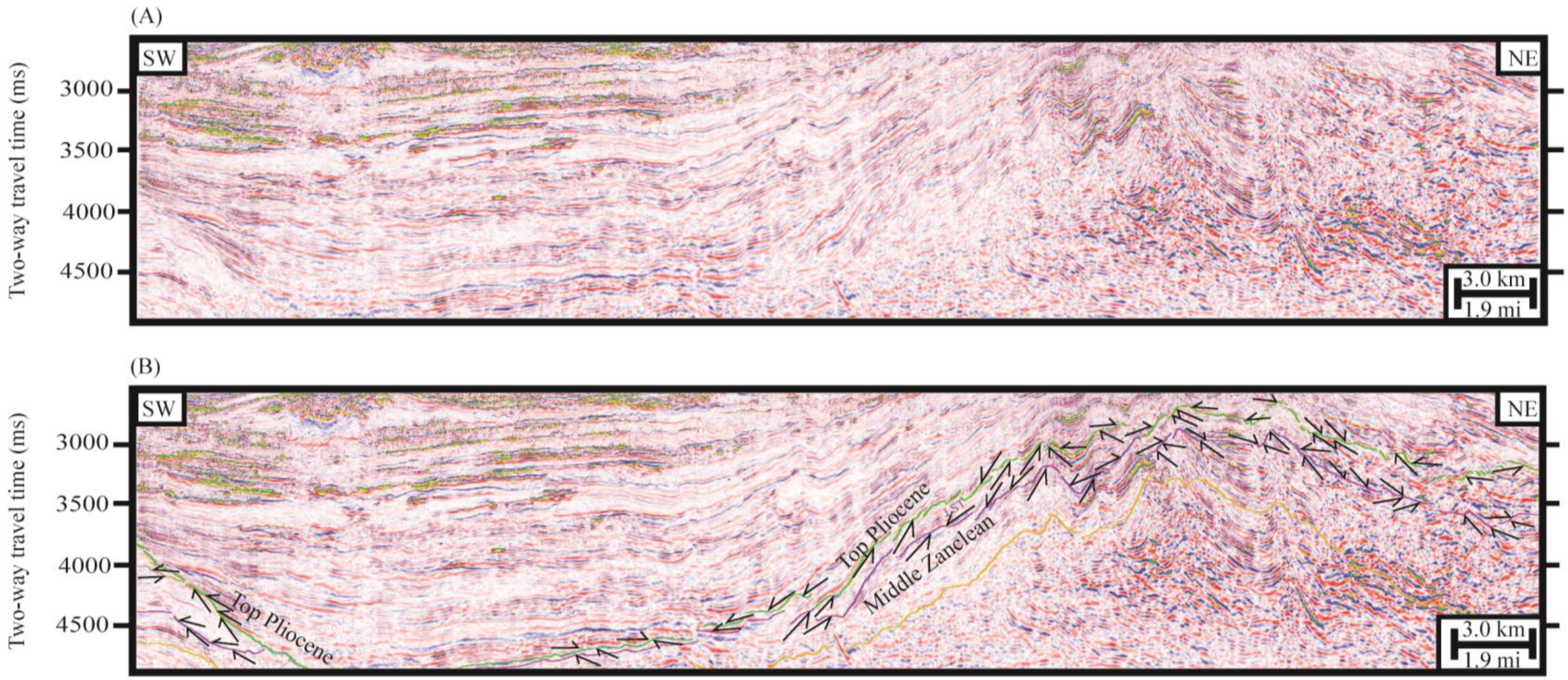

Figure 76: Seismic profile showing megasequence 6 across the 2016 3D-PSTM, strike-line number 3900. **(A)** uninterpreted **(B)** interpreted including sequence boundaries and stratal terminations. LST = Low-Stand system tract.

Location of this seismic section is shown in Figures 77 - 79.

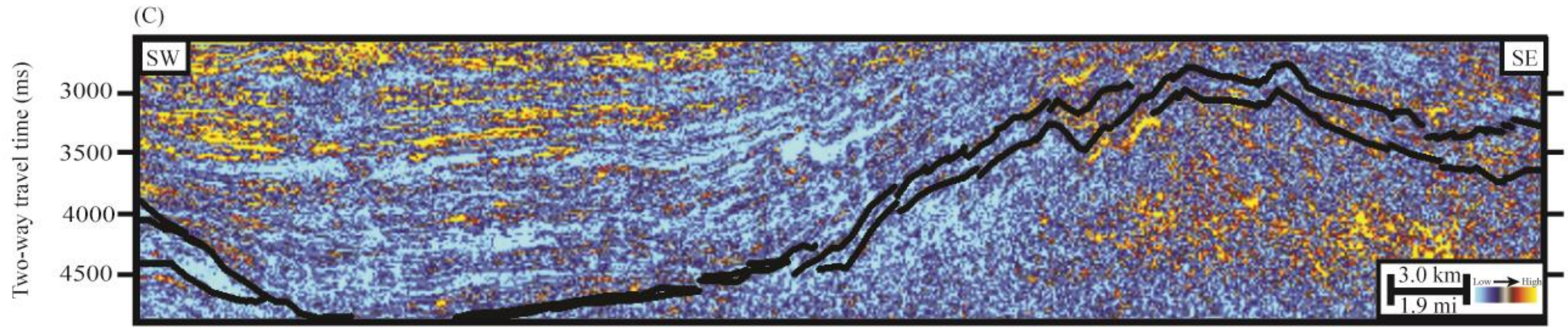

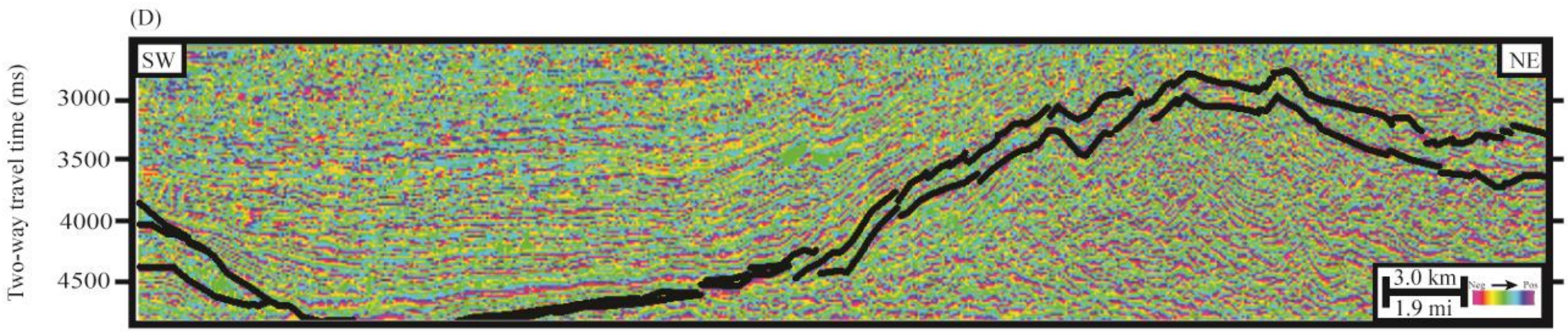

Figure 76: (C) Envelope seismic attribute **(D)** Instantaneous Phase seismic attribute.

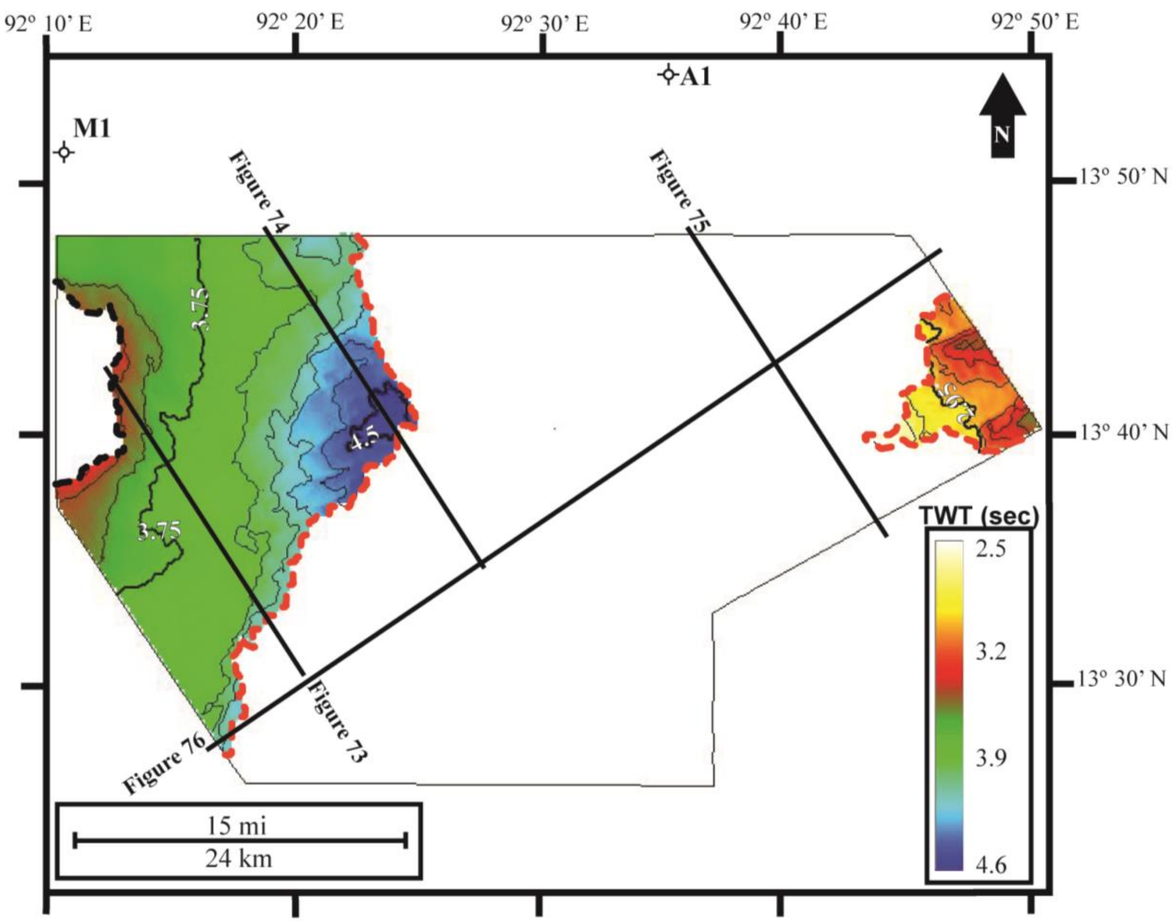

Figure 77: Time structure map of early Pliocene (TWT). Contour interval is 200 milliseconds with bold contour in every second. Black dash-line is onlap edge and red dash-line is truncation edge.

Locations of Figures 73 – 76 are shown.

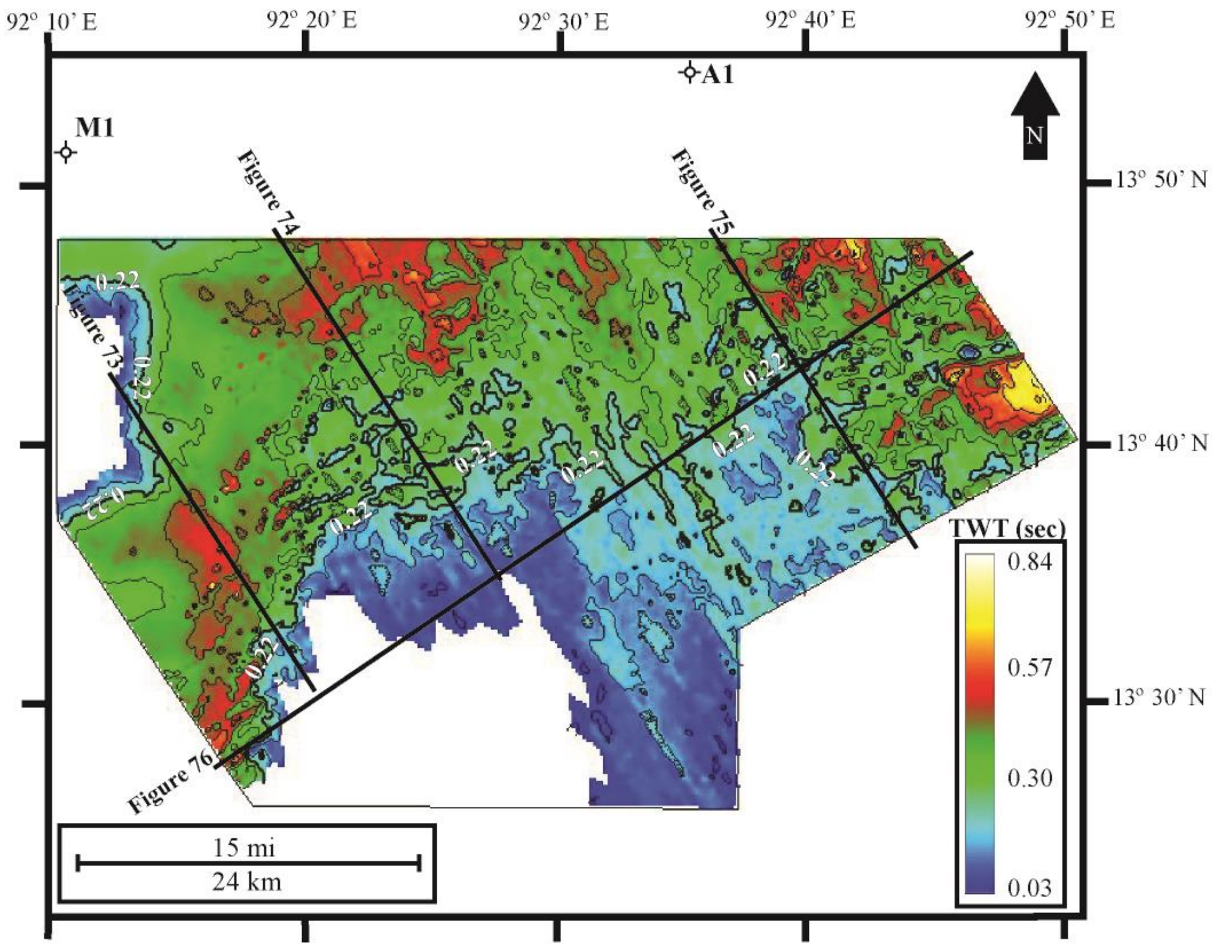

Figure 78: Isochron map of late Zanclean megasequence (TWT). Contour interval is 200 milliseconds with bold contour in every second.

Locations of Figures 73 – 76 are shown.

Seismic Facies: Three seismic and geological facies were interpreted based on the seismic attributes, i.e. instantaneous phase and envelope (Figure 79). Overall, the facies trending N-S. All facies consist of parallel and sub-parallel reflection. Facies 1 is characterized by moderate to high amplitude and good continuity (Figures 73 - 76). Facies 2 includes hummocky reflections (Figures 74 - 76), and facies 3 has different amplitude values (Figures 73, 76).

Geological Interpretation: The depositional environment map (Figure 80) was interpreted based on seismic facies (Figure 79) and seismic attributes (Figure 80). Sand channel belts are interpreted for facies 1. Levees that are associated with the channel are interpreted in facies 1 and facies 2. Facies 3 is interpreted as distal of overbank deposits. The overall channel belts trend in N-S direction (Figures 80, 81). The stratal transformation calculation also suggests N-S trending channel features (Figure 82).

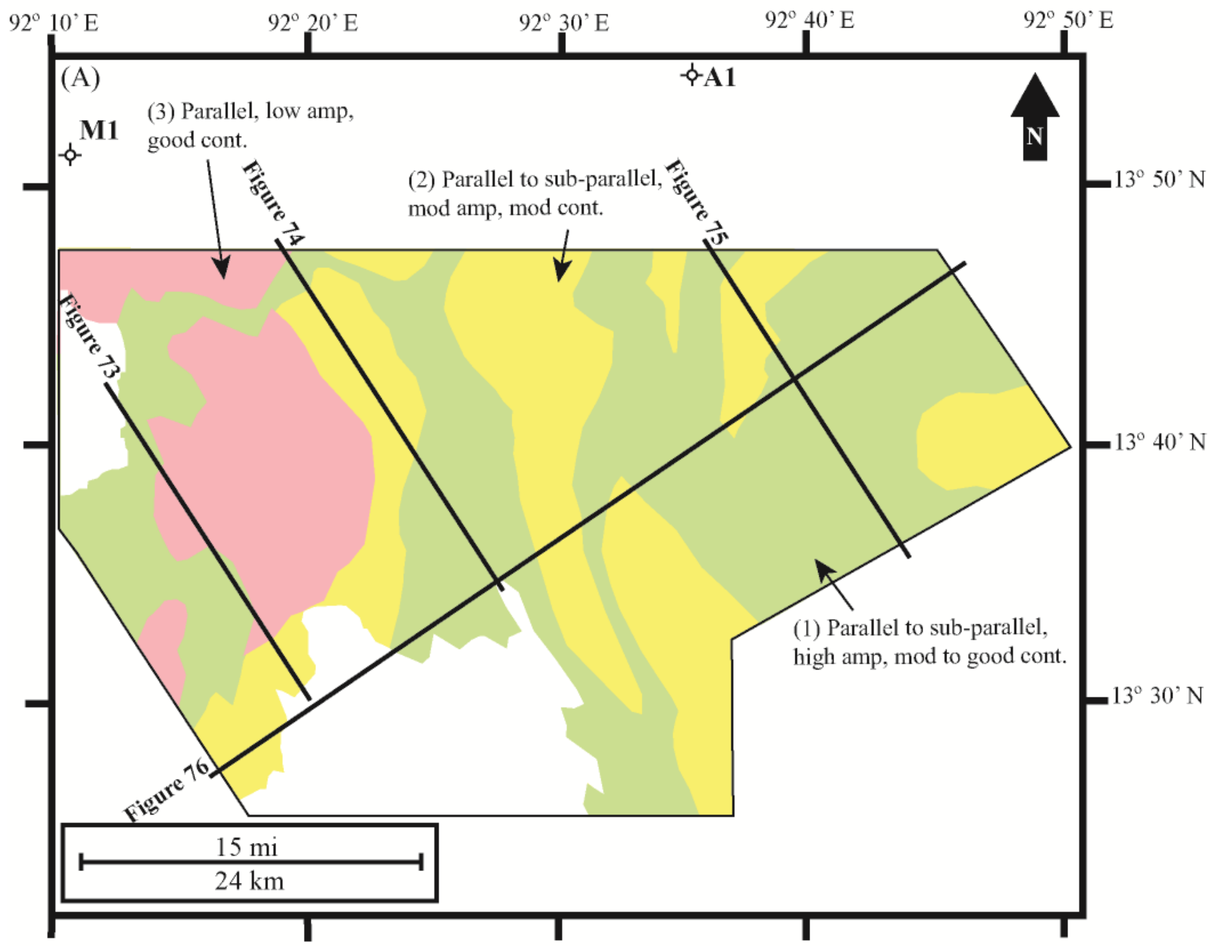

Figure 79: (A) Interpreted seismic facies map as green color is facies 1, yellow color is facies 2 and pink color is facies 3. Each facies is listed by reflection configuration, following by amplitude (amp.) and continuity (cont.) classifications. **(B)** Envelope attribute map, calculated at 30 milliseconds above middle Zanclean surface. Map is twt unit. **(C)** Instantaneous Phase attribute map, calculated at 30 milliseconds above middle Zanclean surface. Map is degree of phase unit.

Locations of Figures 73 – 76 are shown.

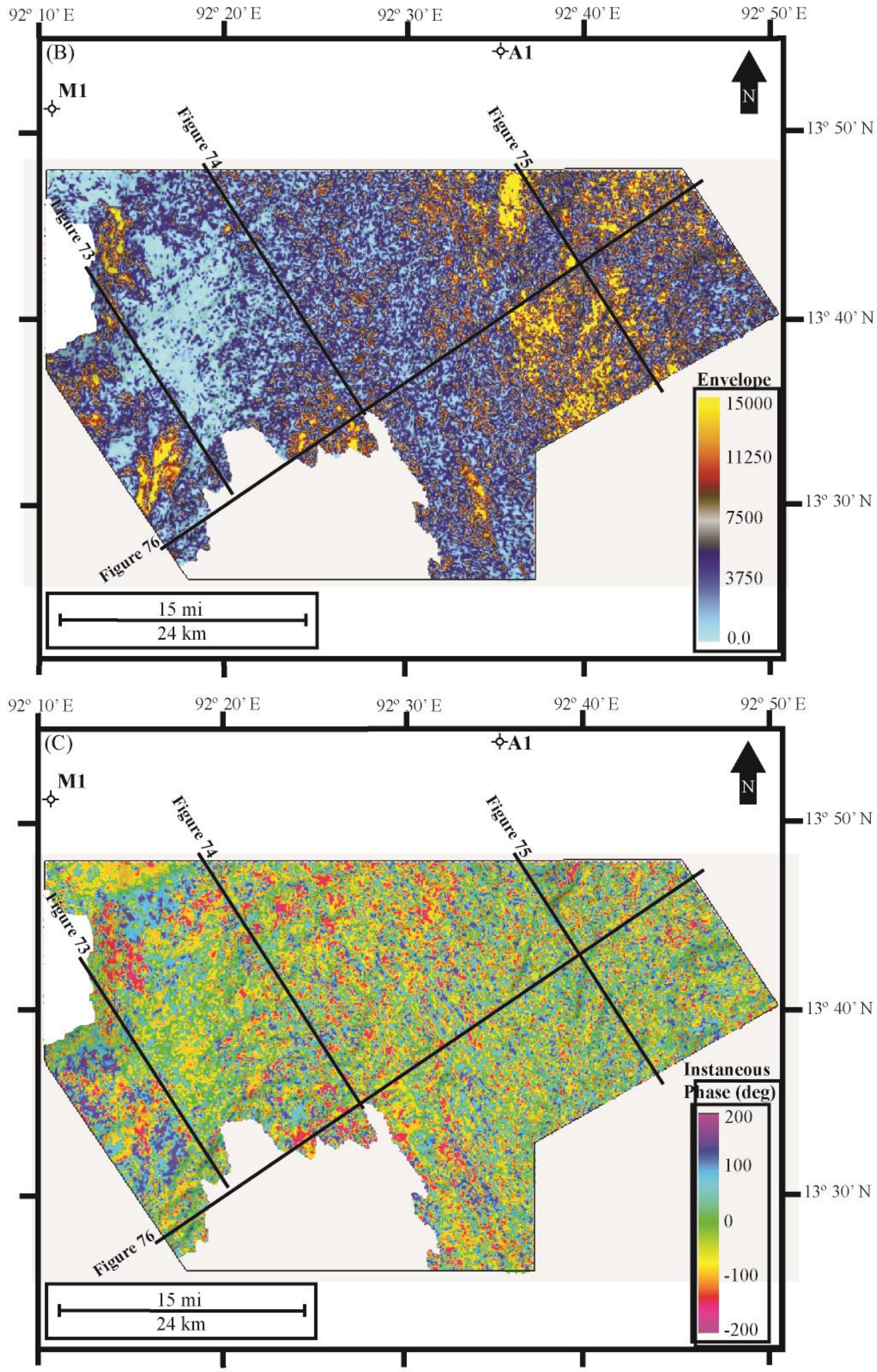
92° 10' E
92° 20' E
92° 30' E
92° 40' E
92° 50' E
(B)
A1
M1
N
Figure 74
Figure 75
Figure 73
Figure 76
13° 50' N
13° 40' N
13° 30' N
Envelope
15000
11250
7500
3750
0.0
15 mi
24 km
(C)
Instaneous
Phase (deg)
200
100
0
-100
-200

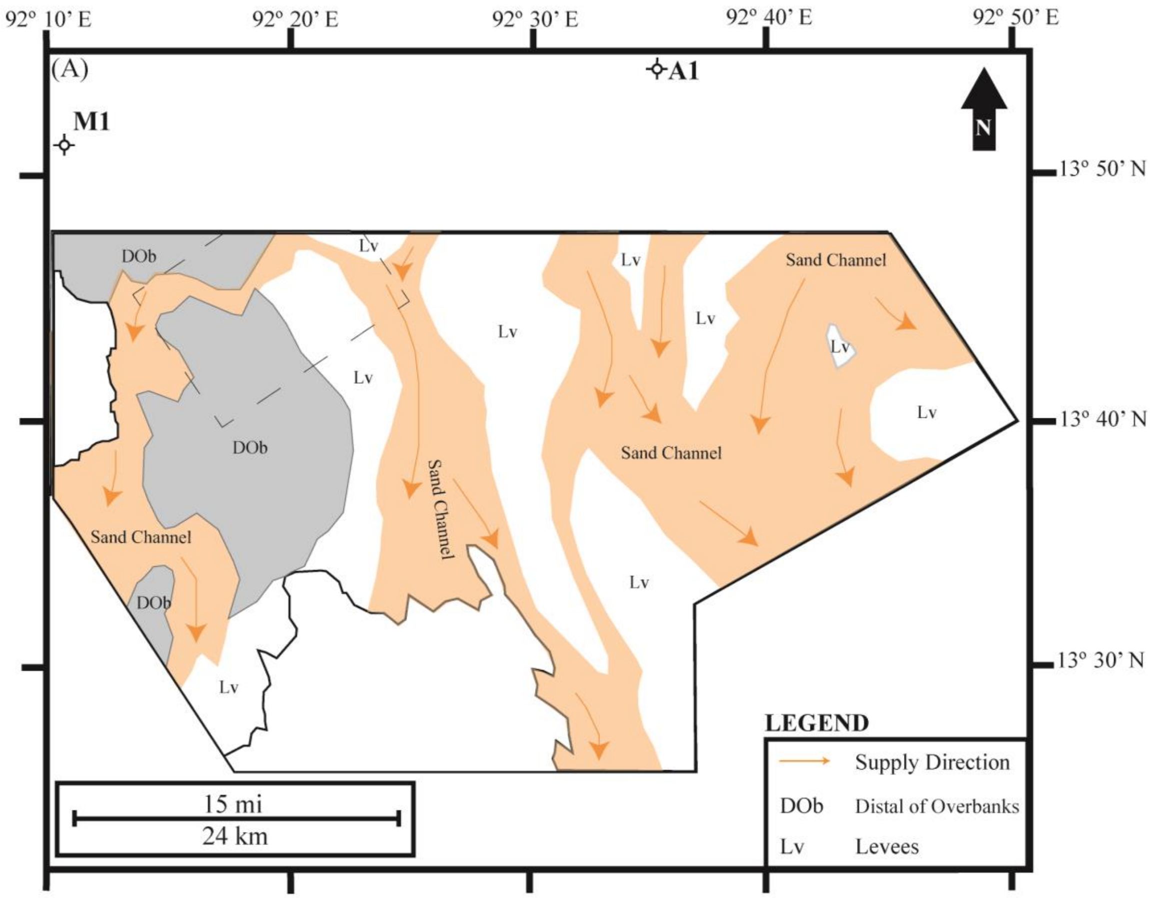

Figure 80: (A) Depositional setting map **(B)** Sweetness attribute map, calculated at 30 milliseconds above middle Zanclean surface. Map is absolute amplitude value in twt unit. **(C)** Coherency attribute map, calculated at 30 milliseconds above middle Zanclean surface.

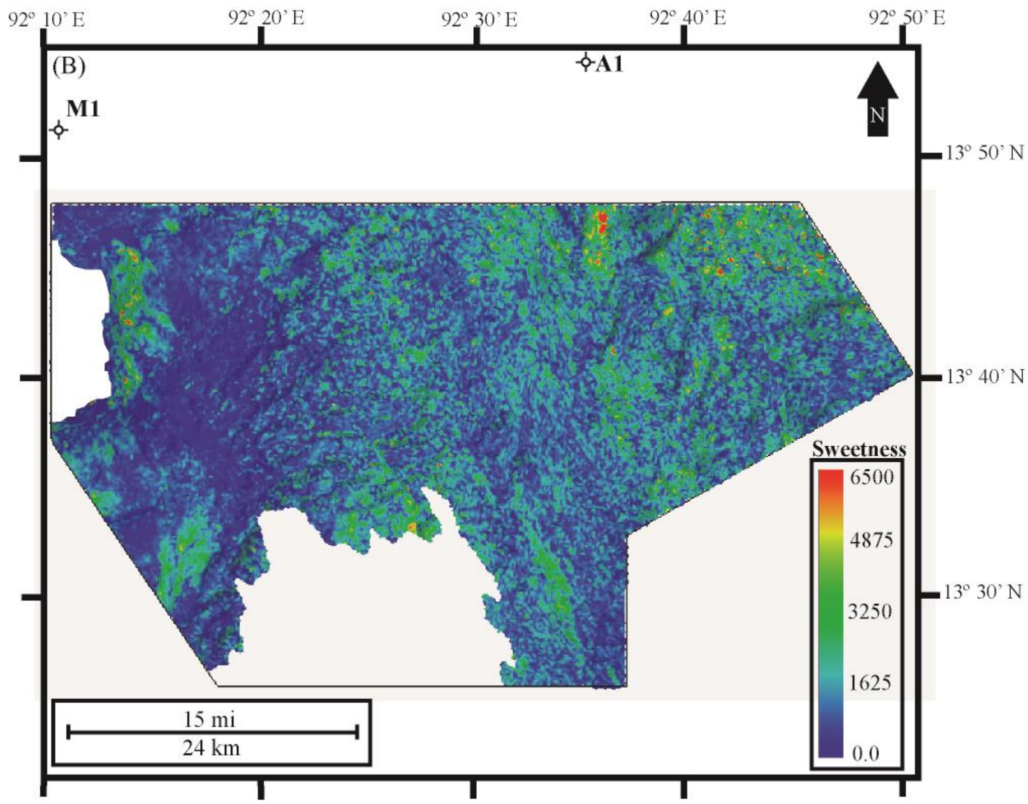
92º 10' E
92º 20' E
92º 30' E
92º 40' E
92º 50' E
(B)
A1
M1
N
13º 50' N
13º 40' N
13º 30' N
Sweetness
6500
4875
3250
1625
0.0
15 mi
24 km

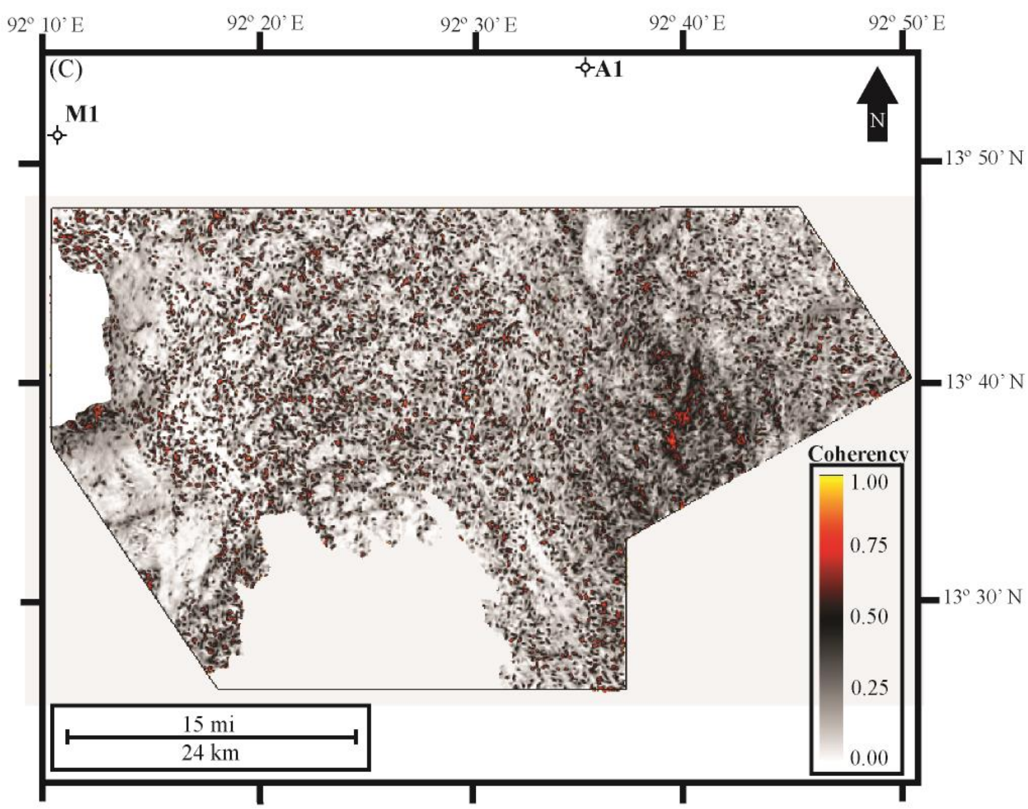
92º 10' E
92º 20' E
92º 30' E
92º 40' E
92º 50' E
(C)
A1
M1
N
13º 50' N
13º 40' N
13º 30' N
Coherency
1.00
0.75
0.50
0.25
0.00
15 mi
24 km

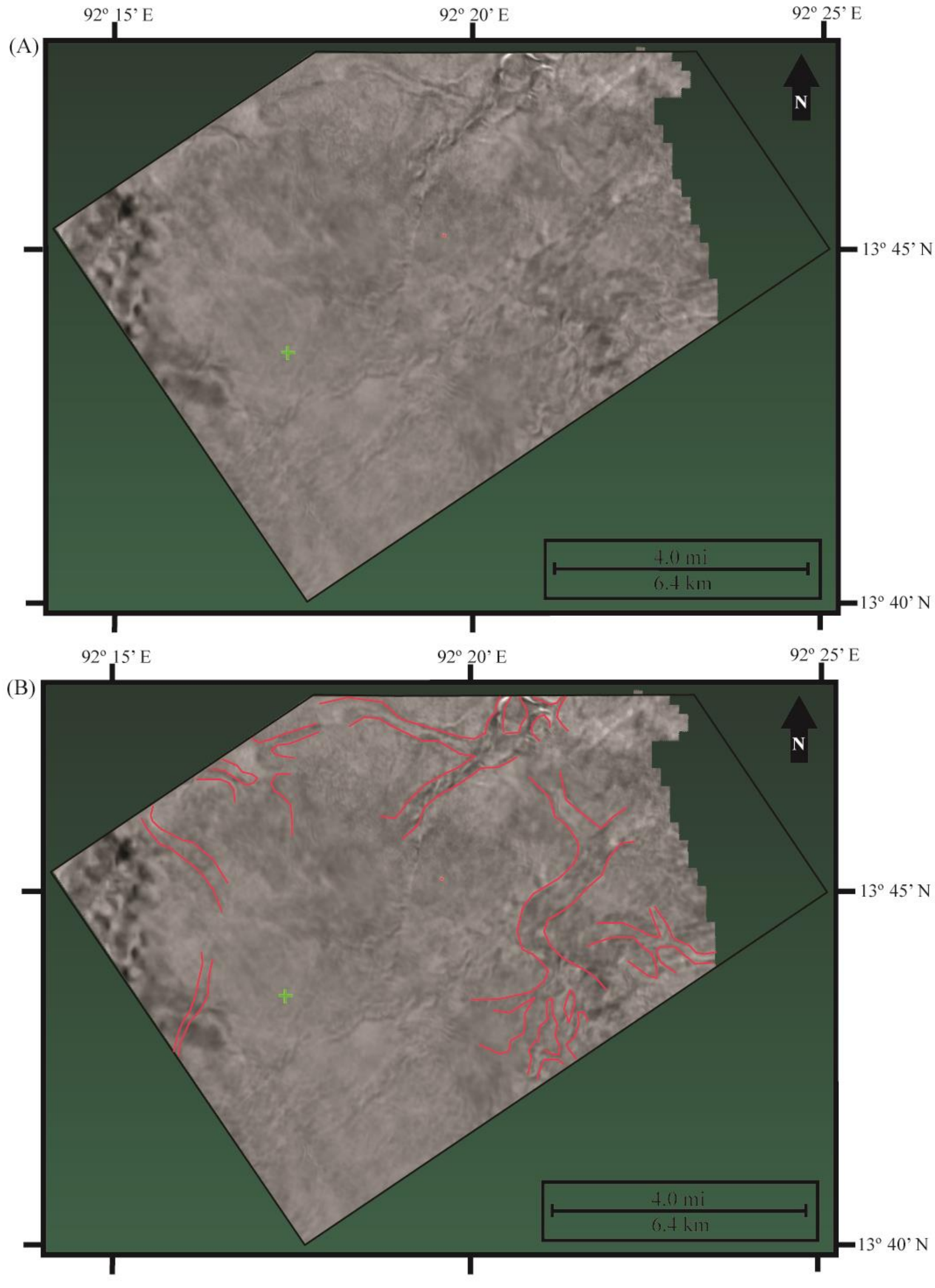

Figure 81: Strata transformation calculation horizon map about 30 milliseconds above middle Zanclean surface. **(A)** Uninterpreted **(B)** Interpreted depositional environment showing possible channel features. For location, see in figure 15B and 80.

Megasequence 7: early Piacenzian

Key Surfaces: The lower sequence boundary corresponds to the merging of three surfaces early Miocene, early Pliocene and middle Zanclean (Figures 20, 22, 82). Stratal onlap and erosional truncation are present along the surface (Figures 82 - 84). The moderate to high amplitude peak seismic reflection correspond to the sequence boundary.

The upper sequence boundary corresponds to two merged surfaces -- late Pliocene sequence boundary (SB) and Top Pliocene surfaces -- with obvious onlap and erosional truncation above and below the horizon, respectively (Figures 82 – 84). The seismic reflection that corresponds to the top Pliocene surface is a moderate amplitude peak association together with high amplitude trough association.

Time-Structure Map: The structure map of one of upper sequence boundary (late Pliocene sequence boundary (SB)) shows a homoclinal dip to the east with two-way travel time values ranging from 2.81 to 3.90 seconds (Figure 85). The horizon pinches-outs to the west, (Figure 82 – 84).

Isochron Map: The early Piacenzian megasequence has two-way travel time values that range from 0.02 to 0.50 seconds interval (Figure 87), with most of this megasequence between 0.27 to 0.37 seconds twt (Figures 82 - 84). The thickest part is located to the central part of the map (0.29 to 0.41 seconds twt) (Figure 83). The megasequence thins is to the west due to onlap and to the east due to the erosional (Figures 82, 83).

Age: This megasequence is penetrated by the M11 well (Figure 28), where the megasequence is relatively thin. The age is interpreted as early Piacenzian (upper Pliocene) (Table 2).

Seismic Facies: Three seismic and geological facies that were interpreted based on the seismic attributes, i.e. instantaneous phase and envelope (Figure 87). All facies consist of parallel

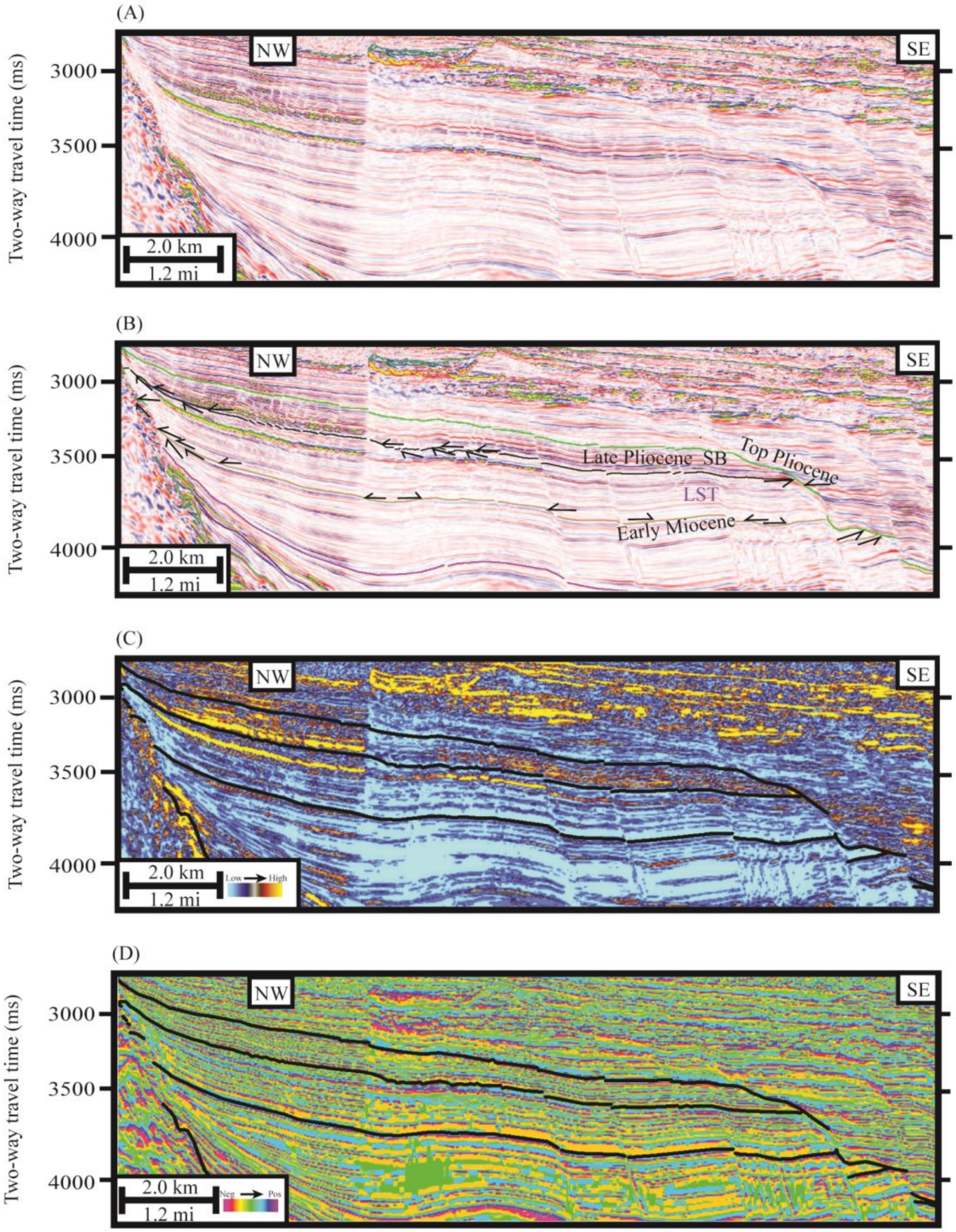

Figure 82: Seismic profile showing megasequence 7 across the 2016 3D-PSTM, dip-line number 2300. **(A)** uninterpreted **(B)** interpreted including sequence boundaries and stratal terminations. LST = Low-Stand system tract. **(C)** Envelope seismic attribute **(D)** Instantaneous Phase seismic attribute.

Location of this seismic section is shown in Figures 85 - 87.

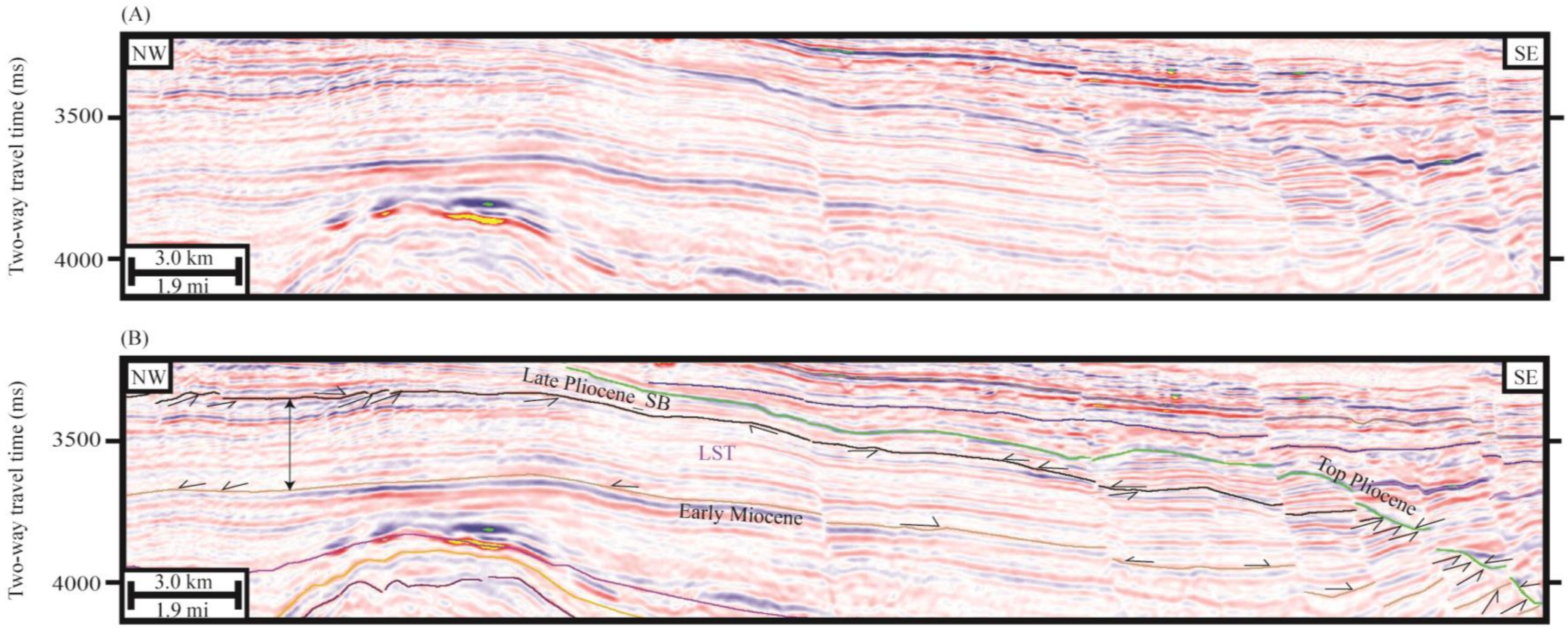

Figure 83: Seismic profile showing megasequence 7 across the 2016 3D-PSTM, dip-line number 3100. **(A)** uninterpreted **(B)** interpreted including sequence boundaries and stratal terminations. LST = Low-Stand system tract. Double-arrow indicates the thickest zone of this megasequence.

Location of this seismic section is shown in Figures 85 - 87.

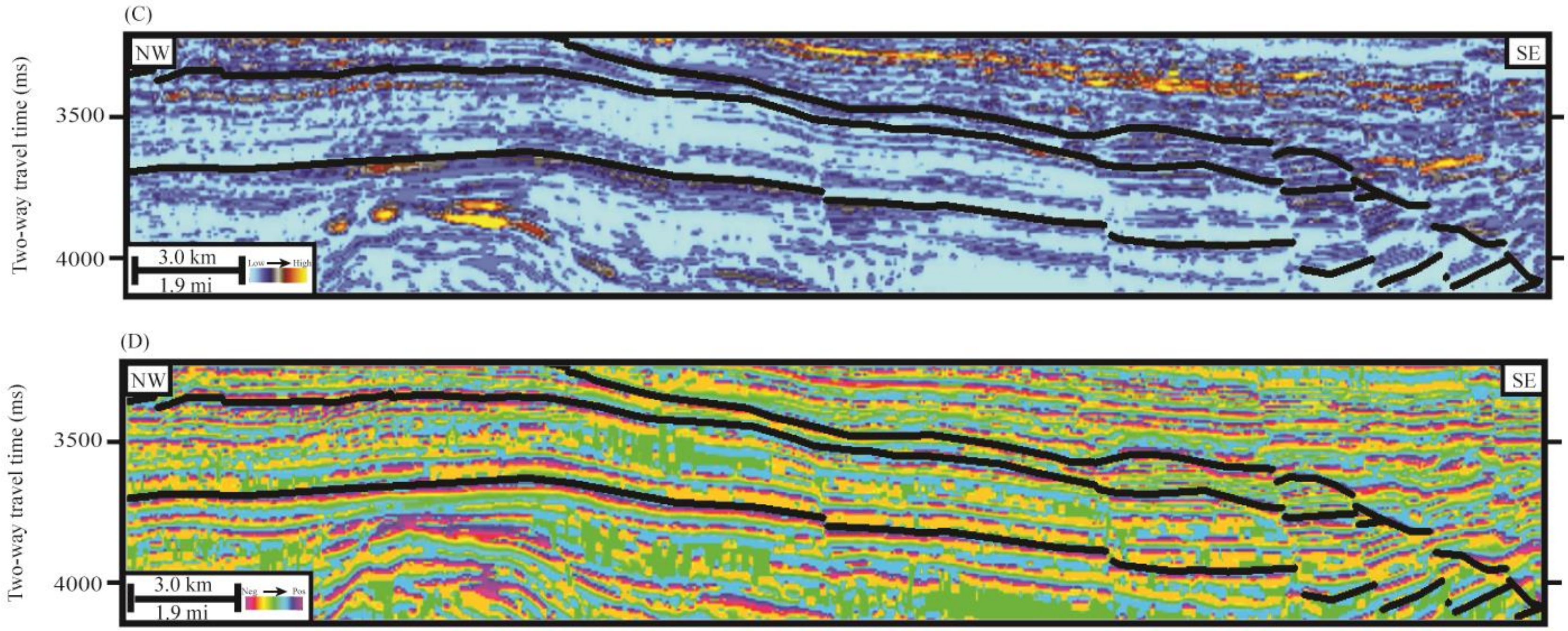

Figure 83: (C) Envelope seismic attribute **(D)** Instantaneous Phase seismic attribute.

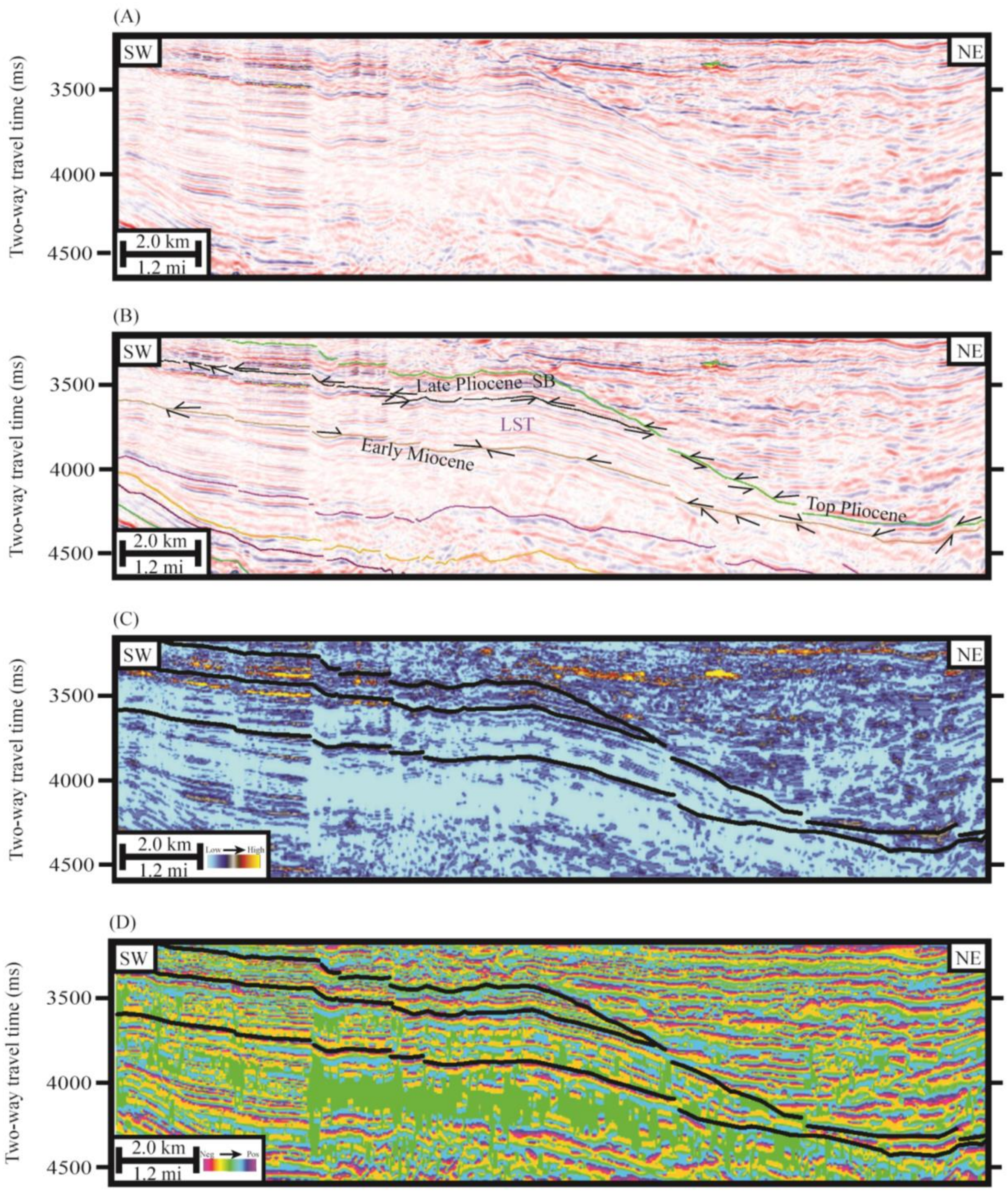

Figure 84: Seismic profile showing megasequence 7 across the 2016 3D-PSTM, strike-line number 5100. **(A)** uninterpreted **(B)** interpreted including sequence boundaries and stratal terminations. LST = Low-Stand system tract. **(C)** Envelope seismic attribute **(D)** Instantaneous Phase seismic attribute.

Location of this seismic section is shown in Figures 85 - 87.

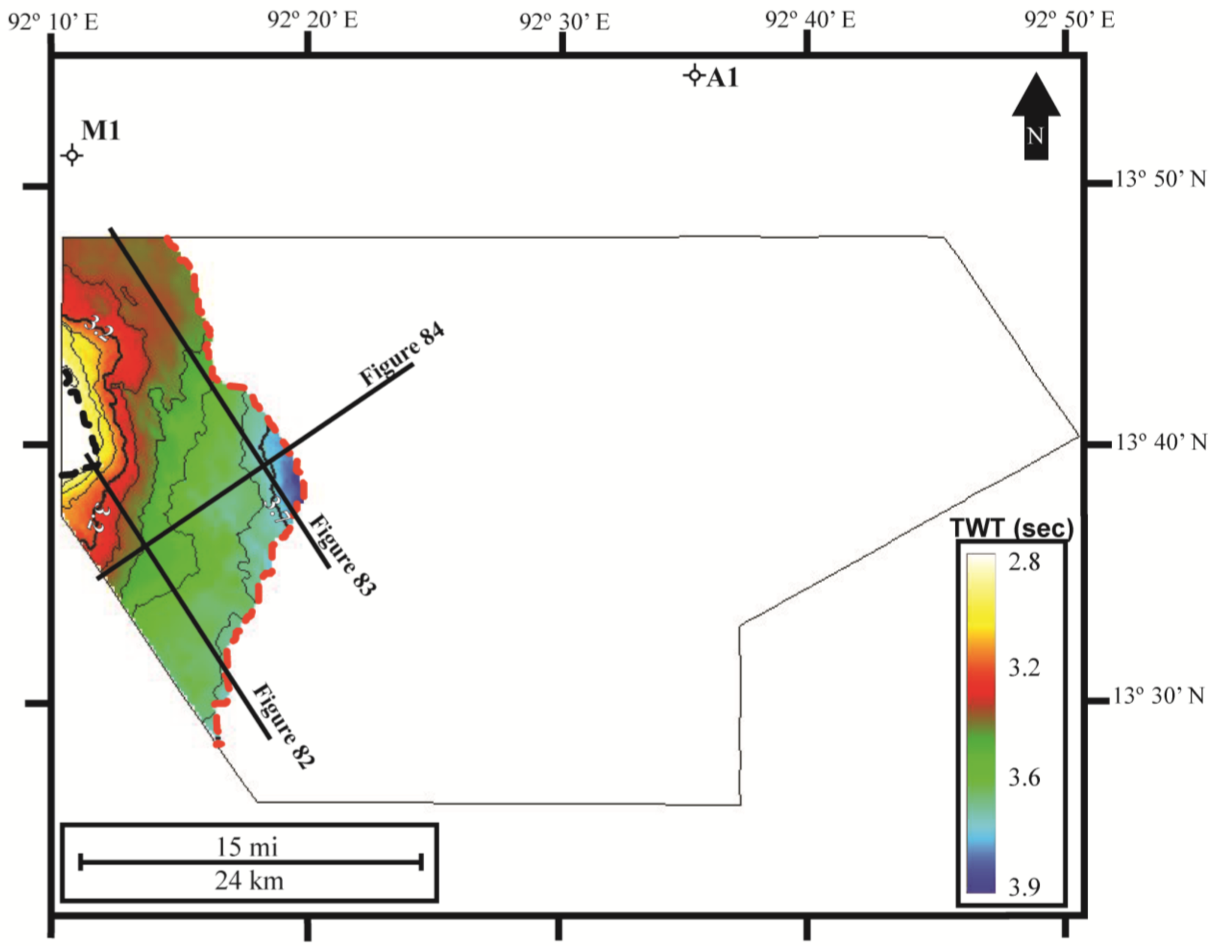

Figure 85: Time structure map of late Pliocene sequence boundary (SB) (TWT). Contour interval is 200 milliseconds with bold contour in every second. Black dash-line is onlap edge and red dash-line is truncation edge.

Locations of Figures 82 – 84 are shown.

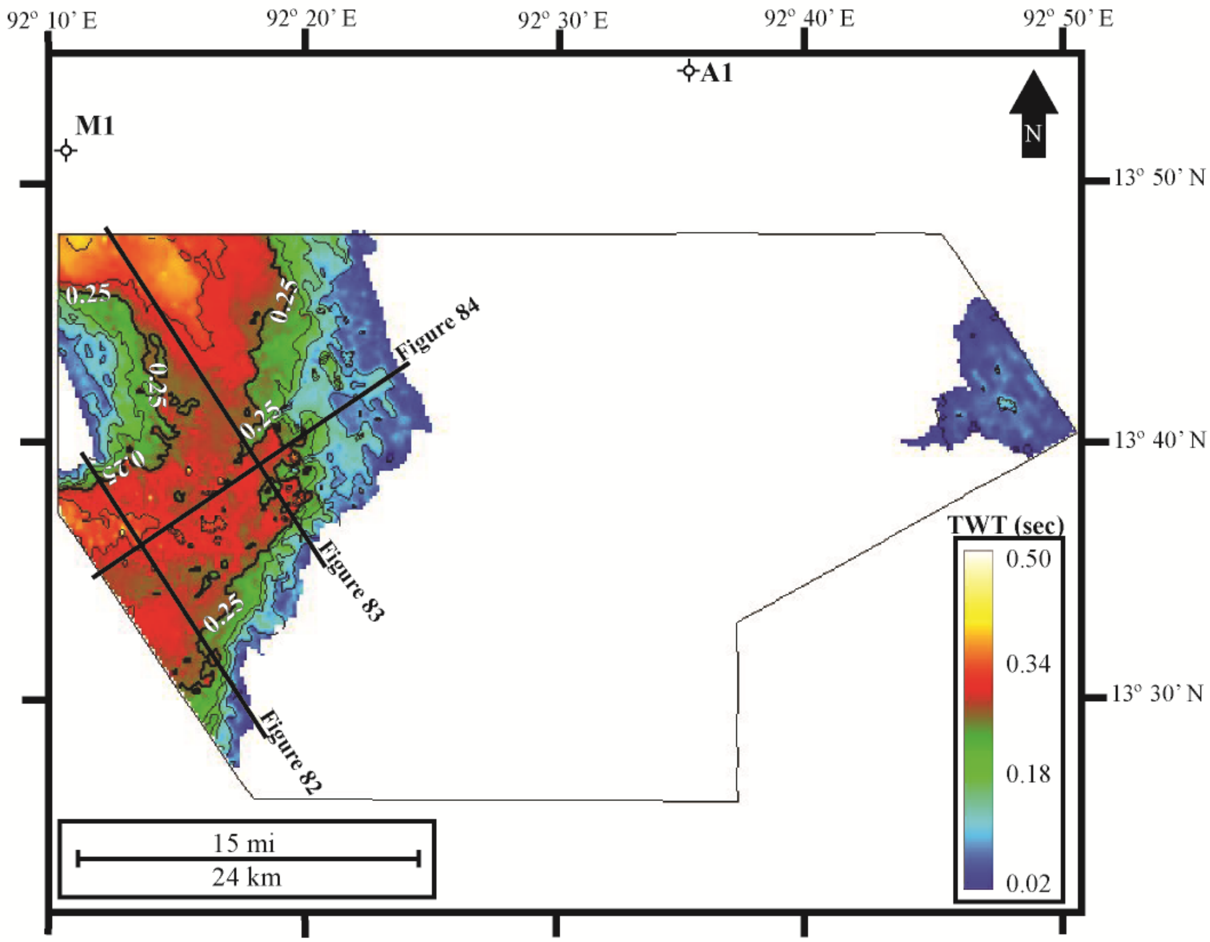

Figure 86: Isochron map of early Piacenzian megasequence (TWT). Contour interval is 200 milliseconds with bold contour in every second.

Locations of Figures 82 – 84 are shown.

reflections (Figures 82 – 84). Each facies differs in amplitude values and continuity of the reflections.

Geological Interpretation: The depositional environment map (Figure 88) was interpreted based on seismic facies (Figure 87) and seismic attributes (Figures 87, 88). The remnant of sand channel belts are interpreted in facies 1 (Figure 88). Muddy levees, where are associated with muddy channels, are part of facies 3 and facies 2, respectively. The overall channel belts trend N-S direction (Figures 87, 88); the stratal transformation calculation also suggests N-S channelize features (Figure 89).

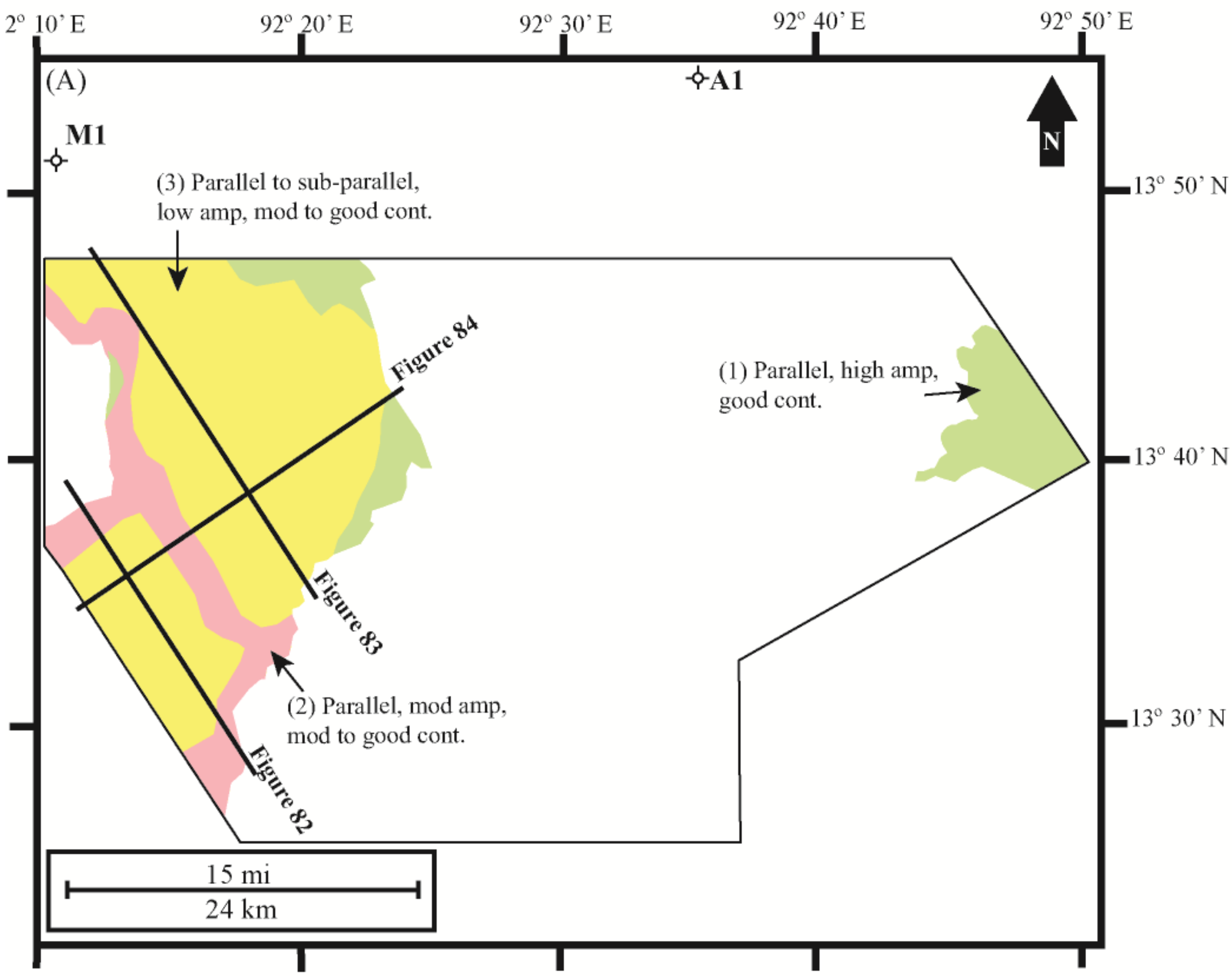

Figure 87: (A) Interpreted seismic facies map as green color is facies 1, pink color is facies 2 and yellow color is facies 3. Each facies is listed by reflection configuration, following by amplitude (amp.) and continuity (cont.) classifications. **(B)** Envelope attribute map, calculated at 20 milliseconds above early Pliocene surface. Map is twt unit. **(C)** Instantaneous Phase attribute map, calculated at 20 milliseconds above early Pliocene surface. Map is degree of phase unit.

Locations of Figures 82 – 84 are shown.

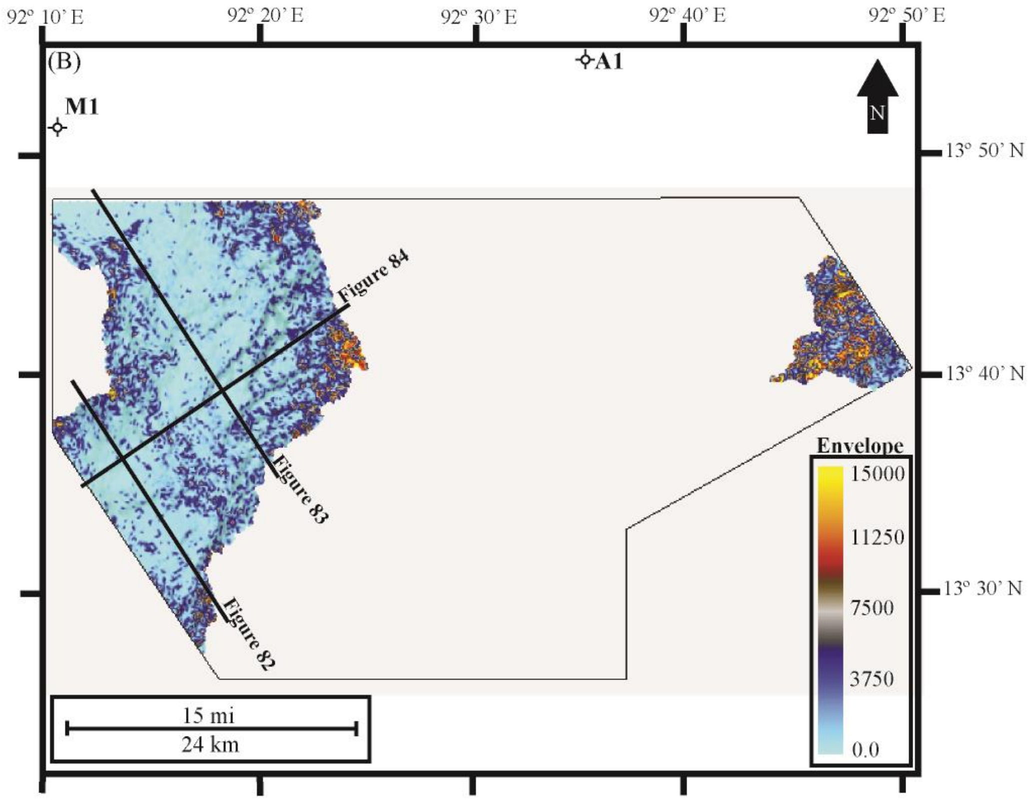

92º 10' E
92º 20' E
92º 30' E
92º 40' E
92º 50' E
(B)
A1
M1
N
13º 50' N
13º 40' N
13º 30' N
Figure 84
Figure 83
Figure 82
Envelope
15000
11250
7500
3750
0.0
15 mi
24 km

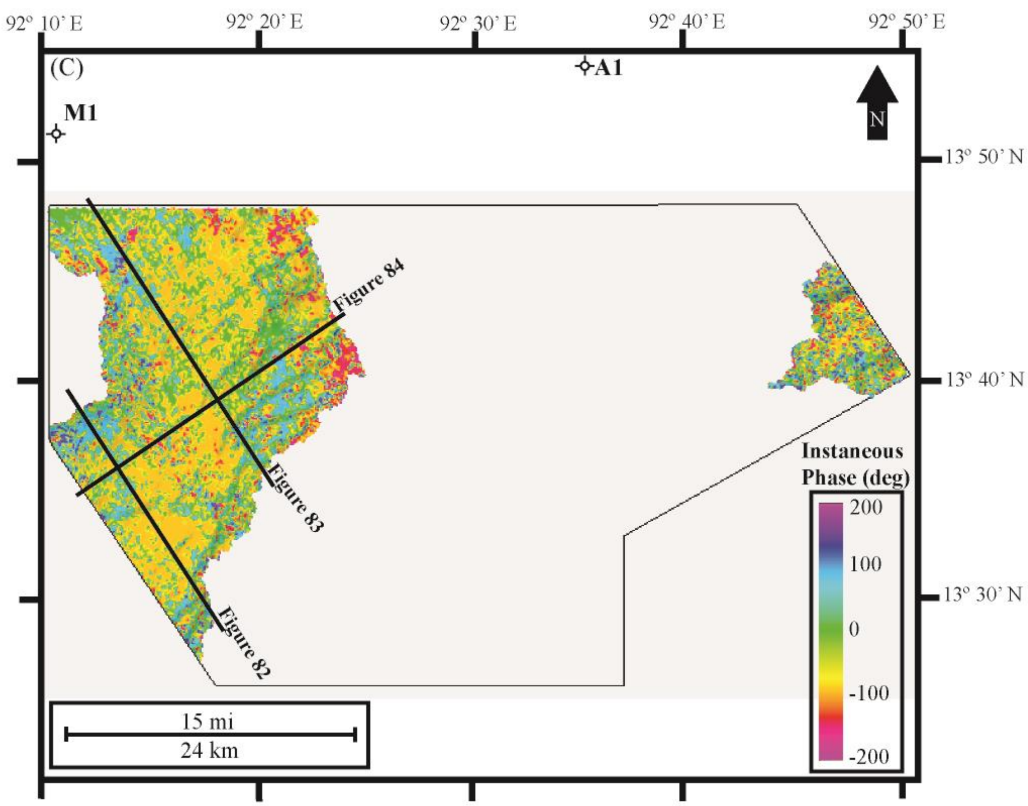

92º 10' E
92º 20' E
92º 30' E
92º 40' E
92º 50' E
(C)
A1
M1
N
13º 50' N
13º 40' N
13º 30' N
Figure 84
Figure 83
Figure 82
Instaneous Phase (deg)
200
100
0
-100
-200
15 mi
24 km

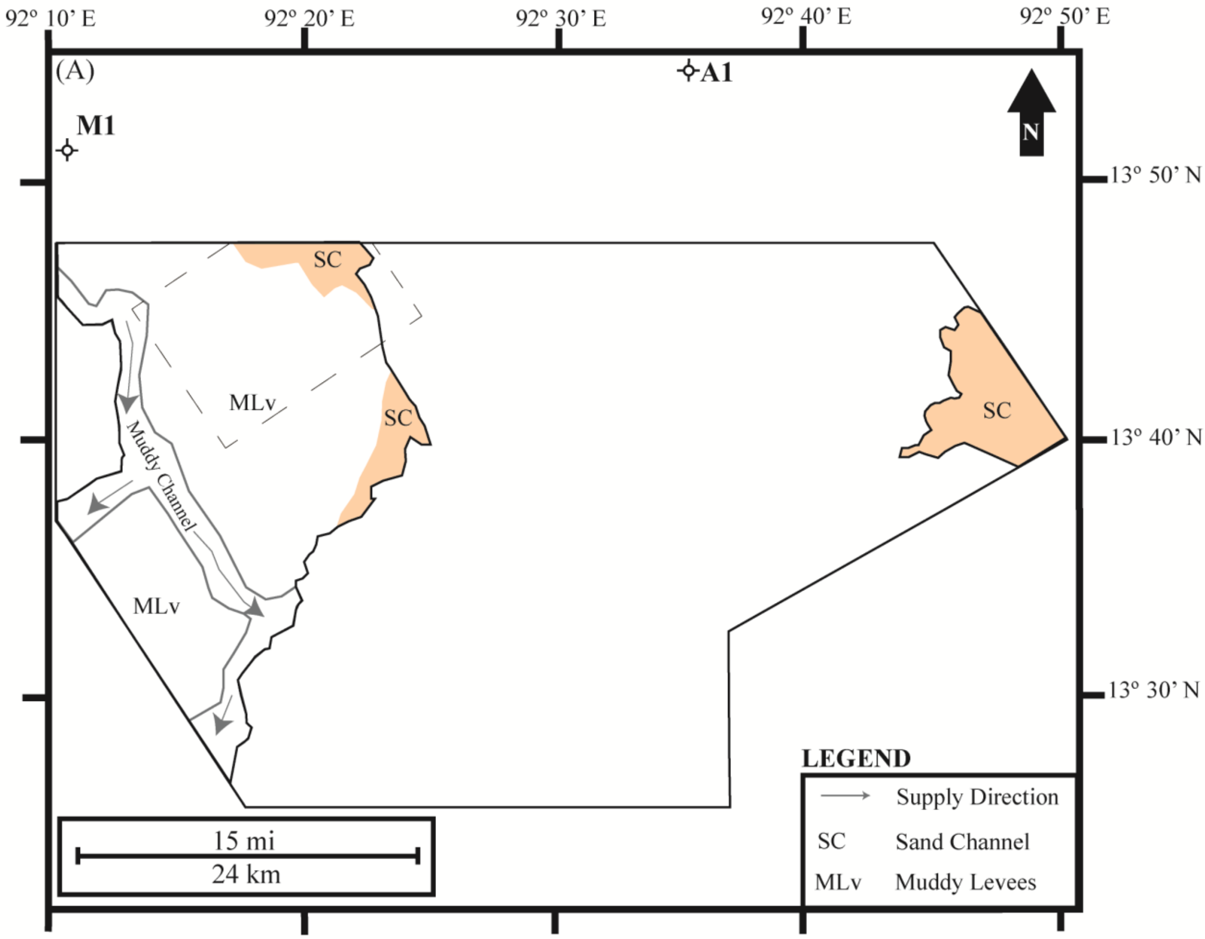

Figure 88: (A) Depositional setting map **(B)** Sweetness attribute map, calculated at 20 milliseconds above early Pliocene surface. Map is absolute amplitude value in twt unit. **(C)** Coherency attribute map, calculated at 20 milliseconds above early Pliocene surface.

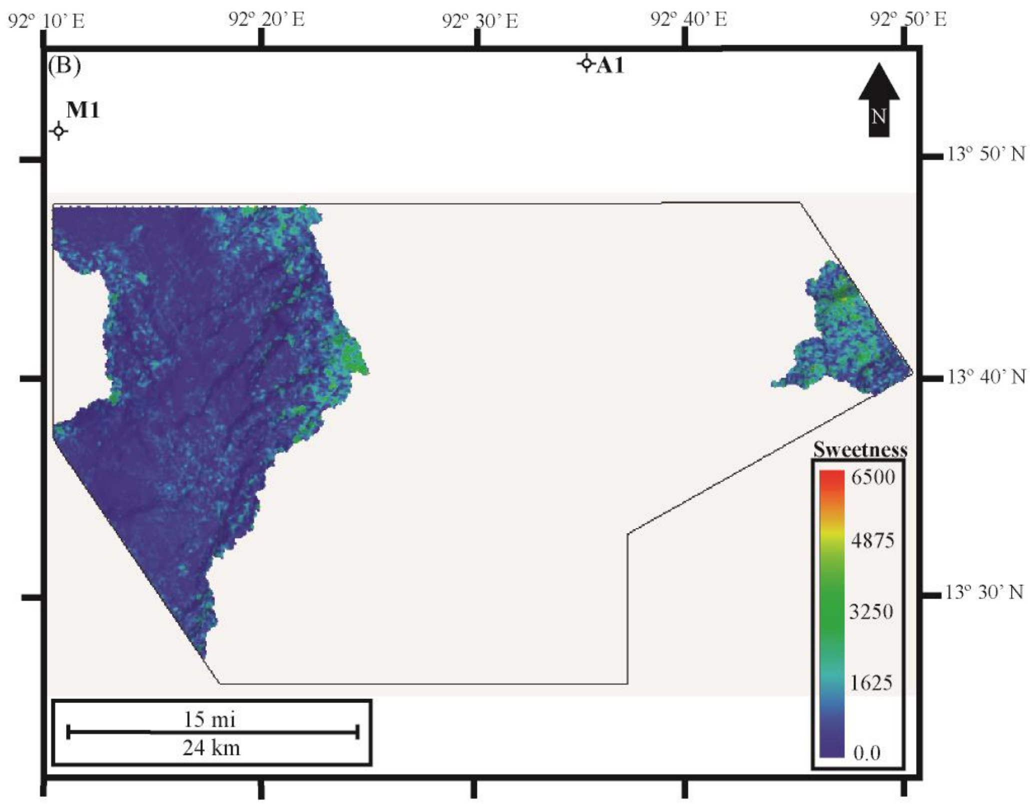
92º 10' E
92º 20' E
92º 30' E
92º 40' E
92º 50' E
(B)
A1
M1
N
13º 50' N
13º 40' N
13º 30' N
Sweetness
6500
4875
3250
1625
0.0
15 mi
24 km

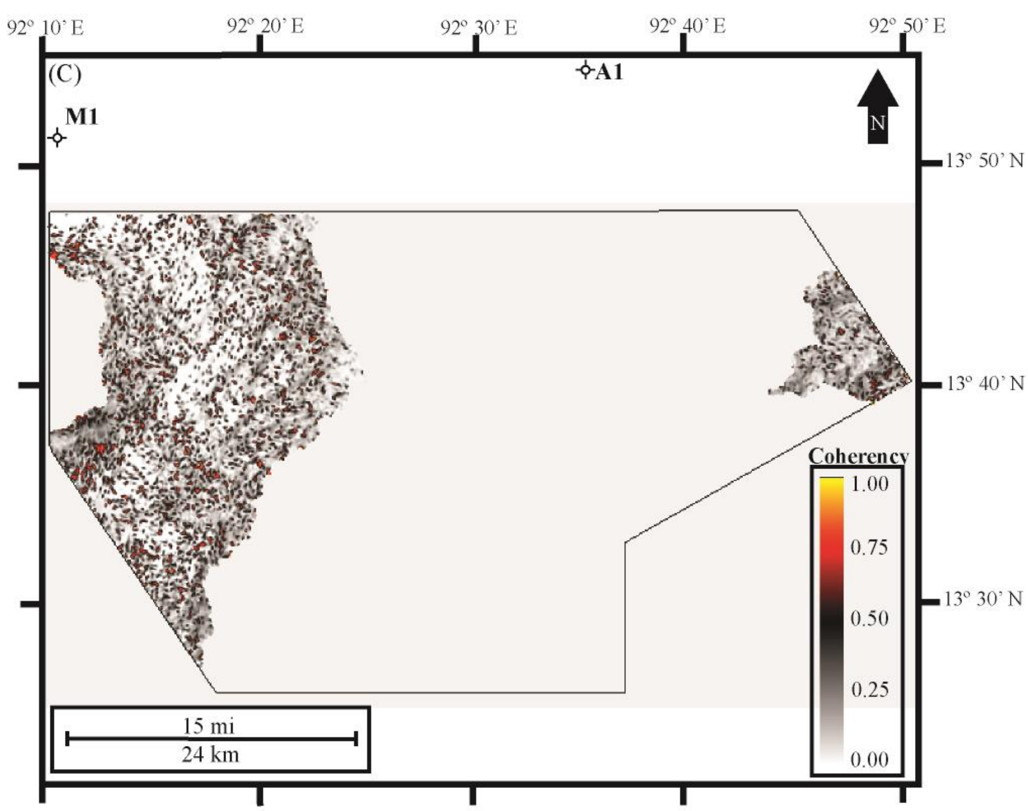
92º 10' E
92º 20' E
92º 30' E
92º 40' E
92º 50' E
(C)
A1
M1
N
13º 50' N
13º 40' N
13º 30' N
Coherency
1.00
0.75
0.50
0.25
0.00
15 mi
24 km

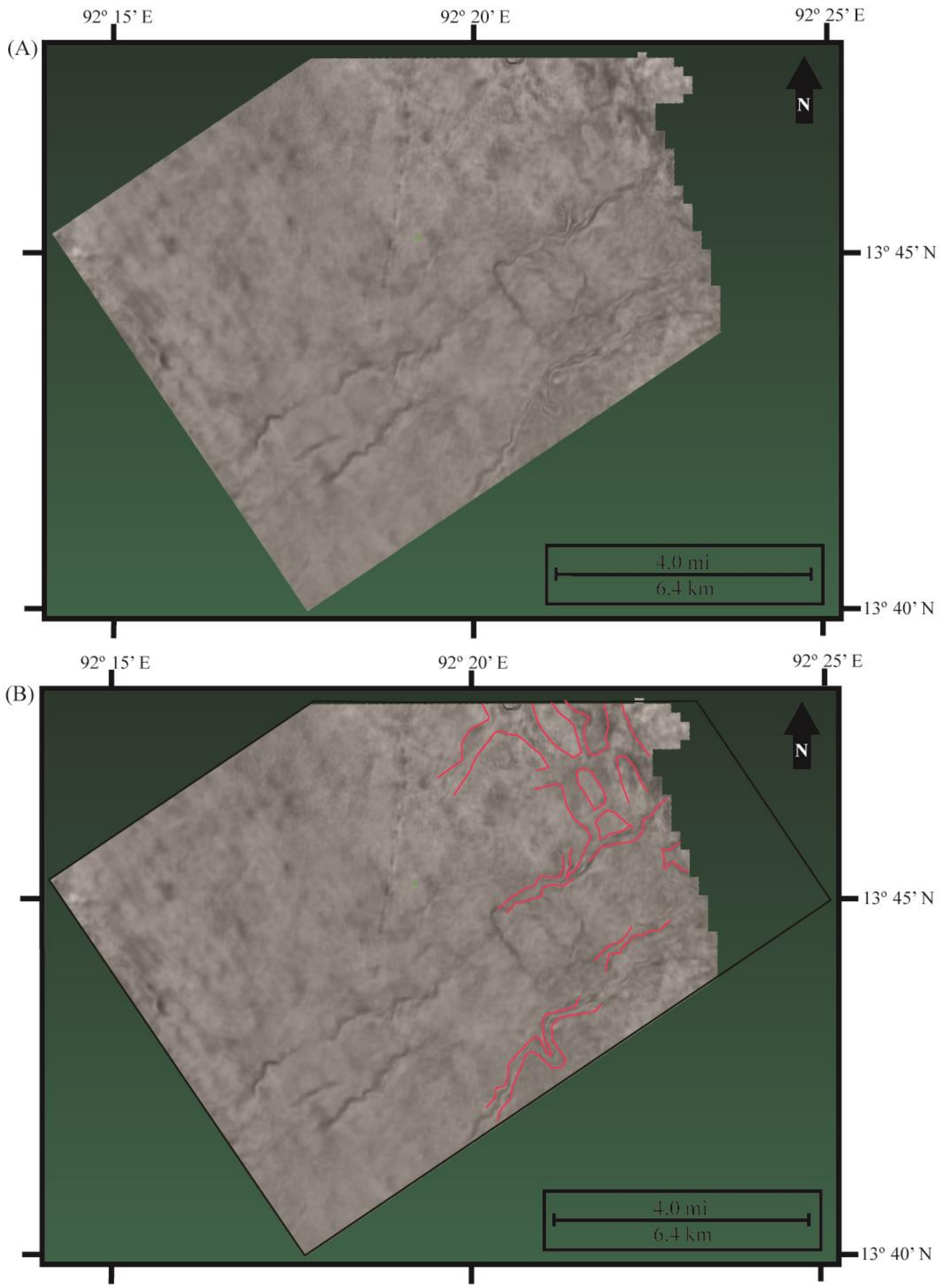

Figure 89: Strata transformation calculation horizon map about 20 milliseconds above early Pliocene surface. **(A)** Uninterpreted **(B)** Interpreted depositional environment showing possible channel features. For location, see in figure 15B and 88.

Megasequence 8: late Piacenzian

Key Surfaces: The lower sequence boundary was defined by the merged surfaces consisting of early Miocene, late Pliocene sequence boundary (SB), and middle Zanclean horizons (Figures 20, 90 - 92). Stratal onlap is extensive along the lower boundary, as well as erosional truncation below the horizon (Figures 90 – 92). This sequence boundary corresponds to a moderate to high amplitude peak seismic reflection.

The upper sequence boundary was identified by Top Pliocene surface with clear onlap above and truncation below the horizon (Figures 20, 90 – 92). The seismic reflection picking as the high amplitude trough association, corresponds to Top Pliocene surface.

Isochron Map: The late Piacenzian megasequence has two-way travel time values ranging from 0.02 to 0.27 seconds interval (Figure 93), with most of this megasequence between 0.08 to 0.19 seconds twt (Figures 90 – 92). The thickest part is located to the north (0.22 to 0.27 seconds twt) (Figure 91). The megasequence thins to the west and to the east due to the sediment deposited onto the high structure area and the erosional feature, respectively (Figures 90, 92).

Age: This megasequence is penetrated by the M11 well (Figure 28), where the megasequence is relatively thin. The age is interpreted as late Piacenzian, (upper Pliocene) (Table 2).

Seismic Facies: Two seismic and geological facies that were interpreted based on the seismic attributes, i.e. instantaneous phase and envelope (Figure 94). Their Overall trend is N-S. All facies consist of parallel reflections with the variable amplitude and continuity.

Geological Interpretation: Depositional environment map (Figure 95) was interpreted based on the seismic facies (Figure 94) and the seismic attributes (Figures 94, 95). Sand channel belts and levees are interpreted in facies 1 and facies 2, respectively (Figure 95).

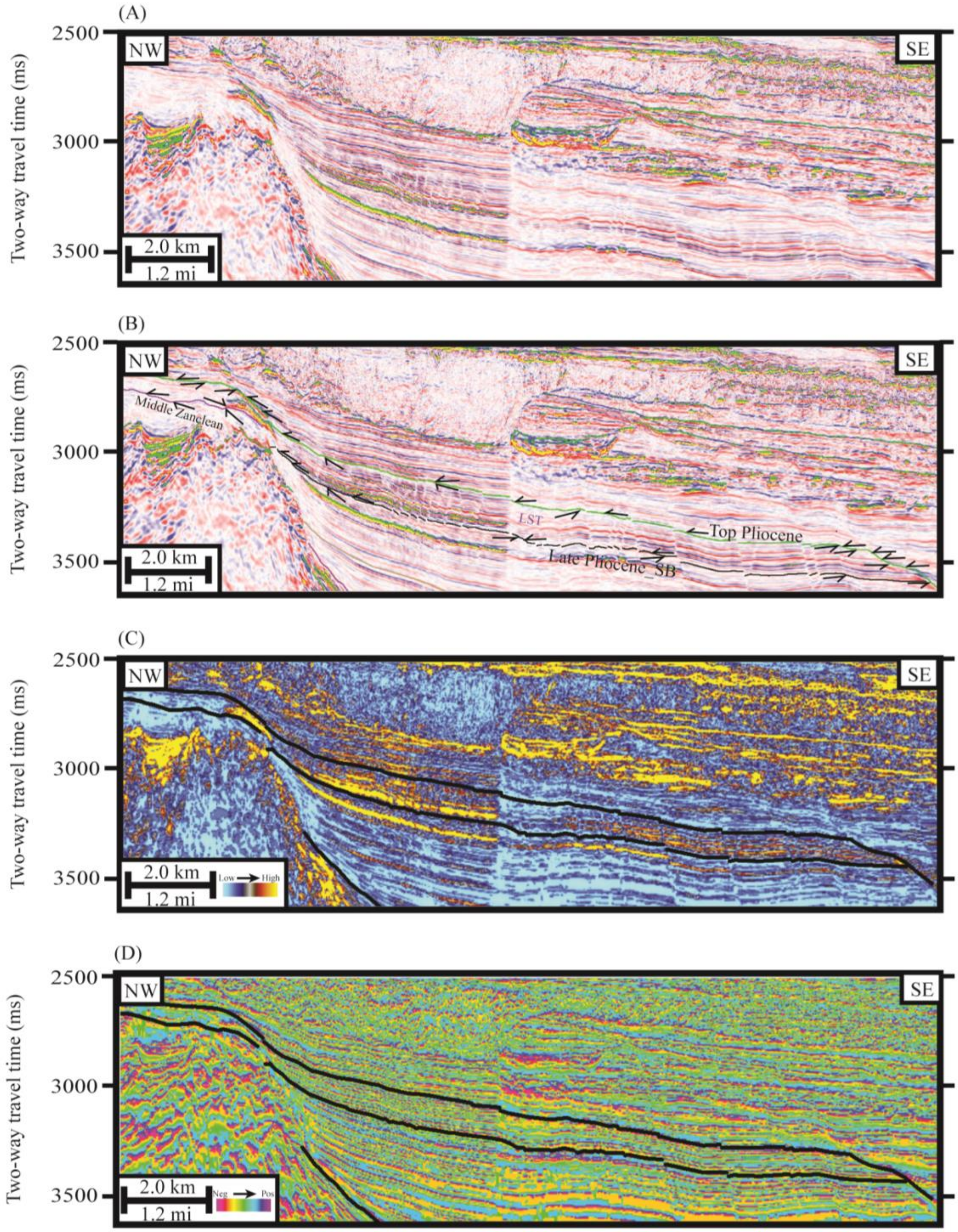

Figure 90: Seismic profile showing megasequence 8 across the 2016 3D-PSTM, dip-line number 2300. **(A)** uninterpreted **(B)** interpreted including sequence boundaries and stratal terminations. LST = Low-Stand system tract. **(C)** Envelope seismic attribute **(D)** Instantaneous Phase seismic attribute.

Location of this seismic section is shown in Figures 93, 94.

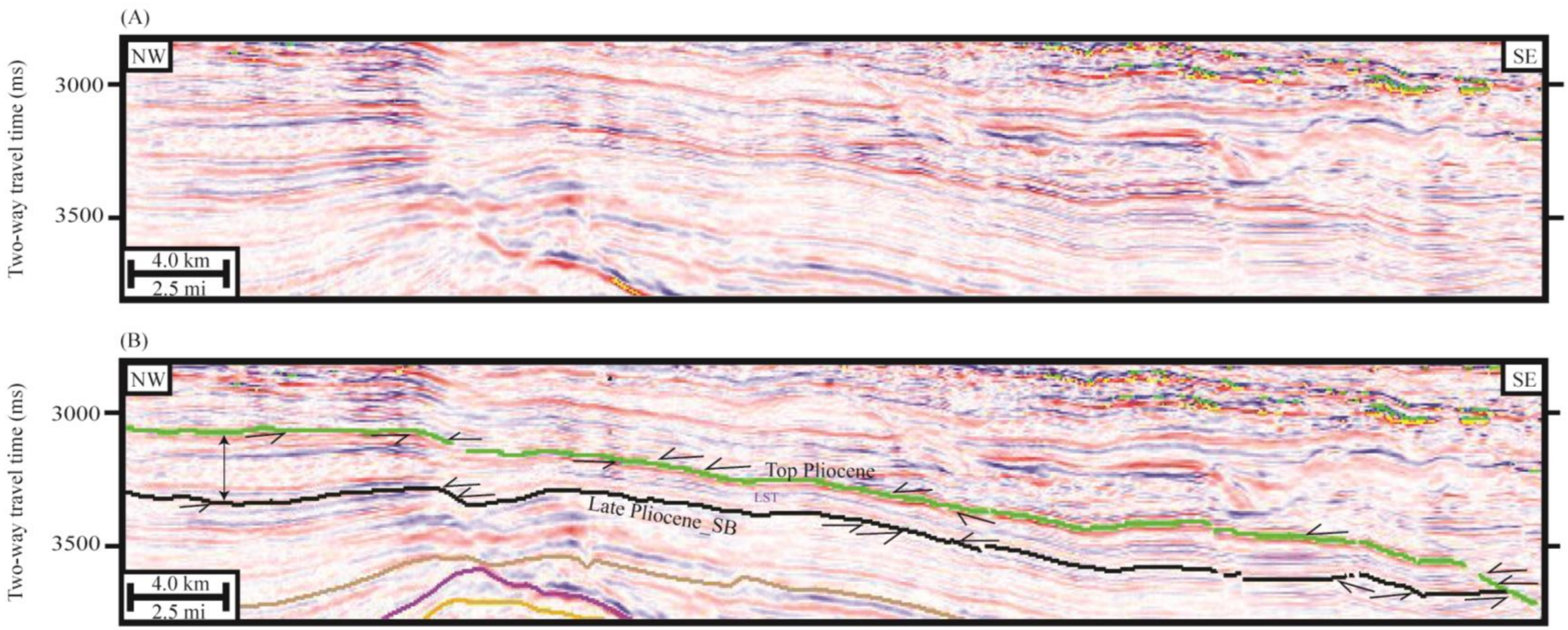

Figure 91: Seismic profile showing megasequence 8 across the 2016 3D-PSTM, dip-line number 2940. **(A)** uninterpreted **(B) i**nterpreted including sequence boundaries and stratal terminations. LST = Low-Stand system tract. Double-arrow indicates the thickest zone of this megasequence.

Location of this seismic section is shown in Figures 93, 94.

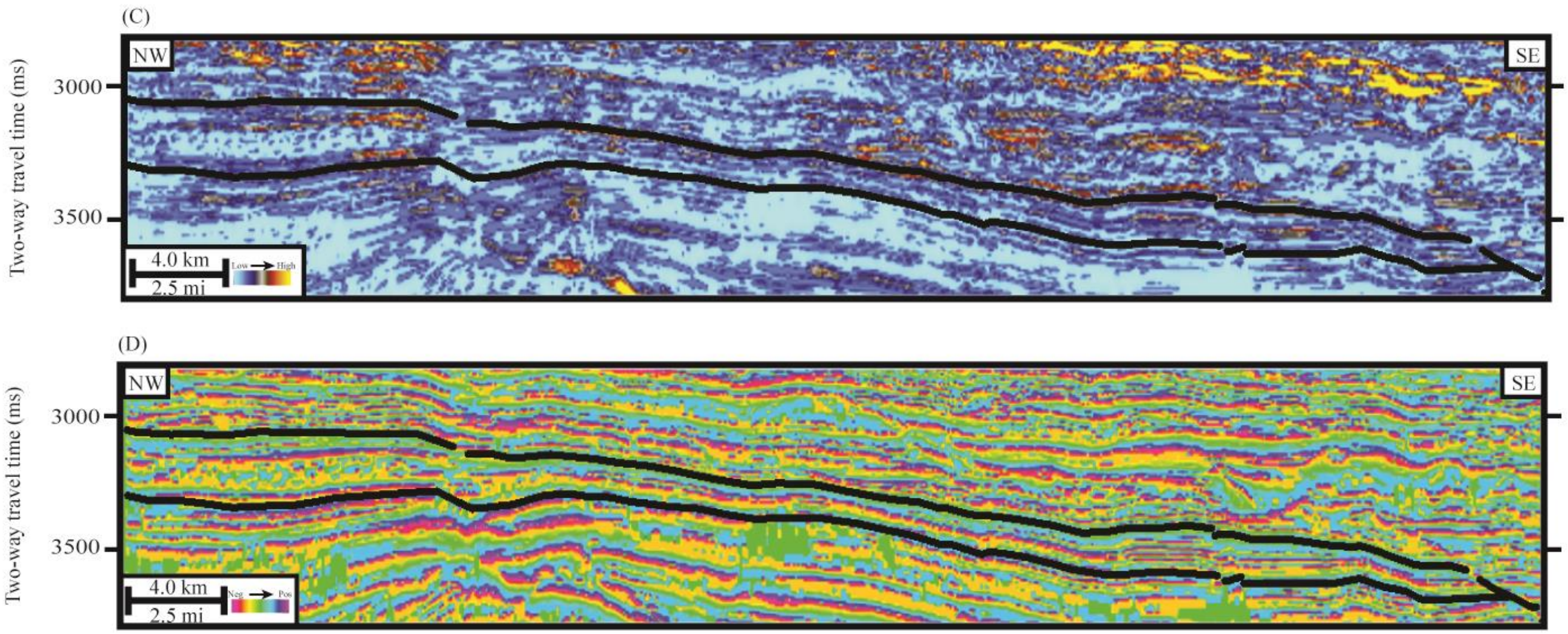

Figure 91: (C) Envelope seismic attribute **(D)** Instantaneous Phase seismic attribute.

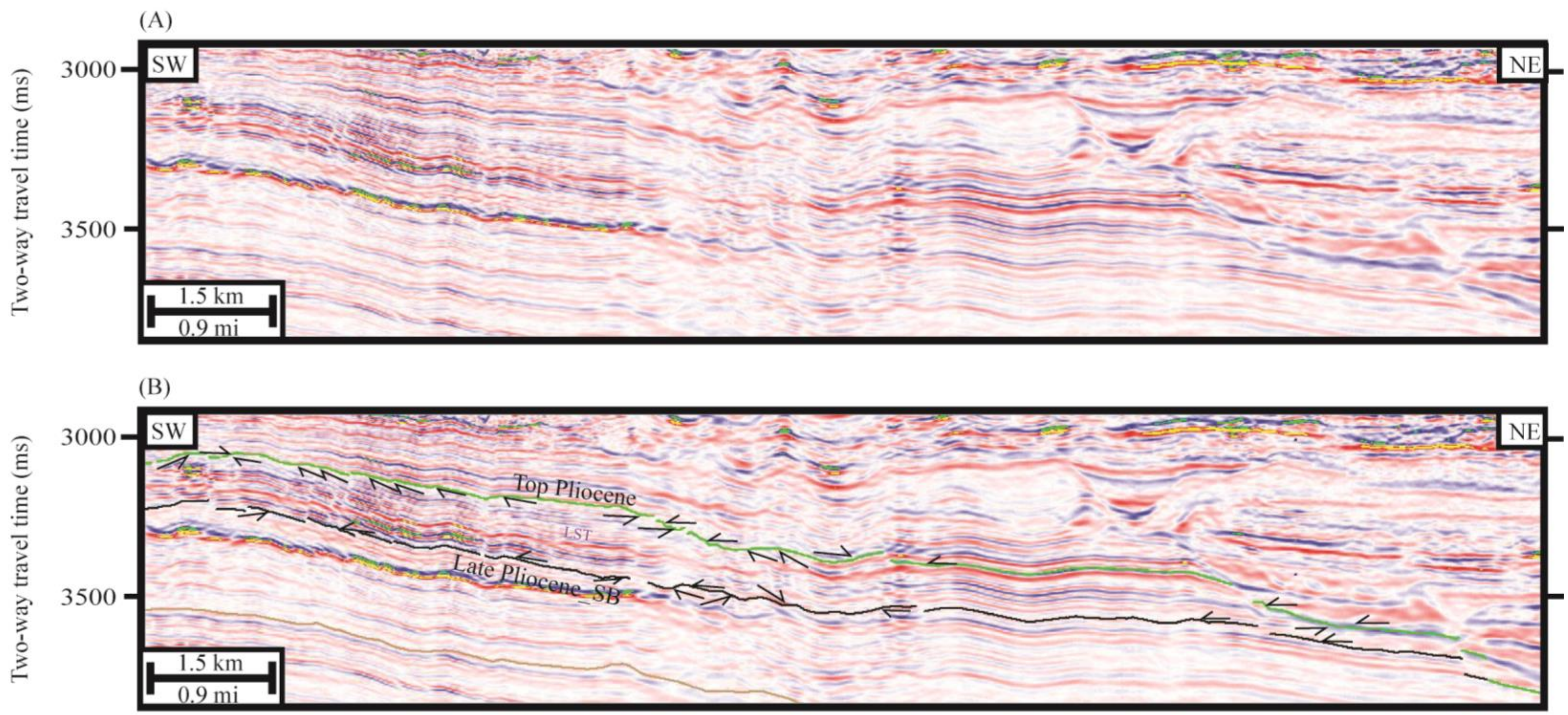

Figure 92: Seismic profile showing megasequence 8 across the 2016 3D-PSTM, strike-line number 5300. **(A)** uninterpreted **(B)** interpreted including sequence boundaries and stratal terminations. LST = Low-Stand system tract.

Location of this seismic section is shown in Figures 93, 94.

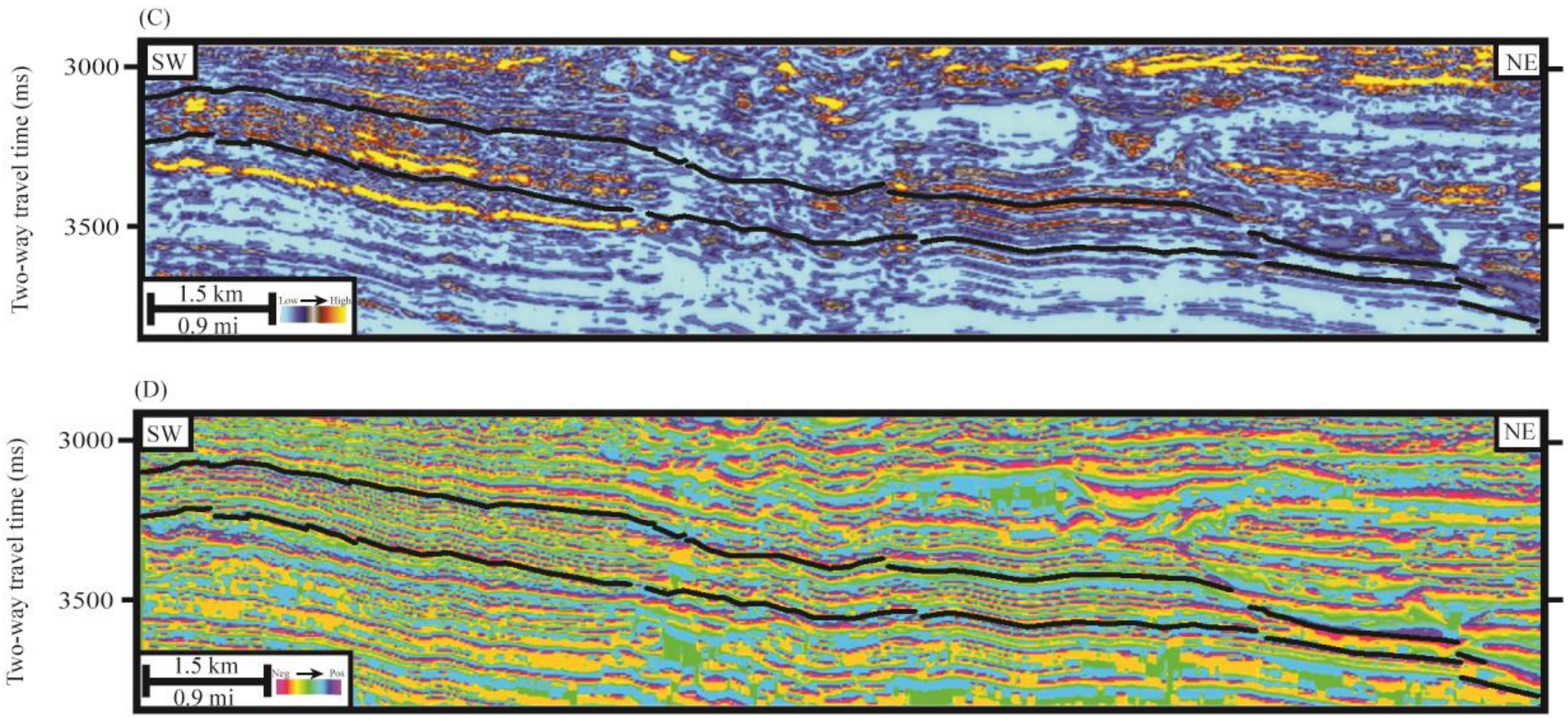

Figure 92: (C) Envelope seismic attribute **(D)** Instantaneous Phase seismic attribute.

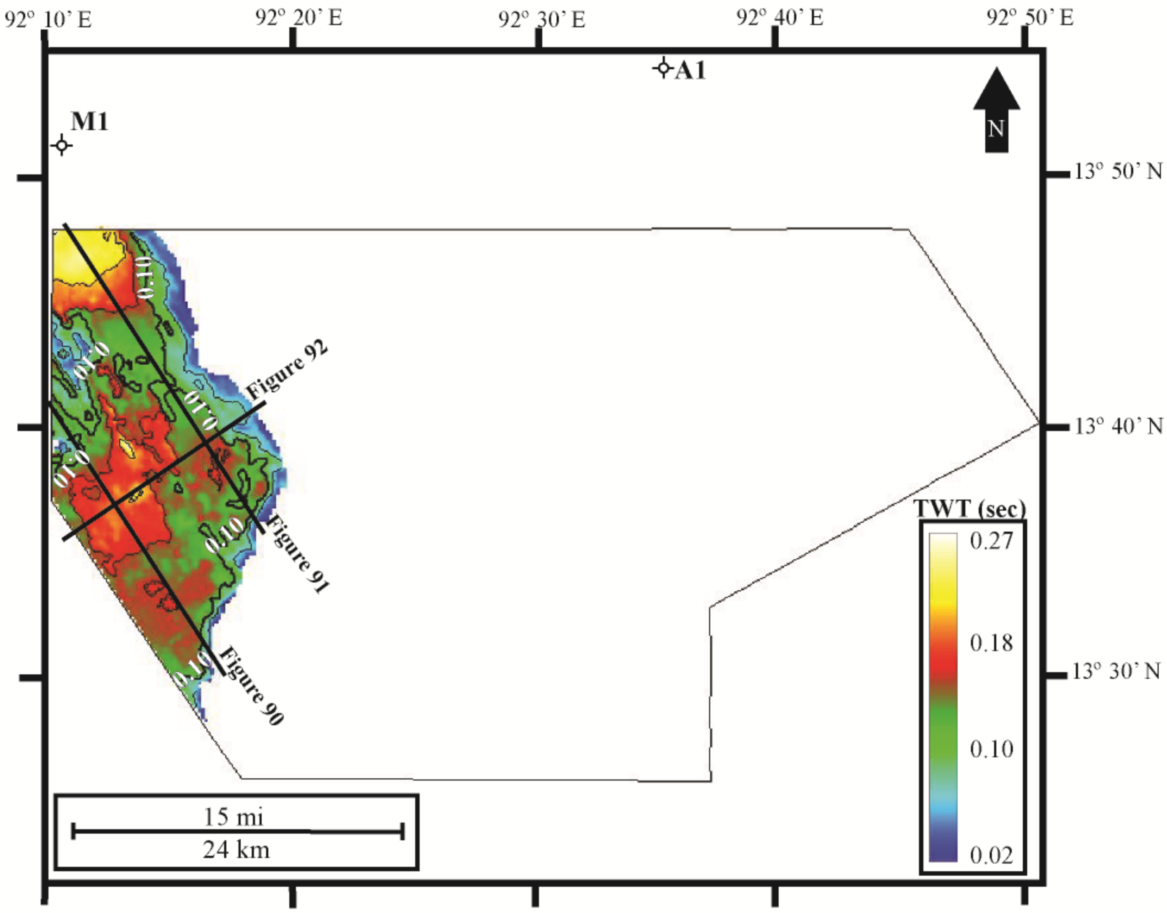

Figure 93: Isochron map of late Piacenzian megasequence (TWT). Contour interval is 200 milliseconds with bold contour in every second.

Locations of Figures 90 – 92 are shown.

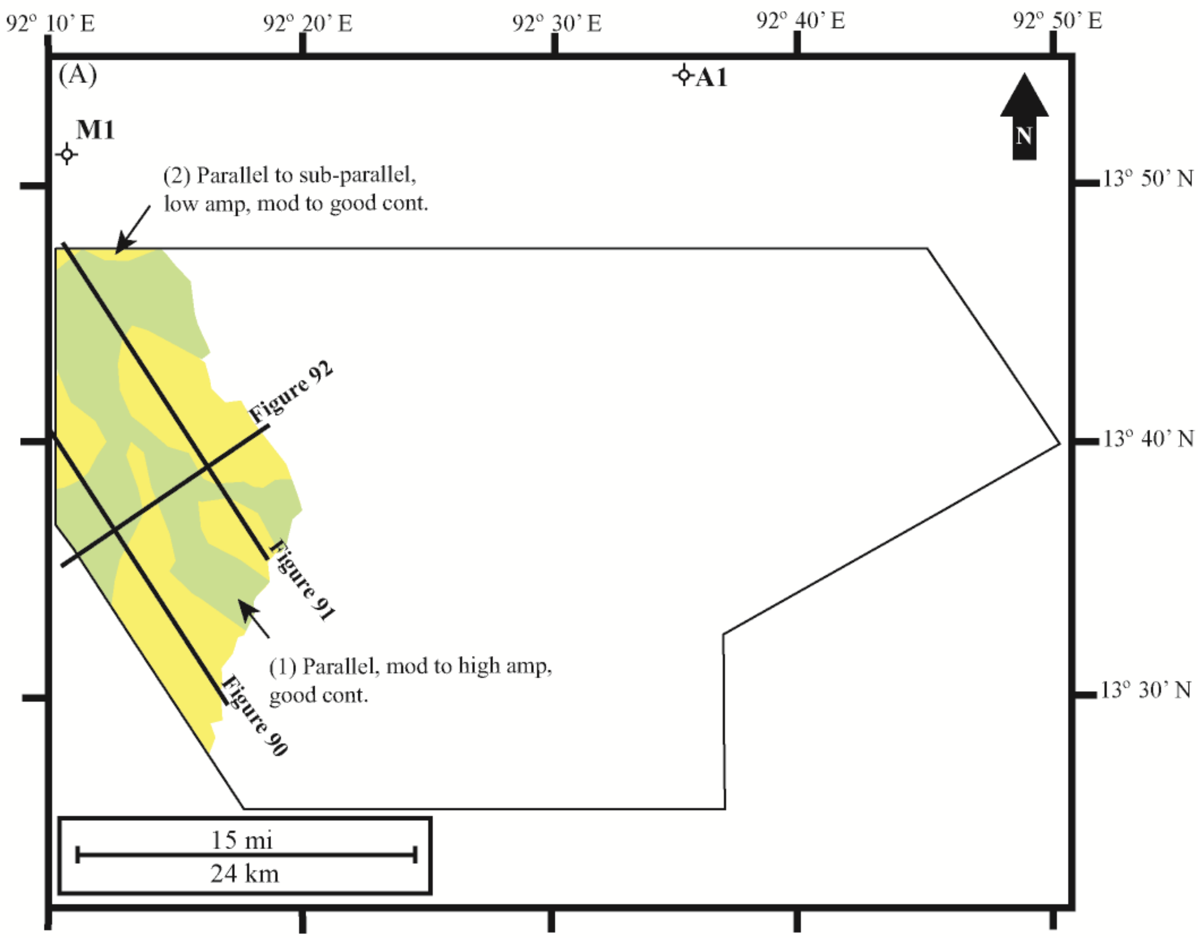

Figure 94: (A) Interpreted seismic facies map as green color is facies 1 and yellow color is facies 2. Each facies is listed by reflection configuration, following by amplitude (amp.) and continuity (cont.) classifications. **(B)** Envelope attribute map, calculated at 10 milliseconds above late Pliocene sequence boundary (SB). Map is twt unit. **(C)** Instantaneous Phase attribute map, calculated at 10 milliseconds above late Pliocene sequence boundary (SB). Map is degree of phase unit.

Locations of Figures 90 – 92 are shown.

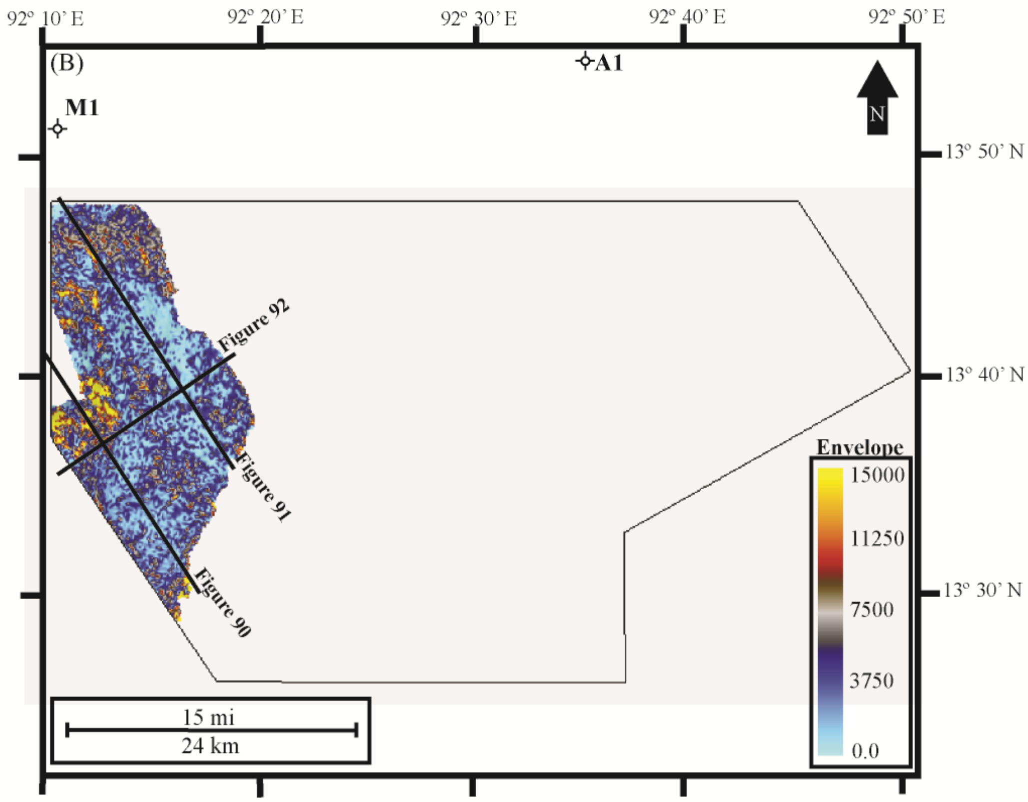

92° 10' E
92° 20' E
92° 30' E
92° 40' E
92° 50' E
(B)
A1
M1
N
13° 50' N
13° 40' N
13° 30' N
Figure 92
Figure 91
Figure 90
Envelope
15000
11250
7500
3750
0.0
15 mi
24 km

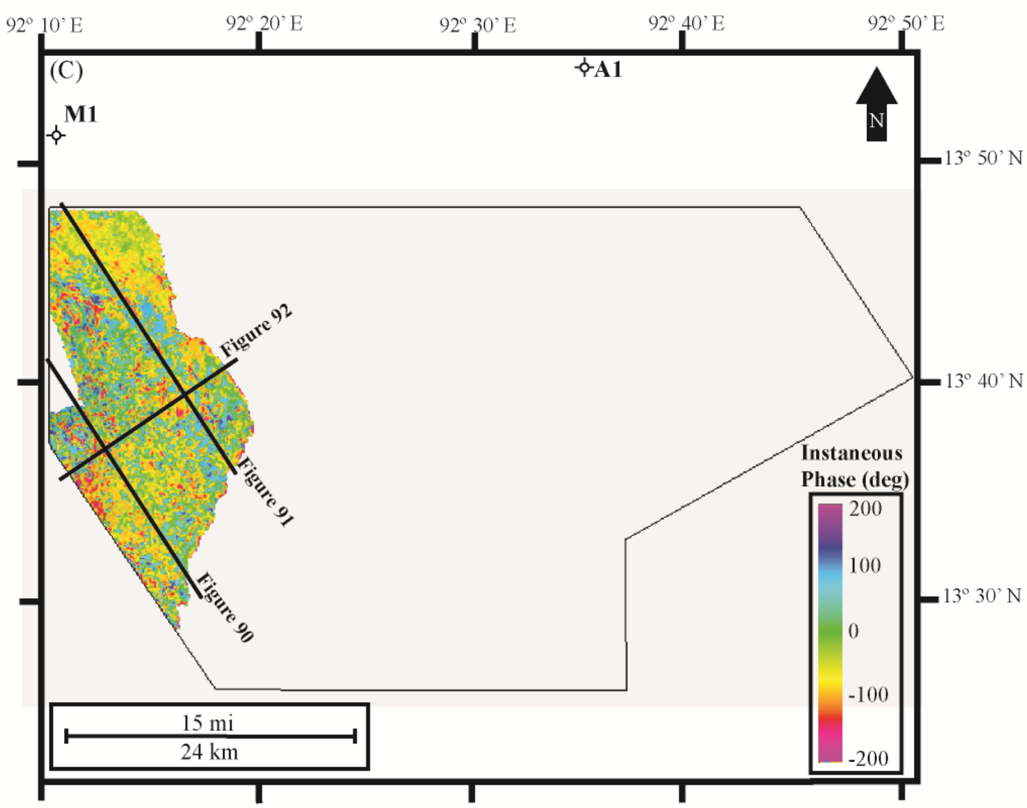

92° 10' E
92° 20' E
92° 30' E
92° 40' E
92° 50' E
(C)
A1
M1
N
13° 50' N
13° 40' N
13° 30' N
Figure 92
Figure 91
Figure 90
Instaneous Phase (deg)
200
100
0
-100
-200
15 mi
24 km

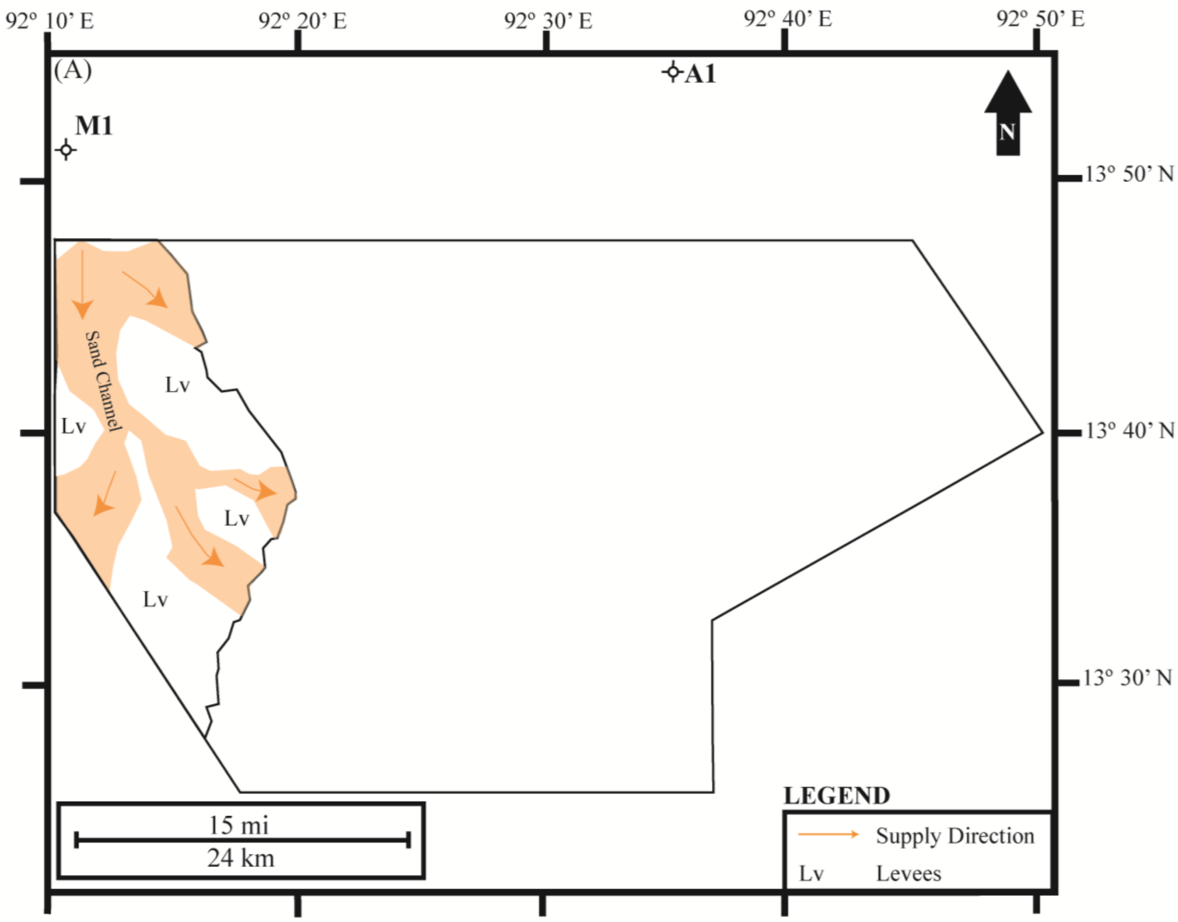

Figure 95: (A) Depositional setting map **(B)** Sweetness attribute map, calculated at 10 milliseconds above late Pliocene sequence boundary (SB). Map is absolute amplitude value in twt unit. **(C)** Coherency attribute map, calculated at 10 milliseconds above late Pliocene sequence boundary (SB).

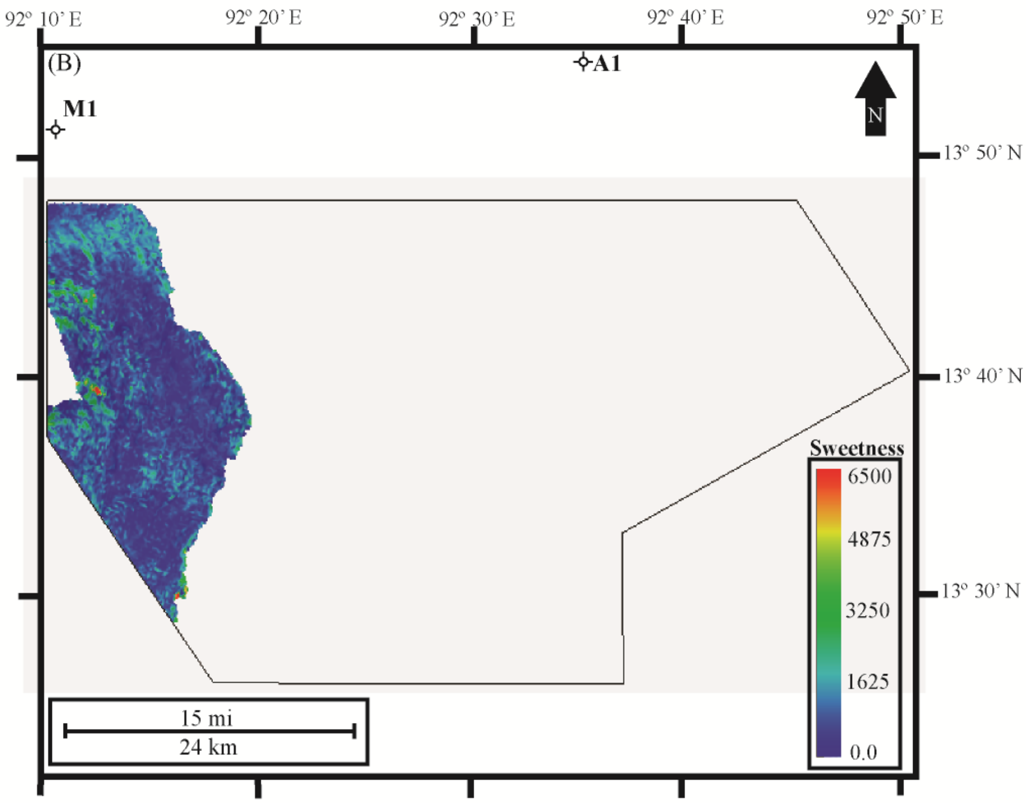
92° 10' E
92° 20' E
92° 30' E
92° 40' E
92° 50' E
(B)
A1
M1
N
13° 50' N
13° 40' N
13° 30' N
Sweetness
6500
4875
3250
1625
0.0
15 mi
24 km

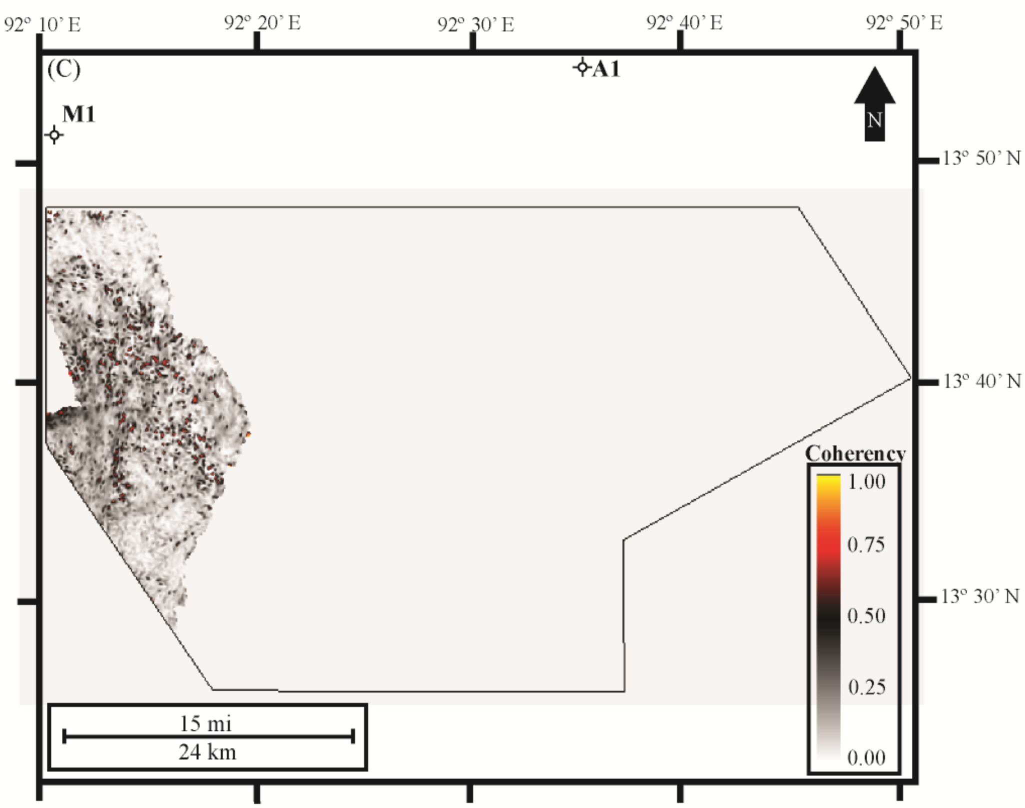
92° 10' E
92° 20' E
92° 30' E
92° 40' E
92° 50' E
(C)
A1
M1
N
13° 50' N
13° 40' N
13° 30' N
Coherency
1.00
0.75
0.50
0.25
0.00
15 mi
24 km

DISCUSSION

This discussion addresses the geological evolution, sequence stratigraphy, structural controls, reservoir potential, and petroleum elements of the study area. All of these interpretations were derived from the seismic interpretation and generation of time-structure and isochron maps. The seismic facies and the geological interpretation were also used to understand the petroleum system analysis.

Geological Evolution

The study area is segmented into three parts, based on different tectonic settings in the focus stratigraphic section (Figure 15): (1) basement high structure to the west, which is overlain by a late Miocene carbonate buildup; (2) an extensional zone consists of a central graben associated with trans-tension and back-arc rifting, and filled with thick Neogene deepwater siliciclastics sediments; and (3) a compressional zone, consisting of a thrusted fold belt that developed associated with transpression due to oblique subduction. Pliocene sediments were deformed. However, this structure zone defining in this area can be more complex, if whole stratigraphic section of Paleogene- Neogene basin is taking into account.

The tectonic and stratigraphic evolution of the Martaban basin is similar to the other sedimentary basins in SE Asia. Isolated carbonate buildups developed during late Oligocene. These isolated buildups developed on top of rift-related, basement horst blocks that were within and above the photic zone in waters with a low volume of suspended sediment.

During the early Miocene, the entire area subsided regionally, which caused the carbonate platform to be flooded and drowned. The entire study area subsided into relatively deep water depths due to tectonic subsidence. As subsidence developed, the type of sediments that were deposited in the area shifted to deepwater silciclastics in the central graben area.

The Ayeyarwardy delta supplied the clastic sediments to the study area from late

Miocene (Figure 12). In the study area, most sediment was derived from the NNE since the middle Miocene (Figure 36). The, during the late Miocene to Pliocene, the sediment supply shifted to the North (Figures 44, 52, 61, 71, 80, 88, 95).

Sequence Stratigraphy

A clear sequence stratigraphic framework for the Neogene sediments has been defined. Eight megasequences are recognized (Figures 20 – 23), and are shown in a chronostratigraphic chart (Figure 96). The overall relative changes of coastal onlap in this area present a broad moving to landward, from the reference point (Figure 96). The interpretation from the movement of coastal onlap is referring to relative sea level rising. The highest relative sea level in this specific area is at Megasequences 3 or Messinian.

Based on the biostratigraphic report interpretation (Figure 7), the relative rising of sea level is interpreted to lower Bathyal zone. The biostratigraphic data can support to perform the relative changes of coastal onlap or cycles (Figure 96), however the data from the nearby well is not good correlation enough to accurately date the Miocene megasequences (Figure 7). At the M1 well location that was located at paleo- structural high, most of the Miocene megasequences were not penetrated, so their exact ages are unknown (Figures 25 - 28). Attempts to tie to the global sea-level curve for age-dating are problematic.

The erosional nature of sequence boundaries varies from the older (Megasequences 1-4) to the younger (Megasequences 5-8). Up to 300 meters of erosion in the Miocene and lower Pliocene megasequences, is present possibly enhanced by tectonism in the source area. These might be 2nd order of sequence boundaries. In Pliocene, less erosion is present at the lower boundaries. Possibly 3rd order of sequence boundaries is interpreted in Pliocene, with less tectonic enhancement (Figures 20 - 23).

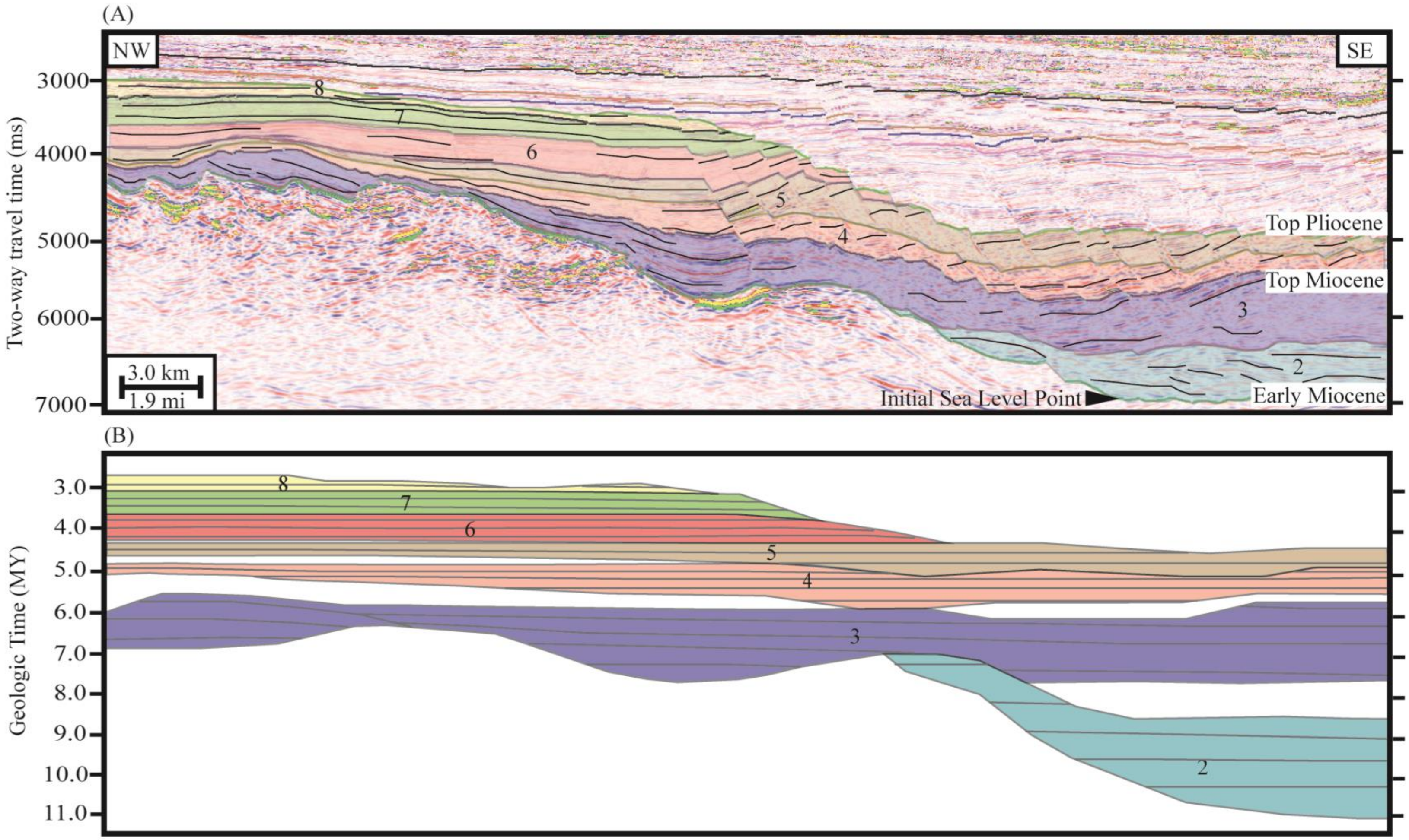

Figure 96: Chronostratigraphic chart of this study area, which was derived from **s**eismic profile across the 2016 3D-PSTM, dip-line number 3100. **(A)** Stratigraphic cross section referenced from Figure 20 **(B)** Chronostratigraphic chart **(C)** Relative changes of coastal onlap.

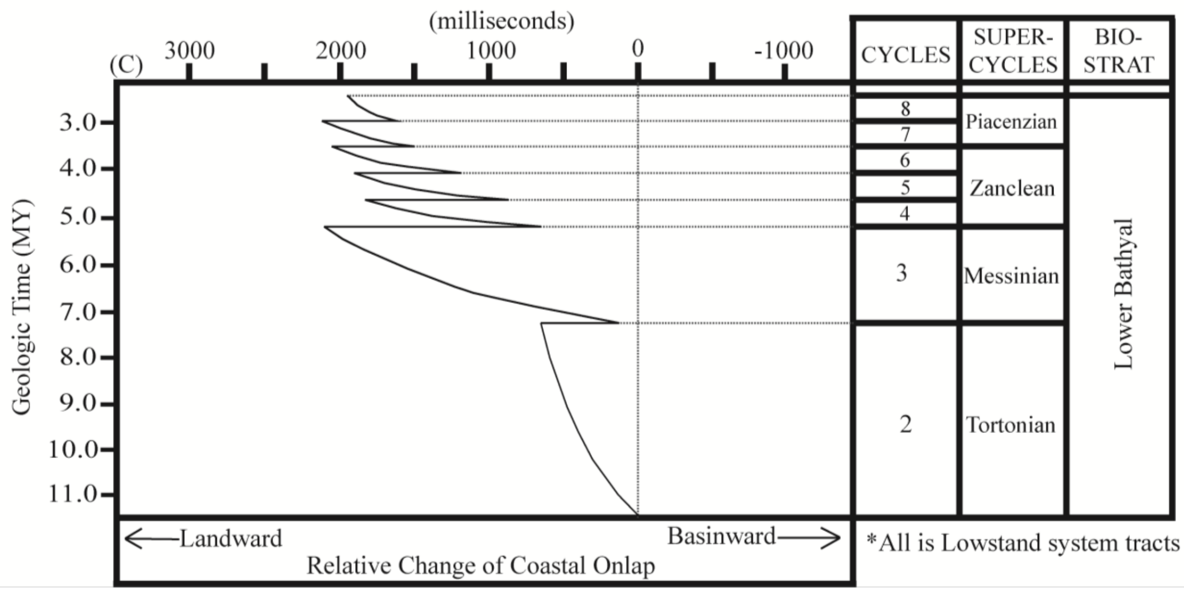
(milliseconds)
(C)
3000
2000
1000
0
-1000
CYCLES
SUPER-CYCLES
BIO-STRAT
3.0
4.0
5.0
6.0
7.0
8.0
9.0
10.0
11.0
Geologic Time (MY)
8
7
6
5
4
3
2
Piacenzian
Zanclean
Messinian
Tortonian
Lower Bathyal
Landward
Basinward
Relative Change of Coastal Onlap
*All is Lowstand system tracts

Likely significant increases in erosion at lower four megasequences due to the sudden increase in volume of the sediment gravity flows. Possibly substantial sand deposits are located south of the study area, which is for reservoir potential (Figures 36, 44, 52, and 61).

For system tracts interpretation, all of megasequences consist primarily of thick LSTs, with thin condensed sections that are the basinal equivalents to PGC, TST and HST. All clinoforms of HST and prograding complex of LST are located north of the study area, and thin southward into the condensed section in the study area.

Structural Controls

Extensive syn-depositional normal faulting in the Miocene through Pliocene sediments throughout the central graben primarily developed due to regional subsidence and high rates of siliciclastic sedimentation. The faults die-out upward into Pleistocene sediments (Figures 16 – 23). In addition, these normal faults, in general, become younger from north to south, and align with the direction of sedimentary transport.

The obvious increase in thickness can be seen in downthrown blocks or hanging walls in many places (Figures 20, 22). The effects of the faulting on reservoir distribution are unknown. Trap, migration, and entrapment are quite likely affected by these faults.

To the east, thrust and fold structures deform Pliocene sediments (Figures 16, 17, 19, 28), which is affected to retention of accumulation. To the west, the carbonate high remained until late Miocene, as part of megasequence 3 (Figures 20, 45, 52). This is another reservoir potential with main clastic reservoir.

Reservoir Potential

In the central graben, the sediment comprises stacked, base-of-slope, turbidite systems. Primary sediment supply was from N and NNE direction (Figures 36, 44, 52, 61, 71, 80, 88, 94). These strata are primarily channel-fill, levee, and overbank sediments. Each element has the distinct seismic facies and seismic attributes' response (Figures 35-36, 43-44, 51-53, 60- 62, 70-72, 79-81, 87-89, 93-94).

Attributes for each reservoir element are shown in Table 3. The potential channel-fill reservoirs are thicker in the shallow megasequences in both Miocene and Pliocene. In the Pliocene, two zones are recognized as lower (Megasequences 4–6) and upper Pliocene (Megasequences 7-8). Levees and overbank thickness vary based on the width and the channel geometry, which cut through the area. In addition, the possible carbonate reservoir in late Miocene must be included in the summary (Figure 53).

Reservoir Characters - Channel-filled								
Megasequences	**1**	**2**	**3**	**4**	**5**	**6**	**7**	**8**
Avg. Thickness	20 m	10 m	32 m	30 m	42 m	50 m	n/a	30 m
Width	1.8 km	0.8 km	1.5 km	1 km	1.5 km	1.2 km	n/a	2.2
Geometry	Medium Sinuosity	n/a	Low Sinuosity	Medium Sinuosity	Low Sinuosity	Medium Sinuosity	n/a	Low Sinuosity
	Lens	Lens	Lens	Lens	Lens	Lens	n/a	Lens

Reservoir Characters- Levees								
Megasequences	**1**	**2**	**3**	**4**	**5**	**6**	**7**	**8**
Avg. Thickness	12 m	n/a	8 m	17 m	28 m	22 m	n/a	28 m
Width	0.8 km	n/a	0.2 km	0.5 km	1 km	1 km	n/a	1.8 km
Geometry	Wedge	n/a	Wedge	Wedge	Wedge	Wedge	n/a	Wedge

Reservoir Characters- Overbank								
Megasequences	**1**	**2**	**3**	**4**	**5**	**6**	**7**	**8**
Avg. Thickness	18 m	n/a	25 m	10 m	22 m	22 m	n/a	15 m
Width	2 km	n/a	1.5 km	0.8 km	0.8 km	1.5 km	n/a	1.5 km
Geometry	Sheet-like	n/a	Thick sheet	Sheet-like	Sheet-like	Sheet-like	n/a	Sheet-like

Table 3: Table of Reservoir Characters in each Element

Petroleum Elements

The summary of the petroleum systems for lower Miocene to Pliocene strata in this area is shown in an events chart (Figure 97). However, the main potential source rock needed for generation is located in deeper than our study target. Maturity and present-day transformation ratios have been modeled by PTTEP and are summarized in Figure 98.

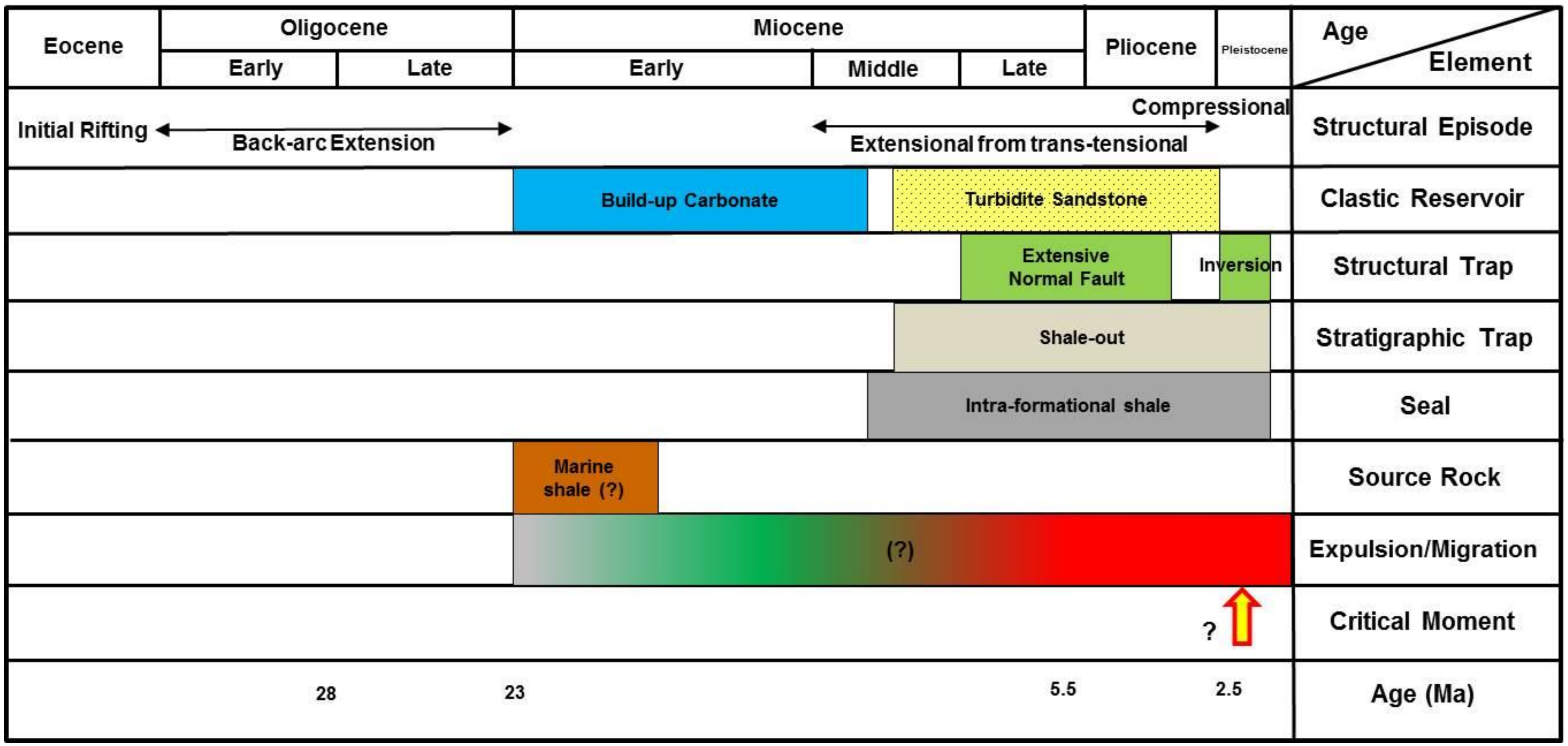

Figure 97: Petroleum event chart of middle Miocene-Pliocene play in M11, Martaban basin

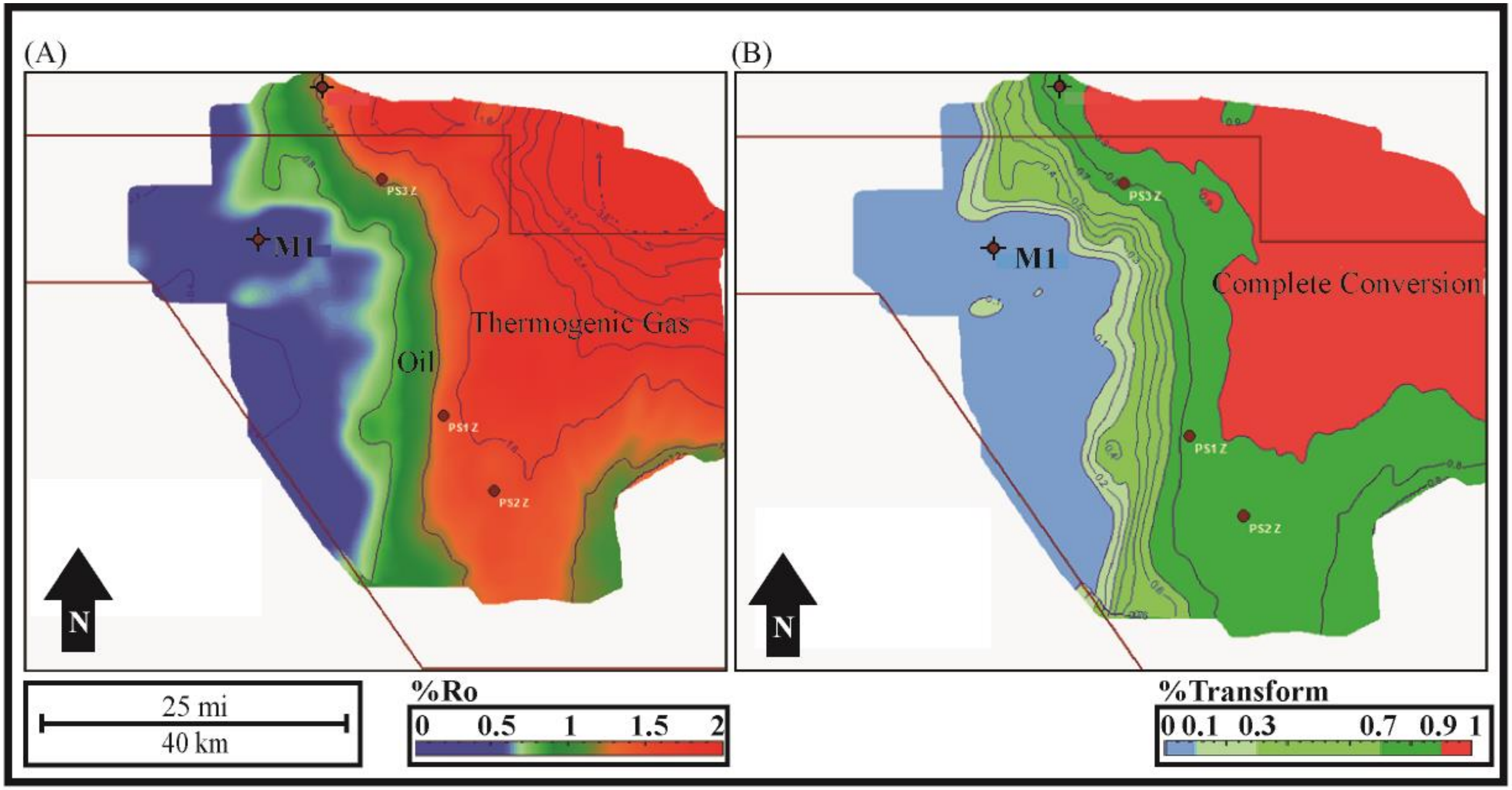

Figure 98: Map showing **(A)** thermal maturity of lower Miocene source rock, as measured by calculated vitrinite reflectance (Ro) and **(B)** present-day transformation (Modified from PTTEP internal report, 2017).

(1) Source Rocks

- No clear source rocks are identified on seismic sections in this area (Figure 97).
- In Miocene-Pliocene sediments, the dominantly muddy deposits from turbidity currents that over spilled into overbank, likely contain type III kerogen as gas-prone source rock (Figures 36, 44, 52, 61, 71, 80, 88, 94).
- Possible oil-prone source rocks, analogous Nipa palm Leaves from Sabah and Kalimantan are present. No clear evidence about this interpretation can be recognized in this area. This is possible (?) source rock were deposited in fine-grained turbidity sediments within the channel-fill.
- However, the producing fields in the northern Martaban basin have both microbial and thermogenic gas (Figure 3), which are generated from Pleistocene and early Miocene, respectively. The interpretation of thermogenic source rock is from PTTEP internal study, 2017 (Figure 98).

(2) Seals

- Mudrocks or shale deposited in the turbidity system are probably good for seals system (Figure 97).
- The extensive faults may also be the potential seal, as lateral seal from fault smear (Figure 15).

(3) Reservoir See, refer to reservoir potential topic (Figure 97).

(4) Trap

- Different trap styles are recognized in different areas, which were controlled by structural controls in each zone (Figure 15).

- To the west, 4-way dip closure on the structural high is present, which is part of carbonate reservoir potential (Figures 49, 97).
- In the central part of the study area, both 3-way dip closures against extensional faults, 4-way closures, and stratigraphic traps (onlap and truncation features) are present (Figures 33, 41, 49, 58, 67, 68, 77, 97). Any discoveries with 3-way or 4-way dip closures
- To the east, several 4-way closures are recognized due to thrust faults or detachment faults effects (Figures 33, 41, 49, 58, 67, 68, 77, 97).
- Seismic amplitude anomalies or Direct Hydrocarbon Indicators (DHIs) are possibly present (Figures 35, 43, 51, 60, 70, 79, 87). Given the age of sediment, high rates of sedimentation and recent burial, the rock physics are assumed to be favorable to amplitude anomalies, analogous to the Zawtika field to the North.

(5) Generation / Migration / Entrapment

- A 2D basin modeling study by PTTEP (internal report, 2017) indicated that the generation of early Miocene source rock produced thermogenic gas. However, the generation window is located in the depocenter of the Martaban basin, to the east and the southeast of the study area (Figure 98).
- Hydrocarbon migration is expected from the modeled transformation area charge to the reservoir at the east after critical moment (Figures 15, 16 – 22, 97).
- However, to the east, the thrusting developed during Pleistocene, probably affected the migration and entrapment in the Pliocene reservoirs (Figures 16, 17, 97).

CONCLUSION

(1) The Martaban basin, offshore Myanmar, consists of thick Neogene siliciclastic deepwater deposits. Local and regional tectonics control the distribution of Neogene sediment, with thickest sediments in the central part of the study area, overlying a post-rift graben. To the west, a basement high is present. To the east, thrust fold belt can be observed.

(2) Eight megasequences, ranging in age from early Miocene (?) to Top Pliocene, are defined. Each megasequence consists of base-of-slope turbidite system, comprising channel-fill, levee, and overbanks. The overall sedimentary section is primarily mud, with sands restricted to specific environments. Sedimentary supply was primarily to N and NNE, part of Ayeyarwardy delta (Figures 35-36, 43-44, 51-53, 60-62, 70-72, 79-81, 87-89, 93-94).

(3) In M11 block, the overall sea level changes present major in relative sea level rise, which is part of lower Bathyal from biostratigraphic report. The highest relative sea level in this specific area is in Megasequences 3 or Messinian.

(4) The typical stacked reservoir from the prediction of channel-fill is about 120 meters, with each individual channel averaging 30 meters (Table 3).

(5) Possible trap types include 3-way, 4-way, and stratigraphic traps (both onlap and truncation) (Figure 97).

(6) Significant unknown of petroleum systems elements (Figures 97, 98):

- Source rock presence and kerogen types.
- Timing of the HC generation and charging.

REFERENCE

CGG Service (Singapore) PTE LTD, 2017, Myanmar Block M-11 Broadband 3D Prestack Time Migration, Seismic data processing report, 1-233.

Curray Joseph R., 2004, Tectonics and History of the Andaman Sea region, *Journal of Asian Earth Sciences 25 (2005)*, 187-232.

Khan P.K. and Chakraborty Partha Pratim, 2004, Two-phase opening of Andaman Sea: a new Seismotectonic insight, *Earth and Planetary Science Letters 229 (2005)*, 259-271.

Laitrakull K., Myint K.H., and Iamboon J., 2016, Exploration history and Studies summary report of Myanmar deepwater block M11, *PTT Exploration and Production Public Company Limited.*, 1-61.

Li Quan, Yu Shui, Wu Wei, Tong Liqing, and Kang Hongquan, 2017, Detection of a deep-water channel in 3D seismic data using the sweetness attribute and seismic geomorphology: a case study from the Taranaki basin, New Zealand, *New Zealand Journal of Geology and Geophysics*, 60:3, 199-208.

Moeremans Raphaele E., and Singh Satish C., 2015, Fore-arc basin deformation in the Andaman- Nicobar segment of the Sumatra-Andaman subduction zone: Insight from high-resolution seismic reflection data, *AGU Publications,* 1736-1750.

Racey Andrew and Ridd Michale F., 2012, Chapter 6: Myanmar offshore petroleum overview, Petroleum Geology of Myanmar, *The Geological Society of London Memoir 45*, 57-62.

Racey Andrew and Ridd Michale F., 2012, Chapter 7: Petroleum geology of the Moattama Region, Myanmar, Petroleum Geology of Myanmar, *The Geological Society of London Memoir 45*, 63-81.

Raphaële E. M., and Satish C. S., 2015, Fore-arc basin deformation in the Andaman-Nicobar segment of the Sumatra-Andaman subduction zone: Insight from high-resolution seismic reflection data, *AGU Publication,* 1736-1750.

Rodolfo K. S., 1969, Bathymetry and marine geology of the Andaman Basin, and tectonic implications for Southeast Asia, *Geol. Soc. Am. Bull.,* 80(7), 1203-1230.

Rungsai Khunamai., 2015, Seismic interpretation for high-resolution seismic sequence stratigraphy in Moattama Basin, Myanmar, *IFP*, 1-10.

Pugin A., Pullan S.E., and Sharpe D.R., 1999, Seismic facies and regional architecture of the Oak Ridges Moraine area, southern Ontario, Can. J. Earth Sci. 36, 409-432.

Tapponnier P., G. Peltzer., A. Y. Le Dain., R. Armijo., and P. Cobbold., 1982, Propagating extrusion tectonics in Asia: New insights from simple experiments with plasticine, *Geology, 10(12),* 611–616.

Thiha, 2014, Myanmar oil & gas block map deep sea shallow water, Rakhine, Moattama, Tanintharyi, *Journal of Consult-Myanmar,* https://consult-myanmar.com/myanmar-oil-gas-block-map- deep-sea-shallow-water-rakhinemoattama-tanintharyi-consultmyanmar-4oct2014/.

Vail P.R., and Mitchum JR. R.M., 1978, Seismic Stratigraphy and Global Changes of Sea Level, Part1 Overview, *AAPG Bulletin Volume 62 Number 5*, 51-52.

Uzma Engineering in association with BSI Lab, 2012, Biostratigraphy and Paleoenvironments of Cutting Samples from well Manizawta (Interval 2090-3580 meters), offshore Myanmar, *PTT Exploration and Production Public Company Limited.*, 1-19.